How intestinal commensals affect the immune system and the outcome of inflammatory disorders: novel molecular insights

Dissertation

der Mathematisch-Naturwissenschaftlichen Fakultät

der Eberhard Karls Universität Tübingen

zur Erlangung des Grades eines

Doktors der Naturwissenschaften

(Dr. rer. nat.)

vorgelegt von

Alexander Steimle

aus Neuenbürg/Württ.

Tübingen

2016

Gedruckt mit Genehmigung der Mathematisch-Naturwissenschaftlichen Fakultät der Eberhard Karls Universität Tübingen.

Tag der mündlichen Qualifikation:	03.02.2017
Dekan:	Prof. Dr. Wolfgang Rosenstiel
1. Berichterstatter:	Prof. Dr. Julia-Stefanie Frick
2. Berichterstatter:	Prof. Dr. Ingo B. Autenrieth

Table of contents

Abbreviations

ABPs	activity based probes
AID	autoimmune disease
ALDH	aldehyd dehydrogenase
APC	antigen presenting cell
BMDC	bone marrow derived dendritic cells
CD	Crohn's disease
CTSB	cathepsin B
CTSL	cathepsin L
CTSS	cathepsin S
DC	dendritic cell
GALT	gut-associated lymphoid tissue
IBD	inflammatory bowel disease
iDC	immature dendritic cells
IFN-γ	interferon-γ
Kdo	3-deoxy-d-manno-octulosonic acid
LPS	lipopolysaccharide
MΦ	macrophage
MAMP	Microbe-associated molecular pattern
MD-2	myeloid differentiation-2
mDC	mature dendritic cells
MHC-II	major histocompatibility class-II
MyD88	myeloid differentiation primary response gene 88
OS	oligosaccharide
PAMP	pathogen-associated molecular pattern
PMGLP	Mca-GRWPPMGLPWE-Lys(Dnp)-DArg-NH_2
PRR	Pattern recognition receptor
SBP	Substrate based probes
smDC	Semi-mature dendritic cells
STAT3	Signal transducer and activator of transcription 3
TCR	T cell receptor
TLR	toll-like receptor
TNF	tumor necrosis factor
tolDC	tolerogenic dendritic cells
Treg	regulatory T cell
UC	ulcerative colitis

Summary (English)

The gut is considered to be the biggest immunological organ in mammals and the composition of the intestinal microbiota is therefore assumed to have widespread effects on the immune system of its host. During past years, more and more insights were gained concerning the correlation of intestinal microbiota composition and onset and progress of various autoimmune diseases, i.e. Inflammatory Bowel Diseases (IBD). Nevertheless, insights in defined molecular mechanisms underlying these observations are rare. However, a deeper knowledge of these mechanisms is necessary for proper drug development for gut-associated and immune system-related pathologies. With this work, knowledge gaps concerning molecular events of the interplay between commensal gut bacteria and the host immune system shall be closed. In this context, we focused on how different intestinal commensals, symbionts and pathobionts, differentially influence the host immune system.

Briefly summarized, *B. vulgatus* mpk, a Gram negative model symbiont of the intestinal microbiota, was able to prevent from induction of intestinal inflammation in a mouse model for experimental colitis. This effect was not restricted to prevention, as even already established colonic inflammation was reduced by oral administration of this bacterium, resulting in complete healing of damaged colonic tissue. Furthermore, isolated lipopolysaccharide from *B. vulgatus* mpk, providing a unique core oligosaccharide structure, was able to mimic both observed bacteria-mediated therapeutic effects. Additionally and for the first time, a symbiotic commensal such as *B. vulgatus* mpk was demonstrated to prevent from cathepsin S activity upregulation in host dendritic cells by a regulation mechanism involving the endogenous protein cystatin C. Cathepsin S activity regulation is a decisive criterion for the prevention of pathological $CD4^+$ T cell mediated immune responses. Since many autoimmune diseases were already demonstrated to be associated with cathepsin S activity dysregulation, our observation might explain why and how the microbiota composition influences the progress of autoimmune diseases in various mouse models. We furthermore showed that cathepsin S activity regulation in dendritic cells is part of DC semi-maturation. Semi-mature DCs provide a a tolerant and tolerogenic phenotype contributing to (re-)establishment of intestinal homeostasis and prevention of pathological inflammation.

Taken together, we hereby offer novel therapeutic approaches for the treatment of inflammatory bowel disease in specific and autoimmune diseases in general. First, lipopolysaccharides of symbiotic commensals might act as therapeutic agents and insights gained from the structural analysis of *B. vulgatus* mpk LPS might help to chemically design novel inflammation-silencing drugs. Second, *B. vulgatus* mpk was shown to prevent from pathological cathepsin S activitiy increase, making this bacterium an attractive alternative to chemical cathepsin S inhibitors which are widely considered to be promising drugs for the treatment of autoimmune diseases.

Zusammenfassung (Deutsch)

Der Darm wird im Allgemeinen als größtes immunologisches Organ im Säugetierorganismus betrachtet. Daher ist es schlüssig anzunehmen, dass die Zusammensetzung der Darmmikrobiota weitreichende Auswirkungen auf das Wirtsimmunsystem besitzt. In den vergangenen Jahren konnten immer mehr Zusammenhänge zwischen der Mikrobiotazusammensetzung und der Induktion beziehungsweise dem Verlauf verschiedener Autoimmunerkrankungen aufgezeigt und nachgewiesen werden. Obwohl diese generellen Beobachtungen gut dokumentiert sind, fehlt es weiterhin an detaillierten und schlüssig nachgewiesenen molekularen Grundlagen, die diese Beobachtungen zufriedenstellend erklären. Es ist jedoch nötig, genau diese molekularen Mechanismen zu kennen, um neue Therapieansätze für darmassoziierte immunologische Erkrankungen zu entwickeln. Diese Arbeit soll daher einen Beitrag dazu leisten, die Kenntnisse molekularer Ereignisse bei der Wechselwirkung kommensaler Darmbakterien mit dem Wirtsimmunsystem zu erweitern. Dabei steht insbesondere die unterschiedliche Wirkung von symbiotischen und pathobiontischen Kommensalen auf das Immunsystem des Wirts im Fokus.

In früheren Arbeiten konnte bereits gezeigt werden, dass *B. vulgatus* mpk, ein gramnegativer kommensaler Modellsymbiont der intestinalen Mikrobiota in einem Mausmodell vor experimenteller Kolitis schützen kann. Diese entzündungsregulierende Eigenschaft ist nicht nur darauf beschränkt, einen gesunden Darm vor beginnender Inflammation zu bewahren. Vielmehr ist dieses Bakterium auch in der Lage, bereits stattfindende entzündliche Prozesse in einer etablierten Kolitis derart zu reduzieren, dass eine komplette Regeneration des betroffenen Kolongewebes stattfindet und ein immunologisches Gleichgewicht wiederhergestellt wird. Aufgereinigtes Lipopolysaccharid dieses Bakteriums, dessen molekulare Struktur bisher einzigartig unter kommensalen Darmbakterien ist, spielt hierbei eine entscheidende Rolle. Des Weiteren konnte zum ersten Mal gezeigt werden, dass ein darmkommensaler Symbiont wie *B. vulgatus* mpk über einen Cystatin C-vermittelten Regulationsmechanismus vor einer pathologischen Erhöhung der enzymatischen Aktivität von Cathepsin S im Wirt schützt. Die Regulation der enzymatischen Aktivität dieser Protease ist entscheidend, um eine pathologische Aktivierung $CD4^+$ T-Zellen zu verhindern. Da viele Autoimmunerkrankungen mit einer pathologisch veränderten Cathepsin S-Aktivität einhergehen, könnte diese Beobachtung erklären, warum die Mikrobiotazusammensetzung die eingangs beschriebenen Auswirkungen auf den Verlauf von Autoimmunerkrankungen in verschiedenen Tiermodellen hat. Es ist weiterhin bereits bekannt, dass $CD11c^+$ Zellen im Intestinum eine entscheidene Rolle dabei spielen, die Immunhomöostase im Darm aufrecht zu erhalten und damit wichtig sind, um vor pathologischen entzündlichen Prozessen zu schützen. Wir konnten zeigen, dass

B. vulgatus mpk diese $CD11c^+$ Zellen in einen sowohl toleranten, als auch tolerogenen Zellphänotyp konvertiert, der direkt mit der strikten Regulation der Cathepsin S-Aktivität assoziiert ist.

Zusammenfassend wollen wir mit den in dieser Arbeit diskutierten Ergebnissen neue therapeutische Ansätze, die zur Behandlung chronisch entzündlicher Darmerkrankungen im Speziellen und zur Verhinderung pathologischer Immunreaktionen im Allgemeinen geeignet sind, anbieten. Oberflächenbestandteile von gramnegativen Bakterien (wie Lipopolysaccharide) könnten als Therapeutika für die erwähnten Pathologien fungieren. Zusätzlich könnten Erkentnisse, die aus der detaillierten Strukturanalyse des *B. vulgatus* mpk LPS gewonnen wurden, dazu beitragen, neuartige entzündungshemmende Substanzen chemisch zu generieren. Außerdem konnten wir zeigen, dass *B. vulgatus* mpk in der Lage ist, die proteolytische Aktivität von Cathepsin S zu regulieren. Somit liegt der Schluss nahe, dass dieses Bakterium eine attraktive Alternative zu chemischen Cathepsin S Inhibitoren darstellt, die weithin als vielversprechende Therapeutika für die Behandlung verschiedenster Autoimmunerkrankungen diskutiert werden.

List of publications in the thesis

Accepted manuscripts:

1. **Role of CD40 ligation in dendritic cell semi-maturation.**
   Gerlach AM, Steimle A, Krampen L, Wittmann A, Gronbach K, Geisel J, Autenrieth IB, Frick JS.
   BMC Immunol. 2012 Apr 26;13:22. doi: 10.1186/1471-2172-13-22.

2. **A novel approach for reliable detection of cathepsin S activities in mouse antigen presenting cells.**
   Steimle A, Kalbacher H, Maurer A, Beifuss B, Bender A, Schäfer A, Müller R, Autenrieth IB, Frick JS.
   J Immunol Methods. 2016 May;432:87-94. doi: 10.1016/j.jim.2016.02.015. Epub 2016 Feb 18.

3. **Molecular Mechanisms of Induction of Tolerant and Tolerogenic Intestinal Dendritic Cells in Mice.**
   Steimle A, Frick JS.
   J Immunol Res. 2016;2016:1958650. doi: 10.1155/2016/1958650. Epub 2016 Feb 11. Review.

4. **Structure and function: Lipid A modifications in commensals and pathogens.**
   Steimle A, Autenrieth IB, Frick JS.
   Int J Med Microbiol. 2016 Aug;306(5):290-301. doi: 10.1016/j.ijmm.2016.03.001. Epub 2016 Mar 5.

5. **The challenge of specific Cathepsin S activity detection in experimental settings**
   Steimle A, Frick JS
   J Neurol Neuromed. 2016: 1(3): 6-12

6. **Symbiotic gut commensal bacteria act as host cathepsin S activity regulators.**
   Steimle A, Gronbach K, Beifuss B, Schäfer A, Harmening R, Bender A, Maerz JK, Lange A, Michaelis L, Maurer A, Menz S, McCoy K, Autenrieth IB, Kalbacher H, Frick JS.
   J Autoimmun. 2016 Jul 30. pii: S0896-8411(16)30117-2. doi: 10.1016/j.jaut.2016.07.009.

Submitted manuscripts:

7. ***Bacteroides vulgatus* mpk lipopolysaccharide acts as an inflammation-silencing agent for the treatment of intestinal inflammatory disorders**
   Steimle A, Di Lorenzo F, Gronbach K, Kliem T, Fuchs K, Öz HH, Schäfer A, Bender A, Lange A, Maerz JK, Menz S, Silipo A, Autenrieth IB, Pichler BP, Bisswanger H, Łakomiec E, Jachymek W, Molinaro A, Frick JS
   Submitted to Nature Communications in November 2016

Personal contribution to the papers in the thesis

Paper No.	Accepted for publication yes/no	Number of all authors	Position of the candidate in list of authors	Scientific ideas of candidate (%)	Data generation by candidate (%)	Analysis and Interpretation by candidate (%)	Paper writing by candidate (%)
1	yes	8	2*	25	25	25	25
2	yes	9	1	100	90	90	100
3	yes	2	1	100	100	90	100
4	yes	3	1	80	80	80	80
5	yes	2	1	100	100	90	100
6	yes	15	1	90	90	100	100
7	no	17	1	60	60	60	85

* Shared first authorship

Introduction

1. The intestinal microbiota

1.1 Evolution and function of the intestinal microbiota

During the evolution of complex eukaryotic organisms, these organisms became hosts to so-called commensal microbes. Commensals are hereby defined as organisms that live in a relationship in which the host derives food or other benefits from commensals without being negatively affected by their presence. Besides fungi, intestinal commensals mainly consist of bacteria [1]. This symbiotic co-evolution of a eukayrotic host and commensals resulted in the formation of huge metaorganisms consisting of prokaryotic and eukaryotic cells. These metaorganisms share a common metabolome despite having a separate metagenome [2, 3]. The entirety of commensal microorganisms, which are adapted to a certain host, are termed “microbiota”. Since these microorganisms are present in abundant numbers in and on mammals and other complex organisms, this symbiotic form of life made up of a single eukaryotic and several million prokaryotic organisms is often called a “superorganism” [4, 5].

The biggest numbers and the greatest variety of commensal bacteria in a mammalian organism is found in the intestine with the largest number of microorganisms existing in the colon and distal ileum [6]. This intestinal microbiota consists of a pool of approximately 10^{12} microorganisms per gram luminal content with 99% of these microorganisms being obligate or facultative anaerobes [7]. The resulting interplay between host and intestinal microbiota influences and regulates various functions of the host organisms, such as (I) nutrition, (II) metabolism, (III) integrity maintenance of the intestinal epithelial barrier, (IV) inhibition of pathogen attachment and proliferation, (V) general homeostasis and promotion of gut microbial diversity as well as (VI) development and regulation of the innate and the adaptive immune system [8-12]. For example, microbiota components produce and secrete vitamins in excess of their own requirements therefore being important for host vitamin supply [13]. Besides vitamins, also other bacterially produced substances are important for the host organism by supporting the growth of the gut epithelium and influencing metabolic functions. Indeed, bacterial colonization is required for the induction of host digestive enzymes [13, 14]. Additionally, a normal microbiota is crucial for the development of the adaptive immune system and lymphatic structures [15, 16]. The gut-associated lymphoid tissue (GALT) harbours immune structures where antigens are taken up and presented via antigen-presenting cells (APCs). The requirement of the intestinal microbiota for the development of the GALT has been convincingly demonstrated by studies using germfree mice underlying the importance of the intestinal microbiota for host immune system development [17].

1.2. The composition of the gut microbiota

The intestinal microbiota of mice and humans (as the most well studied mammalian organisms) mainly consists of seven major bacterial phyla: Gram positive *Firmicutes* and *Actinobacteria* as well as Gram negative *Bacteroidetes*, *Proteobacteria*, *Fusobacteria*, *Verrumicrobia* and *Cyanobacteria*. Among these, *Firmicutes* and *Bacteroidetes* bacteria alone account for more than 90% of all bacterial strains in an "average" intestinal microbiota [18, 19]. However, the composition of the microbiota is not static. Nutrition, the presence of toxins, medication such as antibiotics and various other environmental factors influence a certain individual's microbiota composition [20, 21]. Besides these extrinsic factors, instrinsic properties of the host, such as its genetic background, greatly affect the constitution of the intestinal microbiota [22-24]. Importantly, this host genetic background is decisive whether a specific microbiota composition is healthy or, in other words "balanced" for a certain host. Therefore, host genetics is relevant for the definition of a so-called "microbiota dysbiosis" or "imbalance". The term "dysbiosis" often refers to describe a microbiota composition that is considered to be harmful, or potentially harmful, for a certain host individual by disrupting a normal and balanced state of the gut [25].

1.3. Subgroups of intestinal commensals: the concept of "symbionts" and "pathobionts"

Although mostly consisting of bacteria belonging to a handful of different bacterial phyla, the intestinal microbiota is a highly heterogeneous mixture of microorganisms. However, microbiota components can be classified and subgrouped into different functional classes, dependent on their effect on the host immune system [17]. In general, the intestinal microbiota is composed of commensals and, sometimes, pathogens. Commensals are generally considered to be harmless or even beneficial for the host, while pathogens cause infections or diseases. However, it remains largely unclear how exactly the host immune system manages to discriminate between pathogens and commensals. According to a certain definition concept, commensals can be further subdivided into symbionts and pathobionts. Pathobionts are hereby defined as commensal and resident bacteria that may cause non-beneficial effects on the host such as induction of overshooting inflammatory reactions in the gut. However, pathobionts exhibit these potentially pathological properties only when the host provides certain genetic or environmental preconditions [26], which defines the decisive difference between pathobionts and pathogens. Contrariwise, symbiotic commensals never trigger intestinal inflammatory reactions [17] and symbionts rather actively suppress pathological properties of pathobionts by the induction of regulatory immune functions, i.e. via interleukin-10 (IL-10) and the induction of regulatory T cells (Tregs). These different properties of symbionts and pathobionts concerning induction of inflammatory reactions in the gut have been demonstrated in various studies focusing on the induction of colitis in mice [27-29].

1.5 *Bacteroides vulgatus* mpk – a model symbiotic commensal

Some commensals have been already reported to exhibit either symbiotic or pathobiotic properties. Examples for commensal pathobionts include (among others) *Bilophila wadsworthia* [30], *Escherichia coli* [28, 31], *Porphyromonas gingivalis* [32], *Clostridium difficile* [33], *Enterococcus faecalis* and members of the *Prevotellaceae* family [34]. Prominent examples of commensal symbionts comprise members of the genera *Bifidobacterium* [35], *Lactobacillus* [36] and *Ruminococcus* [37, 38]. Concerning *Bacteroides*, it seems to be more complicated to class this genus adequately into such a bipolar symbiont/pathobiont classification scheme. While some groups consider the whole *Bacteroidetes* phylum to be pathobiotic [39, 40], others classify the entire genus *Bacteroides* as symbionts [41]. Supporting the latter classification, *Bacteroides fragilis* [42, 43] and *Bacteroides thetaiotaomicron* [44, 45] as prominent members of this genus were convincingly reported to be symbionts.

Our group has extensively reported on another intestinal commensal of the *Bacteroides* genus: *B. vulgatus* mpk. So far, this bacterium was demonstrated to provide strikingly symbiotic features in mice and we therefore assume *B. vulgatus* mpk to be a model symbiont for the mouse intestine. We could already demonstrate that this strain protects from colitis induction in *Rag1*$^{-/-}$ mice [46] and promotes survival in *Il2*$^{-/-}$ [28] mice, with both mouse models for experimental colitis being highly dependent on microbiota composition and both studies underlying the symbiotic properties of this commensal bacterium. Detailed analysis of the *B. vulgatus* mpk genome revealed a high genomic plasticity [47] which we consider to be a survival and adaption strategy to different intestinal environments, helping this strain to mediate and exhibit its immune system-silencing properties.

2. Inflammatory disorders of the gut

Due to their different immunogenic properties, intestinal symbionts and pathobionts exhibit distinct effects on the mucosal immune system and immune system-related pathologies. Therefore, microbiota-driven or –influenced pathological inflammatory reactions in the intestine may lead to the manifestation of Inflammatory Bowel Disease (IBD). IBD is characterised by chronic relapsing intestinal inflammation with Crohn's Disease (CD) and Ulcerative Colitis (UC) being the most frequent and clinically relevant forms of this disease complex in humans [48, 49]. IBD is associated with either an inappropriate immune response to normally harmless commensal microbes, an inefficient clearance of immune response-stimulating microorganisms leading to a continuous activation of the immune system or failing to turn from an adequate proinflammatory response to inflammation-reducing anti-inflammatory immune reactions [50, 51]. It is furthermore considered to be a

multifactorial disease with genetics [52], environmental factors [53] and intestinal microbiota composition [54] contributing to its pathology [49]. In fact, changes in the microbiota composition were observed in IBD patients and a decrease in general diversity but also an increase in certain species [55, 56] was associated with IBD development [49]. In UC patients, the proportion of *Bacteroides* species is markedly decreased [57] supporting the idea of *Bacteroides* strains being important symbionts in the intestinal microbiota [49]. Concerning the influence of host genetic predisposition on IBD pathology, single nucleotide polymorphisms in more than 160 human genes are associated with an increased incidence of IBD [52, 58]. However, these genetic risk factors are not specific for either UC or CD [58]. Since the human genetic pool remained relatively constant during past generations, the increasing incidence and prevalence of IBD in developed countries is therefore traced back to be most likely provoked by environmental factors [59]. Thus, changes in the microbiota composition are considered to be relevant for IBD incidence. In general, a more diverse microbiota is regarded to be beneficial for the host. In fact, changes in microbiota composition in the colon of IBD patients were demonstrated in various studies [54, 60-64].

3. Bacterial structural compounds and their influence on the immune system

An important factor for the interplay between commensals and the host immune system is an adequate recognition of bacteria and bacterial compounds in the intestine. Therefore, recognizing bacterial structures is a prerequisite for an efficient host innate immune system and important for the clearance of initial or persisting bacterial infections. The host immune system is able to detect and recognize conserved bacterial molecular structures which are termed microbe-associated molecular patterns (MAMPs) with MAMPs being originally defined as *conserved molecules present in whole classes of microbes (nonself) with an essential function for these microbes* [65].

3.1. Lipopolysaccharides of Gram negative bacteria

One of the most important MAMPs of Gram negative bacteria are lipopolysaccharides (LPS). LPS is anchored in the outer bacterial membrane providing a barrier against surrounding environments that could be harmful for bacterial survival [49, 66]. Usually, LPS consists of a lipid A part, a core oligosaccharide (OS) and sometimes additionally of a so-called O-antigen. Figure 1 illustrates the general structure of LPS which is embedded in the outer leaflet of the bacterial cell wall via the hydrophobic acyl chains of its lipid A part [67, 68]. *E. coli* lipid A is considered to be the “prototype” lipid A and consists of a β(1→6)-linked glucosamine disaccharide backbone, mostly phosphorylated at position 1 and 4’, which is additionally acylated at positions 2

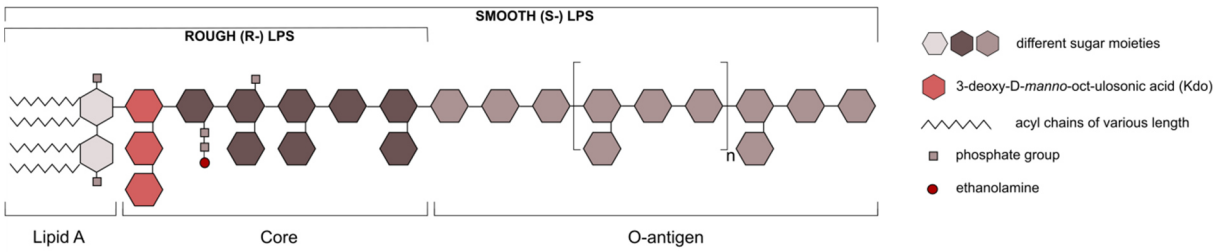

Figure 1: Schematic diagram of the general structure of lipopolysaccharides of Gram negative bacteria. Lipolysaccharides of Gram negative bacteria consist of three main subunits (from left to right): lipid A, the core region and the O-antigen. Lipid A and the core region form rough (R)-type LPS. Lipid A, the core-region and the O-antigen together form smooth (S)-type LPS. The number and chemical structure of the acyl chains can vary. Suger moieties are depticted as hexagons in different colors. The number and chemical structure of these sugar moieties can vary. Taken from Steimle & Frick (2016) [68] and slightly changed.

and 3 of each monosaccharide residue [68-71]. The immunogenicity of LPS, or the strength of the host immune response to bacterial LPS, is regarded to be mainly mediated by lipid A [49, 68, 72, 73]. However, despite LPS of all Gram negative bacteria follows this general structural make up, slight differences in the phosphorylation pattern as well as in the number, length and distribution of the acyl chains may influence the immunogenicity of lipid A and therefore of LPS as a whole (reviewed in [68, 74]). The LPS core OS is coupled to lipid A via at least one residue of 3-deoxy-D-manno-oct-ulosonic acid (Kdo) and contains up to 15 sugar residues [68]. Adjacent to the core oligosaccharide, repeating units of usually not more than five different sugar moieties build up the so-called O-antigen [68]. However, the O-antigen is not always part of LPS. LPS structures missing an O-antigen are called “rough”, the ones containing the O-antigen are named “smooth” [75].

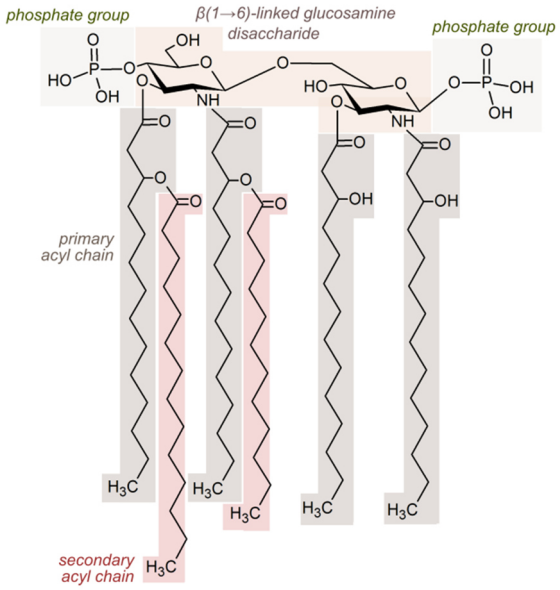

Figure 2: Detailed structure of *E. coli* lipid A.
E. coli lipid A contains a β(1→6)-linked glucosamine disaccharide backbone (light brown). The hydroxyl group (light yellow) of the distal glucosamine links lipid A to the Core region. The two phosphate groups are depicted in light green. Primary acyl chains (light grey) are directly linked to the sugar moieties, secondary acyl chains (light red) are esterified with the hydroxyl groups of primary acyl chains. All primary acyl chains of E. coli lipid are hydroxymyristates, one of the two secondary acyl chains is myristate while the other one being laurate. Taken from Steimle & Frick (2016) [68]

3.2. MAMP recognition receptors – a focus on the MD-2/TLR4 receptor complex

The general conservatism of LPS structures allowed for the development of evenly conserved LPS recognition structures in mammals [76]. Extracellular recognition of LPS occurs via the myeloid differentiation-2/Toll-like receptor receptor 4 (MD-2/TLR4) receptor complex [76]. This receptor complex belongs to the group of pattern recognition receptors (PRR), which allow host cells to sense microbiota component-derived MAMPs [9]. Expressed on intestinal epithelial cells and dendritic cells [41], the MD-2/TLR4 receptor complex stands in the front line of the host microbe-sensing machinery. In general, LPS is a potent MD-2/TLR4 receptor complex agonist, leading to strong intracellular signalling in target cells and resulting in transcription of genes associated with pro-inflammatory immune responses [49, 77]. For the cellular detection of low LPS concentrations, a series of different proteins is necessary: the LPS binding protein (LBP) [78, 79] which is supposed to deliver LPS monomers to soluble or membrane bound CD14 [80] followed by LPS binding of MD-2 which forms a heterodimer with the TLR4 ectodomain [81, 82]. LPS binding of MD-2/TLR4 results in a conformational change of the heterodimer resulting in $(MD\text{-}2/TLR4)_2$ heterotetramerization leading to activation of intracellular signalling [49, 83-85]. However, LPS is not only recognized in extracellular environments but also intracellularly inside target cells. Recently, caspase-11 (Casp11) has been identified as such an intracellular LPS recognition receptor [86-91] which is able to bind the lipid A part via its CARD-domain, resulting in secretion of pro-inflammatory cytokines [68, 92, 93]. However, intracellular Casp11-mediated LPS sensing requires previous transcription of the *Casp11* gene which can be initiated by recognition of bacterial components not only via TLR4, but also via TLR2 and/or TLR7 [68, 94].

4. Dendritic cells: major players in immunity

Although not being the only TLR4 expressing cells in mammals, dendritic cells (DCs) are major components of the innate as well as of the adaptive immune system and represent the most important cell type connecting both immune responses [95, 96]. They provide important functions in mucosal immunity since, besides intestinal epithelial cells, DCs are among the first PRR-expressing cells encountering microbiota components (see above). In general, DCs comprise a heterogenous leukocyte population of different developmental origin and with distinct surface markers and biological functions [51]. DCs patrol virtually all lymphoid and non-lymphoid organs and are specialized antigen presenting cells (APCs) which are able to induce a variety of different immune responses [51, 95]. One of the most prominent functions of DCs is to induce an adaptive immunity against pathogens while simultaneously maintaining tolerance to self-antigens and, importantly, to the own commensal microbiota [51, 97].

4.1 Dendritic cell tolerance, tolerogenicity and semi-maturation

Usually, antigen encounter leads to induction of a maturation program in DCs and certain components of complex antigens are sufficient to induce DC maturation. As an example, binding of agonistic LPS to the MD-2/TLR4 receptor complex leads to complete maturation of DCs. DC maturation is characterized by efficient antigen sampling from the extracellular environment and effective subsequent antigen processing [51]. These cellular effects are accompanied by upregulation of major histocompatibility class-II (MHC-II) and T cell co-stimulatory molecules like CD40, CD80 and CD86 which are essential for proper T cell activation [51]. Secretion of pro-inflammatory cytokines such as IL-1β, IL-6, TNF, IL-12 and others complete this mature DC phenotype [95, 98].

However, dependent on the nature of the encountered antigen, DCs can be prevented to become fully mature but rather develop into different other phenotypes. Many groups have already characterized a DC phenotype called semi-mature [99-106] which is strongly distinct from a classical mature state [51]. However, the exact definition of DC semi-maturation is less distinct and depends on the agent that is used to induce this certain phenotype [51]. The most important property of semi-mature DCs, uniting different definitions, is the inability to induce a pro-inflammatory Th1 or Th17 immune response and to be non-responsive, or in other words “tolerant” towards subsequent maturation stimuli [51, 99, 107]. Semi-mature or “tolerant” DCs often provide additional “tolerogenic” properties. This means, they possess one, several or all of the following criteria: (1) induction of unresponsiveness of T cells, (2) active induction of regulatory T cells (Tregs), (3) active inhibition of pro-inflammatory T cell responses and (4) promotion of T cell apoptosis or T cell anergy [51, 108].

4.2 The connection between inflammatory disorders, gut microbiota and phenotypes of intestinal DCs

As mentioned above, the composition of the intestinal microbiota plays an important role in manifestation, onset or progress of intestinal inflammatory disorders like IBD, not only in mouse models for experimental colitis but also in human patients [109]. The distinct components of the intestinal microbiota have different effects on the phenotype and maturation state of intestinal dendritic cells which are crucial for driving immune responses into either a proinflammatory or a rather homeostatic condition [51]. In this context, tolerogenic and semi-mature DCs have been reported to play decisive roles for the maintenance of intestinal homeostasis and the prevention of pathological intestinal inflammatory processes [28, 31, 46, 51, 110]. Most notably, symbiotic commensals are able to induce tolerogenic intestinal DCs via direct interaction with this important type of APCs [41]. This initial interaction at the mucosal interface is a crucial event for the subsequent onset of a series of immunological cellular reactions that finally define the overall

inflammatory status of the intestine. As mentioned, the microbiota-induced DC phenotype decides on whether intestinal T cells are polarized into an inflammation-promoting Th1 and, notably, Th17 directions or the induction of $Foxp3^+$ Tregs is favoured. While intestinal $Foxp3^+$ Tregs favour mucosal homeostasis, Th17 T cells play a pivotal role for the manifestation of inflammatory disorders. These Th17 T cells are associated with the induction of autoimmune diseases in general [111], a fact that also highlights their role for onset and development of IBD [112]. We could already provide evidence, that symbiotic and pathobiotic commensals differentially modulate DC maturation phenotypes which, in turn, directly affect the polarization type of T cells and therefore the induction or prevention of intestinal inflammation. In various mouse models, pathobionts induced maturation of intestinal DCs leading to enhanced Th1/Th17 T cell polarization resulting in enhanced colonic inflammation while symbionts induced DC semi-maturation which was associated with lower Th1/Th17 responses and a prevention of pathological inflammation [28, 31, 110].

5. The role of cathepsin S for MHC-II surface expression and DC maturation

Dendritic cells activate T cells and influence their polarization profile via the secretion of a certain cytokine pattern and the surface expression of proteins that directly interact with receptors on the T cell surface. Among these DC surface proteins, MHC-II is one of the most important activators for $CD4^+$ T cells and the extent of MHC-II surface expression is one major criterion for the determination of the DC phenotype and therefore for the ability to induce or prevent inflammatory responses [46, 51]. MHC-II expression is regulated on transcriptional and post-transcriptional levels [113] and TLR signalling leads to enhanced MHC-II protein synthesis [114]. However, in immature DCs, large amounts of already synthesized MHC-II molecules are present in endosomal and lysosomal compartments [115, 116]. Upon induction of DC maturation, MHC-II protein complexes are translocated from these intracellular vesicular compartments to the cell surface [115, 116]. One of the most important post-transcriptional regulation mechanisms for MHC-II surface expression is cleavage of the MHC-II associated invariant chain, a proteolytical step that is catalyzed and therefore regulated by cathepsin S (CTSS) in professional antigen-presenting cells (APCs) [117].

5.1 CTSS as an important general regulator of immune responses

Cathepsin S (CTSS) is a lysosomal single-chain protease that is expressed APCs like macrophages, dendritic cells (DC) [118] and B cells as well as in non-professional APCs like intestinal epithelial cells [46, 119, 120]. It belongs to the papain-like cysteine protease family that currently comprises eleven known members in humans [46, 121]. It is mainly involved in the stepwise degradation of the MHC-II associated chaperone invariant chain (Ii) [46, 122]. These proteolytic events are crucial for the

loading of antigen-derived peptides on MHC-II and the subsequent transport of this MHC-II-peptide complex to the APC surface where it promotes $CD4^+$ T cell activation [46, 117]. CTSS activity can be influenced by transcriptional and post-translational regulation or by protein-protein-interaction with endogenous inhibitors, mainly cystatins [46, 123]. However, there are contradictory reports on cystatin-mediated CTSS activity regulation [46, 124-127]. Though, adequate regulation of CTSS is necessary to retain the steady state of $CD4^+$ T cell dependent immune responses, which, in turn, is crucial for the onset of CD4+ T cell mediated autoimmune diseases (AID) [46].

5.2 Impact of cathepsin S on IBD and onset or progression of autoimmune diseases – a short overview

In fact, dysregulation of CTSS activity, expression or secretion into the extracellular space is associated with the pathogenesis of various AID, i.e. arthritis [128, 129], type-I-diabetes [130], Sjögren's syndrome [131, 132], multiple sclerosis [125, 133] and atherosclerosis [134, 135]. Furthermore, CTSS secretion contributes to pain induction during inflammatory bowel disease (IBD) [136]. Due to the implications of CTSS dysregulation for the pathogenesis of AID, there is an intense search ongoing for the development of drugs that are able to specifically inhibit CTSS proteolytic activity [137] in order to offer novel therapeutic approaches for the treatment of AID.

Aim of this work

Insights of molecular events caused by gut microbiota leading to novel therapeutic strategies for the treatment of IBD and AID

In previous studies, we could demonstrate that the composition of the intestinal microbiota is a decisive factor for the induction or prevention of pathological immune responses in mouse models for experimental colitis. We could show that a certain mouse-associated symbiotic gut commensal, *Bacteroides vulgatus* mpk, is able to prevent from pro-inflammatory immune responses by induction of semi-maturation in dendritic cells, thus favouring homeostatic conditions in the intestine [28, 31, 99]. Furthermore, we could show that not only the microbiota composition but also the detailed structure of LPS from Gram negative gut commensals determines the outcome of inflammation in *Rag1*$^{-/-}$ mice [110].

Due to these implications, we were interested, (I) in the exact molecular mechanisms that underly induction and preservation of DC semi-maturation, (II) if the proteolytic activity of cathepsin S as a major mediator of $CD4^+$ T cell driven immune responses is regulated by commensal bacteria (and especially by *B. vulgatus* mpk), (III) if *B. vulgatus* mpk is not only able to prevent from intestinal inflammation, but might also be able to actively reduce already established intestinal inflammation and (IV) if the anti-inflammatory and DC semi-maturation inducing properties of *B. vulgatus* mpk requires living bacteria or whether isolated LPS as a MD-2/TLR4 receptor complex ligand might mimic these immunomodulatory effect.

All these questions to be answered aim to find new therapeutical approaches not only for the treatment of IBD, but also for AID in general. Since cathepsin S is a crucial enzyme for the induction of almost all known AID, a proven microbiota-dependent (or microbiota-derived component dependent) regulation of this enzyme might be a major step forward into the development of novel drugs.

Results and discussion

Gerlach et al. BMC Immunology 2012, 13:22
http://www.biomedcentral.com/1471-2172/13/22

BMC Immunology

RESEARCH ARTICLE Open Access

Role of CD40 ligation in dendritic cell semimaturation

Anna-Maria Gerlach†, Alexander Steimle†, Lea Krampen, Alexandra Wittmann, Kerstin Gronbach, Julia Geisel, Ingo B. Autenrieth and Julia-Stefanie Frick*

Paper 1: Role of CD40 ligation in dendritic cell semi-maturation

Research paper

Anna-Maria Gerlach†, **Alex Steimle**†, Lea Krampen, Alexandra Wittmann, Kerstin Gronbach, Julia Geisel, Ingo B Autenrieth and Julia-Stefanie Frick

BMC Immunol (2012) 13:22 [138]

† both authors contributed equally to this work

Dendritic cells play a crucial role in the activation of T cell-mediated immune responses. The exact DC phenotype is thereby decisive if T cells are activated and if yes, how these activated T cells are polarized. We and others could already demonstrate that this immature-versus-mature phenotype characterisation is not as bipolar as it seems to be since other DC phenotypes with different immunomodulating properties have been discovered. We could show that a certain symbiotic gut commensal bacterium, *B. vulgatus* mpk, converts DCs into a semi-mature phenotype which is distinct from an immature or mature phenotype [31, 99, 105]. This semi-mature phenotype was demonstrated to be crucial for maintenance of intestinal homeostasis, thus preventing from pathological inflammatory reactions [28, 31, 99, 110].

A characteristic feature of a semi-mature DC phenotype is, besides others, their low to intermediate expression of CD40, a T cell co-activating surface protein. In general, activation of T cells by dendritic cells includes three different ligation events resulting in activating processes in the T cell (reviewed in [139]). The first event is recognition of MHC-II which is loaded with antigenic peptide by binding to the corresponding T cell receptor (TCR) on the T cell surface. The second event is the ligation of CD80 or CD86 on the DC surface with CD28 on the T cell surface and the third and last required signal is mediated by ligation of CD40 on DCs with the corresponding CD40 ligand (CD40L) on T cells. CD40 expression on DCs is therefore important for the induction of a $CD4^+$ T cell mediated immune response [140, 141]. Binding of CD40L to CD40 leads to increased expression of CD83, CD80, CD86

and MHC-II on dendritic cells, therefore acting as an expression booster of these surface proteins [142-145]. CD40 ligation may also positively influence survival of DCs [146, 147] as well as enhancing the secretion of pro-inflammatory cytokines [143-145, 148].

These findings underly that there are two principal mechanisms how CD40 expression on DCs can be regulated or activated. The first mechanism is antigenic encounter leading to DC maturation and enhanced expression of T cell activating surface proteins and cytokines. The second mechanism is feedback activation by ligation of CD40 and CD40L.

We already know that once a DC was converted into a semi-mature phenotype with a characteristic low to intermediate expression of CD40 cannot be overcome by additional antigenic encounter. We were therefore interested if and how the binding of CD40L to CD40 of semi-mature DCs alters their phenotype and in consequence their immunomodulatory properties or, in other words, can DC semi-maturation be overcome by T cell binding and activation?

In order to clarify the impact of CD40 expression on the T-cell activation capacity of semi-mature DC, we examined the effect of CD40 ligation on immature, semi-mature and mature DCs [138]. Semi-mature DC were induced by stimulation with *B. vulgatus* and are characterized by a low positive expression of co-stimulatory molecules like e.g. CD40, secretion of only IL-6, and nonresponsiveness toward subsequent TLR activation [99, 105, 138]. We could demonstrate that, upon CD40 ligation with an α-CD40 antibody, *B. vulgatus* primed semi-mature DCs secrete increased amounts of IL-12p40 and IL-6, but not IL-12p70 in contrast to E. coli primed mature DCs which secrete high amounts of all three cytokines [138]. CD40-ligated semi-mature DCs express slightly more T cell co-stimulatory molecules (such as CD80, CD86 and CD40) than their non-CD40-ligated semi-mature counterparts. However, this slight increase in surface expression of CD40, CD80 and CD86 upon CD40 ligation led to an expression level that was still significantly lower than the expression level of these proteins in *E. coli*-stimulated mature DCs. These findings prompted us to check for intracellular signalling events upon CD40 ligation in immature, mature and semi-mature DCs. Usually, binding of CD40L to CD40 leads to enhanced intracellular signalling in DCs resulting in phosphorylation, and therefore activation, of the MAP kinase p38. We could demonstrate that in mature and immature DCs, CD40 ligation leads to enhanced phosphorylation of p38. However, this was not observed in semi-mature DCs. Mature DCs which were treated with a p38-inhibitor before CD40 ligation provided reduced secretion rates of IL-12p70 compared to non-inhibitor treated samples. However, this effect was not observed in immature or semi-mature DCs. Taken together, we conclude that inhibited p38-phosphorylation in semi-mature DCs is, at least in part, responsible for their reduced secretion of IL-12p70 [138]. A graphical summary of the obtained results is depicted in Figure 3.

With this study, we demonstrated that CD40 ligation does not overcome DC semi-maturation in terms of expression of activation surface markers and results in production of only IL-6 and IL-12p40, but not the bioactive form of IL-12, IL-12p70 [138]. The slightly reduced p38 phosphorylation levels in semi-mature DC as compared to mature DC might at least partially contribute to this effect [138]. In line with other studies [149, 150], we observed that on mature DCs no significant further increase in the expression levels of the already highly expressed co-stimulatory molecules CD40, CD80 and CD86 could be triggered upon additional stimulation by CD40 ligation [138]. Upon CD40 ligation immature and semi-mature DC expressed intermediate levels of CD40, CD80 and CD86, but did not reach the expression level of mature DC [138] (Figure 3). However, the intermediate expression of co-stimulatory molecules was not associated with production of pro-inflammatory cytokines like IL-12p70 [138]. It is known that immature DCs, which are characterized by low expression levels of co-stimulatory molecules and by lacking secretion of pro-inflammatory cytokines, induce tolerance by promoting T-cell anergy, apoptosis or differentiation into Treg cells via antigen presentation in the absence of co-stimulatory signals [138, 151, 152]. Additionally, CD40 deficient DCs or DCs with a suppressed CD40 expression were shown to have a reduced potential to activate T-cell proliferation and polarization into Th1 or Th2 direction [138, 153-157]. This effect might also contribute to the inhibited T cell activation induced by the intermediate expression of co-stimulatory molecules on semi-mature lamina propria (lp) DC of *B. vulgatus* mono-colonized *Il2*$^{-/-}$ mice [31, 138]. On the other hand, it was shown that a high positive expression of co-stimulatory molecules in absence of pro-inflammatory mediators like e.g. TNF-α or IL-12p70 favours T-cell tolerance and suppression of T-cell activation [138]. This type of DC is mainly induced by autocrine or paracrine stimulation with inflammatory mediators like e. g. TNF [138, 158, 159]. The cytokine secretion pattern upon CD40 ligation differed between immature/semi-mature DC and mature DC [138]. In immature and semi-mature DC, CD40 ligation did not result in induction of IL-12p70 secretion, in contrast to mature DC where CD40 ligation led to increased IL-12p70 secretion [138]. This is in line with other studies showing that TLR4 stimulation and CD40 ligation synergize in inducing IL-12p70 secretion [138, 150, 160]. The additive microbial priming signals are necessary to trigger the production of the IL-12p35 subunit [161] which was shown to be not induced by CD40 ligation only [138, 162, 163]. Additionally, these accessory stimuli have the potential to augment the CD40 expression on antigen presenting cells (APC) [164-166] which results in a more effective CD40 ligation [138]. However, DCs primed with *B. vulgatus* as a microbial stimulus do not secrete IL-12p70 upon CD40 ligation [138] (Figure 3). This mechanism might also contribute to the tolerogenic effects of *B. vulgatus* in the maintenance of intestinal homeostasis [28, 31]. Upon CD40 ligation, semi-mature DC produced significantly enhanced levels of IL-6 but not TNF-α or IL-12p70 [138]. This is in line with our previous studies showing a crucial role for IL-6 in induction of DC semi-maturation and tolerance [99, 105]. This is interesting as

the secretion of IL-6 upon CD40 ligation by semi-mature DC might help to sustain the semi-mature differentiation state and influence the T-cell activation pattern [138]. We hypothesize that the inability of CD40 ligation in overcoming DC semi-maturation might contribute to the tolerogenic phenotype of semi-mature DC and at least partially account for maintenance of intestinal homeostasis [138].

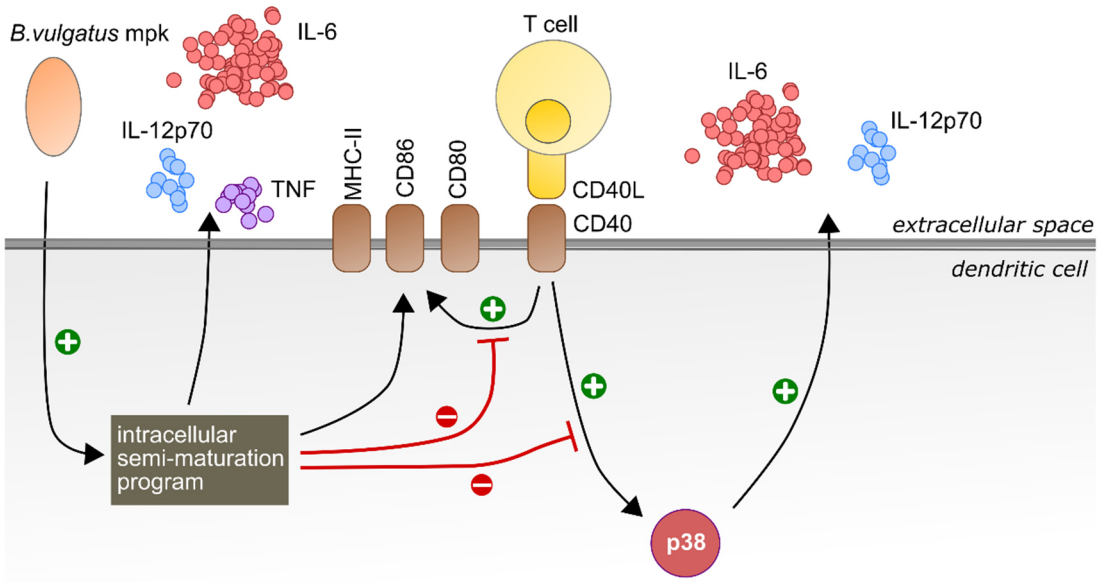

Figure 3: Schematic depiction of intracellular events upon CD40 ligation of semi-mature dendritic cells. *B. vulgatus* mpk stimulation of immature dendritic cells leads to induction of a certain intracellular semi-maturation program resulting in characteristic immunological properties as published [46, 99]. Among other features, semi-mature DCs secrete only low amounts of IL-12p70 and TNF but remarkable amounts of immune response-modulating IL-6. Additionally, *B. vulgatus* mpk stimulation only leads to low to intermediate expression of MHC-II and T cell co-stimulatory molecules, such as CD40. CD40 ligation usually leads to an increase in surface expression of these proteins. However, semi-maturation of dendritic cells prevents from these CD40-ligation induced events. CD40 ligation is also reported to result in intracellular p38 phosphorylation, resulting in enhanced secretion of IL-6 and IL-12p70. p38 phosphorylation upon CD40 ligation is reduced in semi-mature dendritic cells. (+) stands for activation, secretion or expression increase, (-) stands for inhibition.

Hindawi Publishing Corporation
Journal of Immunology Research
Volume 2016, Article ID 1958650, 12 pages
http://dx.doi.org/10.1155/2016/1958650

Hindawi

Review Article

Molecular Mechanisms of Induction of Tolerant and Tolerogenic Intestinal Dendritic Cells in Mice

Alex Steimle and Julia-Stefanie Frick

University of Tübingen, Institute of Medical Microbiology and Hygiene, Elfriede-Aulhorn-Strasse 6, 72076 Tübingen, Germany

Paper 2: Molecular mechanisms of induction of tolerant and tolerogenic intestinal dendritic cells in mice

Review

Alex Steimle and Julia-Stefanie Frick

J Immunol Research (2016) 2016:1958650 [51]

How does the host manage to tolerate its own intestinal microbiota? A simple question leading to complicated answers [51]. In order to maintain balanced immune responses in the intestine, the host immune system must tolerate commensal bacteria in the gut while it has to simultaneously keep the ability to fight pathogens and clear infections [51]. If this tender equilibrium is disturbed, severe chronic inflammatory reactions might result [51]. Tolerogenic intestinal dendritic cells fulfil a crucial role in balancing immune responses and therefore creating homeostatic conditions and preventing from uncontrolled inflammation [51]. Although several dendritic cell subsets have already been characterised to play a pivotal role in this process, less is known about definite molecular mechanisms how intestinal dendritic cells are converted into tolerogenic ones [51]. Different commensal bacteria can have distinct effects on the phenotype of intestinal dendritic cells and these effects are mainly mediated by impacting toll-like receptor signalling in dendritic cells [51].

The gut-associated lymphoid tissue (GALT) is the largest immune organ of the body [51]. The GALT has to ensure that there is a dynamic balance between protective immunity by fighting pathogens and regulatory mechanisms to prevent autoimmunity [51, 167]. Since the GALT is constantly exposed to large amounts of luminal antigens like food metabolites, foreign pathogens and commensal microbes, this balance has to be well adjusted in order to create homeostatic conditions in the

intestine [51]. Dendritic cells are hereby the players for the maintenance of intestinal homeostasis [51, 108]. They are spread out in the connective tissue underlying the epithelial layer of the gut [51, 168].

The capability of initiating an immune response depends on the current DC maturation state [51]. Usually, antigen encounter results in rapid DC maturation which is characterized by efficient endocytosis and antigen processing [51]. Furthermore, upregulation of MHC-II, T cell co-stimulatory molecules like CD40, CD80 and CD86, enhanced expression of chemokine receptors and the secretion of pro-inflammatory cytokines like IL-1β, IL-6, TNF and IL-12 are part of DC maturation [51]. These events influence and activate other cellular components of an induced immune response like macrophages, neutrophils and especially T cells [51, 98]. Induction of DC maturation is accompanied by a loss of the capacity to take up and process antigen [51, 169]. However, they literally develop into professional antigen presenting cells (APCs) which are characterized by powerful antigen presentation to naïve T cells, as well as by their ability to migrate to secondary lymphatic organs where they present antigens to T cells [51]. Immature DCs (iDCs) express low amounts of MHC-II and T cell co-stimulatory molecules [51]. They tend to promote T cell anergy and to generate Tregs, with both effects being crucial for intestinal homeostasis [51, 151]. iDCs furthermore express high levels of PRRs with which they mediate the recognition of potential antigens and therefore their endocytosis [51, 169]. The definition of a semi-mature DC phenotype is less distinct [51]. The most important property of smDCs, uniting different definitions, is the inability to induce a pro-inflammatory Th1 or Th17 response and to be non-responsive, or in other words “tolerant”, towards subsequent maturation stimuli [99, 107] with the latter being the criterium that mediates the tolerogenic functions of smDCs [51, 107]. DC semi-maturation leads to a certain expression of T cell activation and a cytokine secretion pattern that is distinct from the ones of immature and mature DCs [51]. The definite phenotype varies from one semi-maturation inducing strategy to another [51]. SmDCs that are generated by treating immature DCs with TNF display a phenotype that can be summarized as $CD11c^{+}MHCII^{hi}CD86^{hi}CD80^{hi}CD40^{lo}CD54^{+}CD205^{hi}CD25^{hi}TNF^{lo}IL\text{-}12p40^{lo}IL\text{-}10^{lo}$ [51, 100]. Induction of semi-maturation via low-dose LPS and subsequent dexamethasone treatment results in $CD14^{+}CD1a^{lo}CD80^{hi}CD86^{hi}MHCII^{hi}IL\text{-}10^{hi}TNF^{lo}$ DCs [51, 101]. We use a Gram negative gut commensal, *Bacteroides vulgatus*, to induce semi-maturation and define the smDC phenotype as $CD11c^{+}MHCII^{int}CD40^{lo}CD80^{lo}CD86^{lo}TNF^{lo}IL\text{-}12^{lo}IL\text{-}6^{int}$ [51, 99]. Besides these strategies, DC semi-maturation can be induced by treating immature DCs with ATP and LPS [170], low dose *Salmonella* LPS [105], α-1 antitrypsin [106], *Bacteroides fragilis* PSA [102] or *Echinococcus multilocularis* cell aggregates [51, 171].

While mature DCs (mDCs) promote efficient induction of inflammatory immune responses, iDCs and smDCs fail to do so. They rather have the property to actively prevent from inflammatory reactions and are therefore also termed tolerogenic DCs (tolDCs) [51].

More generally, regulatory or tolerogenic DCs keep their ability to present antigens, but at the same time they downregulate the expression of T cell co-stimulatory molecules and pro-inflammatory cytokines, but in turn upregulate inhibitory molecules like PD-L1, CD95L or IDO as well as anti-inflammatory cytokines such as TGF-β and IL-10 [51, 172]. Furthermore, they are resistant to a second maturation-inducing signal [51, 172]. Importantly, DCs also influence the differentiation of naïve T cells into Th1, Th2, Th17 or Treg cells, mostly due to supplying a certain cytokine environment [51, 173]. In a healthy individual, the presence of tolDCs is important and a loss of tolDCs can result in the development of AID [51, 97]. Semi-mature DCs are potent tolerant and tolerogenic DCs since they fulfil many to all of the above mentioned criteria, dependent on the agent with which seminaturation is induced [51]. As already mentioned before, the main characteristic that makes semi-mature DCs tolerogenic is their unresponsiveness (tolerance) towards subsequent maturating stimuli [51, 99, 105, 106].

Less is known about defined mechanisms of tolerance induction in intestinal DCs [51]. However, knowledge about tolerance induction mechanisms of other DC subsets or of *in vitro* generated DCs can be transferred to intestinal DCs to explain how they manage to tolerate luminal bacterial or food antigens and therefore prevent from uncontrolled inflammatory reactions [51]. Here, we want to present latest research results and discuss how and if these findings can be assigned also to intestinal DCs. All proposed mechanisms are summarized in figure 4 [51].

(1) Cell-to-cell-contact and STAT3 signaling

Epithelial cells of the intestine express the surface protein CD47 which can directly interact with signal regulatory protein α (SIRPα) expressed on the surface of DCs which underlie the intestinal epithelial cell layer [51]. This protein-protein-interaction has been shown to result in a janus kinase-2 (JAK-2) dependent signal transducer and activator of transcription 3 (STAT3) activation downstream of SIRPα in DCs [51, 174]. STAT3 activation, in turn, leads to enhanced IL-10 secretion from DCs and therefore promotes tolerogenic properties in the intestinal environment [51, 174]. STAT3 has long been known as a crucial negative regulator of immunity [51]. Disruption of STAT3 leads to a loss of T cell tolerance in mice and efficient STAT3 signaling is associated with the immature DC phenotype, general IL-10 secretion and tolerance induction [51, 175]. Therefore, not only DC alone seem to be important for homeostasis maintenance but also the “teamwork” with neighbouring epithelial cells seems to contribute to tolerance mechanisms [51].

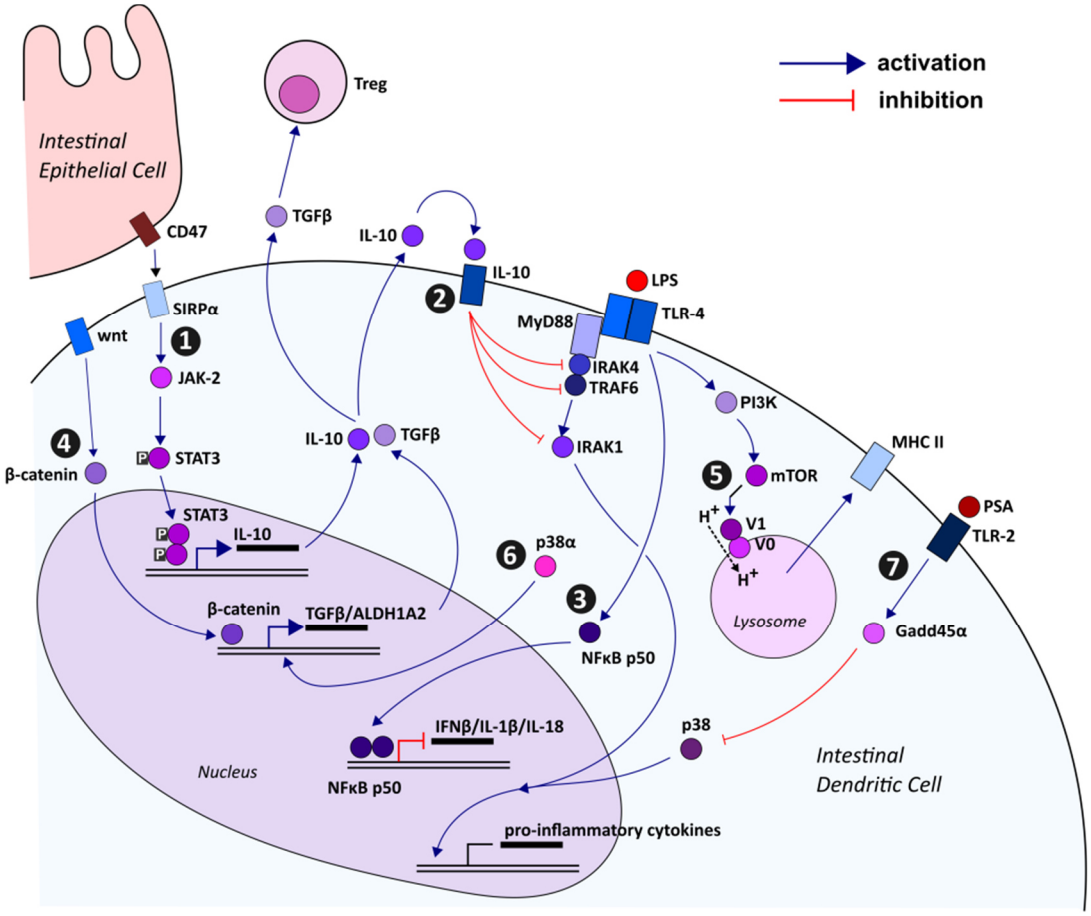

Figure 4: Possible molecular mechnisms of tolerance induction in intestinal dendritic cells.
The white numbers in black circles refer to the numbering of regulation mechanisms in the text. See text for details.

(2) IL-10 as a central cytokine for intestinal homeostasis

Interleukin-10 is a key inhibitory cytokine in T cell activation and a mediator of intestinal homeostasis [51, 176]. It is secreted by T cells, B cells and most myeloid-derived cells [51, 177]. Mice lacking functional IL-10 or its IL-10R receptor counterpart spontaneously develop severe intestinal inflammation supporting the idea of IL-10 being a crucial mediator for intestinal homeostasis [51, 178]. Also humans with defective mutations in the genes encoding for IL-10 or IL-10R develop a severe form of enterocolitis within the first months after birth [51, 179]. These observations made IL-10 a promising therapeutic candidate in order to treat chronic inflammatory conditions of the intestine. However, results were not convincing since in mice as well as in humans, IL-10 administration did not ameliorate the inflammatory conditions [51, 180]. IL-10 does not only affect T

cell responses but can also provide autocrine and paracrine effects on DCs. Since DCs express the IL-10 receptor (IL10R), IL-10 can bind to IL10R resulting in a negative regulation of myeloid differentiation primary response 88 (MyD88) signaling inside DCs. MyD88 is an adaptor molecule of TLRs and is required for downstream TLR signalling. IL-10/IL10R interaction mediates this negative regulation by a downregulation of interleukin 1 receptor associated kinase 4 (IRAK4) on the protein level without altering IRAK4 gene transcription rates [51, 181]. It also leads to dissociation of MyD88 from TLRs and subsequently promotes proteasomal degradation of IRAK1, IRAK4 and TRAF6, therefore silencing MyD88-dependend TLR signalling [51, 181]. However, this is just the case if LPS as a TLR4 ligand is present at the same time to induce TLR signaling. IL-10 silencing of MyD88 signaling seems to be crucial for the maintenance of intestinal homeostasis since *Il10*$^{-/-}$ mice fail to develop intestinal inflammation if these mice simultaneously lack MyD88 [51, 182]. As a consequence, the cytokine environment does also affect DCs in their ability to induce tolerance mechanisms.

(3) NFκB signalling as a mediator for tolerogenicity

A key regulator for DC maturation and inflammatory reactions in general is NFκB [51, 183, 184]. NFκB family members do not only have an activating potential for the induction of pro-inflammatory cytokines. Two NFκB proteins, p50 and p52 have been associated with transcription repression functions and therefore induction of tolerance [51, 185, 186]. Both proteins lack the carboxyterminal transactivation domain and can form inhibitory homodimer complexes that prevent from transcription of pro-inflammatory genes [51]. NFκB p50 has been shown to promote a tolerogenic DC phenotype by negatively affecting DC survival and their capacity to efficiently activate T cells [51, 187]. Accumulation of p50 in the nucleus of tolerogenic DCs can be accompanied by enhanced expression of tolerance-promoting molecules like indoleamine deoxygenases (IDOs) and decreased expression of pro-inflammatory cytokines like IFNβ, IL-1β and IL-18 [51, 187]. These implications for p50 in the induction of tolDCs is supported by the finding that p50-deficient DCs are weak inducers of a Foxp3^{+} Treg differentiation [51, 188]. Formation of p50-p50 homodimers contribute to LPS tolerance in MΦ [189] and p50 expression in immature DCs is crucial to prevent from autoreactive T cells [51, 187].

(4) β-catenin promotes DC tolerogenicity

β-catenin is a transcription factor and part of the wnt signalling pathway. It could be demonstrated that this signalling pathway with the subsequent release of β-catenin into the nucleus results in the induction of tolDCs [51, 190]. Gene expression profiles of intestinal LP DCs revealed that this signalling pathway is decisive for the DC to become either mature or tolerogenic. β-catenin

translocation into the DC nucleus resulted in the expression of various tolerance-associated factors like retinoic acid-metabolizing enzmyes, IL-10 and TGF-β [51, 190].

(5) Prevention of V-ATPase domain assembly induces tolerogenic DCs

Vacuolar (H^+)-ATPases (V-ATPases) are ATP-driven proton pumps. They are composed of two domains: a peripheral V_1 domain and membrane-embedded V_0 domain [51, 191]. V-ATPases are involved in acidification of lysosomes by shuffling protons from the cytosol into the lysosomic lumen [51, 192]. The pH value of lysosomes is a crucial regulator for the efficiency of antigen processing since lysosomal proteases being involved in antigen proteolysis require acidic environments [51, 191]. The most important mechanism to regulate lysosomal acidification is to control the assembly of the two V-ATPase domains which is a required event for forming a functional proton pump [51]. It is known that activation of TLRs promotes domain assembly and therefore supports DC maturation [51, 192]. Domain assembly seems to be a PI-3 kinase and mTOR mediated event since inhibitory substances for both molecules could block V-ATPase domain assembly and therefore prevent from DC maturation and promote the induction of a tolerogenic phenotype [51, 191]. Also, stimulation of integrins and E-cadherins by cluster disruption of DC prevents from domain assembly and supports induction of a tolerogenic phenotype [51, 192, 193].

(6) p38α expression influences expression of ALDH1A2

MAP kinases like ERK, JNK and p38α form central pathways that are activated by innate immune signals like PAMPs [194, 195] and excessive activation of MAP kinases are reported to be associated with many autoimmune and inflammatory diseases [51, 195]. However, the MAP kinase p38α provides a dichotomic role. Besides being involved in promoting pro-inflammatory responses its activity also seems to be crucial for the induction of a tolerogenic phenotype in intestinal $CD103^+$ DCs [51]. In these DCs, p38α is constitutively active and this activity is crucial for the expression of TGF-β and aldehyde dehydrogenase 1A2 (ALDH1A2), the latter being involved in metabolizing retinoic acid (RA) [51]. TGF-β and RA are involved in Treg generation and therefore promote gut homing properties of T cells [51, 195].

(7) Gadd45α-mediated TLR2 signalling contributes to tolerogenic features of intestinal DCs

An abundant bacterial gut commensal, *B. fragilis*, is able to protect from the induction of EAE and experimental colitis and increases the proportions of $CD103^+CD11c^+$ DCs [51, 196, 197]. It could be demonstrated that this effect is mediated by polysaccharide A (PSA), an immunomodulatory component present in outer membrane vesicles derived from *B. fragilis* bacteria [51, 102]. PSA promotes immunological tolerance by inducing IL-10 producing $Foxp3^+$ Tregs and protect animals from experimental colitis [51, 198]. The PSA caused induction of tolDCs is dependent on TLR2 and

growth arrest and DNA-damage-inducible 45 α (Gadd45α), since Gadd45α-deficient DCs are unable to mediate PSA-induced protection of experimental colitis [51, 102]. Gadd45α itself inhibits an alternative way of MAPK p38-mediated signalling [199] and PSA-containing outer membrane vesicles lead to an upregulation of Gadd45α [51, 102].

In order to be suitable as an administrable therapeutic, tolerogenic DCs (tolDCs) have to be generated *in vitro* [51]. One efficient way to induce tolDCs is co-incubating them with apoptotic cells [51]. Phagocytosis of apoptotic cells through DCs results in production of TGF-β which in turn contributes to immune tolerance [51]. Apoptotic cell-treated DCs efficiently converted naïve $CD4^+$ T cells into $Foxp3^+$ Tregs. [51, 200, 201]. In general, apoptotic cell induced tolDCs are important for induction of immune tolerance [51, 202, 203]. They provide upregulation of Galectin-1 and CD205 [204], two molecules that facilitate the manifestation of immune tolerance [51, 205, 206]. At the same time, apoptotic cell treated DCs downregulate Gr-1 and B-220 [204], two molecules triggering inflammatory responses [51]. These DCs furthermore downregulate the transcription factor RORγt which is the decisive transcription factor for Th17 differentiation [51]. Not only treatment with apoptotic cells leads to induction of tolDCs but also treatment with herbal coumarins [207] and the macrocyclic antibiotic rapamycin [208] lead to tolDC induction [51]. *In vitro* generated tolDCs have already been successfully used for the treatment of autoimmune disorders in animal models and peripheral tolerance could be restored by administrating tolerogenic DCs [51, 209]. Approaches to treat autoimmune type 1 diabetes in a mouse model using non-obese diabetic (NOD) mice with tolerogenic DCs were very successful [51, 204]. To do so, apoptotic islet cells were used to induce DC mediated tolerance against own islet cells [51, 210]. All these applications lead to the question, if transfer of tolerogenic dendritic cells would also be an approach to treat IBD. And if yes, which method to induce DC tolerance would be the method of choice [51]. A published approach for the treatment of Crohn's Disease patients is *in vitro* generation of DCs followed by pulsing with dexamethasone, pro-inflammatory cytokines IL-6, IL-1β and TNFα as well as PGE_2 [51, 211]. Concerning our findings that a certain gut commensal, *B. vulgatus* mpk, efficiently induces tolerant and tolerogenic DCs *in vitro* as well as *in vivo* [28, 31, 99], we would recommend to use host gut commensal bacteria for *in vitro* tolDC generation [51]. In order to provide more potential luminal antigens presented by MHC-II of tolDCs a defined mixture of commensal bacteria could be used [51]. This would enlarge the amount of antigenic peptides against which tolerance would be induced [51].

A novel approach for reliable detection of cathepsin S activities in mouse antigen presenting cells

Alex Steimle [a], Hubert Kalbacher [b], Andreas Maurer [c], Brigitte Beifuss [a], Annika Bender [a], Andrea Schäfer [a], Ricarda Müller [a], Ingo B. Autenrieth [a], Julia-Stefanie Frick [a,*]

[a] Institute of Medical Microbiology and Hygiene, University of Tübingen, Germany
[b] Interfacultary Institute of Biochemistry, University of Tübingen, Germany
[c] Institute of Radiology, University of Tübingen, Germany

Paper 3: A novel approach for reliable detection of cathepsin S activities in mouse antigen presenting cells

Research Paper

Alex Steimle, Hubert Kalbacher, Andreas Maurer, Brigitte Beifuss, Annika Bender, Andrea Schäfer, Ricarda Müller, Ingo B. Autenrieth and Julia-Stefanie Frick

J Immunol Method (2016) 432: 87-94 [212]

In enzyme-related research, detecting activities of the enzyme-of-interest is of special importance. Concerning cathepsins, activity detection of one specific cathepsin causes difficulties in experimental procedures since cathepsins in general provide a broad and overall very similar substrate specificity towards endogenous and exogenous substrates [212, 213]. This physiologically valuable property makes cathepsins poor targets for specific activity detection in experimental settings [212]. We were especially interested in the reliable detection of cathepsin S activities in mouse-derived antigen presenting cells. Several different methods have already been described in the literature (reviewed in [120]). However, most of these methods have only been shown to be suitable for human samples, do not deliver quantitative results or the experimental procedure requires technical equipment that is not commonly available in a standard laboratory [212]. Therefore it was necessary to establish a novel method for a reliable detection of mouse cathepsin S activities which fits into our experimental scheme. The method we established is based on a fluorogen substrate that has previously been described to be exclusively cleaved by human CTSS [214]. However we could demonstrate that this substrate is also suitable for detection of mouse-derived samples by using a novel protocol [212].

This method is cheap, specific, reliable and easy to perform in a standard laboratory without the requirement of special technical equipment, besides the requisition of a fluorescence compatible photometer [212].

The substrate we intended to use for CTSS activity detection was Mca-GRWPPMGLPWE-Lys(Dnp)-DArg-NH2 (PMGLP) [214]. In a first step, we checked for PMGLP cleaving specificity using various recombinant murine cathepsins. We could demonstrate that PMGLP was cleaved by recombinant murine CTSS as efficiently as by recombinant human CTSS. However, we could also detect slight PMGLP turnover caused by recombinant murine cathepsin L (CTSL) at pH 5.0, yet not at pH 7.5. Since we could not detect any loss of CTSS activity at pH 7.5 we decided to perform all prospective activity assays at this pH in order to prevent from potential PMGLP cleavage caused by CTSL [212].

In a second step, we used complex protein solutions by lysing bone-marrow derived dendritic cells (BMDCs) and checked for PMGLP turnover rates caused by components of these lysates. We tested several lysing methods and buffer systems and discovered hypotonic lysis avoiding addition of detergents as the most effective lysing method. Furthermore, detection of PMGLP hydrolysis was best using a phosphate buffer system at pH 7.5. In order to elucidate the contribution of CTSS to PMGLP turnover in cell lysates, we compared lysates of BMDCs generated from wt mice to lysates derived from BMDCs of *Ctss*$^{-/-}$ mice. Thereby, we could demonstrate that PMGLP is cleaved by murine CTSS in cell lysates and no other cathepsin contributes to PMGLP turnover. However, a yet unidentified cellular component causes PMGLP hydrolysis. Nevertheless this “background” hydrolysis occuring in every mouse cell-derived lysate, is not dependent on any DC maturation inducing stimuli and remains relatively constant. We therefore define the difference between overall PMGLP hydrolysis and background PMGLP hydrolysis as specific CTSS activity in mouse cell-derived samples and CTSS activity was proven to be higher in mature BMDCs compared to CTSS activity in immature DCs [212]. In summary, we recommend the following workflow using PMGLP as a fluorogen substrate for the detection of cathepsin S activities from mouse derived cells (Fig. 5) [212]. Cells are harvested as carefully as possible followed by hypotonic lysis as described in the methods and materials section [212]. In order to compare cathepsin S activities in different samples, equal protein amounts should be used in all tested samples [212]. Each sample is then devided into two: one sample is pre-incubated with cathepsin inhibitor E-64, whereas the other one is not [212]. PMGLP is added into both samples followed by measuring fluorescence intensity increase as a function of time [212]. PMGLP turnover

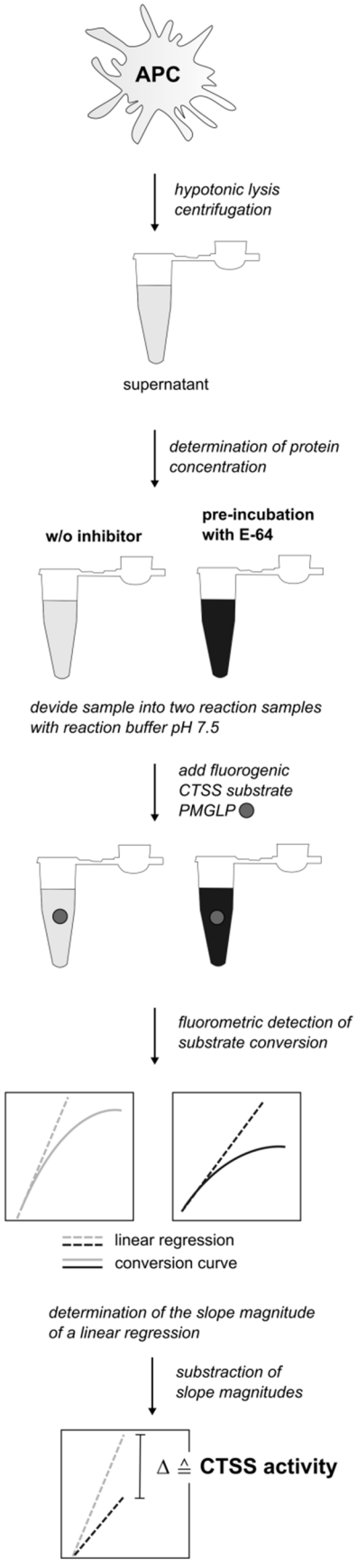

Figure 5: Experimental workflow for the detection of CTSS activities in mouse APC. Cells of interest are lysed hypotonically followed by blast freezing in liquid nitrogen as described in materials and methods section. Supernatant is used for CTSS activity detection. Out of each sample, two reaction samples containing the same amount of whole cell protein are created. The first sample contains the fluorogen substrate, the second both, the substrate and the cathepsin inhibitor E-64. Reaction buffer provides a pH of 7.5 to minimize false positive substrate conversion caused by other cathepsins. Substrate conversion is monitored for 60 min at 37 °C. A linear regression at the very beginning of the sigmoidal conversion curve is performed for both reaction samples. The slope magnitude of this linear regression is equivalent to the substrate conversion per time unit. The difference in the slope magnitude of both reaction samples is equivalent to the CTSS activity in the sample the lysate was taken from. CTSS activities can therefore be expressed as the difference of fluorescence intensity per µg cell protein and time unit, i.e. $\Delta AU\ min^{-1}\mu g^{-1}$. Taken from Steimle *et al.* (2016) [212]

rates are computed as described [212]. The mathematical difference between the PMGLP turnover rates in the E-64 pre-incubated sample and the non-inhibited sample is directly equivalent to the activity of mouse cathepsin S [212]. We want to underline that it is crucial for a successful CTSS activity detection to keep the samples on ice throughout the entire experiment [212]. Unfortunately, after blast freezing in liquid nitrogen, samples cannot be frozen again for longtime storage since this leads to a dramatic loss of enzymaticv activity. Additionally, long time storage in liquid nitrogen, starting directly after adding deionized water for the hypotonic lysis, also leads to a remarkable, yet not complete, reduction of enzymatic activity [212]. Hence, the whole experimental setup should be performed in

one go in order to obtain the best possible results [212]. In contrast to the cleavage behavior in human APC [214], mouse bone marrow derived dendritic cells provide a certain background cleavage of this substrate that is not caused by CTSS or any other protease that can be inhibited by E-64 or the Roche Complete Protease Inhibitor [212]. We still do not know what the cause for this background hydrolysis of PMGLP is [212]. We could demonstrate that this background hydrolysis is not abolished through addition of any tested protease inhibitor. Furthermore, crude cell lysates and spontaneous substrate hydrolysis do not contribute to this effect. However, our recommended workflow (Fig. 5) offers a possibility to detect specific mouse CTSS activities besides background substrate hydrolysis [212]. After hypotonic lysis of the cells, we recommend to create two different reaction samples out of one sample of interest [212]. The first sample contains the substrate, the second both, the substrate and E-64, an inhibitor against all cysteine cathepsins to detect the background activity [212]. CTSS activity is therefore equivalent to the difference in PMGLP conversion between the reaction sample containing no inhibitor and the sample containing E-64 [212].

Since CTSS is exclusively expressed in professional antigen presenting cells, we recommend using cell populations which are as homogenous as possible for CTSS activity detection [212]. Otherwise the cell amount of CTSS expressing cells can fall below a critical level for reliable CTSS activity detection [212].

In summary, we have shown (I) that a specific CTSS inhibitor is not necessary for the detection of background activity, therefore the easily commercially available E-64 can be used and (II) that the background activity is not different between differentially stimulated APC [212]. Therefore, this PMGLP assisted CTSS activity assay is also useable for high-throughput experiments within a short period of time and we think that this experimental assay contributes to simplify CTSS related research [212].

Steimle A and Frick JS, J Neurol Neuromed (2016) 1(3): 6-12
www.jneurology.com

Journal of Neurology & Neuromedicine

Mini Review Open Access

The challenge of specific Cathepsin S activity detection in experimental settings

Alex Steimle and Julia-Stefanie Frick*

Institute of Medical Microbiology and Hygiene, University of Tuebingen, Tübingen, Germany

Paper 4: The challenge of specific Cathepsin S activity detection in experimental settings

Mini Review

Alex Steimle and Julia-Stefanie Frick

J Neurol Neuromed (2016) 1(3): 6-12 [120]

As mentioned above, cathepsins in general provide a broad and overall similar substrate specifity [213]. This makes CTSS activity detection a challenge, *in vitro*, *ex vivo* and especially *in vivo*. But how can an experimentator achieve the goal to reliably detect CTSS activity in the biological system of choice? [120] There are several possibilities how CTSS activity can be detected, all of them with their characteristic advantages and limitations [120]. A suitable CTSS activity detection method should match the following four criteria: (i) high specifity, (ii) high sensitivity since CTSS expression is restricted to APCs, (iii) the experimental workflow should be able to be performed in a more or less standard laboratory without the requirement of highly special technical equipment and (iv) the method should deliver reproducible and quantifiable results [120]. We summarize some currently available techniques for CTSS activity detection with their characteristic pros and cons in table 1.

Popular approaches for CTSS activity detection include activity based probes (ABPs) [120]. These are small reporters of proteolytic activity which bind covalently and irreversibly to the active site of the target enzymes [215] leading to a loss of enzymatic activity [120]. This irreversible CTSS inhibition should be kept in mind if *in vivo* monitoring shall be performed [120]. ABPs usually consist of three distinct functionalities (Fig. 6): (1) The so-called warhead functionality leads the probe to enzymes sharing a common catalytic mechanism, (2) the recognition element that enhances specificity for one or more specific enzymes and (3) a tag for a later detection of the tagged enzymes [120]. Such ABPs are available for the

Table 1: Summary of various CTSS activity detection techniques. The techniques are grouped into the major functional classes. Taken from Steimle *et al.* (2016) [120]

Application category	Characteristic	Example	target	Year published	Quantification method	Limitation	Outstanding advantage
Activity based probe (ABPs)	covalent binding to CTSS active site leading to enzyme inhibition	GB123 [216]	Human CTSS and CTSB	2015	Fluorescent label	Binds also to CTSB. Gel-assisted enzyme separation or IP needed	Non invasive in vivo imaging possible
		Probe 7 [217]	Human CTSS	2015	Fluorescent label	Not cell permeable	Specificity for CTSS
		Z-PraVG-DMG [218]	Human CTSS, CTSB and CTSL	2016	Rhodamine azide labelling	Similar K_i values for CTSS, CTSB and CTSL	Cell-permeability of the substrate
		CM-279 [219]	Human CTSS and CTSL	2013	Luciferase assisted light detection	Also labels CTSL	Reliable detection of combined CTSS and CTSL activity
		BMV157 [220]	Mouse CTSS	2015	Fluorescent label	aviailability	Highly specific, in vivo and in vitro application possible
		BIL-DMK [221]	Human CTSS	2011	Radioactive label	Radioactivity	Specificity for CTSS
		Probe 10 [222]	Human CTSS, CTSL, CTSB and CTSK	2014	Fluorescent label	Not specific for CTSS	Suitable for complex protein mixtures
		Biot-$(PEG)_2$-Ahx-LeuValGly-DMK [223]	Human CTSS, CTSL, CTSB and CTSL	2015	SDS Page assisted chemi-luminescence	Not specific for CTSS	Easy to perform
Substrate based probes (SBP)	Substrate turnover; enzyme is not inhibited and remains proteolytically active	PMGLP	Human CTSS [214] and mouse CTSS [212]	2016	Fluorescence increase	Requires cell lysis and inhibition control	Simple enzymatic assay, easy-to-perform, time saving.
		Ac-KQKLR-AMC	Mouse CTSS	2014	Fluorescence increase	Requires cell lysis and inhibition control	Simple enzymatic assay
		NB200 [224]	Mouse CTSS, CTSK and CTSB	2015	Fluorescence increase	Detects also CTSK at pH7.5 and CTSB at pH 5.5	Simple enzymatic assay
		Z-FR-AMC	Mouse CTSS, CTSB and CTSL	2002	Fluorescence increase	Unspecificity, requires extensive experimental setting	Simple enzymatic assay
Indirect detection methods	Does not directly interact with CTSS	Detection of CTSS substrate accumulation by western blotting [135]	Mouse invariant chain p10 detection	2015	Western blot band intensity of Iip10	Does not detect CTSS activity directly	Simple to perform
		Western blotting of 24 kDa CTSS [225]	Human CTSS	2014	Western blot band intensity of 24 kDa CTSS	Does not consider potential binding of endogenous inhibitors and does not refer to activity	Simple to perform

detection of human and mouse CTSS [120]. General disadvantages of such ABPs include a lack of specificity for CTSS for some of these ABPs since other cathepsins with similar substrate specifity might deliver false positive detection [120]. This has then to be compensated by further time-consuming experimental approaches like western blotting, immunoprecipitations etc [120]. Additionally, CTSS activity can often only be determined in a semi-quantitative manner like detection of band intensities on a gel or a detection of overall fluorescence intensity [120]. However, the potential labelling of proteolytically active CTSS in live cells due to cell permeability is a big advantage of some ABPs [120]. Veilleux *et al.* developed a radioiodinated ABPs to selectively label active CTSS in human whole blood [120, 221]. Ben-Aderet *et al.* [216] and Oresic Bender *et al.* [220] used fluorogenic ABPs to monitor enzymatically active CTSS in human cells or live mice, respectively [120]. Other examples of recent ABPs development for CTSS activity detection include the publications of Barlow *et al.* [224], Hughes *et al.* [218], Mertens *et al.* [222] and Garenne *et al*. [223], [120]. However, some of them provide a lack of specificity for CTSS and also label other cathepsins [216, 218, 219, 222, 223] while other ABPs selectively label human or mouse CTSS [217, 220, 221], [120]. Another general disadvantage of ABPs include the requirement of more specialized detection techniques that a non-specialized lab could tentatively not afford [120].

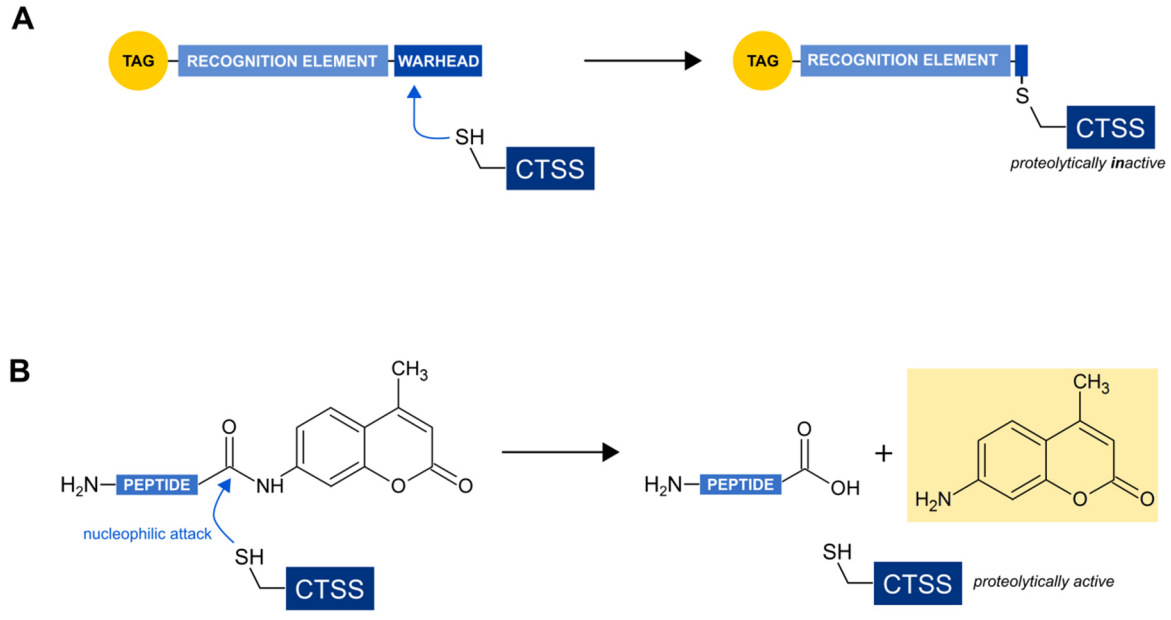

Figure 6: Functional comparison of the two major classes of probes for direct CTSS activity detection

(A) activity based probes (ABPs): The so-called warhead covalently links the probe with CTSS, leading to the inhibition of its enzymatic activity. The recognition elements supports the specificity for CTSS alone or some related cysteine cathepsins. The tag allows for later detection of the tagged enzymes.

(B) substrate based probes (SBPs): The thiol group at the active site of CTSS nucleophilically attacks the peptide bond of the peptidyl substrate leading to a deliberation of the aminomethylcoumarin. The resulting change in the fluorogenic behaviour of free aminomethylcoumarin can then be detected in a fluorescent compatible photometer. Taken from Steimle *et al.* (2016) [120]

Other approaches include an indirect method to determine CTSS proteolytic (table 1) activity by not directly assessing the enzymatic activity but rather determining the intracellular amount of the MHC II-bound invariant chain fragment (Iip10), which is a substrate for CTSS [120]. Therefore, decreased amounts of Iip10 is stated to correlate with enhanced CTSS activity [226], [120]. Since CTSS is translated into an inactive pro-enzyme requiring proteolytical cleaving which results in a 24 kDa active enzyme, some publications refer to the band intensities of this 24 kDa band when making statements on CTSS activity [225], [120]. However this does not take the potential binding of endogenous inhibitors into account [120].

Another possibility for direct CTSS activity determination is to use substrate-based probes (SBP) like i.e. fluorochrome-coupled peptidyl substrates (Figure 6) [120]. Prominent examples are Z-VVR-AMC [127] , Z-FR-AMC [217, 227] or Ac-KQKLR-AMC [228, 229], [120] . All of them share the aminomethyl coumarin group. Coumarins are popular fluorescent labels due to their large stoke's shifts [230] and their small size allowing for incorporation into small peptides [222], [120]. These peptidyl substrates generally provide the disadvantage to be usable only in cell lysates and not in living cells or organisms [120]. The major potential problem with these peptidyl substrates is the unsatisfactory specificity for CTSS [120]. Due to the already mentioned similar substrate specificity among cysteine cathepsins, other cathepsins than CTSS can deliver false positive results due to unspecific cleavage of the substrate [120].

We could recently report on an alternative method for reliable CTSS activity detection using the peptide-derived substrate-based probe Mca-GRWPPMGLPWE-Lys(Dnp)-DArg-NH_2 (PMGLP) [212], [120]. PMGLP was shown to be cleaved specifically by murine CTSS at a pH of 7.5 with no other murine cathepsin contributing to substrate cleaving in cell lysates [212], [120]. The obtained results were easily quantifiable and highly reproducible as demonstrated in mouse bone marrow derived dendritic cells that were differentiated from the bone marrow of different individuals [120]. The presented method therefore delivers specific CTSS activities and only requires a phosphate buffer system and a fluorescence compatible heatable photometer making the application attractive for less specialized laboratories [120].

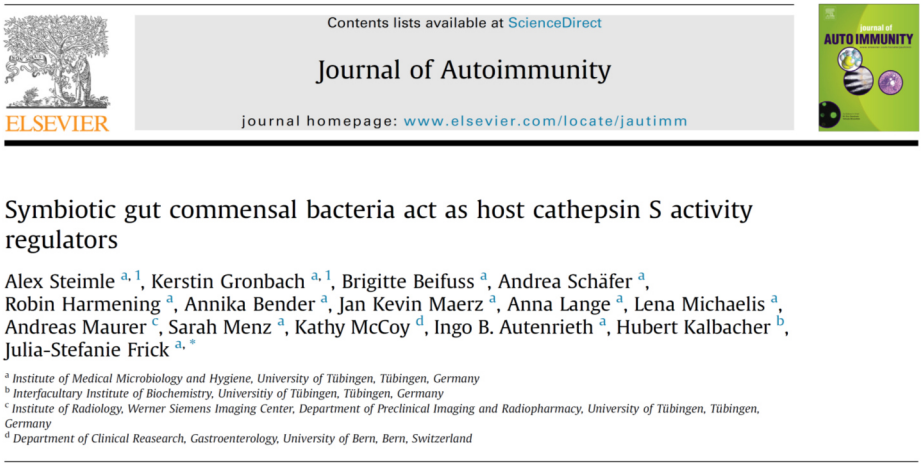

Contents lists available at ScienceDirect

Journal of Autoimmunity

journal homepage: www.elsevier.com/locate/jautimm

Symbiotic gut commensal bacteria act as host cathepsin S activity regulators

Alex Steimle [a, 1], Kerstin Gronbach [a, 1], Brigitte Beifuss [a], Andrea Schäfer [a], Robin Harmening [a], Annika Bender [a], Jan Kevin Maerz [a], Anna Lange [a], Lena Michaelis [a], Andreas Maurer [c], Sarah Menz [a], Kathy McCoy [d], Ingo B. Autenrieth [a], Hubert Kalbacher [b], Julia-Stefanie Frick [a, *]

[a] Institute of Medical Microbiology and Hygiene, University of Tübingen, Tübingen, Germany
[b] Interfacultary Institute of Biochemistry, Universitiy of Tübingen, Tübingen, Germany
[c] Institute of Radiology, Werner Siemens Imaging Center, Department of Preclinical Imaging and Radiopharmacy, University of Tübingen, Tübingen, Germany
[d] Department of Clinical Reasearch, Gastroenterology, University of Bern, Bern, Switzerland

Paper 5: Symbiotic gut commensal bacteria act as host cathepsin S activity regulators

Research paper

Alex Steimle, Kerstin Gronbach, Brigitte Beifuss, Andrea Schäfer, Robin Harmening, Annika Bender, Jan Maerz, Anna Lange, Lena Michaelis, Andreas Maurer, Sarah Menz, Kathy McCoy, Ingo B. Autenrieth, Hubert Kalbacher and Julia-Stefanie Frick

J Autoimmun (2016) xxx:1-14 (Epub, ahead of print) [46]

Cathepsin S (CTSS) is a lysosomal protease whose activity regulation is important for MHC-II signaling and subsequent activation of $CD4^+$ T cell mediated immune responses [46]. Dysregulation of its enzymatic activity or enhanced secretion into extracellular environments is associated with the induction or progression of several autoimmune diseases [46]. Here we demonstrate that commensal intestinal bacteria influence secretion rates and activity of CTSS and that symbiotic bacteria, i.e. *Bacteroides vulgatus* mpk, may actively regulate this process and help to maintain physiological levels of CTSS activities in order to prevent from induction of inflammation [46]. Dysregulation of CTSS activity, expression or secretion into the extracellular space is associated with the pathogenesis of various autoimmune diseases (AID) making CTSS a popular drug target for the treatment of these diseases [46]. Eventually, we demonstrate that an alteration of the gut microbiota composition can contribute to host CTSS regulation and that the microbiota composition itself could be decisive to control host CTSS secretion and activity, hence treatment with chemical drugs might not be necessary [46]. As most autoimmune diseases are associated with dysbiosis of the intestinal microbiota [46, 231], we compared effects of symbiotic or pathobiotic commensals on host CTSS activities and protein levels *in vivo* and *in vitro*. *B. vulgatus* mpk could already be demonstrated to be

a symbiotic bacteria, mediating anti-inflammatory effects [28, 31, 99] which are directly associated with the induction of a tolerant DC phenotype termed semi-mature [28, 31, 46, 110].

It is known that apathogenic commensal bacteria can have either symbiotic or pathobiotic properties concerning the activation of the immune system [46]. In previous work, we identified symbiotic *B. vulgatus* mpk which protects *Il2*$^{-/-}$ mice from induction of colitis, hence promoting the immunological equilibrium, whereas pathobiont *E. coli* mpk promotes induction of colitis, thus featuring pathobiotic effects [28, 31, 46]. Likewise, in IBD patients, *Bacteroidetes* proportions in the intestine are decreased while *Enterobacteriaceae* proportions are enhanced [46, 232, 233]. Therefore, we consider *B. vulgatus* mpk and *E. coli* mpk to represent adequate symbiotic and pathobiotic model organisms, respectively [46]. Thus, we wanted to elucidate the distinct T cell activation potential of these two model organisms [46]. We could demonstrate that monocolonization of T cell transplanted *Rag1*$^{-/-}$ mice with symbiotic *B. vulgatus* mpk induces tolerant semi-mature colonic lamina propria (cLP) DCs and does not promote T cell proliferation whereas monocolonization with of T cell transplanted *Rag1*$^{-/-}$ mice pathobiotic *E. coli* mpk induces DC maturation and clearly promotes proliferation of transplanted T cells [46]. Since the semi-mature phenotype of cLP DCs, especially the MHC-II surface expression, plays a pivotal role for the observed prevention of T cell activation in *B. vulgatus* mpk monocolonized and *B. vulgatus* mpk and *E. coli* mpk cocolonized gnotobiotic mice, we had a closer look on the molecular mechanisms of semi-maturation in vitro [46]. We could demonstrate the significance of CTSS activity control for the induction of tolerant semi-mature DCs since complete DC maturation could not be induced in *Ctss*-deficient BMDCs [46]. Thus, we demonstrate that *B. vulgatus* mpk stimulated, semi-mature DC also provide non-responsiveness in terms of CTSS activity which therefore seems to be part of the tolerant semi-mature DC phenotype [46]. Since we detected different CTSS activities in BMDCs that were stimulated with either *B. vulgatus* mpk or *E. coli* mpk finally resulting in different MHC-II surface expression and T cell activation the question of the regulation mechanism arised [46]. It is known that upon increase of intracellular ROS amounts, cystatin C monomers preferentially form protein homodimers leading to a loss of the inhibitory potential [46, 234]. We could demonstrate that *B. vulgatus* mpk stimulation of BMDCs does not induce ROS production [46]. This would, in turn, promote maintenance of cystatin C monomers that are able to bind to CTSS, therefore inhibiting CTSS proteolytic activity [46]. *E. coli* mpk stimulation, however, leads to significantly higher intracellular ROS amounts compared to *B. vulgatus* mpk stimulated cells. *E. coli* mpk induced higher ROS levels would favor homodimerisation of cystatin C which would subsequently lead to a loss of CTSS inhibition, resulting in CTSS activity increase [46]. Therefore we conclude that lower intracellular ROS amounts are, at least in part, responsible for CTSS activity control in semi-mature DC. Furthermore, application of *B. vulgatus* mpk protects T cell transplanted *Rag1*$^{-/-}$ mice from induction of $CD4^+$ T cell driven transfer colitis and *B.*

vulgatus mpk dependent prevention of colitis is associated with prevention of CTSS secretion into serum [46]. Additionally, feeding symbiont *B. vulgatus* to T cell transplanted *Rag1*$^{-/-}$ mice is equally effective in prevention of colitis induction and intestinal inflammation as administration of a chemical CTSS inhibitor, since both therapeutic approaches led to significant less inflammation in this mouse model for experimental colitis [46]. In summary, we demonstrate that regulation of cathepsin S (CTSS) activity importantly contributes to the maintenance of the intestinal immune equilibrium [46]. CTSS activity can be regulated by the intestinal microbiota with symbionts triggering physiological CTSS activity and pathobionts inducing pathological CTSS activity increase, the latter resulting in T cell activation and proliferation which, in turn, supports pro-inflammatory host immune responses [46]. The microbiota dependent regulation of CTSS activity is mediated by the induction of reactive oxygen species (ROS) [46]. Pathobionts, but not symbionts, induced high intracellular ROS levels in DCs, allowing for homodimerization of cystatin C (CysC) and resulting in an abrogation of the CysC- mediated inhibition of CTSS activity.This promotes intestinal inflammatory host responses, in

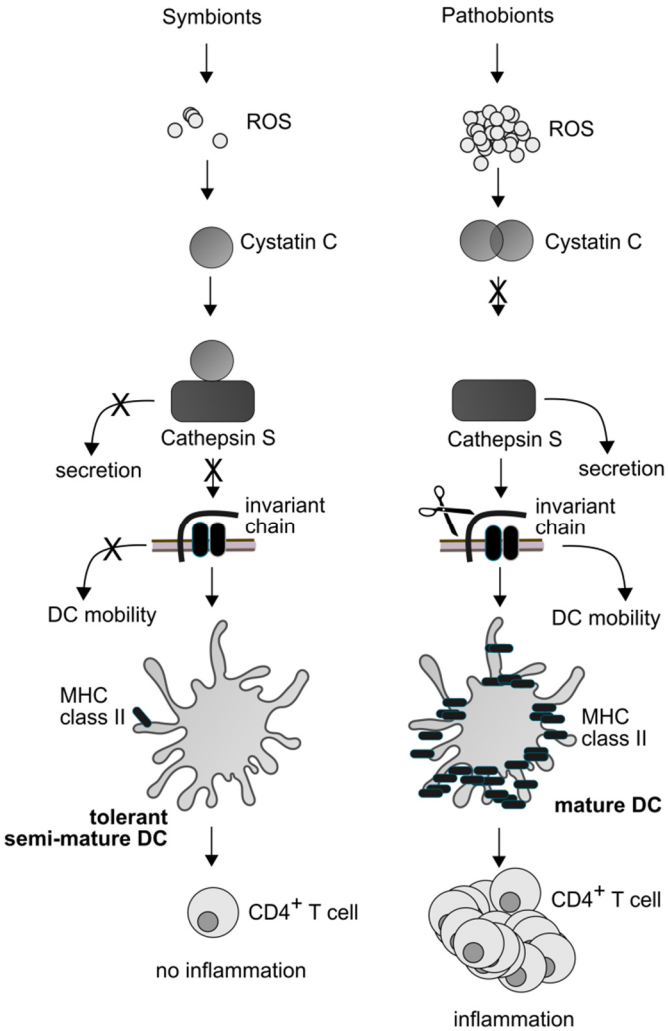

Figure 7: Postulated mechanism how commensal symbiont *Bacteroides vulgatus* mpk prevents from inflammation induction via cathepsin S activity regulation. Left panel: *B. vulgatus* mpk is suspected to promote only a weak immunological signal resulting in low amounts of reactive oxygen species (ROS). These low ROS amounts favour cystatin C monomers which can therefore efficiently bind to cathepsin S (CTSS) and thus cause inhibition of CTSS proteolytic activity. This results in less efficient cleaving of the invariant chain (Ii) and therefore in lower amounts of surface MHC-II and reduced DC mobility. Additionally, CTSS secretion into the extracellular space is omitted. These events lead to the conversion of immature DC into tolerant semi-mature DC that fail to induce a $CD4^+$ T cell mediated immune response and therefore protect from inflammatory reactions. Right panel: In contrast to symbiont commensals, pathobionts like *E. coli* mpk induce intracellular ROS formation promoting homodimerization of Cystatin C leading to a loss of its inhibitory capacity towards CTSS. This leads to enhanced invariant chain cleaving, high MHC-II expression, increased DC mobility and high CTSS secretion. These events characterize a mature DC which are finally capable to induce a $CD4^+$ T cell mediated immune response. Taken from Steimle *et al.*, 2016 [46]

our mouse model resulting in induction of colitis [46]. The symbiont induced low intracellular ROS levels lead to a preservation of CysC monomers, mediating inhibition of CTSS via direct protein-protein-interactions, which therefore results in physiological CTSS activity levels and maintenance of intestinal homeostasis [46].

Pathogenesis of most autoimmune diseases (AID), and of IBD in particular, is associated with an induction of a $CD4^+$ T cell mediated immune responses, highlighting the importance of the MHC-II mediated antigen presenting pathway for the onset of AID [46]. Therefore a strict regulation of the CTSS activity is important to retain a balanced immune system homeostasis [46]. CTSS exerts its physiological functions intracellularly [46]. However, secretion can occur since CTSS is part of the lysosomal compartment [46]. This might cause additional pathophysiological processes in the extracellular space [46]. Upon secretion, cathepsins end in extracellular environments whose pH values strongly affect their proteolytical activity [46]. Among all cathepsins, CTSS is the only enzyme with significant activity within a broader pH range since it is also capable of catalysing peptide bond cleavage at neutral pH [46, 235]. All other cathepsins provide their maximum activity at acidic pH values [46, 236]. Since in extracellular environments a neutral pH is dominant, CTSS is not automatically inactivated like other cathepsins [46]. Extracellular or, in other words, secreted CTSS is involved in the pathology of a variety of autoimmune diseases [46]. For example, increased CTSS levels in the serum or cerebrospinal fluid can be found in multiple sclerosis patients [46, 125]. In the mouse model of experimental autoimmune encephalomyelitis (EAE), resembling the multiple sclerosis phenotype in humans, increased CTSS levels could be detected [46, 237]. Its extracellular pathological function might be proteolysis of the myelin basic protein which could be observed *in vitro* [46, 238]. In Sjögren's syndrome patients, enhanced CTSS activity could be detected in tear fluid [46, 131], therefore making CTSS activity in tears an appropriate biomarker for the diagnosis of this disease [132]. Especially the atheriosclerosis phenotype is affected by extracellular CTSS. Secreted CTSS cleaves proteins of the extracellular matrix (ECM) like laminin, collagen or elastin [46, 239]. Resulting elastin peptides are able to incite inflammation and stimulate macrophage chemotaxis [46, 240]. Concerning inflammatory bowel disease, general ECM degradation therefore could promote epithelial damage or relieve bacterial contact to APC leading to accelerated T cell responses and IBD promotion [46]. CTSS secretion into the colonic lumen might cause damage of the epithelial barrier leading to intensified colitis symptoms as enhanced encounter of gut bacteria with immune cells on the basolateral side of the epithelium would be possible [46]. We could now demonstrate in a mouse model for T cell mediated colitis, using *Rag1*$^{-/-}$ mice, that feeding symbiotic *B. vulgatus* mpk via drinking water protects mice from colitis induction and we provide evidence that this is due to a strict regulation of CTSS activity and a prevention of secretion from DCs into extracellular environments [46]. There is a clear correlation between the CTSS concentration in blood serum and

severity of colonic damage and we could demonstrate that administration of a chemical CTSS inhibitor prevents from colitis induction in a $CD4^+$ T cell mediated mouse model for experiment colitis using *Rag1*$^{-/-}$ mice [46]. We could confirm this observation *in vitro* by detecting low CTSS secretion rates in *B. vulgatus* mpk stimulated bone marrow derived dendritic cells (BMDCs) [46]. It has already been shown that CTSS secretion promotes pain induction during colitis via cleaving of the PAR-2 receptor [46, 136]. However, our data support the idea that CTSS activity dysregulation and enhanced secretion is the decisive trigger for colitis induction [46].

Intracellular CTSS activity also requires precise regulation. CTSS is the main protease in DCs that is responsible for cleaving the MHC-II associated chaperone invariant chain (Ii) [46]. This cleaving event is the major regulation step for loading antigen-derived peptides onto the MHC-II binding groove and the subsequent transport of peptide-loaded MHC-II to the cell surface [46]. We could show that DC maturation induced by the pathobiotic commensal *E. coli* mpk results in strong intracellular CTSS activity increase and therefore enhanced MHC-II surface expression which is required for a powerful $CD4^+$ T cell mediated immune response [46]. Symbiotic commensal *B. vulgatus* mpk priming of DC, however, prevents from *E. coli* mpk induced CTSS activity increase and therefore from Ii cleaving and enhanced MHC-II surface expression [46]. We have previously shown that *B. vulgatus* mpk converts DC into a tolerant semi-mature phenotype [31, 99]. These tolerant semi-mature DCs are non-responsive to further stimuli, they fail to activate $CD4^+$ T cells and they are associated with the prevention of colitis in various mouse models [31, 99]. We now demonstrate that CTSS activity regulation is one of the most important reasons for induction of DC semi-maturation and the circumvention of T cell activation [46]. Prevention of CTSS activity increase results in less efficient Ii cleaving [46]. It was shown that CTSS deficiency significantly impairs DC mobility since Ii seems to interact with cellular myosin II [241] and efficient Ii cleaving therefore seems to be required for adequate interaction of Ii with myosin II and thus for DC mobility [46]. Therefore, reduced Ii cleaving might contribute to impaired mobility of semi-mature DC [31]. Furthermore, CTSS catalysed Ii cleaving leads to NFκB activation resulting in enhanced secretion of pro-inflammatory cytokines [242]. In fact, smDCs express only low amounts of pro-inflammatory cytokines [99] and this might be, at least in part, due to reduced cleaving of MHC-II bound Ii in smDCs [46].

The question emerges which intracellular regulation mechanisms are involved in *B. vulgatus* mpk mediated CTSS activity regulation [46]. In principle, CTSS activity can be regulated by various mechanisms. Possible regulation via transcriptional control, i.e. induced by IL-10 binding and STAT3 dimerisation [243] can be excluded in this case since we could not detect any transcriptional regulation of the *Ctss* gene [46]. Another potential regulation mechanism is control of the lysosomal pH, but this might not be of importance in case of CTSS due to the broad pH range in which CTSS

provides remarkable activity [46]. Possible post-translational regulation might occur through inhibition by chondroitin-4-sulfate [121] or the creation of an oxidizing environment by NADPH oxidase NOX2 [244, 245]. Another prominently discussed endogenous CTSS inhibitor is cystatin C (CysC) [46]. However, there are contradictory reports about the role of CysC for CTSS activity regulation [46]. Although some groups claim CysC to be the major CTSS activity regulator [124-126], Magister *et al.* published that CysF might be the more important regulator protein [127]. In order to elucidate the role of CysC during *B. vulgatus* mpk induced DC semi-maturation and the effect on CTSS activity, we first performed immunoprecipitations against CysC that proved convincing interaction between CysC and CTSS [46]. We could further demonstrate that *B. vulgatus* mpk fails to induce DC semi-maturation in Cystatin C-deficient *Cst3*$^{-/-}$ DCs indicating a central role for CysC in this process [46]. We conclude that *B. vulgatus* mpk mediates its CTSS regulating functions via Cystatin C [46]. There are different possibilities how a bacterial stimulus on DCs might affect the interaction between CysC and CTSS [46]. Transcriptional regulation of the CysC gene might be the first possibility since it could be shown that transcription factors like IRF-8 and PU.1 enhance CysC mRNA transcription [46, 246]. However, we could not detect any alteration in CysC gene transcription during the DC maturation or semi-maturation process [46]. In line with this, we could also not detect any differences in the amount of CysC protein in DCs of different maturation states [46]. CysC inhibits target proteases like CTSS by forming tight and non-covalent complexes [46, 247]. Complex forming with CTSS is limited to CysC monomers [46]. However, CysC protein expression in the endoplasmatic reticulum (ER) does not only yield in the formation of monomers but also in dimers that do not form inhibitory complexes with target proteases [46, 248]. Xu *et al.* demonstrated that the formation of non-inhibitory CysC dimers is dependent on the amount of ROS inside the cell, whereupon ROS presence promotes dimer formation [234]. Since bacterial lipopolysaccharide (LPS) induced DC maturation leads to an increase in intracellular ROS concentrations [249], we hypothesized that a weaker *B. vulgatus* mpk LPS signalling leads to less ROS formation and therefore enhanced levels of monomeric CysC compared to completely mature DC [46]. In fact, *B. vulgatus* mpk stimulation does not lead to an increase of intracellular ROS amounts, in contrast to *E. coli* mpk stimulation which efficiently enhances ROS production [46]. We therefore assume that *B. vulgatus* mpk stimulation leads to less CysC dimer formation, thus resulting in increased proportions of monomeric cystatin C [46]. These enhanced amounts of monomeric CysC can subsequently form inhibitory complexes with CTSS, which we could prove via immunoprecipitation, resulting in permanently low CTSS activities [46]. In line with this, we could detect a CysC-regulation dependent MHC-II surface expression of DCs supporting the findings of Pierre *et al.* [250] but opposing findings of El-Sukkari *et al.* [251], [46]. In line with this, we detected extremely efficient Ii cleavage in *Cst3*$^{-/-}$ BMDCs, with Ii cleaving being the precondition for MHC-II translocation to the cell surface [46].

There is an intense ongoing research for adequate CTSS inhibitors for the use as potential drugs in order to treat autoimmune diseases [46]. Some groups developed chemical CTSS inhibitors and chemical CTSS inhibition could attenuate atherosclerosis in mice [135] and T cell mediated inflammation in the murine central nervous system [252], [46]. However, a non site-directed complete inhibition of CTSS might have severe side effects on the host organism [46]. Furthermore, the effectiveness of chemical substances is dependent on bioavailability and membrane passage behaviour if inhibitors are supposed to act intracellularly [46]. In contrast to a chemical inhibitor, *B. vulgatus* mpk does not lead to a complete CTSS inhibition as demonstrated in our experiments [46]. This is a strong advantage over a chemical inhibitor that usually leads to a complete inhibition of its target enzyme [46]. Therefore, *B. vulgatus* mpk treatment still allows for CTSS to achieve its physiological role and only prevents from pathophysiological activation [46].

We could show that *B. vulgatus* mpk prevents from pathological reactions of the immune system via regulation of host CTSS activity and therefore contributes to the maintenance of the intestinal homeostasis [46]. This could be underlined by the observation that the *B. vulgatus* mpk associated protection of *Rag1*$^{-/-}$ mice from colitis induction is accompanied by inducing DC semi-maturation and inhibition of CTSS secretion [46]. This makes *B. vulgatus* mpk a promising candidate for the treatment for IBD and other CTSS-associated AID [46]. We think that *B. vulgatus* mpk might be an even better tool than a chemical inhibitor to treat CTSS-associated AID since (i) it is easily administrable, (ii) it does not completely suppress physiological functions of CTSS but only suppresses pathological activities and (iii) it acts as a commensal symbiont [46]. It does not influence a normal immune response due to acute infections but strongly inhibits pathological gut microbiota associated immune responses [46]. Therefore severe side effects of symbiont-mediated CTSS activity regulation should not occur and could not be observed in the used mouse model, another advantage over a chemical inhibitor [46].

Taken together, we demonstrate that symbionts of the intestinal microbiota regulate host CTSS activity and secretion and might therefore be an attractive approach to deal with CTSS associated autoimmune diseases [46].


Contents lists available at ScienceDirect

International Journal of Medical Microbiology

journal homepage: www.elsevier.com/locate/ijmm

Structure and function: Lipid A modifications in commensals and pathogens

Alex Steimle, Ingo B. Autenrieth, Julia-Stefanie Frick*

Institute of Medical Microbiology and Hygiene, University of Tübingen, Elfriede-Aulhorn-Str. 6, D-72076 Tübingen, Germany

Paper 6: Structure and Function: Lipid A modifications in commensals and pathogens

Review

Alex Steimle, Ingo B. Autenrieth and Julia-Stefanie Frick

Int J Med Microbiol (2016) 306(5):290-301 [68]

Lipopolysaccharides (LPS) of Gram negative bacteria are one of the most potent stimulators of the host innate immune system and LPS recognition is essential for the host organism to clear infections of invading bacterial pathogens [68] A lot is known about host immunological reactions to fight pathogens via recognition of their LPS, as well as of strategies of pathogens to modulate their LPS structure in order to evade the immune system [68]. However, less is published about differential sensing of lipopolysaccharides of commensal bacteria in the intestine and how this contributes to manifestation or destruction of the intestinal homeostasis [68]. LPS sensing is necessary to fight pathogens [68]. However, sensing of LPS of gut commensal bacteria can simultaneously be disadvantageous for the genetically predisposed host, since this might lead to damage of the intestinal homeostasis and therefore to chronic intestinal inflammation [68]. However, less immunogenic LPS could also serve as therapeutics to antagonize an overreacting innate immune system [68]. Therefore, commensal gut bacteria-derived LPS could prevent from uncontrolled intestinal immune response in the intestine which makes LPS an attractive therapeutical approach to treat IBD [68].

As already mentioned, LPS structure, especially its lipid A chemistry, differs among distinct bacterial species [68]. Indeed, the exact LPS structure, and in this context mainly the lipid A structure, determines LPS immunogenicity and is therefore decisive for its function [68, 72, 73]. LPS triggering strong pro-inflammatory reactions of host cells are named “agonistic” lipolysaccharides. In contrast, structurally different lipid A can also result in weak inflammatory host responses, hence being called

"weak agonistic" [68]. Certain lipid A can even completely block any pro-inflammatory reactions by binding to corresponding host receptors [68]. These latter lipopolysaccharides are therefore called "antagonistic" [68]. Most Gram negative bacteria possess agonistic hexaacylated LPS like *E. coli* LPS, which is one of the most potent agonists of the human innate immune system [68, 253-255]. Usually the number of lipid A acyl chains directly correlates with the ability to induce cytokine production whereat the hexaacylated forms are the most immunostimulating ones [68, 256]. Within a biological system, distinct lipid A structures compete for binding to host receptors [68]. Antagonistic lipid A might therefore compete with agonistic LPS for host receptor binding [68]. Hexaacylated lipid A seems to promote the strongest proinflammatory immune reactions after binding to TLR4 [68]. This is due to the fact that the first five acyl chains are buried in a hydrophobic cavity of the TLR4 adaptor molecule MD-2 while the sixth chain mediates the binding to TLR4, the precondition for TLR4-mediated intracellular signalling [68, 77, 257]. Therefore, TLR4-mediated signalling is usually drastically reduced if this sixth acyl chain is missing [68]. However, due to the already mentioned differences in the structures of the lipid A binding cavity of the TLR4 receptor between different mammalian species, distinct lipid A structures can provide a different immunogenic potential among these species [68].

However, not only acyl chains contribute to the immunogenic properties of lipid A, but also the number of phosphate groups [68]. A deletion of a phosphate group results in a loss of endotoxic activity [68, 253]. Most lipid A structures contain two phosphate residues, one on each sugar moiety [68]. However, some bacterial lipid As lack one or even both of them, therefore altering its immunogenic potential [68]. For example, *Francisella tularensis* lacks one or both phosphate groups and this is considered to be, at least in part, the reason for its weak agonistic property [68, 74]. Furthermore, the non-phosphorylation might also be seen as an immune evasion strategy for certain bacteria since some antimicrobial peptides (AMPs) specifically target negative charges on bacterial surfaces and a loss of negatively charged phosphate residues therefore renders bacteria to be invisible for these AMPs [68].

It is widely accepted that in inflammatory bowel diseases (IBD) which are chronic inflammatory disorders of the intestine, the mucosal immune system reacts inappropriately towards the endogenous intestinal commensal microbiota [68, 258]. However and until now, no particular microbial species was consistently linked to IBD pathogenesis, but some symbiotic bacteria species have been shown to prevent from pathological inflammatory host responses [26, 30, 55, 68, 259, 260].

For example, the mono-colonization of *Il2*$^{-/-}$ mice with *E. coli* is reported to induce severe colitis, whereas monocolonization with *Bacteroides vulgatus* does not and *B. vulgatus* even inhibits the

E. coli induced inflammation in co-colonized *Il2*$^{-/-}$ mice [28, 68]. Recently we showed that a low endotoxicity of the intestinal microbiota was associated with mucosal immune homeostasis in a mouse model of chronic intestinal inflammation [68, 110]. T cell transplanted *Rag1*$^{-/-}$ harboring a low endotoxic complex intestinal microbiota, characterized by high numbers of *Bacteroidetes* and low numbers of *Enterobacteriaceae* did not develop colitis, whereas T cell transplanted *Rag1*$^{-/-}$ mice harboring a high endotoxic complex intestinal microbiota, characterized by high numbers of *Enterobacteriaceae* and low numbers of *Bacteroidetes* developed severe intestinal inflammation [68, 110]. In line with this, administration of commensal but pathobiontic *E. coli* JM83 to *Rag1*$^{-/-}$ mice harboring a low endotoxic microbiota resulted in intestinal inflammation, whereas the administration of an *E. coli* JM83 mutant containing an acyltransferase from *Porphyromonas gingivalis* (*E. coli*$_{MUT}$) protected *Rag1*$^{-/-}$ mice harboring the high endotoxic microbiota from induction of disease [68, 261]. We isolated and purified LPS from both *E. coli*$_{WT}$ and *E. coli*$_{MUT}$ and characterized its fatty acid composition [68]. Investigations by high-resolution electrospray ionization Fourier transform ion cyclotron mass spectrometry revealed the same hexaacetylated lipid A molecules in both strains [68]. In addition, *E. coli*$_{MUT}$ contained a major portion of lipid A, in which a 12 carbon atom laurate acyl chain is replaced by a 16 carbon atom palmitate acyl chain[68, 110]. This minor modification in *E. coli* JM83 is reported to significantly affect host cell signaling [68, 261]. To verify the altered stimulatory capacity of LPS$_{MUT}$ compared with LPS$_{WT}$, we used TLR4-overexpressing human embryonic kidney cells (HEK293) [68, 110]. Stimulation of cells with the modified LPS$_{MUT}$ resulted in a significantly reduced IL-8 secretion 4 hours after stimulation, as compared with LPS$_{WT}$ indicating a reduced endotoxicity but not TLR4 antagonism of the altered LPS$_{MUT\ [68,\ 110]}$. Feeding of *Rag 1*$^{-/-}$ mice harboring the low endotoxic microbiota with LPS$_{WT}$ resulted in severe intestinal inflammation, however challenging mice which were colonized with the high endotoxic microbiota protected these animal from induction of colitis [68, 110]. This data suggest that the ratio of high endotoxic and low endotoxic LPS is crucial for the regulation of the intestinal immune balance [68]. A predominance of high endotoxic LPS might promote a Th1/Th17 response, subsequently supporting intestinal inflammation, and a predominance of low endotoxic LPS might induce an altered activation of the innate immune system, and either induction of regulatory T cells or prevention of a Th1/Th17 response, associated with intestinal immune homeostasis [68, 110]. Therefore LPS might act as a key microbial symbiosis factor that, depending on its structure, can induce or prevent bowel inflammation by shaping the innate immunity via TLR4-dependent signaling mechanisms [68, 110, 262].

Could LPS be used as a potential drug for the treatment of inflammatory bowel disease?

The role of LPS for the host immune system provides ambivalent features [68]. While LPS is essential for the host organism to sense infections of bacterial pathogens at an early stage, therefore helping

to clear the infection, an imbalanced LPS sensing can have severe effects for the host organism with fatal sepsis being the most severe consequence [68]. When LPS is thought to be used as a potential therapeutic agent, the different modes of LPS sensing in mammalian organisms hast to be kept in mind (Fig. 8). Blocking TLR4 mediated downstream signaling has been implicated to be useful as a drug to prevent from septic shock [68, 263]. Therefore, synthetic antagonistic lipid A structures were invented in order to block TLR4 receptor signaling, such as Eritroran [68]. Eritroran strongly prevents from binding of agonistic lipid A to MD-2 and therefore terminates MD-2/TLR4-mediated signaling *in vitro*, *ex vivo* and *in vivo* [68, 264-266]. Despite these findings, Eritroran failed to improve survival in a phase III trial in patients with severe sepsis [68, 267]. Until now, it is not known why Eritroran gavage failed to prevent from fatal sepsis [68]. Possible explanations might be the delayed administration of this strong TLR4 agonist or a failure in trial design [68, 267, 268]. Nevertheless, antagonistic lipid A structures still seem to be a promising tool for the treatment of bacterially induced sepsis [68]. This strategy to prevent from an uncontrolled, or "imbalanced", TLR4 signaling-mediated immune response might also be an attractive approach to deal with inflammatory disorders of the gut [68]. Inflammatory bowel disease develops from an uncontrolled immune response directed towards the intrinsic microbiota [68]. In this case, not pathogens are the target of the immune system, but rather commensal bacteria located in the intestine [68]. It might therefore be possible that antagonistic or weakly agonistic lipid A structures could prevent from uncontrolled TLR4-mediated immune responses towards the own microbiota [68]. In fact, we could already show that the lipid A structure of commensal bacteria is a decisive trigger for the induction of colitis in a genetically predisposed host [68, 110].

Two main questions remain concerning the administration of isolated LPS (or lipid A) for the treatment of IBD. (I) Which lipid A structure might provide the best results and (II) is TLR4 blocking really "the method of choice"?

The specific structure of lipid A can have profound and even unpredictable effects upon TLR4 signaling [68]. Although detailed studies about the interaction of lipid A with its corresponding MD-2 co-receptors are available [68, 77, 85], the precise immunogenicity cannot be predicted from knowing the structure alone [68]. However, a recent report by Paramo *et al.* means a major advance concerning this issue, since they manage to predict the binding behavior of lipid A structures to MD-2 by measuring their potentials of mean force [68, 269]. The second question is even more complicated to answer. It is possible that TLR4 blocking might not restore homeostasis in every case, since TLR4 signaling seems to be important for the prevention of dextran sodium sulfate (DSS)-induced colitis in mice [68, 270, 271]. Therefore, an antagonistic lipid A structure, completely preventing from TLR4 signaling, might not be the lipid A of choice [68]. Possibly, a rather weakly

agonistic lipid A structure, allowing basic TLR4-mediated signaling, but preventing from uncontrolled TLR4 activation might be a better tool [68]. Additionally, the recent discovery of Caspase-11 as an intracellular lipid A binding LPS sensor [90, 91, 272] leads to the question, if blocking the TLR4 binding cavity is sufficient to influence LPS-mediated induction of the host immune system [68] (Fig. 8). As described, a block of TLR4 is not sufficient to prevent from LPS induced Casp11-mediated inflammasome activation [68]. Other bacterial components, largely present in the intestine, can activate other TLRs than TLR4 to induce an increase in cytosolic amounts of Casp11 being a precondition for intracellular lipid A sensing [68]. Therefore, a potential lipid A-derived drug needs to have access to the cytosol of host target cells [68]. Although being highly speculative, this might be

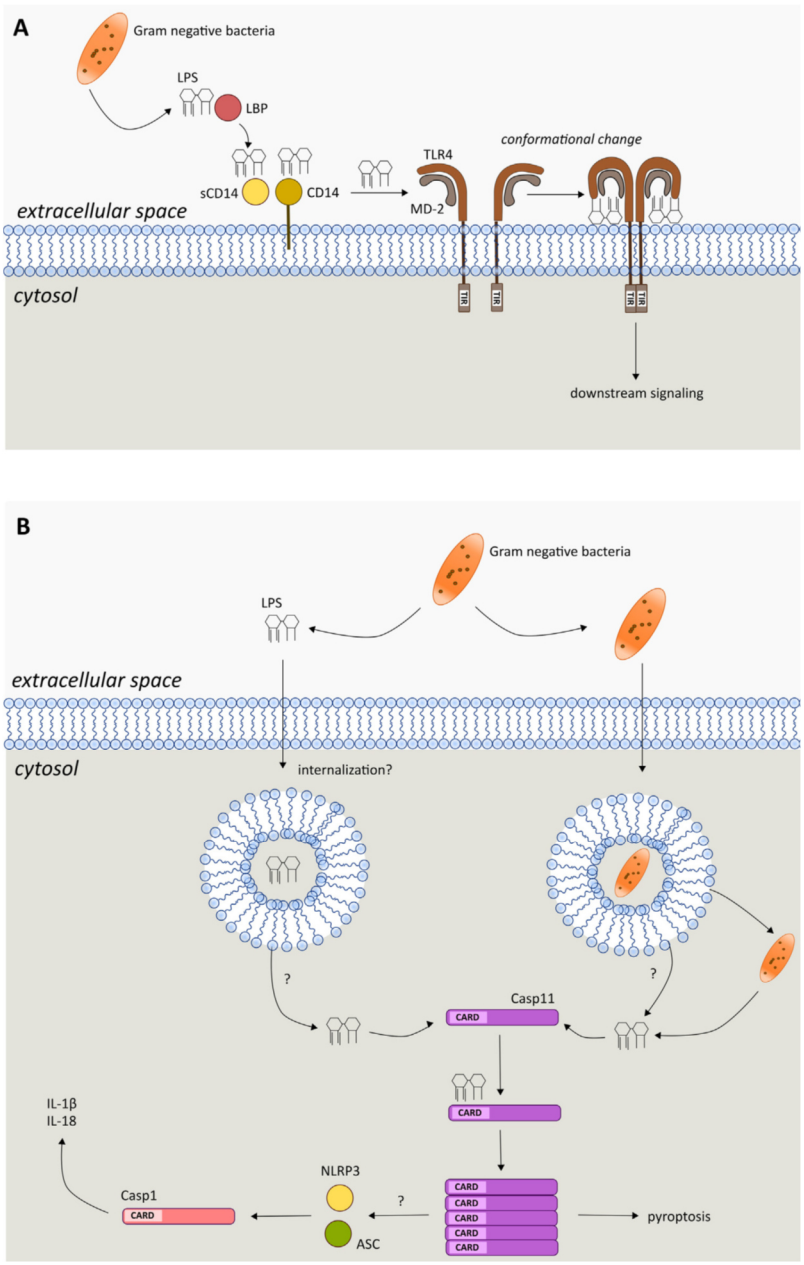

Figure 8: Molecular mechanisms of extracellular and intracellular sensing of bacterial LPS. (A) Extracellular LPS sensing. The host lipid binding protein (LBP) samples LPS from theouter membrane of Gram negative bacteria and mediates its transport to host CD14. CD14 can either be soluble (sCD14) or anchored in the membrane of TLR4 expressing cells. CD14 shuttles LPS to the TLR4 co-receptor protein MD-2 which initiates a conformational change in MD-2 and TLR4, resulting in dimerization of the extracellular and subsequently of the intracellular TIR domains. TIR domain dimerization finally mediates downstream signaling [68]. (B) Intracellular LPS sensing. Left side: LPS that is present in the extracellular space can enter the vacuoles of caspase-11 (Casp11) expressing cells. LPS escapes the vacuoles via a yet unidentified mechanism. Right side: Bacteria can be sampled by phagocytotic cells like Casp11 expressing macrophages. The LPS of non-cell invading bacteria or whole cell invading bacteria are relieved into the cytosol. Both: LPS present in the cytosol actively binds to the CARD domain of Casp11 leading to Casp11 oligomerization that results in Casp11 activation. By a yet unknown mechanism, this Casp11 activation results in inflammasome assembly resulting in Caspase-1 (Casp1) mediated secretion of the pro-inflammatory cytokines IL-1β and IL-18. Casp11 oligomerization can also lead to pyroptosis, a special kind of cell death. Taken from Steimle *et al.*, (2016) [68]

another explanation why Eritroran failed in the clinical study since it was not granted access to the cytosolic compartment [68]. This fact rises drug development to a severe challenge and strategies need to be developped to target therapeutic lipid A to the cytosolic compartment [68]. Since it could be shown that lipid A structures that act antagonistically in TLR4-signaling also prevent from Casp11 oligomerization and activation despite efficient binding [68, 272].Therefore, it seems that the immunogenicity of lipid A structure concerning TLR4 activation, described by the terms agonistic and antagonistic, also accounts for intracellular lipid A induced intracellular inflammasome activation [68].

There is an ongoing research for new lipid A structures in order to be used as therapeutic. Although most research on this topic focuses on the treatment of sepsis, the idea behind it can easily be transferred to the treatment of chronic inflammatory intestinal disorders [68]. Besides synthetic or chemical development of lipid A structure-related TLR4 antagonists, there is an ongoing interest also on LPS structures of more ”exotic” bacteria and how they might contribute to a research progress on this topic [68]. For example, di Lorenzo *et al.* identified a lipid A structure with strong antagonistic activity in a bacterium living in hot springs: *Thermomonas hydrothermalis* [273]. However, a closer and more detailed look on the lipid A structures of symbiotic commensal bacteria might be helpful for the development of a lipid A structure providing weak agonistic activity to prevent from both, TLR4- and Casp11-mediated, uncontrolled immune responses of the host organism towards its own microbiota [68].

Paper 7: *Bacteroides vulgatus* mpk lipopolysaccharide acts as inflammation-silencing agent for the treatment of intestinal inflammatory disorders

Submitted Research Paper

Alex Steimle, Flaviana Di Lorenzo, Kerstin Gronbach, Thorsten Kliem, Kerstin Fuchs, Hasan Halit Öz, Andrea Schäfer, Annika Bender, Anna Lange, Jan Kevin Maerz, Sarah Menz, Ingo B. Autenrieth, Bernd J. Pichler, Hans Bisswanger, Alba Silipo, Antonio Molinaro and Julia-Stefanie Frick

Submitted to *Nature Communications* in November 2016

Inflammatory Bowel Diseases are digestive tract-associated pathologies that are characterised by chronic relapsing intestinal inflammation with Crohn's Disease (CD) and Ulcerative Colitis (UC) being the most frequent and clinically relevant forms of this disease complex [48]. As already mentioned, IBD is considered to be a multifactorial disease with genetics [52], environmental factors [53] and intestinal microbiota composition [54] contributing to the pathology and disease outcome. Therapy of IBD patients is, to date, restricted to general suppression of the patient's immune system [49]. However, scarce data or unsatisfactory treatment effects characterize the properties of available or currently discussed therapeutical approaches for the treatment of IBD [49]. One of the most popular approaches include the utilization of TNF antagonists leading to general immunosuppression [49]. However, only one third of patients treated with TNF antagonists respond to this therapy in a satisfactory way (reviewed in [274]). Other generalized immunomodulatory therapies are currently investigated in experimental trials, such as using anti-adhesive agents which block interactions of lymphocytes with epithelial cells [275], restoring TGFβ activity by blocking pathologically enhanced levels of TGFβ inhibitors in UC patients [276] or targeting Janus kinases to achieve a general reduction of pro-inflammatory cytokine secretion [277]. However, all these therapeutical approaches aim for a generalized reduction of pro-inflammatory responses resulting in general immunosuppression, often associated with many undesirable side effects [49].

We could already demonstrate that mouse symbiotic gut commensal *Bacteroides vulgatus* mpk exhibits anti-inflammatory properties in various mouse models for experimental colitis, such as in *Il2*$^{-/-}$ mice [28, 31] and T cell transplanted *Rag1*$^{-/-}$ mice [46]. These anti-inflammatory properties lead to a prevention of the induction of intestinal inflammation when *B. vulgatus* mpk is administered via drinking water before onset of disease [49]. This considerably demonstrated that, due to the anti-inflammatory properties of the commensal symbiont *B. vulgatus* mpk , this bacterium is not only able to prevent from inducing inflammation but also to actively silence established inflammatory

reactions, alleviating symptoms of colitis in *Rag1*$^{-/-}$ mice [49]. Since one of the major immunoreactive compounds of Gram-negative bacteria is LPS, we were interested whether the administration of pure *B. vulgatus* mpk LPS (LPS_{BV}) exhibits the same anti-inflammatory and inflammation-silencing properties in the colon like the live bacterium [49]. In summary, our data indicate that both, live *B. vulgatus* mpk bacteria and isolated LPS_{BV} are equally capable of silencing established inflammatory processes in the large intestine by downregulation of pro-inflammatory cytokines and by favouring Treg inducing environmental conditions [49].

Due to the immune response silencing properties of isolated LPS_{BV}, we gave a closer look at its chemical structure [49]. LPS_{BV} lipid A resulted to be a heterogeneous mixture of tetra- and pentaacylated species, whose fatty acids nature and distribution was similar to the previously reported lipid A structure of *Bacteroides dorei* [278], a close relative of *Bacteroides vulgatus* [49]. Moreover, the lipid A blend resulted to be phosphorylated only at the reducing glucosamine (α-GlcN) of the lipid A disaccharide, as also observed in *B. dorei* [49, 278]. From the carbohydrate and LPS chemical point of view, it is very important to underline the unusual presence of galactofuranose in the core region [49]. This finding is even more interesting if one takes into account that the presence of five membered rings in the LPS core oligosaccharide is very rare [49, 279].

We were further interested whether the typical immunogenic properties of the used bacteria on dendritic cells *in vitro* can be completely mimicked by their respective isolated LPS, thus explaining the observations made in *in vivo* experiments [49]. In view of this, we also isolated the LPS from *E. coli* mpk (LPS_{EC}) which contains a *bis*phosphorylated and hexaacylated lipid A [49]. Therefore, pure LPS seems to be able to mimic the immunogenic properties of both commensal bacteria with LPS_{BV} providing low and LPS_{EC} providing strong immuno-stimulating properties [49]. Therefore it can be stated that LPS_{BV} is not a TLR4 antagonist since it provides weakly agonistic activity as demonstrated by the low, but still detectable amounts of secreted cytokines and by the slight enhancement of T cell stimulatory surface proteins as MHC-II, CD40, CD80 and CD86 [49]. In summary, differential maturation of DCs by commensal bacteria is highly dependent on their LPS structure and live *B. vulgatus* mpk bacteria are not necessary to induce semi-mature DCs providing immune homeostasis maintaining properties, since using isolated LPS_{BV} was sufficient to induce DC semi-maturation [49]. The observation that both LPS structures, LPS_{BV} and LPS_{EC}, showed different immunological effects on DCs *in vitro*, prompted us to define their binding affinity to the MD-2/TLR4 receptor complex and we determined binding constants K_D for both LPS structures [49]. The K_D of LPS_{BV} could was determined to be 0.412 mg L^{-1} while the K_D of LPS_{EC} was determined to be 0.304 mg L^{-1}, being in the same biologically relevant range as LPS_{BV} K_D [49].

Since both LPS, LPS_{EC} and LPS_{BV}, provided similar binding affinity towards the murine MD-2/TLR4 receptor complex, we tested the capability of each of these two distinct LPS to remove already bound LPS from the receptor complex [49]. We could finally demonstrate that LPS_{BV} was able to remove about 20% of already bound LPS_{EC}, while LPS_{EC} was able to remove about 50% of already bound LPS_{BV} [49].

As already mentioned, LPS_{BV} was able to induce tolerant semi-mature DCs *in vitro*. However, the experiments to demonstrate that were performed in absence of other LPS structures for the first 16h of the semi-maturation process [49]. Physiological conditions in the colonic lumen provide the presence of lots of different LPS structures at the same time [49]. Therefore, we stimulated BMDCs with both LPS molecules, weakly agonistic LPS_{BV} and strong agonistic LPS_{EC}, at the same time and at different concentrations for 16 h [49]. Simultaneous presence of LPS_{BV} could not anticipate LPS_{EC}-induced maturation effects on DCs as it could be demonstrated in case of subsequent stimulation of DCs that were primed with LPS_{BV} and challenged with LPS_{EC} [49].

Figure 9 summarizes the observations of this study into a concluding hypothesis. We have demonstrated that LPS_{BV} provides weakly agonistic activities and binds to the murine MD-2/TLR4 receptor complex with an affinity that is comparable to the binding affinity of strong agonistic LPS_{EC} [49]. Since the downstream signalling, and therefore the immunogenicity, is dependent on effective $(MD\text{-}2/TLR4)_2$ heterotetramerization [77], we hypothesize that the specific and unique overall LPS_{BV} structure blocks the conformational change of the receptor complex which is necessary for tetramer formation (Fig. 9a) [49]. Concerning the therapeutical effects of LPS_{BV} in strongly reducing inflammatory processes in a mouse model for experimental colitis, we conclude that the concentration of LPS_{BV} located in the intestinal lumen must exceed the number of agonistic LPS from other commensal bacteria in order to be able to induce tolerant and semi-mature DCs [49]. Exceeding LPS_{BV} concentrations are thought to enhance the probability that intestinal DCs only encounter weakly agonistic LPS_{BV} since we could demonstrate that simultaneous encounter with another agonistic LPS prevents from DC semi-maturation and induces pro-inflammatory responses mediating DC maturation [49]. In this case, the ability of LPS_{EC} to remove already bound LPS_{BV} from the MD-2/TLR4 receptor more efficiently than *vice versa* would not be relevant [49] (Fig. 9b). As demonstrated, the endotoxicity of LPS_{BV} is dependent on its concentration and very high LPS_{BV} concentration might lead to complete DC maturation [49]. However and as mentioned before, this concentration exceeds physiological LPS levels in the intestine [49]. We could demonstrate that using 160 µg mL^{-1} in the drinking water leads to the observed healing effects in *Rag1*$^{-/-}$ mice, indicating that this concentration is sufficient to exceed the amount of already present LPS in the colon while simultaneously being in a semi-maturation

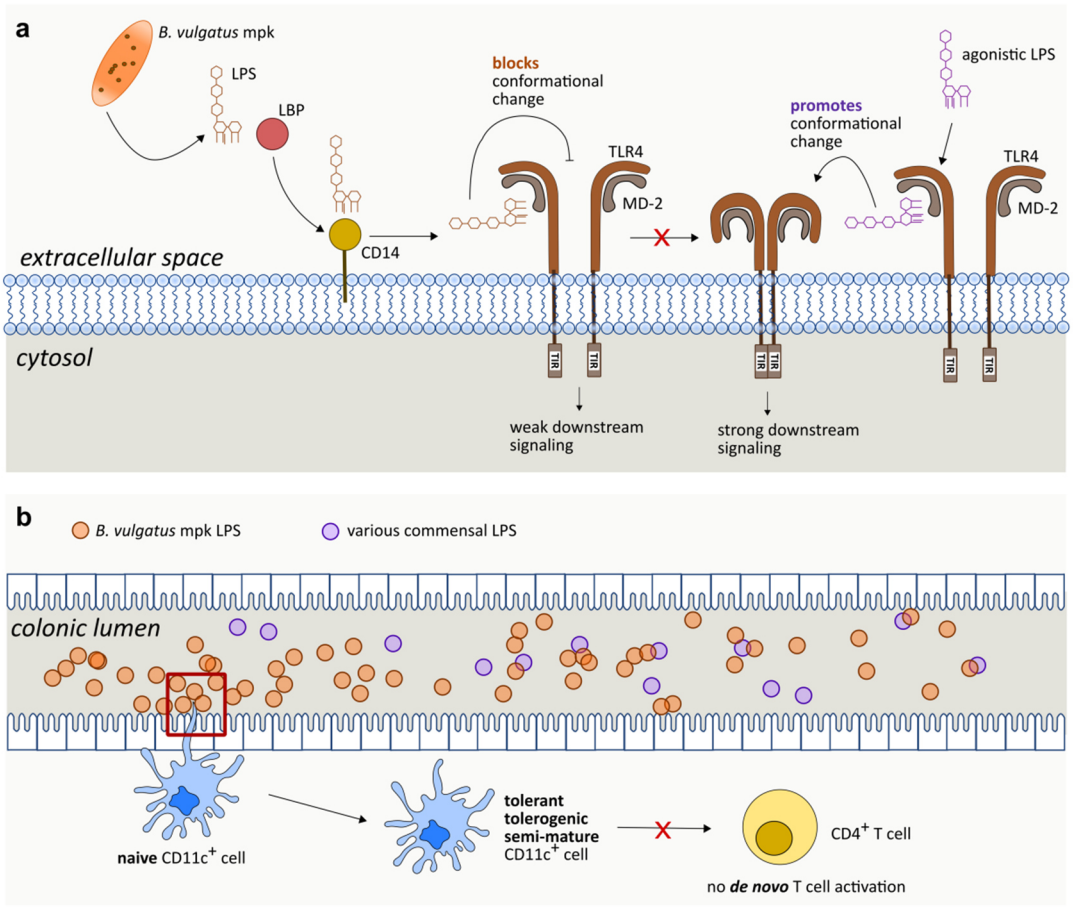

Figure 9: Proposed mechanism how weakly agonistic *B. vulgatus* mpk LPS influences MD-2/TLR4 receptor activation and prevents from initiation of a CD4⁺ T cell mediated immune response via modulation of intestinal CD11c⁺ cells

(a) Right side: agonistic LPS like *E. coli* mpk LPS binds to the MD-2/TLR4 receptor complex. Its LPS structure harbouring a bisphosphylated and hexaacylated lipid A leads to a conformational change in the receptor complex leading to heterotetramerization of two MD-2/TLR4-dimers resulting in efficient intracellular signalling, overshooting a pro-inflammatory signalling threshold. Left side: weakly agonistic *B. vulgatus* mpk LPS binds to the MD-2/TLR4-receptor complex with a similar affinity as strong agonistic *E. coli* mpk LPS. However, its structural characteristics like harbouring a monophosphorylated, mixed tetra- and pentaacylated lipid A, as well as a unique galactofuranose-containing core structure probably lead to a block of the heterotetramer formation resulting in a weak intracellular signalling that does not exceed a pro-inflammatory threshold but rather mediates anti-inflammatory immune responses. (b) Therapeutical administration of LPS from symbiotic *B. vulgatus* mpk ends up in large amounts in the intestine, exceeding the amount of present LPS from other intestinal commensal bacteria. Excess *B. vulgatus* mpk LPS primes naïve CD11c⁺ cells into a tolerant, tolerogenic and semi-mature phenotype that fails to activate CD4⁺ T cells. This prevention of a *de novo* activation of CD4⁺ T cells leads to a phase-out of ongoing inflammatory processes while *de novo* induction of an immune response is prevented. However, our data indicate that this only happens if *B. vulgatus* mpk LPS is the only TLR4 ligand which CD11c⁺ cells encounter when they are still naïve and immature. *B. vulgatus* mpk LPS needs a certain period of time to induce CD11c⁺ cell tolerance. Simultaneous encounter with agonistic LPS does not lead to CD11c⁺ cell tolerance and does therefore not promote abrogation of inflammatory processes. Taken from the manuscript [49], see appendix

inducing concentration range [49]. Once DC semi-maturation is induced, this phenotype cannot be overcome and would therefore lead to a prevention of a *de novo* T cell activation [49]. Therefore, after a phase-out of ongoing inflammatory processes, newly induced smDCs through LPS_{BV} administration would prevent from a continuing T cell activation and therefore promote healing of damaged colonic tissue [49]. With this study, we want to offer an alternative therapeutical approach avoiding disadvantages of current state-of-the art IBD therapies by using intestinal commensal-derived isolated LPS [49]. LPS-like structures acting as TLR4 antagonists have already been considered to be suitable therapeutical agents for the treatment of i.e. sepsis [49]. However an initial trial was not successful [267]. We think, that a complete TLR4 antagonist might not be the right choice for inflammatory disorders, neither for sepsis nor for other immune system-related pathologies like IBD [49]. We therefore want to promote a commensal-derived isolated LPS from mouse gut-associated *B. vulgatus* mpk as a potential immunomodulatory drug for the treatment of IBD [49]. LPS_{BV} does not act antagonistically to the murine MD-2/TLR4 receptor complex but rather weakly agonistic, probably being the key feature of its immune system silencing functions [49]. The observed weakly agonistic activity of *B. vulgatus* LPS is traced back to its unique molecular structure which influences its activating potential towards the murine MD-2/TLR4 receptor complex. Structural analysis of LPS_{BV} revealed a mixture of penta- and tetraacylated *mono*-phosphorylated lipid A, chemically related to the *B. dorei* [278] and *B. fragilis* [280] lipid As, a galactofuranose-containing core OS and an O-chain composed of rhamnose and mannose [49]. Interestingly, the core structure revealed a novel carbohydrate composition that has not yet been detected in any other bacterial LPS [49]. In particular, the presence of galactofuranose in the inner part of the LPS core as well as the presence of a rhamnose residue, as the first sugar linked to the Kdo, are surely an innovative hallmark for LPS [49]. Thus it can be speculated that such an unusual architecture has a key role in the MD-2/TLR4 complexation with LPS and the following downstream signalling [49].

The immunogenicity, or the strength of this intracellular signalling, triggered by LPS is considered to be mostly mediated by the structure of the lipid A part [72, 73]. Hexa-acylated and *bis*-phosphorylated lipid A therefore seems to be the most potent activator of the MD-2/TLR4-receptor complex mediated signalling [82].

In an important study, Park *et al.* [77] revealed the structural basis for the explanation of these observations [49]. Five of the six acyl chains are buried inside the MD-2 binding cavity while the sixth acyl chain points out to the MD-2 surface mediating hydrophobic interactions with the TLR4 ectodomain [49, 77].

This partly explains the lower endotoxicity of hypoacylated lipid A structures lacking this sixth acyl chain and the weakly agonistic activity of hypoacylated LPS_{BV}. Furthermore, both 1- and 4'-

phosphates on the lipid A diglucosamine backbone were demonstrated to be important moieties for MD-2/TLR4 receptor complex activation [49, 77]. Since LPS_{BV} possesses only one phosphate at position 1 of the reducing glucosamine, this may also contribute to its weakly agonistic effects as a missing 4'-phosphate was demonstrated to result in a 100-fold reduction in endotoxic activity [49, 281]. Within this frame, the occurrence of a minor *bis*-phosphorylated lipid A species did not increase the LPS_{BV} immunogenicity as previously demonstrated for the *bis*-phosphorylated LPS lipid A from the mutant strain of *B. thetaiotaomicron* (ΔLpxFI) [49, 282]. Additionally, recent studies revealed that not only the lipid A phosphorylation and acylation pattern determines LPS endotoxicity [49]. Indeed, it was demonstrated that charged groups, other than glucosamine backbone associated phosphates, can increase LPS mediated endotoxicity [49]. The positively charged aminoarabinose residue attached to the lipid A disaccharide backbone combined with longer chained fatty acids rendered the potentially low endotoxic pentaacylated lipid A of *Burkholderia cenocepacia* highly endotoxic [49, 283]. Furthermore, it was previously demonstrated that even chemical modifications of the core OS with additionally charged substituents may have influence on TLR4-mediated signalling [49]. As an example, an additional negatively charged carboxyl group present in the LPS inner core was responsible for the high endotoxicity of a pentaacylated lipid A containing LPS of *Capnocytophaga canimorsus* [49, 284]. These extra charged groups, either in lipid A or in the core OS are likely creating or stabilizing electrostatic interactions between MD-2 and TLR4, resulting in efficient heterotetramerization followed by strong intracellular signalling [74, 77, 283, 284]. Besides Kdo-phosphate, LPS_{BV} does neither contain any further charged groups in the lipid A part nor in the core OS [49]. Therefore, we can hypothesize that LPS_{BV} provides features and properties of a TLR4 antagonist, which is usually able to bind to MD-2 but it failed to induce receptor multimer formation and prevented from induction of any intracellular signalling [49, 285-287]. LPS_{BV} bound to the MD-2/TLR4 receptor complex with a comparable affinity as highly agonistic LPS_{EC} but it did not lead to strong intracellular pro-inflammatory signalling [49]. Nevertheless, LPS_{BV} did not act as a pure antagonist since it actively induced semi-maturation and tolerance in dendritic cells, making it rather weakly agonistic than completely antagonistic [49]. This is highly interesting as Vatanen *et al.* demonstrated that *B. dorei* LPS, which provides the same lipid A structure as LPS_{BV}, acts as a strong MD-2/TLR4 receptor complex antagonist [278]. This difference in immunogenicity of the respective LPS supports the hypothesis of the unique LPS_{BV} core structure to contribute to its weakly agonistic activity [49]. However, this hypothesis remains speculative at the moment and requires further investigation [49]. Nevertheless, the weakly agonistic features of LPS_{BV} seem to be responsible for the observed healing effects in mice suffering from intestinal inflammation [49]. Therefore, LPS_{BV} led to weak intracellular signalling, providing a basic anti-inflammatory intracellular transcription program without exceeding a pro-inflammatory threshold [49]. Furthermore, LPS_{BV} leads to the

induction of tolerogenic DCs [49]. These properties clearly distinguishes LPS_{BV} from strong agonistic LPS_{EC}, which induces endotoxin tolerance but also strong pro-inflammatory signalling, and from antagonistic *B. dorei* LPS, which does not promote pro-inflammatory reactions but does also not promote tolerance induction in TLR4-expressing cells [49, 278]. The property of LPS_{BV} of being an effective ligand for the MD-2/TLR4 receptor complex and, at the same time, of being a weak agonist must of course be attributed to its chemical structure [49]. We are not aware, whether this is a "chemical paradigm" of the intestinal microbiota LPS since so far, only very few chemical structures of intestinal commensals have been established [49]. However, this is a logical follow up of the present work and further work is in progress [49].

These observations led to a speculation on the potential use of such a LPS structure as a suitable tool to restore homeostatic conditions not only in experimental mouse models, but also in IBD patients [49]. Therapy of IBD patients is, to date, restricted to a general suppression of the patient's immune response often associated with undesirable side effects [49].

LPS (derivative)-based treatment might avoid this problem by acting only locally at the site of inflammation: the intestine [5]. Therefore, we would promote pure LPSBV as an alternative for the treatment of intestinal inflammatory disorders or IBD providing evidence that this compound demonstrated its beneficial effects as not being an antagonist but rather a weak agonist [5]. Alternatively, the structure of LPSBV could act as a starting point for a structure-activity relationship study in order to obtain a proper LPS derivative that could be used as a prospective therapeutic agent [5]. Concluding, we hope to contribute to IBD therapy-related research offering a completely new approach avoiding disadvantages of current state-of-the-art IBD therapies [5].

Outlook

The two main findings of this work, a commensal-dependent regulation of host cathepsin S activity and the inflammation-silencing properties of symbiotic *B. vulgatus* mpk lipopolysaccharide, offer widespread possibilities for future investigations.

So far, we were focused on the effect of cathepsin S activity regulation locally in the intestine. However, we could already prove that the secretion of cathepsin S into the blood serum is dependent on the inflammatory status of the gut, indicating generalized effects of cathepsin S secretion and activity regulation by intestinal commensals. This might denote that gut microbiota components regulate the enzymatic activity of this protease not only locally in the gut but also on a more generalized level, making colonic inflammation-dependent cathepsin S secretion interesting concerning the etiology and therapy of autoimmune diseases other than IBD, such as multiple sclerosis and type-1-diabetes.

Non-published data suggest that not only cathepsin S, but other pathology-associated cathepsins like cathepsin B are regulated by symbionts and pathobionts of the intestinal microbiota. This is a highly intriguingly observation since cathepsin B malfunction and dysregulation is reported to be associated with various neurodegenerative diseases such as Parkinson's and Alzheimer's Disease.

Additionally, we proved that not only living symbionts but also isolated surface structures of these commensals, such as *B. vulgatus* mpk lipopolysaccharide, mediate inflammation-silencing properties. We hereby promote this specific surface compound as a potential therapeutic alternative for the treatment of intestinal inflammatory disorders. However, it remains to be elucidated if this specific lipopolysaccharide structure exhibits comparable inflammation-silencing properties not only in mice but also in humans. Furthermore, more detailed insights in the dendritic cell tolerance induction properties of the *B. vulgatus* mpk lipopolysaccharide core compound galactofuranose need to be gained for effective and proper drug development for the treatment of such intestinal inflammatory disorders .

References

[1] Underhill DM, Iliev ID. The mycobiota: interactions between commensal fungi and the host immune system. Nat Rev Immunol, 2014;14:405-16.
[2] Costello EK, Stagaman K, Dethlefsen L, Bohannan BJ, Relman DA. The application of ecological theory toward an understanding of the human microbiome. Science, 2012;336:1255-62.
[3] Bosch TC, McFall-Ngai MJ. Metaorganisms as the new frontier. Zoology (Jena), 2011;114:185-90.
[4] Sleator RD. The human superorganism - of microbes and men. Med Hypotheses, 2010;74:214-5.
[5] Macpherson AJ, McCoy KD. Standardised animal models of host microbial mutualism. Mucosal immunology, 2015;8:476-86.
[6] Turnbaugh PJ, Ley RE, Hamady M, Fraser-Liggett CM, Knight R, Gordon JI. The human microbiome project. Nature, 2007;449:804-10.
[7] Hakansson A, Molin G. Gut microbiota and inflammation. Nutrients, 2011;3:637-82.
[8] McFall-Ngai M, Hadfield MG, Bosch TC, Carey HV, Domazet-Loso T, Douglas AE *et al.* Animals in a bacterial world, a new imperative for the life sciences. Proceedings of the National Academy of Sciences of the United States of America, 2013;110:3229-36.
[9] Chu H, Mazmanian SK. Innate immune recognition of the microbiota promotes host-microbial symbiosis. Nat Immunol, 2013;14:668-75.
[10] Hansen CH, Nielsen DS, Kverka M, Zakostelska Z, Klimesova K, Hudcovic T *et al.* Patterns of early gut colonization shape future immune responses of the host. PLoS One, 2012;7:e34043.
[11] Andrews JM, Tan M. Probiotics in luminal gastroenterology: the current state of play. Intern Med J, 2012;42:1287-91.
[12] Reiff C, Kelly D. Inflammatory bowel disease, gut bacteria and probiotic therapy. Int J Med Microbiol, 2010;300:25-33.
[13] Hooper LV, Gordon JI. Commensal host-bacterial relationships in the gut. Science, 2001;292:1115-8.
[14] Biedermann L, Rogler G. The intestinal microbiota: its role in health and disease. Eur J Pediatr, 2015;174:151-67.
[15] Barreau F, Meinzer U, Chareyre F, Berrebi D, Niwa-Kawakita M, Dussaillant M *et al.* CARD15/NOD2 is required for Peyer's patches homeostasis in mice. PLoS One, 2007;2:e523.
[16] Barreau F, Madre C, Meinzer U, Berrebi D, Dussaillant M, Merlin F *et al.* Nod2 regulates the host response towards microflora by modulating T cell function and epithelial permeability in mouse Peyer's patches. Gut, 2010;59:207-17.
[17] Kamada N, Seo SU, Chen GY, Nunez G. Role of the gut microbiota in immunity and inflammatory disease. Nat Rev Immunol, 2013;13:321-35.
[18] Eckburg PB, Bik EM, Bernstein CN, Purdom E, Dethlefsen L, Sargent M *et al.* Diversity of the human intestinal microbial flora. Science, 2005;308:1635-8.
[19] Ram RJ, Verberkmoes NC, Thelen MP, Tyson GW, Baker BJ, Blake RC, 2nd *et al.* Community proteomics of a natural microbial biofilm. Science, 2005;308:1915-20.
[20] Candela M, Biagi E, Maccaferri S, Turroni S, Brigidi P. Intestinal microbiota is a plastic factor responding to environmental changes. Trends Microbiol, 2012;20:385-91.
[21] Walter J, Ley R. The human gut microbiome: ecology and recent evolutionary changes. Annu Rev Microbiol, 2011;65:411-29.
[22] Ventura M, Turroni F, Motherway MO, MacSharry J, van Sinderen D. Host-microbe interactions that facilitate gut colonization by commensal bifidobacteria. Trends Microbiol, 2012;20:467-76.
[23] Rehman A, Sina C, Gavrilova O, Hasler R, Ott S, Baines JF *et al.* Nod2 is essential for temporal development of intestinal microbial communities. Gut, 2011;60:1354-62.
[24] Backhed F, Ley RE, Sonnenburg JL, Peterson DA, Gordon JI. Host-bacterial mutualism in the human intestine. Science, 2005;307:1915-20.

[25] Honda K, Littman DR. The microbiome in infectious disease and inflammation. Annu Rev Immunol, 2012;30:759-95.
[26] Chow J, Mazmanian SK. A pathobiont of the microbiota balances host colonization and intestinal inflammation. Cell host & microbe, 2010;7:265-76.
[27] Kim SC, Tonkonogy SL, Albright CA, Tsang J, Balish EJ, Braun J *et al.* Variable phenotypes of enterocolitis in interleukin 10-deficient mice monoassociated with two different commensal bacteria. Gastroenterology, 2005;128:891-906.
[28] Waidmann M, Bechtold O, Frick JS, Lehr HA, Schubert S, Dobrindt U *et al.* Bacteroides vulgatus protects against Escherichia coli-induced colitis in gnotobiotic interleukin-2-deficient mice. Gastroenterology, 2003;125:162-77.
[29] Bohn E, Bechtold O, Zahir N, Frick JS, Reimann J, Jilge B *et al.* Host gene expression in the colon of gnotobiotic interleukin-2-deficient mice colonized with commensal colitogenic or noncolitogenic bacterial strains: common patterns and bacteria strain specific signatures. Inflamm Bowel Dis, 2006;12:853-62.
[30] Devkota S, Wang Y, Musch MW, Leone V, Fehlner-Peach H, Nadimpalli A *et al.* Dietary-fat-induced taurocholic acid promotes pathobiont expansion and colitis in Il10-/- mice. Nature, 2012;487:104-8.
[31] Muller M, Fink K, Geisel J, Kahl F, Jilge B, Reimann J *et al.* Intestinal colonization of IL-2 deficient mice with non-colitogenic B. vulgatus prevents DC maturation and T-cell polarization. PLoS One, 2008;3:e2376.
[32] Arimatsu K, Yamada H, Miyazawa H, Minagawa T, Nakajima M, Ryder MI *et al.* Oral pathobiont induces systemic inflammation and metabolic changes associated with alteration of gut microbiota. Sci Rep, 2014;4:4828.
[33] Kamada N, Chen GY, Inohara N, Nunez G. Control of pathogens and pathobionts by the gut microbiota. Nat Immunol, 2013;14:685-90.
[34] Chassaing B, Koren O, Carvalho FA, Ley RE, Gewirtz AT. AIEC pathobiont instigates chronic colitis in susceptible hosts by altering microbiota composition. Gut, 2014;63:1069-80.
[35] Zeuthen LH, Fink LN, Frokiaer H. Epithelial cells prime the immune response to an array of gut-derived commensals towards a tolerogenic phenotype through distinct actions of thymic stromal lymphopoietin and transforming growth factor-beta. Immunology, 2008;123:197-208.
[36] Hornef M. Pathogens, Commensal Symbionts, and Pathobionts: Discovery and Functional Effects on the Host. ILAR J, 2015;56:159-62.
[37] Crost EH, Ajandouz EH, Villard C, Geraert PA, Puigserver A, Fons M. Ruminococcin C, a new anti-Clostridium perfringens bacteriocin produced in the gut by the commensal bacterium Ruminococcus gnavus E1. Biochimie, 2011;93:1487-94.
[38] Hsiao A, Ahmed AM, Subramanian S, Griffin NW, Drewry LL, Petri WA, Jr. *et al.* Members of the human gut microbiota involved in recovery from Vibrio cholerae infection. Nature, 2014;515:423-6.
[39] Biedermann L, Brulisauer K, Zeitz J, Frei P, Scharl M, Vavricka SR *et al.* Smoking cessation alters intestinal microbiota: insights from quantitative investigations on human fecal samples using FISH. Inflamm Bowel Dis, 2014;20:1496-501.
[40] Alhagamhmad MH, Day AS, Lemberg DA, Leach ST. An overview of the bacterial contribution to Crohn disease pathogenesis. J Med Microbiol, 2016.
[41] Edelman SM, Kasper DL. Symbiotic commensal bacteria direct maturation of the host immune system. Curr Opin Gastroenterol, 2008;24:720-4.
[42] Wang Q, McLoughlin RM, Cobb BA, Charrel-Dennis M, Zaleski KJ, Golenbock D *et al.* A bacterial carbohydrate links innate and adaptive responses through Toll-like receptor 2. The Journal of experimental medicine, 2006;203:2853-63.
[43] Coyne MJ, Chatzidaki-Livanis M, Paoletti LC, Comstock LE. Role of glycan synthesis in colonization of the mammalian gut by the bacterial symbiont Bacteroides fragilis.

Proceedings of the National Academy of Sciences of the United States of America, 2008;105:13099-104.
[44] Peterson DA, McNulty NP, Guruge JL, Gordon JI. IgA response to symbiotic bacteria as a mediator of gut homeostasis. Cell host & microbe, 2007;2:328-39.
[45] Lammerts van Bueren A, Saraf A, Martens EC, Dijkhuizen L. Differential Metabolism of Exopolysaccharides from Probiotic Lactobacilli by the Human Gut Symbiont Bacteroides thetaiotaomicron. Applied and environmental microbiology, 2015;81:3973-83.
[46] Steimle A, Gronbach K, Beifuss B, Schafer A, Harmening R, Bender A *et al.* Symbiotic gut commensal bacteria act as host cathepsin S activity regulators. Journal of autoimmunity, 2016.
[47] Lange A, Beier S, Steimle A, Autenrieth IB, Huson DH, Frick JS. Extensive mobilome-driven genome diversification in mouse gut-associated Bacteroides vulgatus mpk. Genome Biol Evol, 2016.
[48] Herfarth H, Rogler G. Inflammatory bowel disease. Endoscopy, 2005;37:42-7.
[49] Steimle A, Di Lorenzo F, Gronbach K, Kliem T, Fuchs K et al. *Bacteroides vulgatus* mpk lipopolysaccharide acts as an anti-inflammatory agent for the treatment of intestinal inflammatory disorders. unpublished manuscript, 2016:1-37.
[50] Steinbach EC, Plevy SE. The role of macrophages and dendritic cells in the initiation of inflammation in IBD. Inflamm Bowel Dis, 2014;20:166-75.
[51] Steimle A, Frick JS. Molecular Mechanisms of Induction of Tolerant and Tolerogenic Intestinal Dendritic Cells in Mice. J Immunol Res, 2016;2016:1958650.
[52] Jostins L, Ripke S, Weersma RK, Duerr RH, McGovern DP, Hui KY *et al.* Host-microbe interactions have shaped the genetic architecture of inflammatory bowel disease. Nature, 2012;491:119-24.
[53] Abegunde AT, Muhammad BH, Bhatti O, Ali T. Environmental risk factors for inflammatory bowel diseases: Evidence based literature review. World journal of gastroenterology : WJG, 2016;22:6296-317.
[54] Duboc H, Rajca S, Rainteau D, Benarous D, Maubert MA, Quervain E *et al.* Connecting dysbiosis, bile-acid dysmetabolism and gut inflammation in inflammatory bowel diseases. Gut, 2013;62:531-9.
[55] Chassaing B, Darfeuille-Michaud A. The commensal microbiota and enteropathogens in the pathogenesis of inflammatory bowel diseases. Gastroenterology, 2011;140:1720-28.
[56] Guarner F. What is the role of the enteric commensal flora in IBD? Inflamm Bowel Dis, 2008;14 Suppl 2:S83-4.
[57] Kumari R, Ahuja V, Paul J. Fluctuations in butyrate-producing bacteria in ulcerative colitis patients of North India. World journal of gastroenterology : WJG, 2013;19:3404-14.
[58] Lees CW, Barrett JC, Parkes M, Satsangi J. New IBD genetics: common pathways with other diseases. Gut, 2011;60:1739-53.
[59] Molodecky NA, Soon IS, Rabi DM, Ghali WA, Ferris M, Chernoff G *et al.* Increasing incidence and prevalence of the inflammatory bowel diseases with time, based on systematic review. Gastroenterology, 2012;142:46-54 e42; quiz e30.
[60] Kang S, Denman SE, Morrison M, Yu Z, Dore J, Leclerc M *et al.* Dysbiosis of fecal microbiota in Crohn's disease patients as revealed by a custom phylogenetic microarray. Inflamm Bowel Dis, 2010;16:2034-42.
[61] Machiels K, Joossens M, Sabino J, De Preter V, Arijs I, Eeckhaut V *et al.* A decrease of the butyrate-producing species Roseburia hominis and Faecalibacterium prausnitzii defines dysbiosis in patients with ulcerative colitis. Gut, 2014;63:1275-83.
[62] Rajilic-Stojanovic M, Shanahan F, Guarner F, de Vos WM. Phylogenetic analysis of dysbiosis in ulcerative colitis during remission. Inflamm Bowel Dis, 2013;19:481-8.
[63] Seksik P, Rigottier-Gois L, Gramet G, Sutren M, Pochart P, Marteau P *et al.* Alterations of the dominant faecal bacterial groups in patients with Crohn's disease of the colon. Gut, 2003;52:237-42.

[64] Sun L, Nava GM, Stappenbeck TS. Host genetic susceptibility, dysbiosis, and viral triggers in inflammatory bowel disease. Curr Opin Gastroenterol, 2011;27:321-7.
[65] Medzhitov R, Janeway CA, Jr. Innate immunity: the virtues of a nonclonal system of recognition. Cell, 1997;91:295-8.
[66] Silipo A, Leone MR, Lanzetta R, Parrilli M, Lackner G, Busch B *et al.* Structural characterization of two lipopolysaccharide O-antigens produced by the endofungal bacterium Burkholderia sp. HKI-402 (B4). Carbohydr Res, 2012;347:95-8.
[67] Alexander C, Rietschel ET. Bacterial lipopolysaccharides and innate immunity. J Endotoxin Res, 2001;7:167-202.
[68] Steimle A, Autenrieth IB, Frick JS. Structure and function: Lipid A modifications in commensals and pathogens. Int J Med Microbiol, 2016.
[69] Galanos C, Freudenberg MA. Bacterial endotoxins: biological properties and mechanisms of action. Mediators Inflamm, 1993;2:S11-6.
[70] Homma JY, Matsuura M, Kanegasaki S, Kawakubo Y, Kojima Y, Shibukawa N *et al.* Structural requirements of lipid A responsible for the functions: a study with chemically synthesized lipid A and its analogues. J Biochem, 1985;98:395-406.
[71] Kotani S, Takada H, Tsujimoto M, Ogawa T, Takahashi I, Ikeda T *et al.* Synthetic lipid A with endotoxic and related biological activities comparable to those of a natural lipid A from an Escherichia coli re-mutant. Infection and immunity, 1985;49:225-37.
[72] Brandenburg K, Mayer H, Koch MH, Weckesser J, Rietschel ET, Seydel U. Influence of the supramolecular structure of free lipid A on its biological activity. Eur J Biochem, 1993;218:555-63.
[73] Seydel U, Oikawa M, Fukase K, Kusumoto S, Brandenburg K. Intrinsic conformation of lipid A is responsible for agonistic and antagonistic activity. Eur J Biochem, 2000;267:3032-9.
[74] Molinaro A, Holst O, Di Lorenzo F, Callaghan M, Nurisso A, D'Errico G *et al.* Chemistry of lipid A: at the heart of innate immunity. Chemistry, 2015;21:500-19.
[75] Raetz CR, Whitfield C. Lipopolysaccharide endotoxins. Annu Rev Biochem, 2002;71:635-700.
[76] Akira S, Takeda K. Toll-like receptor signalling. Nat Rev Immunol, 2004;4:499-511.
[77] Park BS, Song DH, Kim HM, Choi BS, Lee H, Lee JO. The structural basis of lipopolysaccharide recognition by the TLR4-MD-2 complex. Nature, 2009;458:1191-5.
[78] Miyake K. Roles for accessory molecules in microbial recognition by Toll-like receptors. J Endotoxin Res, 2006;12:195-204.
[79] Hansen GH, Rasmussen K, Niels-Christiansen LL, Danielsen EM. Lipopolysaccharide-binding protein: localization in secretory granules of Paneth cells in the mouse small intestine. Histochem Cell Biol, 2009;131:727-32.
[80] Wright SD, Ramos RA, Tobias PS, Ulevitch RJ, Mathison JC. CD14, a receptor for complexes of lipopolysaccharide (LPS) and LPS binding protein. Science, 1990;249:1431-3.
[81] Gioannini TL, Weiss JP. Regulation of interactions of Gram-negative bacterial endotoxins with mammalian cells. Immunol Res, 2007;39:249-60.
[82] Tan Y, Kagan JC. A cross-disciplinary perspective on the innate immune responses to bacterial lipopolysaccharide. Mol Cell, 2014;54:212-23.
[83] Park SH, Kim ND, Jung JK, Lee CK, Han SB, Kim Y. Myeloid differentiation 2 as a therapeutic target of inflammatory disorders. Pharmacol Ther, 2012;133:291-8.
[84] Ohto U, Fukase K, Miyake K, Satow Y. Crystal structures of human MD-2 and its complex with antiendotoxic lipid IVa. Science, 2007;316:1632-4.
[85] Ohto U, Fukase K, Miyake K, Shimizu T. Structural basis of species-specific endotoxin sensing by innate immune receptor TLR4/MD-2. Proceedings of the National Academy of Sciences of the United States of America, 2012;109:7421-6.
[86] Rathinam VA, Vanaja SK, Waggoner L, Sokolovska A, Becker C, Stuart LM *et al.* TRIF licenses caspase-11-dependent NLRP3 inflammasome activation by gram-negative bacteria. Cell, 2012;150:606-19.

[87] Broz P, Ohlson MB, Monack DM. Innate immune response to Salmonella typhimurium, a model enteric pathogen. Gut Microbes, 2012;3:62-70.
[88] Case CL, Kohler LJ, Lima JB, Strowig T, de Zoete MR, Flavell RA *et al.* Caspase-11 stimulates rapid flagellin-independent pyroptosis in response to Legionella pneumophila. Proceedings of the National Academy of Sciences of the United States of America, 2013;110:1851-6.
[89] Aachoui Y, Leaf IA, Hagar JA, Fontana MF, Campos CG, Zak DE *et al.* Caspase-11 protects against bacteria that escape the vacuole. Science, 2013;339:975-8.
[90] Kayagaki N, Wong MT, Stowe IB, Ramani SR, Gonzalez LC, Akashi-Takamura S *et al.* Noncanonical inflammasome activation by intracellular LPS independent of TLR4. Science, 2013;341:1246-9.
[91] Kayagaki N, Warming S, Lamkanfi M, Vande Walle L, Louie S, Dong J *et al.* Non-canonical inflammasome activation targets caspase-11. Nature, 2011;479:117-21.
[92] Mariathasan S, Weiss DS, Newton K, McBride J, O'Rourke K, Roose-Girma M *et al.* Cryopyrin activates the inflammasome in response to toxins and ATP. Nature, 2006;440:228-32.
[93] Schroder K, Tschopp J. The inflammasomes. Cell, 2010;140:821-32.
[94] Takeuchi O, Akira S. Pattern recognition receptors and inflammation. Cell, 2010;140:805-20.
[95] Iwasaki A, Medzhitov R. Regulation of adaptive immunity by the innate immune system. Science, 2010;327:291-5.
[96] Steinman RM. Decisions about dendritic cells: past, present, and future. Annu Rev Immunol, 2012;30:1-22.
[97] Ohnmacht C, Pullner A, King SB, Drexler I, Meier S, Brocker T *et al.* Constitutive ablation of dendritic cells breaks self-tolerance of CD4 T cells and results in spontaneous fatal autoimmunity. The Journal of experimental medicine, 2009;206:549-59.
[98] Delamarre L, Holcombe H, Mellman I. Presentation of exogenous antigens on major histocompatibility complex (MHC) class I and MHC class II molecules is differentially regulated during dendritic cell maturation. The Journal of experimental medicine, 2003;198:111-22.
[99] Frick JS, Zahir N, Muller M, Kahl F, Bechtold O, Lutz MB *et al.* Colitogenic and non-colitogenic commensal bacteria differentially trigger DC maturation and Th cell polarization: an important role for IL-6. European journal of immunology, 2006;36:1537-47.
[100] Menges M, Rossner S, Voigtlander C, Schindler H, Kukutsch NA, Bogdan C *et al.* Repetitive injections of dendritic cells matured with tumor necrosis factor alpha induce antigen-specific protection of mice from autoimmunity. The Journal of experimental medicine, 2002;195:15-21.
[101] Unger WW, Laban S, Kleijwegt FS, van der Slik AR, Roep BO. Induction of Treg by monocyte-derived DC modulated by vitamin D3 or dexamethasone: differential role for PD-L1. European journal of immunology, 2009;39:3147-59.
[102] Shen Y, Giardino Torchia ML, Lawson GW, Karp CL, Ashwell JD, Mazmanian SK. Outer membrane vesicles of a human commensal mediate immune regulation and disease protection. Cell host & microbe, 2012;12:509-20.
[103] Uematsu S, Fujimoto K, Jang MH, Yang BG, Jung YJ, Nishiyama M *et al.* Regulation of humoral and cellular gut immunity by lamina propria dendritic cells expressing Toll-like receptor 5. Nat Immunol, 2008;9:769-76.
[104] Setoguchi R, Hori S, Takahashi T, Sakaguchi S. Homeostatic maintenance of natural Foxp3(+) CD25(+) CD4(+) regulatory T cells by interleukin (IL)-2 and induction of autoimmune disease by IL-2 neutralization. The Journal of experimental medicine, 2005;201:723-35.
[105] Geisel J, Kahl F, Muller M, Wagner H, Kirschning CJ, Autenrieth IB *et al.* IL-6 and maturation govern TLR2 and TLR4 induced TLR agonist tolerance and cross-tolerance in dendritic cells. J Immunol, 2007;179:5811-8.
[106] Ozeri E, Mizrahi M, Shahaf G, Lewis EC. alpha-1 antitrypsin promotes semimature, IL-10-producing and readily migrating tolerogenic dendritic cells. J Immunol, 2012;189:146-53.

[107] Lutz MB. Therapeutic potential of semi-mature dendritic cells for tolerance induction. Front Immunol, 2012;3:123.
[108] Manicassamy S, Pulendran B. Dendritic cell control of tolerogenic responses. Immunol Rev, 2011;241:206-27.
[109] Sartor RB. Microbial influences in inflammatory bowel diseases. Gastroenterology, 2008;134:577-94.
[110] Gronbach K, Flade I, Holst O, Lindner B, Ruscheweyh HJ, Wittmann A *et al.* Endotoxicity of lipopolysaccharide as a determinant of T-cell-mediated colitis induction in mice. Gastroenterology, 2014;146:765-75.
[111] Littman DR, Rudensky AY. Th17 and regulatory T cells in mediating and restraining inflammation. Cell, 2010;140:845-58.
[112] Calderon-Gomez E, Bassolas-Molina H, Mora-Buch R, Dotti I, Planell N, Esteller M *et al.* Commensal-Specific CD4(+) Cells From Patients With Crohn's Disease Have a T-Helper 17 Inflammatory Profile. Gastroenterology, 2016;151:489-500 e3.
[113] Reith W, LeibundGut-Landmann S, Waldburger JM. Regulation of MHC class II gene expression by the class II transactivator. Nat Rev Immunol, 2005;5:793-806.
[114] Villadangos JA, Schnorrer P, Wilson NS. Control of MHC class II antigen presentation in dendritic cells: a balance between creative and destructive forces. Immunol Rev, 2005;207:191-205.
[115] Roche PA, Furuta K. The ins and outs of MHC class II-mediated antigen processing and presentation. Nat Rev Immunol, 2015;15:203-16.
[116] Kleijmeer MJ, Ossevoort MA, van Veen CJ, van Hellemond JJ, Neefjes JJ, Kast WM *et al.* MHC class II compartments and the kinetics of antigen presentation in activated mouse spleen dendritic cells. J Immunol, 1995;154:5715-24.
[117] Conus S, Simon HU. Cathepsins and their involvement in immune responses. Swiss medical weekly, 2010;140:w13042.
[118] Driessen C, Bryant RA, Lennon-Dumenil AM, Villadangos JA, Bryant PW, Shi GP *et al.* Cathepsin S controls the trafficking and maturation of MHC class II molecules in dendritic cells. The Journal of cell biology, 1999;147:775-90.
[119] Beers C, Burich A, Kleijmeer MJ, Griffith JM, Wong P, Rudensky AY. Cathepsin S controls MHC class II-mediated antigen presentation by epithelial cells in vivo. J Immunol, 2005;174:1205-12.
[120] Steimle A, Frick JS. The challenge of specific Cathepsin S activity detection in experimental settings J Neurol Neuromed, 2016;1:7.
[121] Sage J, Mallevre F, Barbarin-Costes F, Samsonov SA, Gehrcke JP, Pisabarro MT *et al.* Binding of chondroitin 4-sulfate to cathepsin S regulates its enzymatic activity. Biochemistry, 2013;52:6487-98.
[122] Hsing LC, Rudensky AY. The lysosomal cysteine proteases in MHC class II antigen presentation. Immunol Rev, 2005;207:229-41.
[123] Lalmanach G, Saidi A, Marchand-Adam S, Lecaille F, Kasabova M. Cysteine cathepsins and cystatins: from ancillary tasks to prominent status in lung diseases. Biol Chem, 2015;396:111-30.
[124] Cox JM, Troutt JS, Knierman MD, Siegel RW, Qian YW, Ackermann BL *et al.* Determination of cathepsin S abundance and activity in human plasma and implications for clinical investigation. Anal Biochem, 2012;430:130-7.
[125] Haves-Zburof D, Paperna T, Gour-Lavie A, Mandel I, Glass-Marmor L, Miller A. Cathepsins and their endogenous inhibitors cystatins: expression and modulation in multiple sclerosis. J Cell Mol Med, 2011;15:2421-9.
[126] Staun-Ram E, Miller A. Cathepsins (S and B) and their inhibitor Cystatin C in immune cells: modulation by interferon-beta and role played in cell migration. J Neuroimmunol, 2011;232:200-6.

[127] Magister S, Obermajer N, Mirkovic B, Svajger U, Renko M, Softic A *et al.* Regulation of cathepsins S and L by cystatin F during maturation of dendritic cells. Eur J Cell Biol, 2012;91:391-401.
[128] Vogel H, Altincicek B, Glockner G, Vilcinskas A. A comprehensive transcriptome and immune-gene repertoire of the lepidopteran model host Galleria mellonella. BMC genomics, 2011;12:308.
[129] Alghoribi MF, Gibreel TM, Dodgson AR, Beatson SA, Upton M. Galleria mellonella infection model demonstrates high lethality of ST69 and ST127 uropathogenic E. coli. PLoS One, 2014;9:e101547.
[130] Hsing LC, Kirk EA, McMillen TS, Hsiao SH, Caldwell M, Houston B *et al.* Roles for cathepsins S, L, and B in insulitis and diabetes in the NOD mouse. Journal of autoimmunity, 2010;34:96-104.
[131] Li X, Wu K, Edman M, Schenke-Layland K, MacVeigh-Aloni M, Janga SR *et al.* Increased expression of cathepsins and obesity-induced proinflammatory cytokines in lacrimal glands of male NOD mouse. Investigative ophthalmology & visual science, 2010;51:5019-29.
[132] Hamm-Alvarez SF, Janga SR, Edman MC, Madrigal S, Shah M, Frousiakis SE *et al.* Tear cathepsin S as a candidate biomarker for Sjogren's syndrome. Arthritis Rheumatol, 2014;66:1872-81.
[133] Giannouli M, Palatucci AT, Rubino V, Ruggiero G, Romano M, Triassi M *et al.* Use of larvae of the wax moth Galleria mellonella as an in vivo model to study the virulence of Helicobacter pylori. BMC microbiology, 2014;14:228.
[134] Samokhin AO, Lythgo PA, Gauthier JY, Percival MD, Bromme D. Pharmacological inhibition of cathepsin S decreases atherosclerotic lesions in Apoe-/- mice. Journal of cardiovascular pharmacology, 2010;56:98-105.
[135] Figueiredo JL, Aikawa M, Zheng C, Aaron J, Lax L, Libby P *et al.* Selective cathepsin S inhibition attenuates atherosclerosis in apolipoprotein E-deficient mice with chronic renal disease. Am J Pathol, 2015;185:1156-66.
[136] Cattaruzza F, Lyo V, Jones E, Pham D, Hawkins J, Kirkwood K *et al.* Cathepsin S is activated during colitis and causes visceral hyperalgesia by a PAR2-dependent mechanism in mice. Gastroenterology, 2011;141:1864-74 e1-3.
[137] Gupta S, Singh RK, Dastidar S, Ray A. Cysteine cathepsin S as an immunomodulatory target: present and future trends. Expert Opin Ther Targets, 2008;12:291-9.
[138] Gerlach AM, Steimle A, Krampen L, Wittmann A, Gronbach K, Geisel J *et al.* Role of CD40 ligation in dendritic cell semimaturation. BMC Immunol, 2012;13:22.
[139] Kapsenberg ML. Dendritic-cell control of pathogen-driven T-cell polarization. Nat Rev Immunol, 2003;3:984-93.
[140] Bennett SR, Carbone FR, Karamalis F, Flavell RA, Miller JF, Heath WR. Help for cytotoxic-T-cell responses is mediated by CD40 signalling. Nature, 1998;393:478-80.
[141] Chang WL, Baumgarth N, Eberhardt MK, Lee CY, Baron CA, Gregg JP *et al.* Exposure of myeloid dendritic cells to exogenous or endogenous IL-10 during maturation determines their longevity. J Immunol, 2007;178:7794-804.
[142] Caux C, Massacrier C, Vanbervliet B, Dubois B, Van Kooten C, Durand I *et al.* Activation of human dendritic cells through CD40 cross-linking. The Journal of experimental medicine, 1994;180:1263-72.
[143] Koch F, Stanzl U, Jennewein P, Janke K, Heufler C, Kampgen E *et al.* High level IL-12 production by murine dendritic cells: upregulation via MHC class II and CD40 molecules and downregulation by IL-4 and IL-10. The Journal of experimental medicine, 1996;184:741-6.
[144] Toso JF, Lapointe R, Hwu P. CD40 ligand and lipopolysaccharide enhance the in vitro generation of melanoma-reactive T-cells. Journal of immunological methods, 2002;259:181-90.
[145] Cella M, Scheidegger D, Palmer-Lehmann K, Lane P, Lanzavecchia A, Alber G. Ligation of CD40 on dendritic cells triggers production of high levels of interleukin-12 and enhances T cell

stimulatory capacity: T-T help via APC activation. The Journal of experimental medicine, 1996;184:747-52.
[146] Bjorck P, Banchereau J, Flores-Romo L. CD40 ligation counteracts Fas-induced apoptosis of human dendritic cells. Int Immunol, 1997;9:365-72.
[147] Wong BR, Josien R, Lee SY, Sauter B, Li HL, Steinman RM *et al.* TRANCE (tumor necrosis factor [TNF]-related activation-induced cytokine), a new TNF family member predominantly expressed in T cells, is a dendritic cell-specific survival factor. The Journal of experimental medicine, 1997;186:2075-80.
[148] Boonstra A, Rajsbaum R, Holman M, Marques R, Asselin-Paturel C, Pereira JP *et al.* Macrophages and myeloid dendritic cells, but not plasmacytoid dendritic cells, produce IL-10 in response to MyD88- and TRIF-dependent TLR signals, and TLR-independent signals. J Immunol, 2006;177:7551-8.
[149] Dohnal AM, Luger R, Paul P, Fuchs D, Felzmann T. CD40 ligation restores type 1 polarizing capacity in TLR4-activated dendritic cells that have ceased interleukin-12 expression. J Cell Mol Med, 2009;13:1741-50.
[150] Lapointe R, Toso JF, Butts C, Young HA, Hwu P. Human dendritic cells require multiple activation signals for the efficient generation of tumor antigen-specific T lymphocytes. European journal of immunology, 2000;30:3291-8.
[151] Dhodapkar MV, Steinman RM, Krasovsky J, Munz C, Bhardwaj N. Antigen-specific inhibition of effector T cell function in humans after injection of immature dendritic cells. The Journal of experimental medicine, 2001;193:233-8.
[152] Steinman RM, Hawiger D, Nussenzweig MC. Tolerogenic dendritic cells. Annu Rev Immunol, 2003;21:685-711.
[153] Fujii S, Liu K, Smith C, Bonito AJ, Steinman RM. The linkage of innate to adaptive immunity via maturing dendritic cells in vivo requires CD40 ligation in addition to antigen presentation and CD80/86 costimulation. The Journal of experimental medicine, 2004;199:1607-18.
[154] Martin E, O'Sullivan B, Low P, Thomas R. Antigen-specific suppression of a primed immune response by dendritic cells mediated by regulatory T cells secreting interleukin-10. Immunity, 2003;18:155-67.
[155] Murugaiyan G, Martin S, Saha B. Levels of CD40 expression on dendritic cells dictate tumour growth or regression. Clinical and experimental immunology, 2007;149:194-202.
[156] Smith DW, Nagler-Anderson C. Preventing intolerance: the induction of nonresponsiveness to dietary and microbial antigens in the intestinal mucosa. J Immunol, 2005;174:3851-7.
[157] Suzuki M, Zheng X, Zhang X, Ichim TE, Sun H, Kubo N *et al.* Inhibition of allergic responses by CD40 gene silencing. Allergy, 2009;64:387-97.
[158] Joffre O, Nolte MA, Sporri R, Reis e Sousa C. Inflammatory signals in dendritic cell activation and the induction of adaptive immunity. Immunol Rev, 2009;227:234-47.
[159] Lutz MB, Schuler G. Immature, semi-mature and fully mature dendritic cells: which signals induce tolerance or immunity? Trends Immunol, 2002;23:445-9.
[160] Snijders A, Kalinski P, Hilkens CM, Kapsenberg ML. High-level IL-12 production by human dendritic cells requires two signals. Int Immunol, 1998;10:1593-8.
[161] Schulz O, Edwards AD, Schito M, Aliberti J, Manickasingham S, Sher A *et al.* CD40 triggering of heterodimeric IL-12 p70 production by dendritic cells in vivo requires a microbial priming signal. Immunity, 2000;13:453-62.
[162] Morelli AE, Zahorchak AF, Larregina AT, Colvin BL, Logar AJ, Takayama T *et al.* Cytokine production by mouse myeloid dendritic cells in relation to differentiation and terminal maturation induced by lipopolysaccharide or CD40 ligation. Blood, 2001;98:1512-23.
[163] Kato T, Hakamada R, Yamane H, Nariuchi H. Induction of IL-12 p40 messenger RNA expression and IL-12 production of macrophages via CD40-CD40 ligand interaction. J Immunol, 1996;156:3932-8.

[164] Alderson MR, Armitage RJ, Tough TW, Strockbine L, Fanslow WC, Spriggs MK. CD40 expression by human monocytes: regulation by cytokines and activation of monocytes by the ligand for CD40. The Journal of experimental medicine, 1993;178:669-74.
[165] Nguyen VT, Benveniste EN. Critical role of tumor necrosis factor-alpha and NF-kappa B in interferon-gamma -induced CD40 expression in microglia/macrophages. J Biol Chem, 2002;277:13796-803.
[166] Wesemann DR, Dong Y, O'Keefe GM, Nguyen VT, Benveniste EN. Suppressor of cytokine signaling 1 inhibits cytokine induction of CD40 expression in macrophages. J Immunol, 2002;169:2354-60.
[167] Maloy KJ, Powrie F. Intestinal homeostasis and its breakdown in inflammatory bowel disease. Nature, 2011;474:298-306.
[168] Gross M, Salame TM, Jung S. Guardians of the Gut - Murine Intestinal Macrophages and Dendritic Cells. Front Immunol, 2015;6:254.
[169] Liu J, Cao X. Regulatory dendritic cells in autoimmunity: A comprehensive review. Journal of autoimmunity, 2015;63:1-12.
[170] Ben Addi A, Lefort A, Hua X, Libert F, Communi D, Ledent C *et al.* Modulation of murine dendritic cell function by adenine nucleotides and adenosine: involvement of the A(2B) receptor. European journal of immunology, 2008;38:1610-20.
[171] Nono JK, Pletinckx K, Lutz MB, Brehm K. Excretory/secretory-products of Echinococcus multilocularis larvae induce apoptosis and tolerogenic properties in dendritic cells in vitro. PLoS Negl Trop Dis, 2012;6:e1516.
[172] Morelli AE, Thomson AW. Tolerogenic dendritic cells and the quest for transplant tolerance. Nat Rev Immunol, 2007;7:610-21.
[173] Iwasaki A, Medzhitov R. Control of adaptive immunity by the innate immune system. Nat Immunol, 2015;16:343-53.
[174] Toledano N, Gur-Wahnon D, Ben-Yehuda A, Rachmilewitz J. Novel CD47: SIRPalpha dependent mechanism for the activation of STAT3 in antigen-presenting cell. PLoS One, 2013;8:e75595.
[175] Cheng F, Wang HW, Cuenca A, Huang M, Ghansah T, Brayer J *et al.* A critical role for Stat3 signaling in immune tolerance. Immunity, 2003;19:425-36.
[176] Seiffart V, Zoeller J, Klopfleisch R, Wadwa M, Hansen W, Buer J *et al.* IL10-Deficiency in CD4 T Cells Exacerbates the IFNgamma and IL17 Response During Bacteria Induced Colitis. Cell Physiol Biochem, 2015;36:1259-73.
[177] Saraiva M, O'Garra A. The regulation of IL-10 production by immune cells. Nat Rev Immunol, 2010;10:170-81.
[178] Shouval DS, Ouahed J, Biswas A, Goettel JA, Horwitz BH, Klein C *et al.* Interleukin 10 receptor signaling: master regulator of intestinal mucosal homeostasis in mice and humans. Adv Immunol, 2014;122:177-210.
[179] Begue B, Verdier J, Rieux-Laucat F, Goulet O, Morali A, Canioni D *et al.* Defective IL10 signaling defining a subgroup of patients with inflammatory bowel disease. Am J Gastroenterol, 2011;106:1544-55.
[180] Buruiana FE, Sola I, Alonso-Coello P. Recombinant human interleukin 10 for induction of remission in Crohn's disease. Cochrane Database Syst Rev, 2010:CD005109.
[181] Chang J, Kunkel SL, Chang CH. Negative regulation of MyD88-dependent signaling by IL-10 in dendritic cells. Proceedings of the National Academy of Sciences of the United States of America, 2009;106:18327-32.
[182] Rakoff-Nahoum S, Hao L, Medzhitov R. Role of toll-like receptors in spontaneous commensal-dependent colitis. Immunity, 2006;25:319-29.
[183] Kawai T, Akira S. TLR signaling. Cell Death Differ, 2006;13:816-25.
[184] Rescigno M, Di Sabatino A. Dendritic cells in intestinal homeostasis and disease. J Clin Invest, 2009;119:2441-50.

[185] Porta C, Rimoldi M, Raes G, Brys L, Ghezzi P, Di Liberto D *et al.* Tolerance and M2 (alternative) macrophage polarization are related processes orchestrated by p50 nuclear factor kappaB. Proceedings of the National Academy of Sciences of the United States of America, 2009;106:14978-83.
[186] Bonizzi G, Karin M. The two NF-kappaB activation pathways and their role in innate and adaptive immunity. Trends Immunol, 2004;25:280-8.
[187] Larghi P, Porta C, Riboldi E, Totaro MG, Carraro L, Orabona C *et al.* The p50 subunit of NF-kappaB orchestrates dendritic cell lifespan and activation of adaptive immunity. PLoS One, 2012;7:e45279.
[188] Shevach EM. Mechanisms of foxp3+ T regulatory cell-mediated suppression. Immunity, 2009;30:636-45.
[189] Ziegler-Heitbrock HW, Petersmann I, Frankenberger M. p50 (NF-kappa B1) is upregulated in LPS tolerant P388D1 murine macrophages. Immunobiology, 1997;198:73-80.
[190] Manicassamy S, Reizis B, Ravindran R, Nakaya H, Salazar-Gonzalez RM, Wang YC *et al.* Activation of beta-catenin in dendritic cells regulates immunity versus tolerance in the intestine. Science, 2010;329:849-53.
[191] Liberman R, Bond S, Shainheit MG, Stadecker MJ, Forgac M. Regulated assembly of vacuolar ATPase is increased during cluster disruption-induced maturation of dendritic cells through a phosphatidylinositol 3-kinase/mTOR-dependent pathway. J Biol Chem, 2014;289:1355-63.
[192] Trombetta ES, Ebersold M, Garrett W, Pypaert M, Mellman I. Activation of lysosomal function during dendritic cell maturation. Science, 2003;299:1400-3.
[193] Vander Lugt B, Beck ZT, Fuhlbrigge RC, Hacohen N, Campbell JJ, Boes M. TGF-beta suppresses beta-catenin-dependent tolerogenic activation program in dendritic cells. PLoS One, 2011;6:e20099.
[194] Huang G, Shi LZ, Chi H. Regulation of JNK and p38 MAPK in the immune system: signal integration, propagation and termination. Cytokine, 2009;48:161-9.
[195] Huang G, Wang Y, Vogel P, Kanneganti TD, Otsu K, Chi H. Signaling via the kinase p38alpha programs dendritic cells to drive TH17 differentiation and autoimmune inflammation. Nat Immunol, 2012;13:152-61.
[196] Ochoa-Reparaz J, Mielcarz DW, Wang Y, Begum-Haque S, Dasgupta S, Kasper DL *et al.* A polysaccharide from the human commensal Bacteroides fragilis protects against CNS demyelinating disease. Mucosal immunology, 2010;3:487-95.
[197] Ochoa-Reparaz J, Mielcarz DW, Ditrio LE, Burroughs AR, Begum-Haque S, Dasgupta S *et al.* Central nervous system demyelinating disease protection by the human commensal Bacteroides fragilis depends on polysaccharide A expression. J Immunol, 2010;185:4101-8.
[198] Round JL, Lee SM, Li J, Tran G, Jabri B, Chatila TA *et al.* The Toll-like receptor 2 pathway establishes colonization by a commensal of the human microbiota. Science, 2011;332:974-7.
[199] Salvador JM, Mittelstadt PR, Belova GI, Fornace AJ, Jr., Ashwell JD. The autoimmune suppressor Gadd45alpha inhibits the T cell alternative p38 activation pathway. Nat Immunol, 2005;6:396-402.
[200] Perruche S, Zhang P, Liu Y, Saas P, Bluestone JA, Chen W. CD3-specific antibody-induced immune tolerance involves transforming growth factor-beta from phagocytes digesting apoptotic T cells. Nat Med, 2008;14:528-35.
[201] Kuang R, Perruche S, Chen W. Apoptotic cell-linked immunoregulation: implications for promoting immune tolerance in transplantation. Cell Biosci, 2015;5:27.
[202] da Costa TB, Sardinha LR, Larocca R, Peron JP, Rizzo LV. Allogeneic apoptotic thymocyte-stimulated dendritic cells expand functional regulatory T cells. Immunology, 2011;133:123-32.
[203] Gleisner MA, Rosemblatt M, Fierro JA, Bono MR. Delivery of alloantigens via apoptotic cells generates dendritic cells with an immature tolerogenic phenotype. Transplant Proc, 2011;43:2325-33.

[204] Zhou F, Lauretti E, di Meco A, Ciric B, Gonnella P, Zhang GX *et al.* Intravenous transfer of apoptotic cell-treated dendritic cells leads to immune tolerance by blocking Th17 cell activity. Immunobiology, 2013;218:1069-76.
[205] Perone MJ, Bertera S, Tawadrous ZS, Shufesky WJ, Piganelli JD, Baum LG *et al.* Dendritic cells expressing transgenic galectin-1 delay onset of autoimmune diabetes in mice. J Immunol, 2006;177:5278-89.
[206] Ilarregui JM, Croci DO, Bianco GA, Toscano MA, Salatino M, Vermeulen ME *et al.* Tolerogenic signals delivered by dendritic cells to T cells through a galectin-1-driven immunoregulatory circuit involving interleukin 27 and interleukin 10. Nat Immunol, 2009;10:981-91.
[207] Xiang M, Lu J, Zhang C, Lan Y, Zhou H, Li X *et al.* Identification and quantification of total coumarins from Urtica dentata Hand and its roles in promoting immune tolerance via TLR4-mediated dendritic cell immaturation. Biosci Biotechnol Biochem, 2013;77:1200-6.
[208] Turnquist HR, Raimondi G, Zahorchak AF, Fischer RT, Wang Z, Thomson AW. Rapamycin-conditioned dendritic cells are poor stimulators of allogeneic CD4+ T cells, but enrich for antigen-specific Foxp3+ T regulatory cells and promote organ transplant tolerance. J Immunol, 2007;178:7018-31.
[209] Marin-Gallen S, Clemente-Casares X, Planas R, Pujol-Autonell I, Carrascal J, Carrillo J *et al.* Dendritic cells pulsed with antigen-specific apoptotic bodies prevent experimental type 1 diabetes. Clinical and experimental immunology, 2010;160:207-14.
[210] Knip M, Siljander H. Autoimmune mechanisms in type 1 diabetes. Autoimmun Rev, 2008;7:550-7.
[211] Cabezon R, Ricart E, Espana C, Panes J, Benitez-Ribas D. Gram-negative enterobacteria induce tolerogenic maturation in dexamethasone conditioned dendritic cells. PLoS One, 2012;7:e52456.
[212] Steimle A, Kalbacher H, Maurer A, Beifuss B, Bender A, Schafer A *et al.* A novel approach for reliable detection of cathepsin S activities in mouse antigen presenting cells. Journal of immunological methods, 2016;432:87-94.
[213] Choe Y, Leonetti F, Greenbaum DC, Lecaille F, Bogyo M, Bromme D *et al.* Substrate profiling of cysteine proteases using a combinatorial peptide library identifies functionally unique specificities. J Biol Chem, 2006;281:12824-32.
[214] Lutzner N, Kalbacher H. Quantifying cathepsin S activity in antigen presenting cells using a novel specific substrate. J Biol Chem, 2008;283:36185-94.
[215] Serim S, Haedke U, Verhelst SH. Activity-based probes for the study of proteases: recent advances and developments. ChemMedChem, 2012;7:1146-59.
[216] Ben-Aderet L, Merquiol E, Fahham D, Kumar A, Reich E, Ben-Nun Y *et al.* Detecting cathepsin activity in human osteoarthritis via activity-based probes. Arthritis Res Ther, 2015;17:69.
[217] Kohl F, Schmitz J, Furtmann N, Schulz-Fincke AC, Mertens MD, Kuppers J *et al.* Design, characterization and cellular uptake studies of fluorescence-labeled prototypic cathepsin inhibitors. Organic & biomolecular chemistry, 2015.
[218] Hughes CS, Shaw G, Burden RE, Scott CJ, Gilmore BF. The application of a novel, cell permeable activity-based probe for the detection of cysteine cathepsins. Biochem Biophys Res Commun, 2016;472:444-50.
[219] Caglic D, Repnik U, Jedeszko C, Kosec G, Miniejew C, Kindermann M *et al.* The proinflammatory cytokines interleukin-1alpha and tumor necrosis factor alpha promote the expression and secretion of proteolytically active cathepsin S from human chondrocytes. Biol Chem, 2013;394:307-16.
[220] Oresic Bender K, Ofori L, van der Linden WA, Mock ED, Datta GK, Chowdhury S *et al.* Design of a highly selective quenched activity-based probe and its application in dual color imaging studies of cathepsin S activity localization. J Am Chem Soc, 2015;137:4771-7.
[221] Veilleux A, Black WC, Gauthier JY, Mellon C, Percival MD, Tawa P *et al.* Probing cathepsin S activity in whole blood by the activity-based probe BIL-DMK: cellular distribution in human leukocyte populations and evidence of diurnal modulation. Anal Biochem, 2011;411:43-9.

[222] Mertens MD, Schmitz J, Horn M, Furtmann N, Bajorath J, Mares M *et al.* A coumarin-labeled vinyl sulfone as tripeptidomimetic activity-based probe for cysteine cathepsins. Chembiochem, 2014;15:955-9.
[223] Garenne T, Saidi A, Gilmore BF, Niemiec E, Roy V, Agrofoglio LA *et al.* Active site labeling of cysteine cathepsins by a straightforward diazomethylketone probe derived from the N-terminus of human cystatin C. Biochem Biophys Res Commun, 2015;460:250-4.
[224] Barlow N, Nasser Y, Zhao P, Sharma N, Guerrero-Alba R, Edgington-Mitchell LE *et al.* Demonstration of elevated levels of active cathepsin S in dextran sulfate sodium colitis using a new activatable probe. Neurogastroenterology and motility : the official journal of the European Gastrointestinal Motility Society, 2015.
[225] Castellano J, Badimon L, Llorente-Cortes V. Amyloid-beta increases metallo- and cysteine protease activities in human macrophages. J Vasc Res, 2014;51:58-67.
[226] Baugh M, Black D, Westwood P, Kinghorn E, McGregor K, Bruin J *et al.* Therapeutic dosing of an orally active, selective cathepsin S inhibitor suppresses disease in models of autoimmunity. Journal of autoimmunity, 2011;36:201-9.
[227] Schwarz G, Boehncke WH, Braun M, Schroter CJ, Burster T, Flad T *et al.* Cathepsin S activity is detectable in human keratinocytes and is selectively upregulated upon stimulation with interferon-gamma. J Invest Dermatol, 2002;119:44-9.
[228] Balce DR, Allan ER, McKenna N, Yates RM. gamma-Interferon-inducible lysosomal thiol reductase (GILT) maintains phagosomal proteolysis in alternatively activated macrophages. J Biol Chem, 2014;289:31891-904.
[229] Zhao P, Lieu T, Barlow N, Metcalf M, Veldhuis NA, Jensen DD *et al.* Cathepsin S causes inflammatory pain via biased agonism of PAR2 and TRPV4. J Biol Chem, 2014;289:27215-34.
[230] Katritzky AR, Cusido J, Narindoshvili T. Monosaccharide-based water-soluble fluorescent tags. Bioconjug Chem, 2008;19:1471-5.
[231] McLean MH, Dieguez D, Jr., Miller LM, Young HA. Does the microbiota play a role in the pathogenesis of autoimmune diseases? Gut, 2015;64:332-41.
[232] Kostic AD, Xavier RJ, Gevers D. The microbiome in inflammatory bowel disease: current status and the future ahead. Gastroenterology, 2014;146:1489-99.
[233] Harding CR, Schroeder GN, Reynolds S, Kosta A, Collins JW, Mousnier A *et al.* Legionella pneumophila pathogenesis in the Galleria mellonella infection model. Infection and immunity, 2012;80:2780-90.
[234] Xu Y, Lindemann P, Vega-Ramos J, Zhang JG, Villadangos JA. Developmental regulation of synthesis and dimerization of the amyloidogenic protease inhibitor cystatin C in the hematopoietic system. J Biol Chem, 2014;289:9730-40.
[235] Qian F, Chan SJ, Gong QM, Bajkowski AS, Steiner DF, Frankfater A. The expression of cathepsin B and other lysosomal proteinases in normal tissues and in tumors. Biomed Biochim Acta, 1991;50:531-40.
[236] Turk B, Turk D, Turk V. Lysosomal cysteine proteases: more than scavengers. Biochim Biophys Acta, 2000;1477:98-111.
[237] Clark AK, Malcangio M. Microglial signalling mechanisms: Cathepsin S and Fractalkine. Exp Neurol, 2012;234:283-92.
[238] Beck H, Schwarz G, Schroter CJ, Deeg M, Baier D, Stevanovic S *et al.* Cathepsin S and an asparagine-specific endoprotease dominate the proteolytic processing of human myelin basic protein in vitro. European journal of immunology, 2001;31:3726-36.
[239] Lohoefer F, Reeps C, Lipp C, Rudelius M, Zimmermann A, Ockert S *et al.* Histopathological analysis of cellular localization of cathepsins in abdominal aortic aneurysm wall. International journal of experimental pathology, 2012;93:252-8.
[240] Simpson CL, Lindley S, Eisenberg C, Basalyga DM, Starcher BC, Simionescu DT *et al.* Toward cell therapy for vascular calcification: osteoclast-mediated demineralization of calcified elastin. Cardiovascular pathology : the official journal of the Society for Cardiovascular Pathology, 2007;16:29-37.

[241] Faure-Andre G, Vargas P, Yuseff MI, Heuze M, Diaz J, Lankar D *et al.* Regulation of dendritic cell migration by CD74, the MHC class II-associated invariant chain. Science, 2008;322:1705-10.
[242] Wilkinson RD, Magorrian SM, Williams R, Young A, Small DM, Scott CJ *et al.* CCL2 is transcriptionally controlled by the lysosomal protease cathepsin S in a CD74-dependent manner. Oncotarget, 2015.
[243] Chan LL, Cheung BK, Li JC, Lau AS. A role for STAT3 and cathepsin S in IL-10 down-regulation of IFN-gamma-induced MHC class II molecule on primary human blood macrophages. Journal of leukocyte biology, 2010;88:303-11.
[244] Rybicka JM, Balce DR, Chaudhuri S, Allan ER, Yates RM. Phagosomal proteolysis in dendritic cells is modulated by NADPH oxidase in a pH-independent manner. The EMBO journal, 2012;31:932-44.
[245] Allan ER, Tailor P, Balce DR, Pirzadeh P, McKenna NT, Renaux B *et al.* NADPH oxidase modifies patterns of MHC class II-restricted epitopic repertoires through redox control of antigen processing. J Immunol, 2014;192:4989-5001.
[246] Xu Y, Schnorrer P, Proietto A, Kowalski G, Febbraio MA, Acha-Orbea H *et al.* IL-10 controls cystatin C synthesis and blood concentration in response to inflammation through regulation of IFN regulatory factor 8 expression. J Immunol, 2011;186:3666-73.
[247] Xu Y, Ding Y, Li X, Wu X. Cystatin C is a disease-associated protein subject to multiple regulation. Immunology and cell biology, 2015;93:442-51.
[248] Janowski R, Kozak M, Jankowska E, Grzonka Z, Grubb A, Abrahamson M *et al.* Human cystatin C, an amyloidogenic protein, dimerizes through three-dimensional domain swapping. Nature structural biology, 2001;8:316-20.
[249] Jiang SL, Liu ZM, Sun ZR, Cao Y, Liu LB. [A method for registration of stomach movement of rabbits in chronic experiments]. Sheng li xue bao : [Acta physiologica Sinica], 1986;38:102-6.
[250] Bender JK, Wille T, Blank K, Lange A, Gerlach RG. LPS structure and PhoQ activity are important for Salmonella Typhimurium virulence in the Galleria mellonella infection model [corrected]. PLoS One, 2013;8:e73287.
[251] El-Sukkari D, Wilson NS, Hakansson K, Steptoe RJ, Grubb A, Shortman K *et al.* The protease inhibitor cystatin C is differentially expressed among dendritic cell populations, but does not control antigen presentation. J Immunol, 2003;171:5003-11.
[252] Fissolo N, Kraus M, Reich M, Ayturan M, Overkleeft H, Driessen C *et al.* Dual inhibition of proteasomal and lysosomal proteolysis ameliorates autoimmune central nervous system inflammation. European journal of immunology, 2008;38:2401-11.
[253] Zahringer U, Lindner B, Rietschel ET. Molecular structure of lipid A, the endotoxic center of bacterial lipopolysaccharides. Adv Carbohydr Chem Biochem, 1994;50:211-76.
[254] Beutler B, Rietschel ET. Innate immune sensing and its roots: the story of endotoxin. Nat Rev Immunol, 2003;3:169-76.
[255] Raetz CR, Whitfield C. Lipopolysaccharide endotoxins. AnnuRevBiochem, 2002;71:635-700.
[256] Munford RS, Varley AW. Shield as signal: lipopolysaccharides and the evolution of immunity to gram-negative bacteria. PLoS pathogens, 2006;2:e67.
[257] Maeshima N, Fernandez RC. Recognition of lipid A variants by the TLR4-MD-2 receptor complex. Front Cell Infect Microbiol, 2013;3:3.
[258] Vijay-Kumar M, Gewirtz AT. Flagellin: key target of mucosal innate immunity. MucosalImmunol, 2009;2:197-205.
[259] Round JL, Mazmanian SK. The gut microbiota shapes intestinal immune responses during health and disease. NatRevImmunol, 2009;9:313-23.
[260] Jeon SG, Kayama H, Ueda Y, Takahashi T, Asahara T, Tsuji H *et al.* Probiotic Bifidobacterium breve induces IL-10-producing Tr1 cells in the colon. PLoS pathogens, 2012;8:e1002714.
[261] Bainbridge BW, Coats SR, Pham TT, Reife RA, Darveau RP. Expression of a *Porphyromonas gingivalis* lipid A palmitylacyltransferase in *Escherichia coli* yields a chimeric lipid A with altered ability to stimulate interleukin-8 secretion. Cell Microbiol, 2006;8:120-9.

[262] Yamamoto M, Akira S. Lipid A receptor TLR4-mediated signaling pathways. AdvExpMedBiol, 2009;667:59-68.
[263] O'Neill LA, Bryant CE, Doyle SL. Therapeutic targeting of Toll-like receptors for infectious and inflammatory diseases and cancer. Pharmacological reviews, 2009;61:177-97.
[264] Rossignol DP, Lynn M. Antagonism of in vivo and ex vivo response to endotoxin by E5564, a synthetic lipid A analogue. J Endotoxin Res, 2002;8:483-8.
[265] Mullarkey M, Rose JR, Bristol J, Kawata T, Kimura A, Kobayashi S *et al.* Inhibition of endotoxin response by e5564, a novel Toll-like receptor 4-directed endotoxin antagonist. The Journal of pharmacology and experimental therapeutics, 2003;304:1093-102.
[266] Rossignol DP, Wasan KM, Choo E, Yau E, Wong N, Rose J *et al.* Safety, pharmacokinetics, pharmacodynamics, and plasma lipoprotein distribution of eritoran (E5564) during continuous intravenous infusion into healthy volunteers. Antimicrobial agents and chemotherapy, 2004;48:3233-40.
[267] Opal SM, Laterre PF, Francois B, LaRosa SP, Angus DC, Mira JP *et al.* Effect of eritoran, an antagonist of MD2-TLR4, on mortality in patients with severe sepsis: the ACCESS randomized trial. JAMA, 2013;309:1154-62.
[268] Tse MT. Trial watch: Sepsis study failure highlights need for trial design rethink. Nature reviews Drug discovery, 2013;12:334.
[269] Paramo T, Tomasio SM, Irvine KL, Bryant CE, Bond PJ. Energetics of Endotoxin Recognition in the Toll-Like Receptor 4 Innate Immune Response. Scientific reports, 2015;5:17997.
[270] Rakoff-Nahoum S, Hao L, Medzhitov R. Role of toll-like receptors in spontaneous commensal-dependent colitis. Immunity, 2006;25:319-29.
[271] Wittmann A, Bron PA, van S, II, Kleerebezem M, Adam P, Gronbach K *et al.* TLR Signaling-induced CD103-expressing Cells Protect Against Intestinal Inflammation. Inflamm Bowel Dis, 2015.
[272] Shi J, Zhao Y, Wang Y, Gao W, Ding J, Li P *et al.* Inflammatory caspases are innate immune receptors for intracellular LPS. Nature, 2014;514:187-92.
[273] Di Lorenzo F, Paciello I, Fazio LL, Albuquerque L, Sturiale L, da Costa MS *et al.* Thermophiles as potential source of novel endotoxin antagonists: the full structure and bioactivity of the lipo-oligosaccharide from Thermomonas hydrothermalis. Chembiochem, 2014;15:2146-55.
[274] Ding NS, Hart A, De Cruz P. Systematic review: predicting and optimising response to anti-TNF therapy in Crohn's disease - algorithm for practical management. Aliment Pharmacol Ther, 2016;43:30-51.
[275] Feagan BG, Rutgeerts P, Sands BE, Hanauer S, Colombel JF, Sandborn WJ *et al.* Vedolizumab as induction and maintenance therapy for ulcerative colitis. N Engl J Med, 2013;369:699-710.
[276] Monteleone G, Neurath MF, Ardizzone S, Di Sabatino A, Fantini MC, Castiglione F *et al.* Mongersen, an oral SMAD7 antisense oligonucleotide, and Crohn's disease. N Engl J Med, 2015;372:1104-13.
[277] Sandborn WJ, Ghosh S, Panes J, Vranic I, Su C, Rousell S *et al.* Tofacitinib, an oral Janus kinase inhibitor, in active ulcerative colitis. N Engl J Med, 2012;367:616-24.
[278] Vatanen T, Kostic AD, d'Hennezel E, Siljander H, Franzosa EA, Yassour M *et al.* Variation in Microbiome LPS Immunogenicity Contributes to Autoimmunity in Humans. Cell, 2016;165:842-53.
[279] Holst O, Molinaro A. Core region and lipid A components of lipopolysacchrides. Microbial glycobiology: structures, relevance and applications, 2009:29-55.
[280] Weintraub A, Zahringer U, Wollenweber HW, Seydel U, Rietschel ET. Structural characterization of the lipid A component of Bacteroides fragilis strain NCTC 9343 lipopolysaccharide. Eur J Biochem, 1989;183:425-31.
[281] Rietschel ET, Kirikae T, Schade FU, Mamat U, Schmidt G, Loppnow H *et al.* Bacterial endotoxin: molecular relationships of structure to activity and function. FASEB J, 1994;8:217-25.

[282] Cullen TW, Schofield WB, Barry NA, Putnam EE, Rundell EA, Trent MS *et al.* Gut microbiota. Antimicrobial peptide resistance mediates resilience of prominent gut commensals during inflammation. Science, 2015;347**:**170-5.
[283] Di Lorenzo F, Kubik L, Oblak A, Lore NI, Cigana C, Lanzetta R *et al.* Activation of Human Toll-like Receptor 4 (TLR4).Myeloid Differentiation Factor 2 (MD-2) by Hypoacylated Lipopolysaccharide from a Clinical Isolate of Burkholderia cenocepacia. J Biol Chem, 2015;290**:**21305-19.
[284] Ittig S, Lindner B, Stenta M, Manfredi P, Zdorovenko E, Knirel YA *et al.* The lipopolysaccharide from Capnocytophaga canimorsus reveals an unexpected role of the core-oligosaccharide in MD-2 binding. PLoS pathogens, 2012;8**:**e1002667.
[285] Ianaro A, Tersigni M, D'Acquisto F. New insight in LPS antagonist. Mini Rev Med Chem, 2009;9**:**306-17.
[286] Meng J, Drolet JR, Monks BG, Golenbock DT. MD-2 residues tyrosine 42, arginine 69, aspartic acid 122, and leucine 125 provide species specificity for lipid IVA. J Biol Chem, 2010;285**:**27935-43.
[287] Meng J, Lien E, Golenbock DT. MD-2-mediated ionic interactions between lipid A and TLR4 are essential for receptor activation. J Biol Chem, 2010;285**:**8695-702.

List of publications

Accepted manuscripts:

1. **Role of CD40 ligation in dendritic cell semi-maturation.**
   Gerlach AM, Steimle A, Krampen L, Wittmann A, Gronbach K, Geisel J, Autenrieth IB, Frick JS.
   BMC Immunol. 2012 Apr 26;13:22. doi: 10.1186/1471-2172-13-22.

2. **A novel approach for reliable detection of cathepsin S activities in mouse antigen presenting cells.**
   Steimle A, Kalbacher H, Maurer A, Beifuss B, Bender A, Schäfer A, Müller R, Autenrieth IB, Frick JS.
   J Immunol Methods. 2016 May;432:87-94. doi: 10.1016/j.jim.2016.02.015. Epub 2016 Feb 18.

3. **Molecular Mechanisms of Induction of Tolerant and Tolerogenic Intestinal Dendritic Cells in Mice.**
   Steimle A, Frick JS.
   J Immunol Res. 2016;2016:1958650. doi: 10.1155/2016/1958650. Epub 2016 Feb 11. Review.

4. **Structure and function: Lipid A modifications in commensals and pathogens.**
   Steimle A, Autenrieth IB, Frick JS.
   Int J Med Microbiol. 2016 Aug;306(5):290-301. doi: 10.1016/j.ijmm.2016.03.001. Epub 2016 Mar 5.

5. **The challenge of specific Cathepsin S activity detection in experimental settings**
   Steimle A, Frick JS
   J Neurol Neuromed. 2016: 1(3): 6-12

6. **Symbiotic gut commensal bacteria act as host cathepsin S activity regulators.**
   Steimle A, Gronbach K, Beifuss B, Schäfer A, Harmening R, Bender A, Maerz JK, Lange A, Michaelis L, Maurer A, Menz S, McCoy K, Autenrieth IB, Kalbacher H, Frick JS.
   J Autoimmun. 2016 Jul 30. pii: S0896-8411(16)30117-2. doi: 10.1016/j.jaut.2016.07.009.

7. **Extensive Mobilome-Driven Genome Diversification in Mouse Gut-Associated Bacteroides vulgatus mpk.**
   Lange A, Beier S, Steimle A, Autenrieth IB, Huson DH, Frick JS.
   Genome Biol Evol. 2016 Apr 25;8(4):1197-207.

Submitted manuscripts:

8. **Gut symbiont or pathogen – the flagellin makes the difference**
   Menz S, Bender A, Tesfazgi Mebrhatu M, Gronbach K, Wagner S, Schwarz S, Linke D, Autenrieth SE, Voehringer D, Steimle A, Korkmaz AG, Alexopoulou L, Lange A, Autenrieth IB, Oelschlaeger T, Frick JS
   Submitted to Cell Host Microbes

8. ***Bacteroides vulgatus* mpk lipopolysaccharide acts as inflammation-silencing agent for the treatment of intestinal inflammatory disorders**
Steimle A, Di Lorenzo F, Gronbach K, Kliem T, Fuchs K, Öz HH, Schäfer A, Bender A, Lange A, Maerz JK, Menz S, Silipo A, Autenrieth IB, Pichler BP, Bisswanger H, Molinaro A, Frick JS

Submitted to Nature Communications

Manuscripts in preparation:

9. **Symbiotic *Bacteroides vulgatus*-derived outer membrane vesicles induce tolerant antigen presenting cells**
Maerz JK, Steimle A, Fehrenbacher B, Lange A, Bender A, Autenrieth IB, Frick JS

10. **How commensal gut bacteria control lysosomal pH values – an unexpected role for cystatin C**
Steimle A, Beifuss B, Michaelis L, Schäfer A, Bender A, Autenrieth IB, Frick JS

11. **Symbiotic gut commensals regulate Proteinkinase C delta activity via cystatin C**
Steimle A, Münzner T, Bender A, Maerz JK, Autenrieth IB, Frick JS

12. **Symbiotic commensals of the intestinal microbiota prevent from induction of an autoimmunity-mediating inflammatory Th17 response by regulation of host IκBζ expression**
Steimle A, Klees J, Birg A, Maerz JK, Menz S, Klameth C, Bender A, Gaffen S, Lorscheid S, Schulze-Osthoff K, Autenrieth IB, Frick JS

13. **Host Cathepsin B activity regulation is essential for intestinal homeostasis**
Steimle A, Michaelis L, Schäfer A, Beifuss B, Harmening R, Bender A, Autenrieth IB, Frick JS

List of oral and poster presentations

List of oral presentations

“Symbiotic gut commensal bacteria act as cathepsin S activity regulators – a novel approach to treat autoimmune diseases”

7th Seeon Conference “Microbiota, Probiota and Host”, Seeon, Germany, June 2016

"Influence of proteolytic activity of cathepsins in intestinal homeostasis”

5th Seeon Conference “Microbiota, Probiota and Host”, Seeon, Germany, June 2014

“Components of bacterial cell walls and their influence on intestinal homeostasis”

SFB766 “Bacterial Cell Envelope” meeting, Freudenstadt, Germany, March 2014

“Immunogenicity of different lipid A structures – the impact of dendritic cell semi-maturation on intestinal homeostasis”

7th Joint Ph.D Student’s Meeting of the SFBs 766, 630 and the FOR 854, Freudenstadt, Germany, November 2012

"Molecular Mechanisms underlying maturation and semi-maturation in murine dendritic cells”

3rd Seeon Conference “Microbiota, Probiota and Host”, Seeon, Germany, June 2012

"The MHC class II pathway in DC semi-maturation and intestinal homeostasis”

62. Jahrestagung der Deutschen Gesellschaft für Hygiene und Mikrobiologie, Essen, Germany, September 2011

List of poster presentations

“IκBζ mediates suppression of secretion of proinflammatory cytokines in dendritic cells”

Cytokines 2015, Bamberg, Germany, October 2015

"Immunogenicity of different lipid A structures”

4th Seeon Conference “Microbiota, Probiota and Host”, Seeon, Germany, June 2013

"Immunogenicity of different lipid A structures”

3rd International SFB 766 Symposium, Kaufbeuren, Germany, May 2013

“Molecular mechanisms underlying maturation and semi-maturation in murine dendritic cells”

Jahrestagung der Vereinigung für Allgemeine und Angewandte Mikrobiologie, Tübingen, Germany, March 2012

“Molecular mechanisms underlying maturation and semi-maturation in murine dendritic cells”

2nd Seeon Conference “Microbiota, Probiota and Host”, Seeon, Germany, June 2011

"Molecular Mechanisms underlying maturation and semi-maturation in murine dendritic cells”

62. Jahrestagung der Deutschen Gesellschaft für Hygiene und Mikrobiologie, Hannover, Germany, September 2011

Acknowledgements

Zuallererst möchte ich den Prüfern, die bei der Disputation anwesend sein werden, einen herzlichen Dank aussprechen: Prof. Dr. Mayer, Prof. Dr. Klaus Hantke, Prof. Dr. Ingo Autenrieth und natürlich Prof. Dr. Julia-Stefanie Frick. Ich hoffe auf eine kurzweilige, interessante und fruchtbare Diskussion .

Ich möchte auch Herrn Prof. Dr. Autenrieth dafür danken, dass er Zweitgutachter dieser Doktorarbeit ist.

Mein größter Dank gilt natürlich Frau Prof. Dr. Julia-Stefanie Frick. Für Unterstützung in jeglichen (auch persönlichen) Lebenslagen, für wissenschaftliche Diskussionen, für nicht-wissenschaftliche Blödeleien, für den unerschütterlichen Glauben an meine Arbeit und für so vieles andere mehr. Danke, Julia.

Andi Schäfer gebürt ein wahnsinnig dickes Dankeschön. Für einfach alles. Fürs zuhören, fürs antworten, fürs Ratschläge geben, für ihr Lachen, fürs über-den-Kopf-streicheln, fürs zu-mir-halten, fürs Raucherpausen-verbringen und generell fürs so-lange-mit-mir-aushalten!

Annika Bender möchte ich danken fürs nie-nein-sagen, wenn ich verzweifelt ihr Hilfe gebraucht habe, fürs immer-gut-zusprechen, wenn es mal wieder schwierige Zeiten gab, fürs mit-mir-Pflanzen-einkaufen, damit ich meinen Balkon zu einem botanischen Alptraum machen konnte, fürs mit-mir-rauchen-gehen, um einige Minuten dem wissenschaftlichen Chaos in meinem Kopf zu entkommen, fürs zuhören, wenn ich mal wieder nicht weiter wusste. Und natürlich auch danke für das ein oder andere Bier (oder neuerdings Pils!).

Die nächsten auf der Liste sind Brigitte Beifuss und Jan Maerz. Danke dafür, dass ihr den ganzen Tag in meiner Nähe seid. Allein das wertet einen Arbeitstag enorm auf! Danke für euren grandiosen Humor, eure Cleverness, euer Verständnis und eure Rücksichtnahme, wenn in meinem Kopf mal wieder Land unter war, eure Unterstützung in fast allen Lebenslagen und natürlich für euren äußerst gesunden Bierdurst. Und wie öde, langweilig und vor allem leise wäre eine Welt ohne das Lachen von Brigitte Beifuss.

Anna Lange möchte ich dafür danken, dass wir so gut miteinander diskutieren können und ich nach jedem Gespräch motiviert bin, noch ein weiteres Projekt in Angriff zu nehmen. Danke für deine beneidenswerte Intelligenz, deinen unnachahmlich herrlichen Humor und deinen Zuspruch und dein Mitgefühl (von Dienstag bis Freitag).

Dem Rest der Arbeitsgruppe möchte ich auch für so vieles danken: Raphael Parusel dafür, dass er mich immer Vatti nennt; Lena Michaelis dafür, dass sie der angenehmste und liebste Mensch ist, der mir seit langem begegnet ist; Thomas Hagemann dafür, dass der erste Mensch ist, mit dem ich mich über chilenische Innenpolitik unterhalten hab und alle anderen, die im Laufe meiner Zeit in diesem Labor gearbeitet haben.

Ein weiterer Dank gebührt allen Menschen, die mich im Laufe meines bisherigen Lebens begleitet haben und einen großen Anteil daran haben, dass diese Arbeit überhaupt entstehen konnte: Mein Bruder Sébastien Peter, meine Ersatzfamilie Silke, Tim und Tobi Meißner, Flo Braun, Jan Kaps, Anna Hertle, Sebastian Hertle, Julia Baturin, Resi Meffert, Doris Zimmermann, Maria Joanna Niemiec, Agostino Ronca, Sarah Menz, Robin Harmening und Suse Hertle.

Ein letztes großes Dankeschön, das größte von allen, geht an meine Eltern Rosi und Charly. Sie wissen, was ich Ihnen verdanke. Nämlich alles. Nicht zu vergessen an dieser Stelle der Rest der Familie: Alex, Tatjana, Sebastian und Sarah.

Appendix

BMC Immunology

RESEARCH ARTICLE Open Access

Role of CD40 ligation in dendritic cell semimaturation

Anna-Maria Gerlach†, Alexander Steimle†, Lea Krampen, Alexandra Wittmann, Kerstin Gronbach, Julia Geisel, Ingo B. Autenrieth and Julia-Stefanie Frick*

Abstract

Background: DC are among the first antigen presenting cells encountering bacteria at mucosal surfaces, and play an important role in maintenance of regular homeostasis in the intestine. Upon stimulation DC undergo activation and maturation and as initiators of T cell responses they have the capacity to stimulate naïve T cells. However, stimulation of naïve murine DC with *B. vulgatus* or LPS at low concentration drives DC to a semimature (sm) state with low surface expression of activation-markers and a reduced capacity to activate T-cells. Additionally, semimature DC are nonresponsive to subsequent TLR stimulation in terms of maturation, TNF-α but not IL-6 production. Ligation of CD40 is an important mechanism in enhancing DC maturation, function and capacity to activate T-cells. We investigated whether the DC semimaturation can be overcome by CD40 ligation.

Results: Upon CD40 ligation smDC secreted IL-12p40 but not the bioactive heterodimer IL-12p70. Additionally, CD40 ligation of smDC resulted in an increased production of IL-6 but not in an increased expression of CD40. Analysis of the phosphorylation pattern of MAP kinases showed that in smDC the p38 phosphorylation induced by CD40 ligation is inhibited. In contrast, phosphorylation of ERK upon CD40 ligation was independent of the DC maturation state.

Conclusion: Our data show that the semimature differentiation state of DC can not be overcome by CD40 ligation. We suggest that the inability of CD40 ligation in overcoming DC semimaturation might contribute to the tolerogenic phenotype of semimature DC and at least partially account for maintenance of intestinal immune homeostasis.

Keywords: Dendritic cells, CD40 ligation, Maturation, Cytokine, MAP Kinase, Homoeostasis, T-cell

Background

Dendritic cells (DC) are among the first antigen presenting cells encountering bacteria at mucosal surfaces and play an important role in maintenance of regular homeostasis in the intestine. Stimulation of DC with e.g. TLR agonists leads to activation and maturation of DC by activation of NF-κB and mitogen-activated protein kinase (MAPK) family members [1]. This results in a rapid production of costimulatory molecules, cytokines and pro-inflammatory mediators that affect T-cell differentiation, for instance.

We identified *Escherichia coli* mpk, a commensal *E. coli* strain which induces colitis in genetically predisposed hosts and *Bacteroides vulgatus* mpk which does not elicit colitis and even prevents the colitis caused by *E. coli* mpk [2,3]. Stimulation of bone marrow derived dendritic cells (BMDC) with *E. coli* [4] or lipopolysaccharide (LPS) at high concentration [5] induced TNF-α, IL-12 and IL-6 secretion and expression of activation-markers, whereas stimulation with *B. vulgatus* or [4] LPS at low concentrations [5] only led to secretion of IL-6 and DC were driven to a semimature state with low expression of activation-markers. Those semimature DC were nonresponsive to subsequent TLR stimulation in terms of maturation and TNF-α but not IL-6 production [4,5]. Moreover, the low positive expression of activation surface marker like e.g. CD40 on semimature DC, was not overcome by a subsequent stimulus via TLR4 [4]. This might contribute to the reduced activation of T-cells by semimature DC [4] as binding of the CD40 ligand (CD40L) on naïve T-cells to

* Correspondence: julia-stefanie.frick@med.uni-tuebingen.de
†Equal contributors
Institute for Medical Microbiology and Hygiene, University Hospital of Tübingen, 72076 Elfriede-Aulhorn-Str. 6, Tübingen D-72076, Germany

CD40 is a crucial signal for generation of effective $CD4^+$ and $CD8^+$ T-cell responses [6,7]. CD40 ligation results in upregulation of CD83, CD80 and CD86 as well as MHC molecules on DC. Additionally, the expression of adhesion molecules ICAM-1 and CD58 [8-11] is upregulated and survival of DC is supported by CD40 ligation [12,13]. Furthermore, CD40 ligation of mature DC results in secretion of proinflammatory cytokines e.g. IL-1, IL-6 and IL-12 [9-11] [14,15].

IL-12 plays an important role in T-cell polarization by promoting Th-1 responses. Its bioactive heterodimer IL-12p70 consists of a p40 and p35 subunit, which are encoded by different genes and therefore independently regulated. IL-12p40 can also form homodimers (IL-12p80) which were shown to inhibit IL-12p70 mediated immune responses [16,17].

Mitogen-activated protein kinase (MAPK) signal transduction pathways play a crucial role in many aspects of immune mediated inflammatory responses [18]. The MAPK ERK, JNK and p38 are important regulators of host immune responses to e.g. bacterial stimuli. Extracellular stimuli induce phosphorylation of MAPK–kinase-kinase (MKKK) which in turn phosphorylate MKK. Specific MKK are necessary to phosphorylate and activate MAPK, which results in activation of downstream kinases and transcription factors [18-20]. The products of inflammatory genes include e.g. cytokines, chemokines and adhesion molecules which promote recruitment of immunocompetent cells to inflammatory sites. Additionally, the MAPK p38 enhances the mRNA stability of many proinflammatory cytokines, e.g. IL-8, TNF-α or IL-6 [21-23].

Within the present study we analyzed the effects of DC semimaturation on cellular responses to CD40 ligation and showed that the semimature differentiation state of DC, induced by stimulation with *B. vulgatus* or LPS^{lo} can not be overcome by CD40 ligation.

Methods

Mice

C57Bl/6x129sv mice were obtained from own breeding. All mice were kept under SPF conditions. Male and female mice were sacrificed at 6–12 weeks of age. Animal experiments were reviewed and approved by the responsible institutional review committee (Regierungspräsidium Tübingen, December 19th 2008).

Abs and reagents

Ultra pure LPS *Salmonella enterica* serovar Minnesota was purchased from Calbiochem (Schwalbach, Germany). The following antibodies were used for flow cytometry: PE conjugated anti-mouse CD11c, clone HL3, Biotin conjugated anti-mouse CD40, clone 3/23, Biotin conjugated anti-mouse CD80, clone 16-10A1, FITC conjugated anti-mouse I-A/I-E clone 2 G9, FITC conjugated anti-mouse CD86, clone GL1. As isotype control hamster IgG_1 λ2, hamster IgG_{2a} κ and rat IgG_{2a} κ were used. For CD40 ligation we used purified NA/LE hamster anti-mouse CD40, clone HM40-3, and purified NA/LE hamster IgM, λ1 isotype control, clone G235-1 (all antibodies from BD, Heidelberg, Germany). p38 MAP kinase inhibitor (SB202190) was purchased from Calbiochem (Schwalbach, Germany), and ERK inhibitor (PD98059) from Promega (Mannheim, Germany).

Western blotting

For p38 and pERK Western blot analysis proteins (50 μg) were solubilized in Laemmli sample buffer. They were separated on SDS-PAGE gels and transferred to nitrocellulose membranes. The membranes were blocked for 1 h at room temperature in 5% dry milk in TBS/T (TBS containing 2,01% Tween). After that the membranes were incubated with mouse anti-p38 MAPK (pT180/pY182) or with mouse anti-ERK 1/2 (pT202/pY204) (both BD Pharmigen, Heidelberg, Germany) at 4°C over night. The antibody solution was diluted 1:1000 in 5% dry milk in TBS/T. After incubation the membranes were washed three times in TBS/T and were treated with the secondary antibody (polyclonal rabbit anti-mouse conjugated to horseradish peroxidase, DakoCytomation, Hamburg, Germany; diluted 1:1000 in 5% dry milk in TBS/T) for 2.5 h at room temperature. After repeating the washing step the proteins were detected by enhanced chemiluminescence. Before using ß-actin (mouse anti-mouse β-actin; Sigma, Munich, Germany) as a control for protein loading, the blots were stripped for 20 min with 10 ml stripping-solution (10 mM NaOH and 250 mM guanidinium chloride).

Bacteria and cell lines

The bacteria used for stimulation of the murine dendritic cells were *Escherichia coli* mpk [2] and *Bacteroides vulgatus* mpk [2] . The *E. coli* strain was grown in Luria-Bertani (LB) medium under aerobic conditions at 37°C. *Bacteroides vulgatus* was grown in Brain-Heart-Infusion (BHI) medium and anaerobic conditions at 37°C. In some experiments, J558L/CD40L cells were used for CD40 ligation. The cells were cultured in DMEM (*Dulbecco's modified Eagle's medium*,Invitrogen, Darmstadt, Germany) supplemented with 1 g/l glucose, L-glutamine, pyruvate, 50 μmol/l 2-mercaptoethanol, 10% FCS and penicillin/streptomycin.

Mouse DC isolation

Bone marrow cells were isolated and cultured as described previously [4] with minor modifications. Cells were harvested at day 7 and used to evaluate the effects of cellular challenge with *E. coli* mpk, *B. vulgatus* mpk and LPS on subsequent CD40 ligation. Cytokine release

and expression of surface markers were determined after CD40 ligation as described below.

Stimulation of isolated DC

At day 7, DC were stimulated with viable bacteria at a MOI of 1 at 37°C, 5% CO_2. Gentamicin was added one hour after stimulation and cells were incubated for 24 hour. To exclude bacterial overgrowth, CFU of viable bacteria was determined at the end of incubation period. Respectively, DC were stimulated with LPS (1 ng/ml and 1 μg/ml). After 24 h cell culture supernatant was harvested for analysis of cytokine expression and cells were used for flow cytometry of surface marker expression.

CD40 ligation

To determine the effects of CD40 ligation on DC cytokine production and expression of surface markers DC were restimulated using an agonistic anti-CD40 mAb (BD, Heidelberg, Germany). Therefore, DCs pretreated with *E. coli, B. vulgatus* or LPS were harvested, washed twice and cultured at $1.5x10^5$ DC in the presence of 5 μg/ml anti-CD40 mAb in DC culture medium at 37°C, 5% CO_2. As a control, DCs were incubated with 5 μg/ml of the IgM isotype control antibody (BD, Heidelberg, Germany). After 48 h, DC culture supernatants were harvested and analyzed for cytokine concentrations by ELISA. The expression of CD80 and CD86 on the DC surface was determined by FACS analysis.

For determination of CD40 expression of DC upon CD40 ligation the J558/LCD40L cell line was irradiated with 180 Gy in a Gammacell 1000 Elite® (Nordion, Ottawa, Canada) prior to co-culture with DC. $5x10^4$ J558L/CD40L cells were cultured with $1.5x10^5$ DC in DC culture medium for 48 h at 37°C, 5% CO_2. DC were harvested and analyzed for expression of CD40 by FACS.

Inhibition of MAP kinase signaling

DC were incubated with the p38 MAP kinase inhibitor SB202190 (2 μmol/l) or the ERK inhibitor PD98059 (50 μmol/l) for 30 min prior to CD40 ligation. After 30 min the cells were washed. CD40 ligation with anti CD40 mAb was performed for 24 h. Cell culture supernatants were harvested and used for determination of cytokine concentrations.

Cytokine analysis by ELISA

For analysis of IL-6, IL-12p40 and IL-12p70 concentrations in cell culture supernatants commercially available ELISA kits (BD, Heidelberg, Germany) were used according to the manufacturer's instructions.

Flow cytometry analysis

$3x10^5$ DC were incubated in 150 μl PBS containing 0.5-μl of fluorochrome conjugated antibodies and applied to flow cytometry analysis. 30,000 cells were analyzed using a FACS Calibur (BD, Heidelberg, Germany).

Statistical analysis

Statistical analysis was performed using the two sided unpaired Student's *t*-test. P values < 0.05 were considered significant. Error bars represent ± SEM.

Results

CD40 ligation does not overcome DC semimaturation

Stimulation of DC with *B. vulgatus* or LPS^{lo} (1 ng/ml) leads to induction of DC semimaturation [4,5] whereas stimulation of immature DC with *E. coli* or LPS^{hi} (1 μg/ml) induces DC maturation. The semimature DC phenotype is characterized by tolerance towards a subsequent stimulation via TLR2 or TLR4 in terms of TNF-α and IL-12p70 but not IL-6 secretion and a low positive expression of costimulatory molecules like e.g. CD40, CD80 CD86 [4,5]. Herein we investigated whether CD40 ligation as a TLR independent DC activation signal can overcome the semimature DC phenotype and induce activation and maturation of semimature DC.

By stimulation of immature DC with *B. vulgatus* or LPS^{lo} we induced semimature DC, and by stimulation with *E. coli* or LPS^{hi} DC maturation was induced. Secretion of IL-12p40 (Figure 1A), IL-12p70 (Figure 1B) and IL-6 (Figure 1C) was determined by ELISA. CD40 ligation of semimature DC led to secretion of IL-12p40 but not to secretion of the bioactive heterodimer IL-12p70. In contrast, CD40 ligation of mature DC resulted in significant enhanced secretion of IL-12p70 as compared to cells treated with the anti-CD40 mAb isotype control. Mature DC revealed a high spontaneous production of IL-12p40 which was only slightly enhanced by CD40 ligation (Figure 1A, B). Additionally, CD40 ligation of semimature DC resulted in increased levels of IL-6 compared to immature DC. In mature DC which also showed a high spontaneous secretion rate of IL-6 CD40 ligation only led to a slight further increase of IL-6 production (Figure 1C).

Next, we investigated whether CD40 ligation can overcome the low positive expression of DC activation markers on semimature DC. Therefore, we analysed the expression of CD80 (Figure 2A), CD86 (Figure 2B), and CD40 (Figure 2C) on immature, mature and semimature DC upon CD40 ligation in comparison to mock cells or cells treated with the anti-CD40 mAb isotype control by FACS.

On semimature DC the expression of CD80 was slightly enhanced upon CD40 ligation, as compared to the control cells (mock or isotype treated). However, in comparison to mature DC, in semimature DC the expression of CD80 was still significantly reduced after subsequent CD40 ligation (*E. coli* 76.7% ± 1.5% vs. *B. vulgatus* 37.1% ± 0.6%;

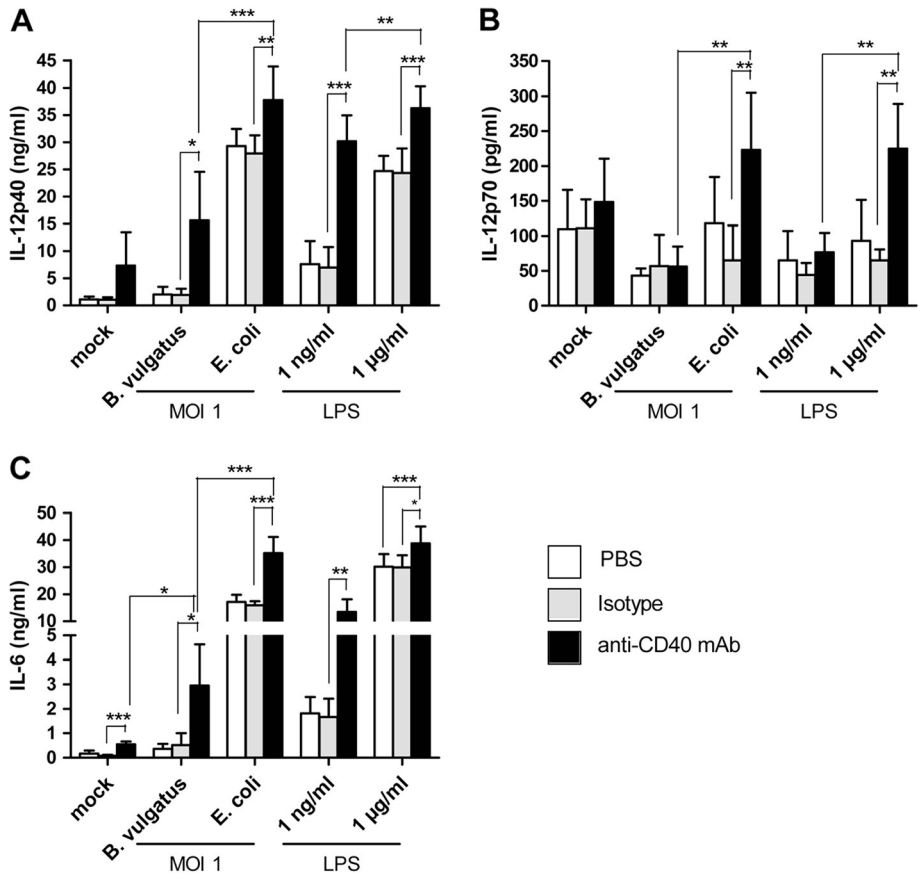

Figure 1 Cytokine secretion of differentially primed BMDC in response to secondary CD40 ligation. Wildtype BMDC were stimulated with B. vulgatus mpk (MOI 1) or E. coli mpk (MOI 1) and LPS at low (1 ng/ml) or high concentration (1 μg/ml), respectively, for 24 hour. Unstimulated DC (PBS) served as a control. Subsequently, these DC were washed twice and were re-stimulated with an agonistic anti-CD40 mAb (5 μg/ml) for 48 hours (black bars). As a control, DC were further incubated in medium only (white bars) or in the presence of the isotype control (grey bars). The concentrations of IL-12p40 (**A**), IL-12p70 (**B**) and IL-6 (**C**) were determined by ELISA. The bars represent the mean values of three independent experiments, each performed as duplicate, + SD. * $p < 0.05$, ** $p < 0.01$, *** $p < 0.001$.

LPS^{hi} 79.0% ± 1.9% vs. LPS^{lo} 53.4% ± 3.7%) (Figure 2A). Analysis of the expression of CD86 on immature, semimature and mature DC upon CD40 ligation revealed a slight increase of CD86 expression in immature (9.1% ± 0.5% to 27.2% ± 4.7%) and semimature DC (*B. vulgatus*: 20.4% ± 5.1% to 42.5% ± 8.6%; LPS^{lo} 44.3% ± 7.9% to 58.7% ± 9.5%). However, the expression levels of CD86 on semimature DC after CD40 ligation did not reach the expression levels of mature DC (*E. coli:* 54.8% ± 6.7% to 59.9% ± 6.5%; LPS^{hi} 56.6% ± 3.3% to 61.3% ± 5.5%) (Figure 2B).

The MHC class II expression on immature, semimature and mature DC was slightly increased upon CD40 ligation. These changes, however, proved not to be statistically significant (data not shown).

As anti-CD40 antibodies used for ligation assays and anti-CD40 antibodies used for FACS analysis might compete for binding of CD40 we used the J558L/CD40L cell line to analyze the influence of CD40 ligation on the expression of CD40 itself on DC. In *B. vulgatus* treated semimature DC we found an increase of CD40 expression upon CD40 ligation (*B. vulgatus* 26.8% ± 7.4% to 55.0% ± 0.1%). In LPS^{lo} treated semimature DC we observed a similar effect, however, the increase in CD40 expression was statistically not significant (57.8% ± 6.6% to 63.5% ± 8.9%). Interestingly, CD40 ligation of semimature DC did not lead to an increase of CD40 resulting in as high expression levels as on mature DC (*E. coli* 77.1% ± 4.2%; LPS^{hi} 75.2% ± 4.0%) (Figure 2C).

In DC semimaturation CD40L induced p38 phosphorylation is inhibited

To analyze phosphorylation of the MAP kinase p38 in response to CD40 ligation, immature, semimature and mature DC were activated by CD40 ligation and pp38 levels were determined by Western blotting. CD40 ligation of immature and mature DC resulted in phosphorylation of

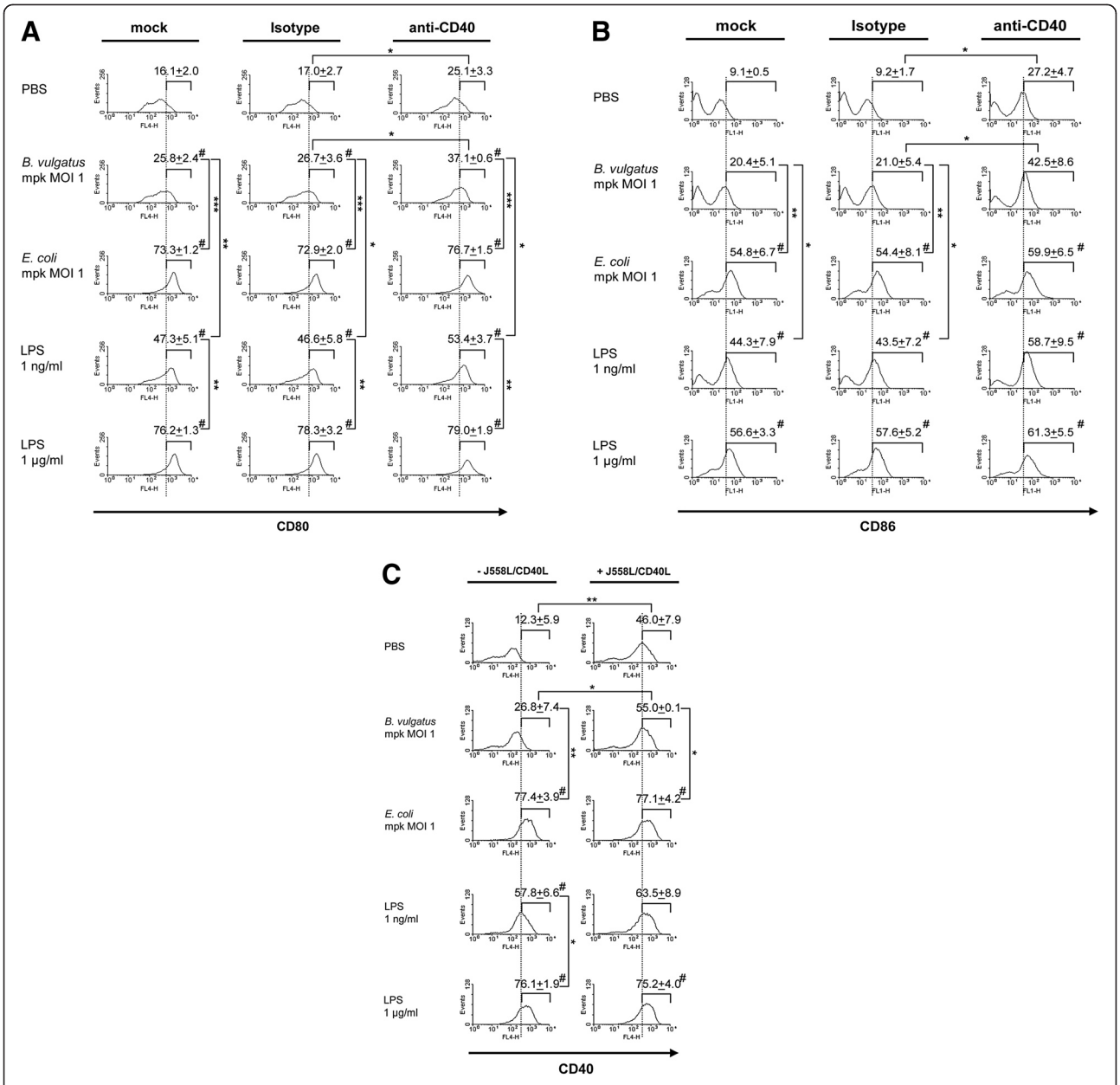

Figure 2 Expression of CD80, CD86 and CD40 on differentially primed BMDC after secondary CD40 ligation. Wildtype BMDC were stimulated with B. vulgatus mpk (MOI 1) or E. coli mpk (MOI 1) and LPS at low (1 ng/ml) or high concentration (1 µg/ml), respectively, for 24 hours. Unstimulated DCs (PBS) served as a control. **Figure 2A** and **2B**: The pre-treated DC were washed twice and were re-stimulated with an agonistic anti-CD40 mAb (5 µg/ml) for 48 hours. As a control, DCs were further incubated in medium only (mock) or in the presence of the isotype control. The expression levels of CD80 (**A**) and CD86 (**B**) were measured by FACS analysis. **Figure 2C**: The pre-treated DC were washed twice and were re-stimulated with CD40L by co-culture with J558L/CD40L transfectants or were cultured in medium only as a control (– J558L/CD40L). After 48 hours, the expression of CD40 was determined by FACS analysis. Each histogram is representative of three independent experiments. The data are mean values of the percentages of the positive cell populations determined in these three experiments, ± SD.
* $p < 0.05$, ** $p < 0.01$, *** $p < 0.001$; # $p < 0.05$ compared to the respective control (PBS).

p38, whereas in semimature DC p38 phosphorylation upon CD40 ligation slightly reduced (Figure 3).

To investigate the biological relevance of p38 MAP kinase activation we treated immature, semimature and mature DC with the p38 inhibitor SB202190 prior to CD40 ligation. Levels of IL-12p40, IL-12p70 and IL-6 were determined in cell culture supernatants by ELISA (Figure 4 A-C).

Inhibition of p38 had no influence on the CD40L induced secretion of IL-12p40 by DC, independent of the maturation state (Figure 4A). However, in mature DC the production of IL-12p70 upon CD40 ligation was

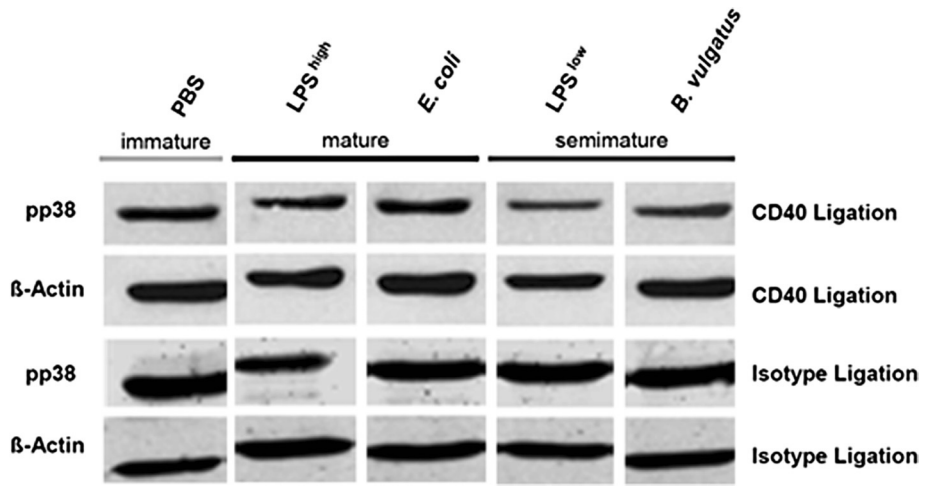

Figure 3 Phosphorylation of p38 MAPK upon secondary CD40 ligation in immature, semimature and mature DC. Wildtype BMDC were stimulated with B. vulgatus mpk or LPS 1 ng/ml (LPS^{low}) to generate semimature DC and E. coli mpk or LPS 1 μg/ml (LPS^{high}), respectively, to generate mature DC. Immature DC were maintained by incubation in the absence of further stimuli (PBS). After 24 hours, DC were re-stimulated with anti-CD40 mAb (1 μg/ml) for 15 minutes or treated with the isotype control (Isotype). The expression of pp38 was analyzed by Western blotting. As loading control, β-actin expression was determined. The results shown are representative of three independent experiments.

inhibited partially by SB202190. Inhibition of p38 did not influence the IL-12p70 expression pattern in immature or semimature DC as CD40 ligation did not induce any IL-12p70 secretion in these cells (Figure 4B). In mature DC, both spontaneous and CD40L induced IL-6 secretion levels were partially reduced by inhibition of the p38 MAP kinase. In contrast, IL-6 production of immature as well as semimature DC upon CD40 ligation was not significantly affected by inhibition of p38 (Figure 4C).

In DC semimaturation ERK suppresses CD40L induced IL-12p40 production

To analyze the role of the extracellular signal regulated kinase (ERK) we used the ERK inhibitor PD98059. Upon CD40 ligation the inhibition of ERK resulted in a significant increase of IL-12p40 in immature and semimature DC but only a slight increase in mature DC (Figure 5A). In contrast, inhibition of ERK had not the ability to induce IL-12p70 production in immature and semimature DC and resulted in only slightly enhanced IL-12p70 secretion levels in mature DC (Figure 5B). The CD40L induced IL-6 production by DC was not affected by ERK inhibition, independent of the maturation state (Figure 5C). In line with this, analysis of pERK levels upon CD40 ligation of immature, semimature and mature DC showed similar levels independent of the DC maturation state (data not shown).

Taken together, our data showed that the semimature differentiation state of DC, induced by stimulation with *B. vulgatus* or LPS^{lo} can not be overcome by CD40 ligation.

Discussion

In order to clarify the impact of CD40 expression on the T-cell activation capacity of semimature DC, we examined the effect of CD40 ligation on immature, semimature and mature DC. Semimature DC were induced by either stimulation with *B. vulgatus* or LPS at low concentration (1 ng/ml), and are characterized by a low positive expression of costimulatory molecules like e.g. CD40, secretion of only IL-6, and nonresponsiveness toward subsequent TLR activation [4,5].

In brief, we showed that CD40 ligation does not overcome DC semimaturation in terms of expression of activation surface markers and results in production of only IL-6 and IL-12p40, but not the bioactive form IL-12p70. The slightly reduced p38 phosphorylation levels in semimature DC as compared to mature DC might at least partially contribute to this effect. The expression of IL-12p40 turned out to be limited by pERK.

In line with other studies [24,25], we observed that on mature DCs no significant further increase in the expression levels of the already highly expressed costimulatory molecules CD40, CD80 and CD86 could be triggered upon additional stimulation by CD40 ligation.

Upon CD40 ligation immature and semimature DC expressed intermediate levels of CD40 CD80 and CD86, but did not reach the expression level of mature DC. However, the intermediate expression of costimulatory molecules was not associated with production of proinflammatory cytokines like IL-12p70.

It is known that immature DCs characterized by low expression levels of costimulatory molecules and lacking secretion of proinflammatory cytokines induce tolerance

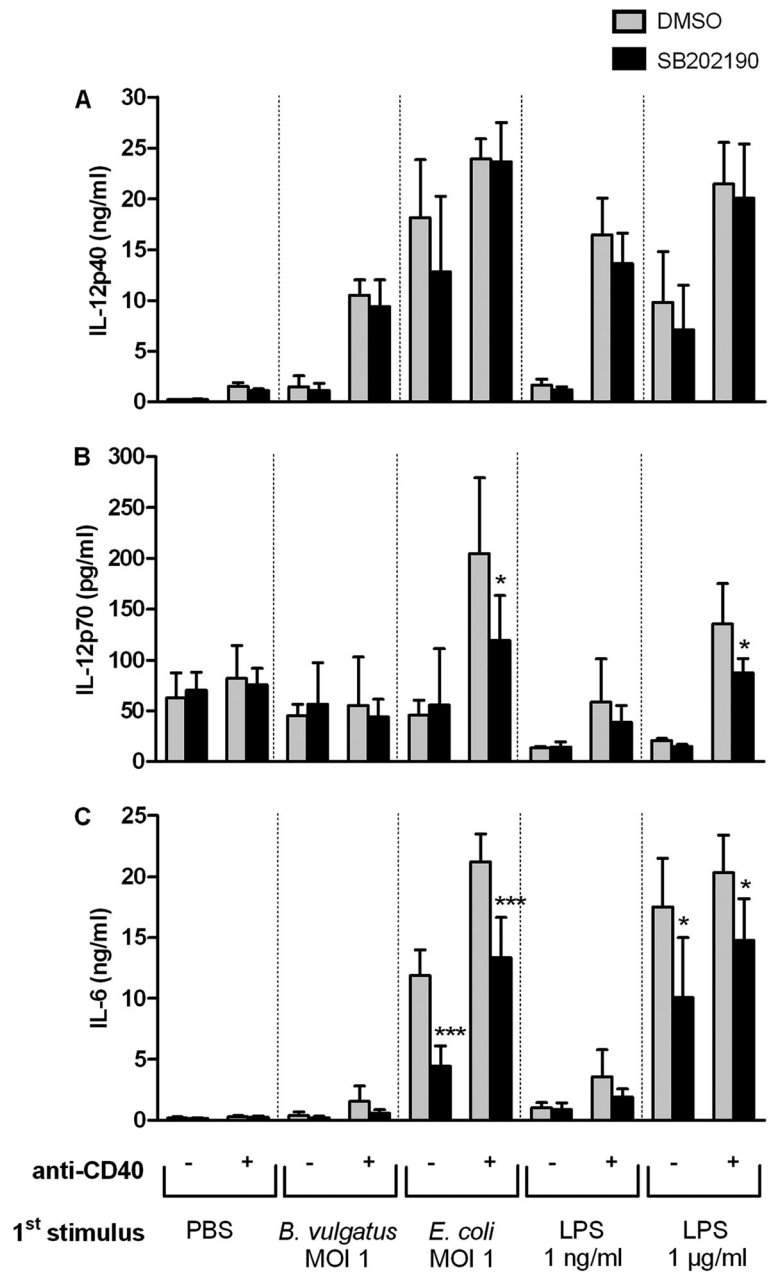

Figure 4 Role of p38 MAPK on CD40L induced cytokine secretion in DC of different maturation status. Wildtype BMDC were primed with B. vulgatus mpk or LPS 1 ng/ml to obtain semimature DC and E. coli mpk or LPS 1 µg/ml, respectively, to obtain mature DC. Immature DC were maintained by incubation in the absence of further stimuli (PBS). Subsequently, the DC were washed and treated with the p38 inhibitor SB202190 (2 µmol/l, black bars) or as a control with DMSO (grey bars) for 30 minutes, washed and re-stimulated with 1 µg/ml anti-CD40 mAb (+) or the isotype control (–). After 24 hours, the concentrations of IL-12p40 (**A**), IL-12p70 (**B**) and IL-6 (**C**) were measured in the cell culture supernatants by ELISA. The bars represent the mean values of three independent experiments, each performed as duplicate, ± SD. * $p < 0.05$, *** $p < 0.001$ for SB202190 compared to DMSO.

by promoting T-cell anergy, apoptosis or differentiation into T_{reg} cells via antigen presentation in the absence of costimulatory signals [26-29]. Additionally, CD40 deficient DCs or DCs with a suppressed CD40 expression were shown to have a reduced potential to activate T-cell proliferation and polarization in Th1 or Th2 direction [30-34]. This effect might also contribute to the inhibited T-cell activation induced by the intermediate expression of costimulatory molecules on semimature *lamina propria* (lp) DC of *B. vulgatus* monocolonized *IL-2*$^{-/-}$ mice [3]. On the other hand it was shown that a high positive expression of costimulatory molecules in absence of

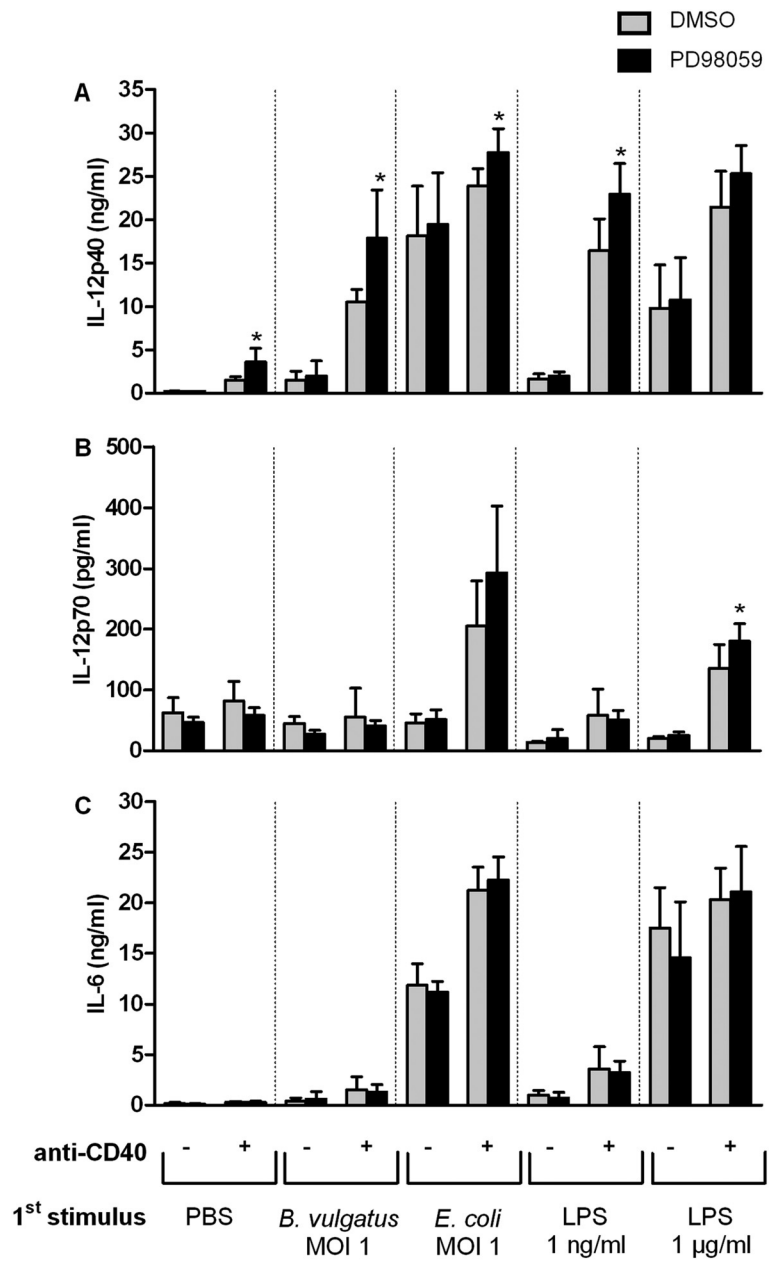

Figure 5 Role of ERK on CD40L induced cytokine secretion in DC of different maturation status. Wildtype BMDC were primed with B. vulgatus mpk or LPS 1 ng/ml to obtain semimature DC and E. coli mpk or LPS 1 µg/ml, respectively, to obtain mature DC. Immature DC were maintained by incubation in the absence of further stimuli (PBS). Subsequently, the DC were washed and treated with the ERK inhibitor PD98059 (50 µmol/l, black bars) or as a control with DMSO (grey bars) for 30 minutes, washed and re-stimulated with 1 µg/ml anti-CD40 mAb (+) or the isotype control (–). After 24 hours, the concentrations of IL-12p40 (**A**), IL-12p70 (**B**) and IL-6 (**C**) were measured in the cell culture supernatants by ELISA. The bars represent the mean values of three independent experiments, each performed as duplicate, ± SD. * $p < 0.05$ for PD98059 compared to DMSO.

pro-inflammatory mediators like e.g. TNF-α or IL-12p70 favours T-cell tolerance and suppression of T-cell activation. This type of DC is mainly induced by autocrine or paracrine stimulation with inflammatory mediators like e. g. TNF-α [35-38].

The cytokine secretion pattern upon CD40 ligation differed between immature/semimature DC and mature DC. In immature and semimature DC, CD40 ligation did not result in induction of IL-12p70 secretion, in contrast to mature DC where CD40 ligation led to increased IL-12p70 secretion. This is in line with other studies showing that TLR4 stimulation and CD40 ligation synergize in inducing IL-12 p70 secretion [25,39]. The additive microbial priming signals are necessary to trigger

the production of the IL-12p35 subunit [40] which was shown to be not induced by exclusive CD40 ligation [41,42]. Additionally, these accessory stimuli have the potential to augment the CD40 expression on antigen presenting cells (APC) [43-45] which results in a more effective CD40 ligation. However, DC primed with *Bacteroides vulgatus* as a microbial stimulus do not secrete IL-12p70 upon CD40 ligation. This might be one mechanism accounting for the tolerogenic effects of *B. vulgatus* in maintenance of intestinal homeostasis [2,3]. As *Porphyromonas gingivalis* which is phylogenetically closely related to *B. vulgatus* signals mainly vial TLR2 [46], this might be also the main receptor for recognition of *B. vulgatus*. In turn, TLR2 activation is reported to result in transcription of the p40 but not the p35 subunit of IL-12p70 [1,47]. This might account for the induction of IL-12p40 but not p70 upon stimulation of *B. vulgatus* primed DC via CD40 ligation. The production of IL-12p40 in the absence of the p35 unit might result in the formation of IL-12p40 homodimers which are known to act as potent antagonists at the IL-12p70 receptor [48-50]. Additionally, in IL-12p40 transgenic mice Th1 responses are significantly reduced suggesting that also *in vivo* p40 functions as an IL-12 antagonist [51].

Upon CD40 ligation semimature DC produced significantly enhanced levels of IL-6 but not TNF-α (data not shown) or IL-12p70. This is in line with our previous studies showing a crucial role for IL-6 in induction of DC semimaturation and tolerance [4,5,52]. This is interesting as the secretion of IL-6 upon CD40 ligation by semimature DC might help to sustain the semimature differentiation state and influence the T-cell activation pattern. IL-6 plays an important role in T-cell differentiation through two independent molecular mechanisms. First, IL-6 stimulation of T-cells leads to an upregulation of nuclear factor of activated T cells (NFAT) [53], a transcription factor regulating IL-4 transcription [54] resulting in IL-4 expression, and thereby promotion of Th2 polarized T cell differentiation [55]. Second, IL-6 upregulates the expression of silencer of cytokine signaling (SOCS) 1 in $CD4^+$ cells which inhibits IFN-γ signaling and thus Th1 differentiation [56]. The presence of IL-6 may shift the Th1/Th2 balance towards Th2 [55].

CD40 ligation of DC is known to result in phosphorylation of MAP kinases like e.g. p38 and ERK [57,58] and the ratio between pp38 and pERK is thought to play a crucial role in directing the cytokine secretion pattern of DC towards pro- or anti-inflammatory host responses [59-61]. CD40 ligation of mature DC resulted in phosphorylation of p38, inhibition of pp38 using the inhibitor SB202190 partially reduced of IL-12p70 and IL-6 but not IL-12p40 levels. Therefore, in mature DC pp38 might contribute to positive regulation of the p35 subunit of IL-12p70 [62]. This is in line with others showing that pp38 is important for production of IL-12p70 [61,63]. Additionally, pp38 is known to increase the stability of IL-6, TNF-α and IL-8 mRNA [22,23,64] which might result in increased secretion of these cytokines. Furthermore, via the mitogen and stress activated protein kinase (MSK) 1 pp38 is involved in NFκB activation [65,66]. In contrast, CD40L induced IL-12p40 secretion from mature DC has been shown to be independent of p38 phosphorylation, but dependent on the NFκB inducing kinase (NIK) [67].

As we observed an only slight reduction of p38 phosphorylation in semimature DC we hypothesize that inhibition of p38 phosphorylation due to DC semimaturation is only one of many factors that may affect in interaction with others the cytokine secretion pattern of semimature dendritic cells in response to secondary CD40 stimulation and thus their reduced pro-inflammatory capability [3-5]. The slight differences in the MAP kinase phosphorylation pattern in response to CD40 ligation might be based on differences in CD40 expression of immature, semimature or mature DC. A strong CD40 signal is known to preferentially activate p38, whereas weak CD40 signals are thought to favour ERK phosphorylation [60].

Inhibition of pERK during CD40 ligation turned out to have no significant effect of cytokine secretion in mature DC. In contrast, in semimature DC phosphorylation of ERK was at least partially responsible for limiting IL-12p40 expression. This is in line with others showing similar effects [68]. However, the Western blot analysis did not reveal significant differences of pERK levels in immature, semimature or mature DC. We speculate that in semimature DC the ERK activation might probably control the IL-12p40 production and therefore contribute to the limitation of the IL-12 p70 production. We are aware that this is highly speculative and that further work has to elucidate the role of ERK in DC semimaturation.

Conclusion

We hypothesize that the inability of CD40 ligation in overcoming DC semimaturation might contribute to the tolerogenic phenotype of semimature DC and at least partially account for maintenance of intestinal homeostasis.

Competing interests

The authors declare that they have no competing interests.

Authors' contributions

AMG: Performance of experiments, analysis of data, writing of manuscript, AS: Performance of experiments, analysis of data, LK: Performance of experiments, AW: Performance of experiments, KG: Performance of experiments, JG: Performance of experiments, IBA: Designing of experiment, JSF: Designing of experiment, analysis of data, data interpretation, writing of manuscript. All authors read and approved the final manuscript.

Acknowledgement

This project was funded by the DFG (Deutsche Forschungsgemeinschaft) (FR 2087/6-1), the BMBF (Bundesministerium für Bildung und Forschung) and the IZKF (Interdisziplinäres Zentrum für Klinische Forschung) Promotionskolleg.

Received: 5 December 2011 Accepted: 16 April 2012
Published: 26 April 2012

References

1. Re F, Strominger JL: **Toll-like receptor 2 (TLR2) and TLR4 differentially activate human dendritic cells.** *J Biol Chem* 2001, **276:**37692–37699.
2. Waidmann M, Bechtold O, Frick JS, Lehr HA, Schubert S, Dobrindt U, Loeffler J, Bohn E, Autenrieth IB: **Bacteroides vulgatus protects against Escherichia coli-induced colitis in gnotobiotic interleukin-2-deficient mice.** *Gastroenterology* 2003, **125:**162–177.
3. Muller M, Fink K, Geisel J, Kahl F, Jilge B, Reimann J, Mach N, Autenrieth IB, Frick JS: **Intestinal colonization of IL-2 deficient mice with non-colitogenic B. vulgatus prevents DC maturation and T-cell polarization.** *PLoS One* 2008, **3:**e2376.
4. Frick JS, Zahir N, Muller M, Kahl F, Bechtold O, Lutz MB, Kirschning CJ, Reimann J, Jilge B, Bohn E, Autenrieth IB: **Colitogenic and non-colitogenic commensal bacteria differentially trigger DC maturation and Th cell polarization: An important role for IL-6.** *Eur J Immunol* 2006, **36:**1537–1547.
5. Geisel J, Kahl F, Muller M, Wagner H, Kirschning CJ, Autenrieth IB, Frick JS: **IL-6 and Maturation Govern TLR2 and TLR4 Induced TLR Agonist Tolerance and Cross-Tolerance in Dendritic Cells.** *J Immunol* 2007, **179:**5811–5818.
6. Bennett SR, Carbone FR, Karamalis F, Flavell RA, Miller JF, Heath WR: **Help for cytotoxic-T-cell responses is mediated by CD40 signalling.** *Nature* 1998, **393:**478–480.
7. Chang WL, Baumgarth N, Eberhardt MK, Lee CY, Baron CA, Gregg JP, Barry PA: **Exposure of myeloid dendritic cells to exogenous or endogenous IL-10 during maturation determines their longevity.** *J Immunol* 2007, **178:**7794–7804.
8. Caux C, Massacrier C, Vanbervliet B, Dubois B, Van KC, Durand I, Banchereau J: **Activation of human dendritic cells through CD40 cross-linking.** *J Exp Med* 1994, **180:**1263–1272.
9. Cella M, Scheidegger D, Palmer-Lehmann K, Lane P, Lanzavecchia A, Alber G: **Ligation of CD40 on dendritic cells triggers production of high levels of interleukin-12 and enhances T cell stimulatory capacity: T-T help via APC activation.** *J Exp Med* 1996, **184:**747–752.
10. Koch F, Stanzl U, Jennewein P, Janke K, Heufler C, Kampgen E, Romani N, Schuler G: **High level IL-12 production by murine dendritic cells: upregulation via MHC class II and CD40 molecules and downregulation by IL-4 and IL-10.** *J Exp Med* 1996, **184:**741–746.
11. Toso JF, Lapointe R, Hwu P: **CD40 ligand and lipopolysaccharide enchance the in vitro generation of melanoma-reactive T-cells.** *J Immunol Methods* 2002 Jan 1, **259**(1-2):181–190.
12. Bjorck P, Banchereau J, Flores-Romo L: **CD40 ligation counteracts Fas-induced apoptosis of human dendritic cells.** *Int Immunol* 1997, **9:**365–372.
13. Wong BR, Josien R, Lee SY, Sauter B, Li HL, Steinman RM, Choi Y: **TRANCE (tumor necrosis factor [TNF]-related activation-induced cytokine), a new TNF family member predominantly expressed in T cells, is a dendritic cell-specific survival factor.** *J Exp Med* 1997, **186:**2075–2080.
14. Boonstra A, Rajsbaum R, Holman M, Marques R, sselin-Paturel C, Pereira JP, Bates EE, Akira S, Vieira P, Liu YJ, Trinchieri G, O'Garra A: **Macrophages and myeloid dendritic cells, but not plasmacytoid dendritic cells, produce IL-10 in response to MyD88- and TRIF-dependent TLR signals, and TLR-independent signals.** *J Immunol* 2006, **177:**7551–7558.
15. Kuniyoshi JS, Kuniyoshi CJ, Lim AM, Wang FY, Bade ER, Lau R, Thomas EK, Weber JS: **Dendritic cell secretion of IL-15 is induced by recombinant huCD40LT and augments the stimulation of antigen-specific cytolytic T cells.** *Cell Immunol* 1999, **193:**48–58.
16. Holscher C: **The power of combinatorial immunology: IL-12 and IL-12-related dimeric cytokines in infectious diseases.** *Med Microbiol Immunol* 2004, **193:**1–17.
17. Trinchieri G: **Interleukin-12 and the regulation of innate resistance and adaptive immunity.** *Nat Rev Immunol* 2003, **3:**133–146.
18. Hommes DW, Peppelenbosch MP, van Deventer SJ: **Mitogen activated protein (MAP) kinase signal transduction pathways and novel anti-inflammatory targets.** *Gut* 2003, **52:**144–151.
19. Chang L, Karin M: **Mammalian MAP kinase signalling cascades.** *Nature* 2001, **410:**37–40.
20. Johnson GL, Lapadat R: **Mitogen-activated protein kinase pathways mediated by ERK, JNK, and p38 protein kinases.** *Science* 2002, **298:**1911–1912.
21. Grassl GA, Kracht M, Wiedemann A, Hoffmann E, Aepfelbacher M, Eichel-Streiber C, Bohn E, Autenrieth IB: **Activation of NF-kappaB and IL-8 by Yersinia enterocolitica invasin protein is conferred by engagement of Rac1 and MAP kinase cascades.** *Cell Microbiol* 2003, **5:**957–971.
22. Brook M, Sully G, Clark AR, Saklatvala J: **Regulation of tumour necrosis factor alpha mRNA stability by the mitogen-activated protein kinase p38 signalling cascade.** *FEBS Lett* 2000, **483:**57–61.
23. Wang SW, Pawlowski J, Wathen ST, Kinney SD, Lichenstein HS, Manthey CL: **Cytokine mRNA decay is accelerated by an inhibitor of p38-mitogen-activated protein kinase.** *Inflamm Res* 1999, **48:**533–538.
24. Dohnal AM, Luger R, Paul P, Fuchs D, Felzmann: **CD40 ligation restores type 1 polarizing capacity in TLR4-activated dendritic cells that have ceased interleukin-12 expression.** *J Cell Mol Med T* 2009, **13:**1741–1750.
25. Lapointe R, Toso JF, Butts C, Young HA, Hwu P: **Human dendritic cells require multiple activation signals for the efficient generation of tumor antigen-specific T lymphocytes.** *Eur J Immunol* 2000, **30:**3291–3298.
26. Dhodapkar MV, Steinman RM, Krasovsky J, Munz C, Bhardwaj N: **Antigen-specific inhibition of effector T cell function in humans after injection of immature dendritic cells.** *J Exp Med* 2001, **193:**233–238.
27. Hawiger D, Inaba K, Dorsett Y, Guo M, Mahnke K, Rivera M, Ravetch JV, Steinman RM, Nussenzweig MC: **Dendritic cells induce peripheral T cell unresponsiveness under steady state conditions in vivo.** *J Exp Med* 2001, **194:**769–779.
28. Steinman RM, Hawiger D, Nussenzweig MC: **Tolerogenic dendritic cells.** *Annu Rev Immunol* 2003, **21:**685–711.
29. van den Broek M: **Dendritic cells break bonds to tolerize.** *Immunity* 2007, **27:**544–546.
30. Fujii S, Liu K, Smith C, Bonito AJ, Steinman RM: **The linkage of innate to adaptive immunity via maturing dendritic cells in vivo requires CD40 ligation in addition to antigen presentation and CD80/86 costimulation.** *J Exp Med* 2004, **199:**1607–1618.
31. Martin E, O'Sullivan B, Low P, Thomas R: **Antigen-specific suppression of a primed immune response by dendritic cells mediated by regulatory T cells secreting interleukin-10.** *Immunity* 2003, **18:**155–167.
32. Murugaiyan G, Martin S, Saha B: **Levels of CD40 expression on dendritic cells dictate tumour growth or regression.** *Clin Exp Immunol* 2007, **149:**194–202.
33. Smith DW, Nagler-Anderson C: **Preventing intolerance: the induction of nonresponsiveness to dietary and microbial antigens in the intestinal mucosa.** *J Immunol* 2005, **174:**3851–3857.
34. Suzuki M, Zheng X, Zhang X, Ichim TE, Sun H, Kubo N, Beduhn M, Shunnar A, Garcia B, Min WP: **Inhibition of allergic responses by CD40 gene silencing.** *Allergy* 2009, **64:**387–397.
35. Joffre O, Nolte MA, Sporri R, Reis e Sousa C: **Inflammatory signals in dendritic cell activation and the induction of adaptive immunity.** *Immunol Rev* 2009, **227:**234–247.
36. Lutz MB, Schuler G: **Immature, semi-mature and fully mature dendritic cells: which signals induce tolerance or immunity?** *Trends Immunol* 2002, **23:**445–449.
37. Menges M, Rossner S, Voigtlander C, Schindler H, Kukutsch NA, Bogdan C, Erb K, Schuler G, Lutz MB: **Repetitive injections of dendritic cells matured with tumor necrosis factor alpha induce antigen-specific protection of mice from autoimmunity.** *J Exp Med* 2002, **195:**15–21.
38. Sporri R, Reis e Sousa C: **Inflammatory mediators are insufficient for full dendritic cell activation and promote expansion of CD4+ T cell populations lacking helper function.** *Nat Immunol* 2005, **6:**163–170.
39. Snijders A, Kalinski P, Hilkens CM, Kapsenberg ML: **High-level IL-12 production by human dendritic cells requires two signals.** *Int Immunol* 1998, **10:**1593–1598.
40. Schulz O, Edwards AD, Schito M, Aliberti J, Manickasingham S, Sher A, Reis e Sousa C: **CD40 triggering of heterodimeric IL-12 p70 production by dendritic cells in vivo requires a microbial priming signal.** *Immunity* 2000, **13:**453–462.
41. Kato T, Hakamada R, Yamane H, Nariuchi H: **Induction of IL-12 p40 messenger RNA expression and IL-12 production of macrophages via CD40-CD40 ligand interaction.** *J Immunol* 1996, **156:**3932–3938.
42. Morelli AE, Zahorchak AF, Larregina AT, Colvin BL, Logar AJ, Takayama T, Falo LD, Thomson AW: **Cytokine production by mouse myeloid dendritic**

cells in relation to differentiation and terminal maturation induced by lipopolysaccharide or CD40 ligation. *Blood* 2001, **98:**1512–1523.
43. Alderson MR, Armitage RJ, Tough TW, Strockbine L, Fanslow WC, Spriggs MK: **CD40 expression by human monocytes: regulation by cytokines and activation of monocytes by the ligand for CD40.** *J Exp Med* 1993, **178:**669–674.
44. Nguyen VT, Benveniste EN: **Critical role of tumor necrosis factor-alpha and NF-kappa B in interferon-gamma -induced CD40 expression in microglia/macrophages.** *J Biol Chem* 2002, **277:**13796–13803.
45. Wesemann DR, Dong Y, O'Keefe GM, Nguyen VT, Benveniste EN: **Suppressor of cytokine signaling 1 inhibits cytokine induction of CD40 expression in macrophages.** *J Immunol* 2002, **169:**2354–2360.
46. Hirschfeld M, Ma Y, Weis JH, Vogel SN, Weis JJ: **Cutting edge: repurification of lipopolysaccharide eliminates signaling through both human and murine toll-like receptor 2.** *J Immunol* 2000, **165:**618–622.
47. Re F, Strominger JL: **IL-10 released by concomitant TLR2 stimulation blocks the induction of a subset of Th1 cytokines that are specifically induced by TLR4 or TLR3 in human dendritic cells.** *J Immunol* 2004, **173:**7548–7555.
48. Ling P, Gately MK, Gubler U, Stern AS, Lin P, Hollfelder K, Su C, Pan YC, Hakimi J: **Human IL-12 p40 homodimer binds to the IL-12 receptor but does not mediate biologic activity.** *J Immunol* 1995, **154:**116–127.
49. Gillessen S, Carvajal D, Ling P, Podlaski FJ, Stremlo DL, Familletti PC, Gubler U, Presky DH, Stern AS, Gately MK: **Mouse interleukin-12 (IL-12) p40 homodimer: a potent IL-12 antagonist.** *Eur J Immunol* 1995, **25:**200–206.
50. Nigg AP, Zahn S, Ruckerl D, Holscher C, Yoshimoto T, Ehrchen JM, Wolbing F, Udey MC, von Stebut E: **Dendritic cell-derived IL-12p40 homodimer contributes to susceptibility in cutaneous leishmaniasis in BALB/c mice.** *J Immunol* 2007, **178:**7251–7258.
51. Yoshimoto T, Wang CR, Yoneto T, Waki S, Sunaga S, Komagata Y, Mitsuyama M, Miyazaki J, Nariuchi H: **Reduced T helper 1 responses in IL-12 p40 transgenic mice.** *J Immunol* 1998, **160:**588–594.
52. Frick JS, Grunebach F, Autenrieth IB: **Immunomodulation by semi-mature dendritic cells: A novel role of Toll-like receptors and interleukin-6.** *Int J Med Microbiol* 2010, **300**(1):19–24.
53. Diehl S, Chow CW, Weiss L, Palmetshofer A, Twardzik T, Rounds L, Serfling E, Davis RJ, Anguita J, Rincon M: **Induction of NFATc2 expression by interleukin 6 promotes T helper type 2 differentiation.** *J Exp Med* 2002, **196:**39–49.
54. Murphy KM, Ouyang W, Farrar JD, Yang J, Ranganath S, Asnagli H, Afkarian M, Murphy TL: **Signaling and transcription in T helper development.** *Annu Rev Immunol* 2000, **18:**451–494.
55. Diehl S, Rincon M: **The two faces of IL-6 on Th1/Th2 differentiation.** *Mol Immunol* 2002, **39:**531–536.
56. Diehl S, Anguita J, Hoffmeyer A, Zapton T, Ihle JN, Fikrig E, Rincon M: **Inhibition of Th1 differentiation by IL-6 is mediated by SOCS1.** *Immunity* 2000, **13:**805–815.
57. Aicher A, Shu GL, Magaletti D, Mulvania T, Pezzutto A, Craxton A, Clark EA: **Differential role for p38 mitogen-activated protein kinase in regulating CD40-induced gene expression in dendritic cells and B cells.** *J Immunol* 1999, **163:**5786–5795.
58. Yu Q, Kovacs C, Yue FY, Ostrowski MA: **The role of the p38 mitogen-activated protein kinase, extracellular signal-regulated kinase, and phosphoinositide-3-OH kinase signal transduction pathways in CD40 ligand-induced dendritic cell activation and expansion of virus-specific CD8+ T cell memory responses.** *J Immunol* 2004, **172:**6047–6056.
59. Dillon S, Agrawal A, Van Dyke T, Landreth G, McCauley L, Koh A, Maliszewski C, Akira S, Pulendran B: **A Toll-like receptor 2 ligand stimulates Th2 responses in vivo, via induction of extracellular signal-regulated kinase mitogen-activated protein kinase and c-Fos in dendritic cells.** *J Immunol* 2004, **172:**4733–4743.
60. Mathur RK, Awasthi A, Wadhone P, Ramanamurthy B, Saha B: **Reciprocal CD40 signals through p38MAPK and ERK-1/2 induce counteracting immune responses.** *Nat Med* 2004, **10:**540–544.
61. Mukherjee P, Chauhan VS: **Plasmodium falciparum-free merozoites and infected RBCs distinctly affect soluble CD40 ligand-mediated maturation of immature monocyte-derived dendritic cells.** *J Leukoc Biol* 2008, **84:**244–254.
62. Goodridge HS, Harnett W, Liew FY, Harnett MM: **Differential regulation of interleukin-12 p40 and p35 induction via Erk mitogen-activated protein kinase-dependent and -independent mechanisms and the implications for bioactive IL-12 and IL-23 responses.** *Immunology* 2003, **109:**415–425.
63. Lu HT, Yang DD, Wysk M, Gatti E, Mellman I, Davis RJ, Flavell RA: **Defective IL-12 production in mitogen-activated protein (MAP) kinase kinase 3 (Mkk3)-deficient mice.** *EMBO J* 1999, **18:**1845–1857.
64. Clark AR, Dean JL, Saklatvala J: **Post-transcriptional regulation of gene expression by mitogen-activated protein kinase p38.** *FEBS Lett* 2003, **546:**37–44.
65. Vanden Berghe W, Plaisance S, Boone E, De Bosscher K, Schmitz ML, Fiers W, Haegeman G: **p38 and extracellular signal-regulated kinase mitogen-activated protein kinase pathways are required for nuclear factor-kappaB p65 transactivation mediated by tumor necrosis factor.** *J Biol Chem* 1998, **273:**3285–3290.
66. Vermeulen L, De Wilde G, Van Damme P, Vanden Berghe W, Haegeman G: **Transcriptional activation of the NF-kappaB p65 subunit by mitogen- and stress-activated protein kinase-1 (MSK1).** *EMBO J* 2003, **22:**1313–1324.
67. Yanagawa Y, Onoe K: **Distinct regulation of CD40-mediated interleukin-6 and interleukin-12 productions via mitogen-activated protein kinase and nuclear factor kappaB-inducing kinase in mature dendritic cells.** *Immunology* 2006, **117:**526–535.
68. Kikuchi K, Yanagawa Y, Iwabuchi K, Onoe K: **Differential role of mitogen-activated protein kinases in CD40-mediated IL-12 production by immature and mature dendritic cells.** *Immunol Lett* 2003, **89:**149–154.

doi:10.1186/1471-2172-13-22
Cite this article as: Gerlach *et al.*: Role of CD40 ligation in dendritic cell semimaturation. *BMC Immunology* 2012 **13**:22.

Hindawi Publishing Corporation
Journal of Immunology Research
Volume 2016, Article ID 1958650, 12 pages
http://dx.doi.org/10.1155/2016/1958650

Review Article

Molecular Mechanisms of Induction of Tolerant and Tolerogenic Intestinal Dendritic Cells in Mice

Alex Steimle and Julia-Stefanie Frick

University of Tübingen, Institute of Medical Microbiology and Hygiene, Elfriede-Aulhorn-Strasse 6, 72076 Tübingen, Germany

Correspondence should be addressed to Julia-Stefanie Frick; julia-stefanie.frick@med.uni-tuebingen.de

Received 22 October 2015; Revised 6 January 2016; Accepted 17 January 2016

Academic Editor: Silvia Beatriz Boscardin

How does the host manage to tolerate its own intestinal microbiota? A simple question leading to complicated answers. In order to maintain balanced immune responses in the intestine, the host immune system must tolerate commensal bacteria in the gut while it has to simultaneously keep the ability to fight pathogens and to clear infections. If this tender equilibrium is disturbed, severe chronic inflammatory reactions can result. Tolerogenic intestinal dendritic cells fulfil a crucial role in balancing immune responses and therefore creating homeostatic conditions and preventing from uncontrolled inflammation. Although several dendritic cell subsets have already been characterized to play a pivotal role in this process, less is known about definite molecular mechanisms of how intestinal dendritic cells are converted into tolerogenic ones. Here we review how gut commensal bacteria interact with intestinal dendritic cells and why this bacteria-host cell interaction is crucial for induction of dendritic cell tolerance in the intestine. Hereby, different commensal bacteria can have distinct effects on the phenotype of intestinal dendritic cells and these effects are mainly mediated by impacting toll-like receptor signalling in dendritic cells.

1. Introduction

The mammalian intestinal immune system has to rise to different challenges. On the one hand, it has to tolerate the intestinal microbiota consisting of commensal bacteria, fungi, and other microbes, thereby profiting from beneficial bacterial metabolites and other advantages. On the other hand, pathogen induced infections of the intestine have to be cleared without spacious damage of the intestinal tissue. Since a loss of tolerance to the own microbiota causes chronic inflammation of the gut, efficient sensing of the intestinal homeostasis is crucial to avoid pathophysiological immune responses. In this context, intestinal tolerogenic dendritic cells play a crucial role as key mediators for the maintenance of the intestinal homeostasis. While the main question "how does the host manage to tolerate its own intestinal microbiota?" is pretty simple, the answer is not trivial.

Here, we want to focus on (1) the molecular mechanisms that might contribute to the induction of tolerogenic DCs in the intestine and (2) the potential clinical applications arising from these findings for the treatment of chronic inflammatory disorders of the gut: inflammatory bowel diseases.

2. Intestinal Dendritic Cells: Subsets and Biological Functions

Dendritic cells (DCs) comprise a heterogeneous leukocyte population of different developmental origin and with distinct surface markers and biological functions. DCs originate from blood monocytes or a common DC progenitor in the bone marrow under steady-state conditions. The differentiation into DCs relies on local presence of GM-CSF [1]. DCs in general are utterly specialized antigen presenting cells (APCs) which are able to induce a variety of different immune responses. They are the most important cell type connecting the innate immune system with adaptive immune responses [2]. DCs patrol almost all lymphoid and nonlymphoid organs and meld properties of the innate and adaptive immunity and therefore link these two mechanistically distinct branches of the immune system [3]. Furthermore, DCs play a pivotal role in mediating a protective adaptive immunity against

pathogens while maintaining immune tolerance to self-antigens. Their crucial role for mediating self-tolerance is confirmed by the observation that DC depletion leads to a loss of self-tolerance and results in myeloid inflammation and the induction of autoimmune processes [4].

The gut-associated lymphoid tissue (GALT) is the largest immune organ of the body. The GALT has to ensure that there is a dynamic balance between protective immunity by fighting pathogens and regulatory mechanisms to prevent autoimmunity [5]. Since the GALT is constantly exposed to large amounts of luminal antigens like food metabolites, foreign pathogens, and commensal microbes, this balance has to be well adjusted in order to create homeostatic conditions in the intestine. Dendritic cells are hereby the key players for maintaining intestinal homeostasis [6]. They are spread out in the connective tissue underlying the epithelial layer of the gut [7].

2.1. Morphological Differences between DCs and Macrophages (MΦ) in the Murine Intestine. DCs belong to the group of mononuclear phagocytes (MPs) with macrophages (MΦ) being another cell type belonging to this group. Discrimination between DCs on one hand and MΦ on the other hand is still a matter of ongoing debate. However, concerning intestinal DCs and MΦ, certain surface markers and transcription factors have been reported to be uniquely expressed by only one of these two groups. In the murine intestine, surface proteins which are exclusively expressed by DCs are CD103 [8–10], CD26, and CD272 [9]. However, CD103 is not expressed from every DC subset (see below) [11–13]. A DC specific transcription factor is Zbtb46 [13]. The only MPs in the murine intestine that express the proteins CD14, MerTK [9, 14], F4/80, and CD64 [15] are intestinal MΦ. The widely used surface markers for DC-macrophage discrimination, CD11c and MHC-II, are not useful to distinguish murine intestinal DCs from MΦ, since both proteins can be expressed in DC or macrophage subpopulations [13, 15–19]. The expression of CD11b and MHC-II varies among DC and MΦ subpopulations [13]. Therefore, the protein expression pattern of murine intestinal DCs under steady state conditions can be summarized as $CD11c^{+}CD103^{+/-}CD11b^{+/-}$MHC-$II^{+}CD26^{+}CD272^{+}Zbtb46^{+}CD14^{-}MerTK^{-}F4/80^{-}CD64^{-}$, while the phenotype of intestinal murine MΦ is $CD11c^{+/-}CD103^{-}CD11b^{+/-}$MHC-$II^{+/-}CD26^{-}CD272^{-}Zbtb46^{-}CD14^{+}MerTK^{+}F4/80^{+}CD64^{+}$. Another distinctive feature between DCs and MΦ is the migratory and proliferation behaviour. In general, intestinal DCs are short-lived, proliferating migratory cells while MΦ are tissue resident, long-lived, and nonproliferating [13].

2.2. DC Subpopulations in the Intestine. As mentioned above, dendritic cells do not comprise a homogenous cell population. Different ways to distinguish one DC from another are published and popular. The most prominent approach to differentiate between distinguishable DC subsets is to focus on different expression of surface proteins, especially CD103 and CD11b [12, 13]. However, Guilliams and van de Laar have recently proposed to distinguish DCs rather by their biological function and cellular origin than their surface marker expression [11, 12]. We will adapt this system, but we will focus on DC subsets located in the intestine and add latest findings on different surface marker expression among these subsets [13]. In general, DCs derive from common dendritic cell progenitors (CDP) which, in turn, develop from hematopoietic precursor cells. CDPs may differentiate into either preplasmacytoid DCs (pre-pDCs) or precommon DCs (pre-cDCs) precursor cells [20, 21]. Murine pDCs are characterized by PDCA1 expression and their development is dependent on the transcription factors BATF3 [22], ID2 [23], NFIL3 [24], E2-2 [25], and IRF8 [22]. Murine cDCs commonly express XCR1 and SIRPα [26] and need RelB [27], RPBJ [28], and IRF4 [29] for differentiation. Intestinal murine cDCs additionally express CD103 and can be further subdivided into two ontogenetically different populations, dependent on their surface expression of CD11b [30]. IRF4 is needed for the $CD11b^{+}$ lineage of these CD103-expressing or CD103-nonexpressing conventional DCs [29, 31, 32]. $CD103^{+}CD11b^{-}$ build up cDC subset 1 (cDC1) whereas $CD103^{+}CD11b^{+}$ form subgroup cDC2 (see Figure 1). One of the most important events for the maintenance of intestinal homeostasis is the induction of regulatory T cells (Tregs) (see below). Besides TGF-β, Treg formation is dependent on the presence of retinoic acid (RA) that is produced by dendritic cells [33, 34]. But only DCs possessing retinaldehyde dehydrogenases (ALDHs) can convert vitamin A-derived retinol to RA. Therefore, ALDH is a crucial enzyme for a subsequent induction of Tregs and thus promotion of intestinal tolerance and homeostasis. It was not clear which $CD103^{+}$ DC subset is responsible for Treg induction, since both $CD103^{+}CD11b^{+}$ and $CD103^{+}CD11b^{-}$ DCs can produce RA and induce Tregs *in vitro* [35, 36]. Meanwhile, it could be demonstrated that each $CD103^{+}$ DC subset ($CD11b^{+}$ versus $CD11b^{-}$) can be subdivided in an ALDH-expressing and a non-ALDH-expressing subset [35]. Therefore, both $CD11b^{+}CD103^{+}$ and $CD11b^{-}CD103^{+}$ DCs are able to induce a RA-mediated Treg formation. This was initially demonstrated in skin-draining lymph nodes [35], but Janelsins et al. confirmed the presence of $CD103^{+}CD11b^{+}ALDH^{+/-}$ DCs also in the murine cLP [37]. Both $CD103^{+}$ DC subsets together monitor the luminal environment in the intestine. Not only are $CD103^{+}$ DCs able to induce Treg-mediated immune tolerance in the intestine but they are also able to promote Th17 differentiation of naïve T cells. Th17 cells contribute to the manifestation of autoimmune diseases [38, 39] and $CD103^{+}CD11b^{+}$ seem to be more efficient in Th17 promotion than their $CD11b^{-}$ counterparts [36, 40]. It can be assumed that $ALDH^{-}CD103^{+}CD11b^{+/-}$ might promote this Th17 immune response, but final evidence is missing until now.

Concerning their distribution in the intestine, $CD103^{+}$ $CD11b^{-}$ DCs are prominent in the colonic lamina propria (cLP), while $CD103^{+}CD11b^{+}$ DCs are mostly found in the LP of the small intestine [29]. Additionally, $CD103^{+}CD11b^{+}$ DCs from the mesenteric lymph nodes (MLN) also express ALDH, which is, surprisingly, abdicable for the induction of Tregs since a loss of ALDH activity in the MLN did not affect Treg induction [29]. This might support the hypothesis that

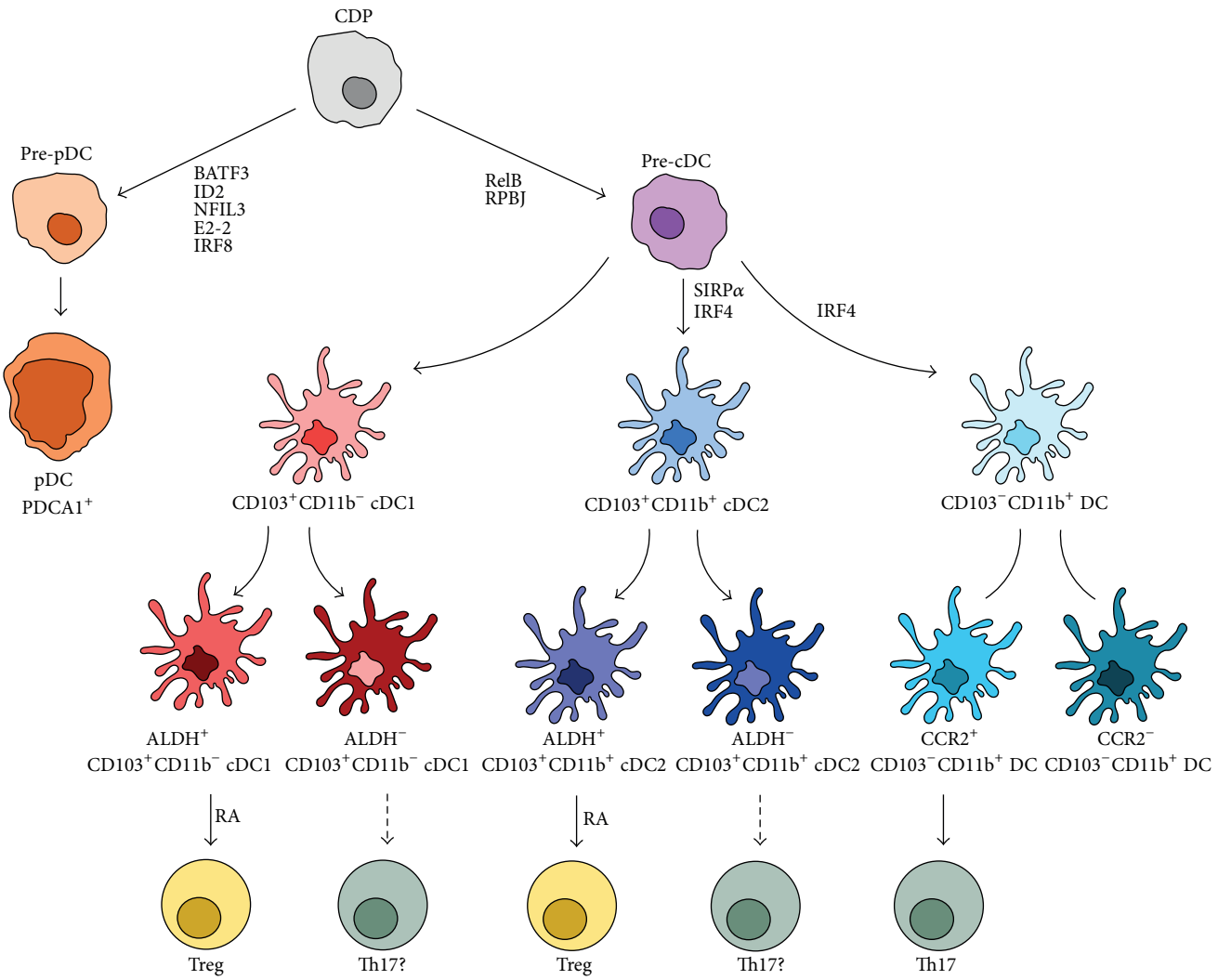

Figure 1: Ontogenetic development of intestinal dendritic cells subpopulations. Adapted from Guilliams et al. [35] and expanded by findings from Scott et al. [13]. See text for details. Common dendritic cell progenitor (CDP), preplasmacytoid dendritic cell (pre-pDC), precommon dendritic cell (pre-cDC), plasmacytoid dendritic cell (pDC), common dendritic cell (cDC), aldehyde dehydrogenase (ALDH), regulatory T cell (Treg), retinoic acid (RA), and T-helper 17 cell (Th17). Arrows with solid lines represent published data, and arrows with broken lines represent speculative hypotheses with missing final evidence.

ALDH activity is more important at other intestinal sites like the lamina propria of the small or large intestine for later Treg induction after DC migration.

Recently, Scott et al. discovered an additional CD103-negative DC population in the murine intestine [13]. There is a $CD11c^+MHC\text{-}II^+CD103^-CD11b^+$ cell population, of which about 15% provide features of DCs like Zbtb64, CD26, and CD272 expression; they respond to Flt3L; they are migratory cells and lack macrophage markers like F4/80 and CD64 [13, 41]. They could be shown to be derived from committed pre-DCs as are $CD103^+$ mucosal DCs [8]. These $CD103^-$ DCs can be further subdivided into two functionally distinct subpopulations dependent on their CCR2 expression. $CCR2^+CD103^+CD11b^+$ DCs are more efficient in Th17 induction than their CCR-negative counterparts and a loss of the $CCR2^+CD103^-CD11b^+$ DCs leads to a defective Th17 response and therefore fails to clear a *Citrobacter* infection *in vivo*.

Another specific protein that is expressed exclusively by intestinal DCs and not by intestinal MΦ or nonintestinal DCs is SIRPα [42, 43]. It seems to be essential for the generation of $CD103^+CD11b^+$ since a loss of function of SIRPα results in a decrease of this DC population in the intestine, accompanied by markedly reduced induction of Th17 immune responses under steady-state and inflammatory conditions [42].

In general, it is important to keep in mind that CD103 expression on DCs is not a marker for universal tolerogenicity, since (1) even $CD103^+$ DCs can fail to induce tolerogenicity if ALDH is not expressed and (2) a tolerogenic environment can be established even in the absence of $CD103^+$ DCs [44].

2.3. Locations of Intestinal DCs. The murine intestine is a multifarious habitat for DCs where distinct sites harbour different DC subsets. A common feature of intestinal DCs distinguishing them from DCs from other nonintestinal tissues

is the expression of CD103, with the already mentioned exception of $CCR2^{+/-}CD103^{-}CD11b^{+}$ DCs, especially DCs in the small intestine (SI) and Peyer's Patches (PP) in mesenteric lymph nodes (MLN) and, with minor occurrence, in the colonic lamina propria (cLP) [8, 29, 41, 43, 45]. DCs from nonlymph node tissues remain some days at their inherent site before migrating to neighbouring draining lymph nodes [35, 46].

3. Antigen Sensing and Sampling by Intestinal Dendritic Cells

Invading microorganisms are recognized by pattern recognition receptors (PRRs) on the DC surface. PRRs include toll-like receptors (TLRs), retinoic acid-inducible gene I-like receptors (RLRs), and nucleotide-binding oligomerization domain-like receptors (NLRs) [47, 48]. PRRs recognize pathogen-associated molecular patterns (PAMPs) [49]. PAMPs comprise a heterogeneous class of different antigens, that is, surface components of bacteria. One of the most prominent PAMPs which usually induces DC maturation is lipopolysaccharide (LPS), an integral cell surface component of all Gram-negative bacteria. Usually, dendritic cells underlie the intestinal epithelium and therefore the connection to the colonic lumen is restricted. However, there are three prominent ways how intestinal dendritic cells can sample luminal antigens: (1) with participation of goblet cells which deliver soluble and preferably low molecular weight antigen to neighbouring DCs [50], (2) with the support of $CX3CR1^{+}$ phagocytotic cells which can actively capture antigen followed by transport to neighbouring DCs via tight junctions [51], and (3) a direct sampling by DCs that extend their dendrites towards the lumen establishing a direct connection to the colonic lumen [52].

4. Intestinal Dendritic Cells and the Gut Microbiota

$CD103^{+}$ DCs are reported to sample mainly bacteria [52] in contrast to $CX3CR1^{+}$ MΦ which also capture soluble proteins and fungi [51, 53]. This illustrates the relevance of the bacterial microbiota composition for intestinal DCs. Interaction of DCs with the gut microbiota can occur directly by sampling bacterial antigen or by interaction with bacterial metabolic products like short chain fatty acids (SCFAs). SCFAs like butyrate can interact with the DC receptor GPR109A which finally leads to an IL-10 mediated induction of Tregs [54]. Since not all gut commensal bacteria produce SCFAs, a microbiota shift leading to dysbiosis can profoundly affect immunological mechanisms in the intestine. Toll-like receptor (TLR) signalling in DCs also seems to be crucial for the maintenance of intestinal homeostasis. Different bacterial components bind to distinct TLRs on the surface of DCs resulting in the activation of intracellular signalling cascades which leads to DC maturation or semimaturation (see below) accompanied by secretion of pro- or anti-inflammatory cytokines. The TLT adaptor molecule TNF-receptor associated factor 6 (TRAF6) seems to play a pivotal role in maintaining intestinal homeostasis since $Traf6^{-/-}$ mice fail to maintain intestinal homeostasis mediated by a reduction of Tregs and an increase of T-helper 2 (Th2) cells, finally resulting in a microbiota composition-dependent induction of colonic inflammation [55].

5. The Different Maturation Phenotypes of Dendritic Cells

The capability of initiating an immune response depends on the current DC maturation state. Usually, antigen encounter results in rapid DC maturation which is characterized by efficient endocytosis and antigen processing. Furthermore, upregulation of MHC-II and T cell costimulatory molecules like CD40, CD80, and CD86 enhanced expression of chemokine receptors and the secretion of proinflammatory cytokines like IL-1β, IL-6, TNFα, and IL-12 are part of DC maturation. These events influence and activate other cellular components of an induced immune response like MΦ, neutrophils, and especially T cells [56].

5.1. Mature DCs (mDCs). Induction of DC maturation is accompanied by a loss of the capacity to take up and process antigen [57]. However, they literally develop into professional antigen presenting cells (APCs) indicated by powerful antigen presentation to naïve T cells [2], as well as by their ability to migrate to secondary lymphatic organs where they present antigens to T cells.

5.2. Immature DCs (iDCs). Immature DCs (iDCs) express low amounts of MHC-II and T cell costimulatory molecules. They tend to promote T cell anergy and to generate Tregs, with both effects being crucial for intestinal homeostasis [58]. iDCs furthermore express high levels of PRRs with which they mediate the recognition of potential antigens and therefore their endocytosis [57].

5.3. Semimature DCs (smDCs) and Tolerant DCs. The definition of a semimature DC phenotype is less distinct. The most important property of smDCs uniting different definitions is the inability to induce a proinflammatory Th1 or Th17 response and to be nonresponsive, or in other words "tolerant," towards subsequent maturation stimuli [59, 60] with the latter being the criterion that mediates the tolerogenic functions of smDCs [60]. DC semimaturation leads to a certain expression of T cell activation and a cytokine secretion pattern that is distinct from the ones of immature and mature DCs. The definite phenotype varies from one semimaturation inducing strategy to another. SmDCs that are generated by treating immature DCs with TNFα display a phenotype that can be summarized as $CD11c^{+}$ $MHCII^{hi}CD86^{hi}CD80^{hi}CD40^{lo}CD54^{+}CD205^{hi}CD25^{hi}TNF^{lo}$ $IL\text{-}12p40^{lo}IL\text{-}10^{lo}$ [61]. Induction of semimaturation via low-dose LPS and subsequent dexamethasone treatment results in $CD14^{+}CD1a^{lo}CD80^{hi}CD86^{hi}MHCII^{hi}IL\text{-}10^{hi}TNF^{lo}$ DCs [62]. We use a Gram-negative gut commensal, *Bacteroides vulgatus*, to induce semimaturation and define the smDC

Table 1: Phenotypes of semimature dendritic cells dependent on semimaturation inducing agent. LPS (lipopolysaccharide), Dex (dexamethasone), and PSA (polysaccharide A); high expression (hi), low expression (lo), intermediate expression (int), and not determined (n.d.).

Semimaturation inducing agent	MHC-II	CD40	CD80	CD86	IL-10	IL-6	TNFα	IL-12	Source
B. vulgatus	int	lo	lo	lo	n.d.	int	lo	lo	[59]
TNFα	hi	lo	hi	hi	lo	n.d.	lo	lo	[61]
LPS + Dex	hi	n.d.	hi	hi	hi	n.d.	lo	n.d.	[62]
B. fragilis PSA	int	n.d.	n.d.	n.d.	hi	n.d.	n.d.	n.d.	[66]
ATP + LPS	hi	lo	hi	hi	hi	n.d.	lo	lo	[120]
E. multilocularis	lo	n.d.	n.d.	lo	int	lo	n.d.	lo	[121]
Low dose LPS	int	lo	lo	lo	n.d.	int	lo	lo	[64]
α-1 Antitrypsin	int	lo	n.d.	int	hi	lo	n.d.	n.d.	[65]

phenotype as $CD11c^+MHCII^{int}CD40^{lo}CD80^{lo}CD86^{lo}$ $TNF\alpha^{lo}IL\text{-}12^{lo}IL\text{-}6^{int}$ [59]. Besides these strategies, DC semimaturation can be induced by treating immature DCs with ATP and LPS [63], low dose *Salmonella* LPS [64], α-1 antitrypsin [65], *Bacteroides fragilis* PSA [66], or *Echinococcus multilocularis* cell aggregates [67]. The resulting phenotypes concerning the most important immunomodulatory molecules are summarized in Table 1.

5.4. Tolerogenic DCs. While mature DCs (mDCs) promote efficient induction of inflammatory immune responses, iDCs and smDCs fail to do so. They rather have the property to actively prevent from inflammatory reactions and are therefore also termed tolerogenic DCs (tolDCs). The term "tolerogenic" includes one, several, or all of the following features DCs must provide to be considered "tolerogenic": (1) the induction of unresponsiveness of T cells, (2) active induction of Tregs, (3) inhibition of proinflammatory T cell responses, and (4) promotion of T cell apoptosis or T cell anergy [6]. In this context, the interplay between the intestinal epithelial cells and the host immune system is of essential importance.

More generally, regulatory or tolerogenic DCs keep their ability to present antigens, but at the same time they downregulate the expression of T cell costimulatory molecules and proinflammatory cytokines but in turn upregulate inhibitory molecules like PD-L1, CD95L, or IDO as well as anti-inflammatory cytokines such as TGF-β and IL-10 [68]. Furthermore, they are resistant to a second maturation inducing signal [68]. Importantly, DCs also influence the differentiation of naïve T cells into Th1, Th2, Th17, or Treg cells, mostly due to supplying a certain cytokine environment [69]. In a healthy individual, the presence of tolDCs is important and a loss of tolDCs can result in the development of AID [4]. Semimature DCs are potent tolerant and tolerogenic DCs since they fulfil many to all of the above-mentioned criteria, dependent on the agent with which semimaturation is induced. As already mentioned before, the main characteristic that makes semimature DCs tolerogenic is their unresponsiveness (tolerance) towards subsequent maturating stimuli [59, 64, 65].

6. The Role of Dendritic Cells in Induction of Inflammatory Bowel Disease (IBD)

The development of inflammatory bowel diseases (IBD) with its two major representatives Crohn's disease (CD) and ulcerative colitis (UC) is associated with (1) an inappropriate immune response to normally benign stimuli like commensal microbes, (2) an inefficient clearance of microbes leading to a continuous stimulation of the immune system, or (3) failing to turn from an adequate proinflammatory response to inflammation resolving anti-inflammatory immune reactions [70]. In this context, the composition of the intestinal microbiota is decisive for the onset of colonic inflammation in most mouse models of experimental colitis [71] and intestinal DCs are crucial for driving immune responses in either a proinflammatory or a rather homeostatic direction [72]. For example, $Il10^{-/-}$ mice develop chronic colitis which results from the absence of suppression of MyD88-dependent commensal-induced inflammation by IL-10 [73].

Under steady-state conditions, circulating $Ly6C^{hi}$ monocytes are repopulated into tolerogenic $F4/80^{low}CD103^+$ $CD11c^+$ LP DCs, which contribute to homeostasis by supporting tolerogenic functions [16]. On the other hand, under inflammatory conditions during colitis, $Ly6C^{hi}$ monocytes develop into $CD103^-CX3CR1^{int}CD11b^+$ LP DCs, which mediate inflammation during colitis [16].

The tolerogenic functions of intestinal DCs are mainly mediated by the induction of regulatory T cells (Tregs). As a characteristic feature, Tregs express the transcription factor forkhead box P3 (Foxp3) [74]. Induction of $CD4^+CD25^+Foxp3^+$ Tregs is essential for intestinal homeostasis [75] and a loss of Tregs leads to a fatal multiple-organ-associated autoimmune disease [76]. Tregs are usually converted in the peripheral immune system with the help of $CD103^+$ dendritic cells [77] whereupon this Treg induction is dependent on the presence of TGF-β and retinoic acid (RA) [78].

However, during colitis, $CD103^-CXCR1^{int}CD11b^+$ DCs, although also present under steady-state conditions, massively infiltrate the colonic LP and mediate proinflammatory

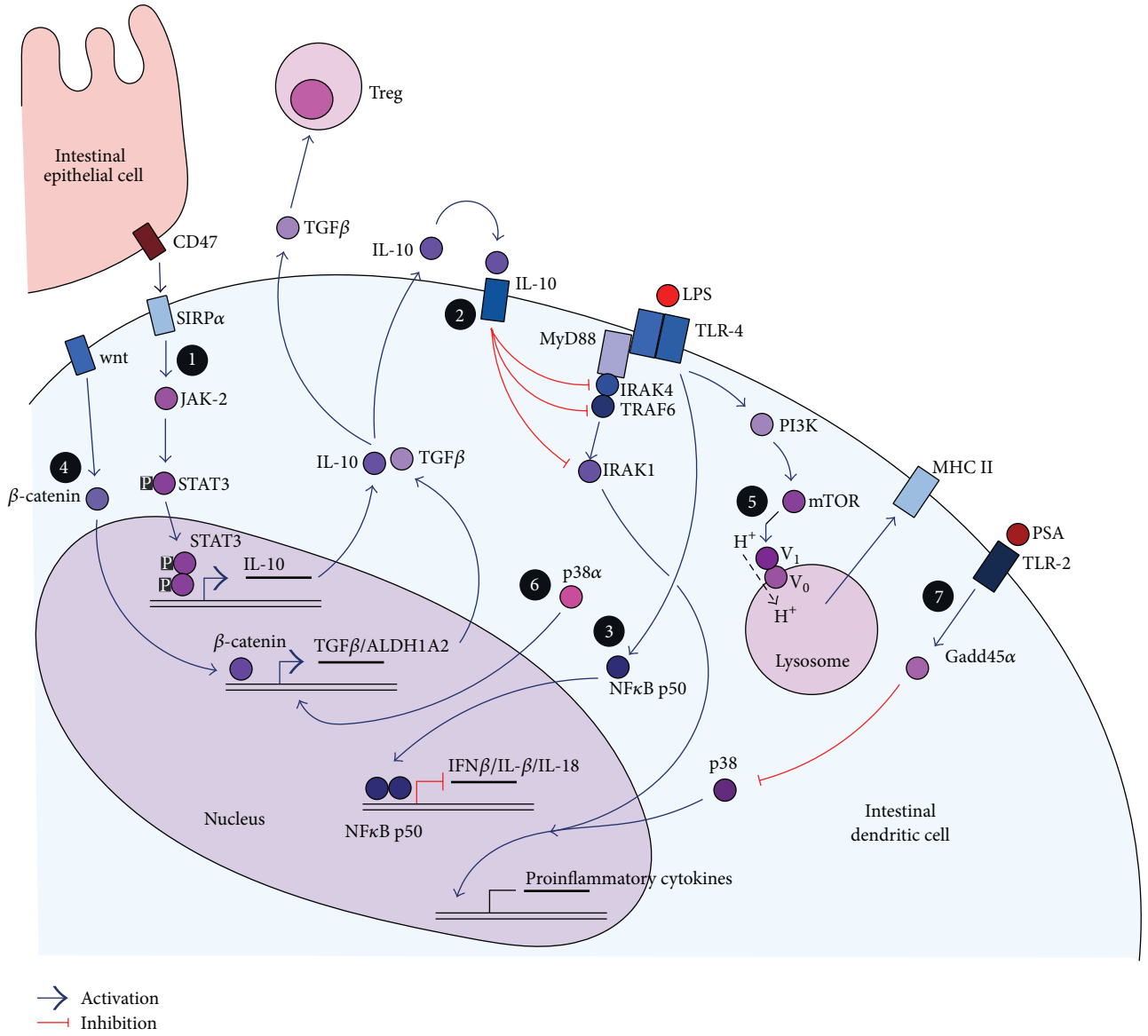

FIGURE 2: Possible molecular mechanisms of tolerance induction in intestinal dendritic cells. The white numbers in black circles refer to the numbering of regulation mechanisms in the text. See text for details.

immune responses by producing IL-12, IL-23, iNOS, and TNF [16].

7. Possible Molecular Mechanisms of DC Tolerance Induction in the Intestine

Less is known about defined mechanisms of tolerance induction in intestinal DCs. However, knowledge about tolerance induction mechanisms of other DC subsets or of *in vitro* generated DCs can be transferred to intestinal DCs to explain how they manage to tolerate luminal bacterial or food antigens and therefore prevent from uncontrolled inflammatory reactions. Here, we want to present latest research results and discuss how and if these findings can be assigned also to intestinal DCs. All proposed mechanisms are summarized in Figure 2.

(1) Cell-to-Cell-Contact and STAT3 Signaling. Epithelial cells of the intestine express the surface protein CD47 which can directly interact with signal regulatory protein α (SIRPα) expressed on the surface of DCs which underlie the intestinal epithelial cell layer. This protein-protein-interaction has been shown to result in a janus kinase-2 (JAK-2) dependent signal transducer and activator of transcription 3 (STAT3) activation downstream of SIRPα in DCs [79]. STAT3 activation, in turn, leads to enhanced IL-10 secretion from DCs and therefore promotes tolerogenic properties in the intestinal environment [79]. STAT3 has long been known as a crucial negative regulator of immunity. Disruption of STAT3 leads to

a loss of T cell tolerance in mice and efficient STAT3 signaling is associated with the immature DC phenotype, general IL-10 secretion, and tolerance induction [80]. Therefore, not only does DC alone seem to be important for homeostasis maintenance but also the "teamwork" with neighbouring epithelial cells seems to contribute to tolerance mechanisms.

(2) IL-10 as a Central Cytokine for Intestinal Homeostasis. Interleukin-10 is a key inhibitory cytokine in T cell activation and a mediator of intestinal homeostasis [81]. It is secreted by T cells, B cells, and most myeloid-derived cells [82]. Mice lacking functional IL-10 or its IL-10R receptor counterpart spontaneously develop severe intestinal inflammation.

Supporting the idea of IL-10 being a crucial mediator for intestinal homeostasis [83]. Also humans with defective mutations in the genes encoding for IL-10 or IL-10R develop a severe form of enterocolitis within the first months after birth [84]. These observations made IL-10 a promising therapeutic candidate in order to treat chronic inflammatory conditions of the intestine. However, results were not convincing since, in mice as well as in humans, IL-10 administration did not ameliorate the inflammatory conditions [85]. IL-10 not only affects T cell responses but can also provide autocrine and paracrine effects on DCs. Since DCs express the IL-10 receptor (IL10R), IL-10 can bind to IL10R resulting in a negative regulation of myeloid differentiation primary response 88 (MyD88) signaling inside DCs. MyD88 is an adaptor molecule of TLRs and is required for downstream TLR signalling. IL-10/IL10R interaction mediates this negative regulation by a downregulation of interleukin 1 receptor associated kinase 4 (IRAK4) on the protein level without altering IRAK4 gene transcription rates [86]. It also leads to dissociation of MyD88 from TLRs and subsequently promotes proteasomal degradation of IRAK1, IRAK4, and TRAF6, therefore silencing MyD88-dependent TLR signalling [86]. However, this is just the case if LPS as a TLR4 ligand is present at the same time to induce TLR signaling. IL-10 silencing of MyD88 signaling seems to be crucial for the maintenance of intestinal homeostasis since *IL-10*$^{-/-}$ mice fail to develop intestinal inflammation if these mice simultaneously lack MyD88 [73]. As a consequence, the cytokine environment does also affect DCs in their ability to induce tolerance mechanisms.

(3) NFκB Signalling as a Mediator for Tolerogenicity. A key regulator for DC maturation and inflammatory reactions in general is NFκB [87, 88]. NFκB family members do not only have an activating potential for the induction of proinflammatory cytokines. Two NFκB proteins, p50 and p52, have been associated with transcription repression functions and therefore induction of tolerance [89, 90]. Both proteins lack the carboxyterminal transactivation domain and can form inhibitory homodimer complexes that prevent from transcription of proinflammatory genes. NFκB p50 has been shown to promote a tolerogenic DC phenotype by negatively affecting DC survival and their capacity to efficiently activate T cells [91]. Accumulation of p50 in the nucleus of tolerogenic DCs can be accompanied by enhanced expression of tolerance-promoting molecules like indoleamine dioxygenases (IDOs) and decreased expression of proinflammatory cytokines like IFNβ, IL-1β, and IL-18 [91]. These implications for p50 in the induction of tolDCs are supported by the finding that p50-deficient DCs are weak inducers of a Foxp3$^+$ Treg differentiation [92]. Formation of p50-p50 homodimers contributes to LPS tolerance in MΦ [93] and p50 expression in immature DCs is crucial to prevent from autoreactive T cells [91].

(4) β-Catenin Promotes DC Tolerogenicity. β-catenin is a transcription factor and part of the wnt signalling pathway. It could be demonstrated that this signalling pathway with the subsequent release of β-catenin into the nucleus results in the induction of tolDCs [94]. Gene expression profiles of intestinal LP DCs revealed that this signalling pathway is decisive for the DC to become either mature or tolerogenic. β-catenin translocation into the DC nucleus resulted in the expression of various tolerance-associated factors like retinoic acid-metabolizing enzymes, IL-10 and TGF-β [94].

(5) Prevention of V-ATPase Domain Assembly Induces Tolerogenic DCs. Vacuolar (H^+)-ATPases (V-ATPases) are ATP-driven proton pumps. They are composed of two domains: a peripheral V_1 domain and membrane-embedded V_0 domain [95]. V-ATPases are involved in acidification of lysosomes by shuffling protons from the cytosol into the lysosomic lumen [96]. The pH value of lysosomes is a crucial regulator for the efficiency of antigen processing since lysosomal proteases being involved in antigen proteolysis require acidic environments [95]. The most important mechanism to regulate lysosomal acidification is to control the assembly of the two V-ATPase domains which is a required event for forming a functional proton pump. It is known that activation of TLRs promotes domain assembly and therefore supports DC maturation [96]. Domain assembly seems to be a PI-3 kinase and mTOR mediated event since inhibitory substances for both molecules could block V-ATPase domain assembly and therefore prevent from DC maturation and promote the induction of a tolerogenic phenotype [95]. Also, stimulation of integrins and E-cadherins by cluster disruption of DC prevents from domain assembly and supports induction of a tolerogenic phenotype [96, 97].

(6) p38α Expression Influences Expression of ALDH1A2. MAP kinases like ERK, JNK, and p38α form central pathways that are activated by innate immune signals like PAMPs [98, 99] and excessive activation of MAP kinases are reported to be associated with many autoimmune and inflammatory diseases [99]. However, the MAP kinase p38α provides a dichotomic role. Besides being involved in promoting proinflammatory responses, its activity seems also to be crucial for the induction of a tolerogenic phenotype in intestinal CD103$^+$ DCs. In these DCs, p38α is constitutively active and this activity is crucial for the expression of TGF-β and aldehyde dehydrogenase 1A2 (ALDH1A2), the latter being involved in metabolizing retinoic acid (RA). TGF-β and RA are involved in Treg generation and therefore promote gut homing properties of T cells [99].

(7) Gadd45α-Mediated TLR2 Signalling Contributes to Tolerogenic Features of Intestinal DCs. An abundant bacterial gut commensal, *B. fragilis*, is able to protect from the induction of EAE and experimental colitis and increases the proportions of $CD103^+CD11c^+$ DCs [100, 101]. It could be demonstrated that this effect is mediated by polysaccharide A (PSA), an immunomodulatory component present in outer membrane vesicles derived from *B. fragilis* bacteria [66]. PSA promotes immunological tolerance by inducing IL-10 producing $Foxp3^+$ Tregs and protects animals from experimental colitis [102]. The PSA caused induction of tolDCs is dependent on TLR2 and growth arrest and DNA-damage-inducible 45 α (Gadd45α), since Gadd45α-deficient DCs are unable to mediate PSA-induced protection of experimental colitis [66]. Gadd45α itself inhibits an alternative way of MAPK p38-mediated signalling [103] and PSA-containing outer membrane vesicles lead to upregulation of Gadd45α [66].

Taken together, all of the mentioned molecular mechanisms of tolerance induction in DCs are potentially able to take place in the intestine, either through participation of neighbouring intestinal epithelial cells or through direct interaction of DCs with luminal content. Concerning luminal content, bacteria and their PAMPs could promote all of the potential mechanisms via interaction with host pattern PRRs, especially TLRs. We identified apathogenic Gram-negative commensal strains, namely, *Bacteroides vulgatus* mpk and *Escherichia coli* mpk, mediating completely contrary effects on DC maturation and, in consequence, the progress of experimental colitis in mice [104, 105]. As mentioned above, *B. vulgatus* interaction with immature DCs converted them into a tolerant and tolerogenic semimature phenotype characterized by low to intermediate expression of MHC-II, CD40, CD80, and CD86, almost absent secretion rates of TNFα and IL-12p70, and remarkable IL-6 secretion [59]. As a characteristic of tolerant DC, this phenotype could not be overcome with a subsequent maturating bacterial stimulus or by CD40 ligation [106]. *E. coli* mpk stimulation, however, resulted in efficient DC maturation. As a consequence, *E. coli* mpk colonization in experimental mouse colitis using $Il2^{-/-}$ mice resulted in colonic inflammation, a feature that could be prevented by simultaneous *B. vulgatus* mpk colonization [104, 105]. We could prove that both bacteria differentially alter the phenotype of dendritic cells not only *in vitro* but also *in vivo* in the colonic LP via adjusted bacterial colonization of the gut [105]. In this context, feeding *B. vulgatus* always induced tolerant and tolerogenic DC in the colonic LP. In another study using distinct *E. coli* bacteria that just differ in the structure of their cell surface LPS, we could prove that the LPS structure alone decides if LP DCs are converted into a mature phenotype and therefore promote inflammation or if they are converted into tolerogenic semimature DCs and thus maintain intestinal homeostasis [107]. As LPS primarily signals via TLR4, tolerance induction mechanisms where NFκB p50, Gadd45α, MyD88-signaling, β-catenin, and/or V-ATPase domain assembly are involved could be possible. Since LPS is a cell wall component of all Gram-negative bacteria, the resulting abundance in the intestinal lumen could largely contribute to tolerance induction in intestinal DCs. As we have demonstrated, different commensal bacteria can have opposite effects on DC maturation. This makes the composition of the microbiota decisive on whether DCs mediate tolerogenic or inflammatory LPS-triggered immune responses.

8. Perspectives for Clinical Approaches for the Treatment of IBD Using Tolerant and Tolerogenic Dendritic Cells

In order to be suitable as an administrable therapeutic, tolerogenic DCs (tolDCs) have to be generated *in vitro*. One efficient way to induce tolDCs is coincubating them with apoptotic cells. Phagocytosis of apoptotic cells through DCs results in production of TGF-β which in turn contributes to immune tolerance. Apoptotic cell-treated DCs efficiently converted naïve $CD4^+$ T cells into $Foxp3^+$ Tregs [108, 109]. In general, apoptotic cell induced tolDCs are important for induction of immune tolerance [110, 111]. They provide upregulation of Galectin-1 and CD205 [112], two molecules that facilitate the manifestation of immune tolerance [113, 114]. At the same time, apoptotic cell treated DCs downregulate Gr-1 and B-220 [112], two molecules triggering inflammatory responses. These DCs furthermore downregulate the transcription factor RORγt which is the decisive transcription factor for Th17 differentiation. Not only does treatment with apoptotic cells lead to induction of tolDCs but also treatment with herbal coumarins [115] and the macrocyclic antibiotic rapamycin [116] leads to tolDC induction. *In vitro* generated tolDCs have already been successfully used for the treatment of autoimmune disorders in animal models and peripheral tolerance could be restored by administrating tolerogenic DCs [117]. Approaches to treat autoimmune type 1 diabetes in a mouse model using nonobese diabetic (NOD) mice with tolerogenic DCs were very successful [112]. To do so, apoptotic islet cells were used to induce DC mediated tolerance against own islet cells [118]. All these applications lead to the question if transfer of tolerogenic dendritic cells would also be an approach to treat IBD and, if yes, which method to induce DC tolerance would be the method of choice. A published approach for the treatment of Crohn's disease patients is *in vitro* generation of DCs followed by pulsing with dexamethasone, proinflammatory cytokines IL-6, IL-1β, and TNFα, and PGE_2 [119]. Concerning our findings that a certain gut commensal, *B. vulgatus* mpk, efficiently induces tolerant and tolerogenic DCs *in vitro* as well as *in vivo* [59, 104, 105], we would recommend using host gut commensal bacteria for *in vitro* tolDC generation. In order to provide more potential luminal antigens presented by MHC-II of tolDCs, a defined mixture of commensal bacteria could be used. This would enlarge the amount of antigenic peptides against which tolerance would be induced.

Disclosure

The authors disclose all commercial affiliations and competing financial interests.

Conflict of Interests

The authors declare that there is no conflict of interests regarding the publication of this paper.

Acknowledgments

Work by Julia-Stefanie Frick was supported by the DFG (DFG FR 2087/6-1, DFG FR 2087/8-1, CRC685, SPP1656), the DFG research training group 1708, the Bundesministerium für Bildung und Forschung (BMBF), and the German Centre for Infection Research (DZIF).

References

[1] S. Rutella, G. Bonanno, L. Pierelli et al., "Granulocyte colony-stimulating factor promotes the generation of regulatory DC through induction of IL-10 and IFN-α," *European Journal of Immunology*, vol. 34, no. 5, pp. 1291–1302, 2004.

[2] A. Iwasaki and R. Medzhitov, "Regulation of adaptive immunity by the innate immune system," *Science*, vol. 327, no. 5963, pp. 291–295, 2010.

[3] R. M. Steinman, "Decisions about dendritic cells: past, present, and future," *Annual Review of Immunology*, vol. 30, pp. 1–22, 2012.

[4] C. Ohnmacht, A. Pullner, S. B. S. King et al., "Constitutive ablation of dendritic cells breaks self-tolerance of CD4 T cells and results in spontaneous fatal autoimmunity," *Journal of Experimental Medicine*, vol. 206, no. 3, pp. 549–559, 2009.

[5] K. J. Maloy and F. Powrie, "Intestinal homeostasis and its breakdown in inflammatory bowel disease," *Nature*, vol. 474, no. 7351, pp. 298–306, 2011.

[6] S. Manicassamy and B. Pulendran, "Dendritic cell control of tolerogenic responses," *Immunological Reviews*, vol. 241, no. 1, pp. 206–227, 2011.

[7] M. Gross, T. M. Salame, and S. Jung, "Guardians of the gut—murine intestinal macrophages and dendritic cells," *Frontiers in Immunology*, vol. 6, article 254, 2015.

[8] M. Bogunovic, F. Ginhoux, J. Helft et al., "Origin of the lamina propria dendritic cell network," *Immunity*, vol. 31, no. 3, pp. 513–525, 2009.

[9] J. C. Miller, B. D. Brown, T. Shay et al., "Deciphering the transcriptional network of the dendritic cell lineage," *Nature Immunology*, vol. 13, no. 9, pp. 888–899, 2012.

[10] C. Varol, A. Vallon-Eberhard, E. Elinav et al., "Intestinal lamina propria dendritic cell subsets have different origin and functions," *Immunity*, vol. 31, no. 3, pp. 502–512, 2009.

[11] M. Guilliams, F. Ginhoux, C. Jakubzick et al., "Dendritic cells, monocytes and macrophages: a unified nomenclature based on ontogeny," *Nature Reviews Immunology*, vol. 14, no. 8, pp. 571–578, 2014.

[12] M. Guilliams and L. van de Laar, "A Hitchhiker's guide to myeloid cell subsets: practical implementation of a novel mononuclear phagocyte classification system," *Frontiers in Immunology*, vol. 6, article 406, 2015.

[13] C. L. Scott, C. C. Bain, P. B. Wright et al., "CCR2(+)CD103(−) intestinal dendritic cells develop from DC-committed precursors and induce interleukin-17 production by T cells," *Mucosal Immunology*, vol. 8, pp. 327–339, 2015.

[14] E. L. Gautier, T. Shay, J. Miller et al., "Gene-expression profiles and transcriptional regulatory pathways that underlie the identity and diversity of mouse tissue macrophages," *Nature Immunology*, vol. 13, no. 11, pp. 1118–1128, 2012.

[15] C. C. Bain, C. L. Scott, H. Uronen-Hansson et al., "Resident and pro-inflammatory macrophages in the colon represent alternative context-dependent fates of the same Ly6Chi monocyte precursors," *Mucosal Immunology*, vol. 6, no. 3, pp. 498–510, 2013.

[16] A. Rivollier, J. He, A. Kole, V. Valatas, and B. L. Kelsall, "Inflammation switches the differentiation program of Ly6chi monocytes from antiinflammatory macrophages to inflammatory dendritic cells in the colon," *Journal of Experimental Medicine*, vol. 209, no. 1, pp. 139–155, 2012.

[17] F. Geissmann, S. Gordon, D. A. Hume, A. M. Mowat, and G. J. Randolph, "Unravelling mononuclear phagocyte heterogeneity," *Nature Reviews Immunology*, vol. 10, no. 6, pp. 453–460, 2010.

[18] D. A. Hume, "Differentiation and heterogeneity in the mononuclear phagocyte system," *Mucosal Immunology*, vol. 1, no. 6, pp. 432–441, 2008.

[19] O. Schulz, E. Jaensson, E. K. Persson et al., "Intestinal CD103$^+$, but not CX3CR1$^+$, antigen sampling cells migrate in lymph and serve classical dendritic cell functions," *The Journal of Experimental Medicine*, vol. 206, no. 13, pp. 3101–3114, 2009.

[20] M. Merad, P. Sathe, J. Helft, J. Miller, and A. Mortha, "The dendritic cell lineage: ontogeny and function of dendritic cells and their subsets in the steady state and the inflamed setting," *Annual Review of Immunology*, vol. 31, pp. 563–604, 2013.

[21] N. Onai, K. Kurabayashi, M. Hosoi-Amaike et al., "A clonogenic progenitor with prominent plasmacytoid dendritic cell developmental potential," *Immunity*, vol. 38, no. 5, pp. 943–957, 2013.

[22] G. E. Grajales-Reyes, A. Iwata, J. Albring et al., "Batf3 maintains autoactivation of Irf8 for commitment of a CD8α^+ conventional DC clonogenic progenitor," *Nature Immunology*, vol. 16, pp. 708–717, 2015.

[23] J. T. Jackson, Y. Hu, R. Liu et al., "Id2 expression delineates differential checkpoints in the genetic program of CD8α^+ and CD103$^+$ dendritic cell lineages," *The EMBO Journal*, vol. 30, no. 13, pp. 2690–2704, 2011.

[24] M. Kashiwada, N.-L. L. Pham, L. L. Pewe, J. T. Harty, and P. B. Rothman, "NFIL3/E4BP4 is a key transcription factor for CD8α^+ dendritic cell development," *Blood*, vol. 117, no. 23, pp. 6193–6197, 2011.

[25] B. Cisse, M. L. Caton, M. Lehner et al., "Transcription factor E2-2 is an essential and specific regulator of plasmacytoid dendritic cell development," *Cell*, vol. 135, no. 1, pp. 37–48, 2008.

[26] S. Gurka, E. Hartung, M. Becker et al., "Mouse conventional dendritic cells can be universally classified based on the mutually exclusive expression of XCR1 and SIRPα," *Frontiers in Immunology*, vol. 6, article 35, 2015.

[27] L. Wu, A. D'Amico, K. D. Winkel, M. Suter, D. Lo, and K. Shortman, "RelB is essential for the development of myeloid-related CD8α- dendritic cells but not of lymphoid-related CD8α^+ dendritic cells," *Immunity*, vol. 9, no. 6, pp. 839–847, 1998.

[28] M. L. Caton, M. R. Smith-Raska, and B. Reizis, "Notch-RBP-J signaling controls the homeostasis of CD8$^-$ dendritic cells in the spleen," *The Journal of Experimental Medicine*, vol. 204, no. 7, pp. 1653–1664, 2007.

[29] E. K. Persson, H. Uronen-Hansson, M. Semmrich et al., "IRF4 transcription-factor-dependent CD103$^+$CD11b$^+$ dendritic cells drive mucosal T helper 17 cell differentiation," *Immunity*, vol. 38, no. 5, pp. 958–969, 2013.

[30] B. T. Edelson, K. C. Wumesh, R. Juang et al., "Peripheral CD103$^+$ dendritic cells form a unified subset developmentally related to CD8α^+ conventional dendritic cells," *Journal of Experimental Medicine*, vol. 207, no. 4, pp. 823–836, 2010.

[31] B. Vander Lugt, A. A. Khan, J. A. Hackney et al., "Transcriptional programming of dendritic cells for enhanced MHC class II antigen presentation," *Nature Immunology*, vol. 15, no. 2, pp. 161–167, 2014.

[32] A. Schlitzer, N. McGovern, P. Teo et al., "IRF4 transcription factor-dependent CD11b$^+$ dendritic cells in human and mouse control mucosal IL-17 cytokine responses," *Immunity*, vol. 38, no. 5, pp. 970–983, 2013.

[33] W. W. Agace and E. K. Persson, "How vitamin A metabolizing dendritic cells are generated in the gut mucosa," *Trends in Immunology*, vol. 33, no. 1, pp. 42–48, 2012.

[34] J. A. Hall, J. R. Grainger, S. P. Spencer, and Y. Belkaid, "The role of retinoic acid in tolerance and immunity," *Immunity*, vol. 35, no. 1, pp. 13–22, 2011.

[35] M. Guilliams, K. Crozat, S. Henri et al., "Skin-draining lymph nodes contain dermis-derived CD103$^-$ dendritic cells that constitutively produce retinoic acid and induce Foxp3$^+$ regulatory T cells," *Blood*, vol. 115, no. 10, pp. 1958–1968, 2010.

[36] T. L. Denning, B. A. Norris, O. Medina-Contreras et al., "Functional specializations of intestinal dendritic cell and macrophage subsets that control Th17 and regulatory T cell responses are dependent on the T cell/APC ratio, source of mouse strain, and regional localization," *The Journal of Immunology*, vol. 187, no. 2, pp. 733–747, 2011.

[37] B. M. Janelsins, M. Lu, and S. K. Datta, "Altered inactivation of commensal LPS due to acyloxyacyl hydrolase deficiency in colonic dendritic cells impairs mucosal Th17 immunity," *Proceedings of the National Academy of Sciences of the United States of America*, vol. 111, no. 1, pp. 373–378, 2014.

[38] K. Honda and D. R. Littman, "The microbiome in infectious disease and inflammation," *Annual Review of Immunology*, vol. 30, pp. 759–795, 2012.

[39] T. Korn, E. Bettelli, M. Oukka, and V. K. Kuchroo, "IL-17 and Th17 cells," *Annual Review of Immunology*, vol. 27, pp. 485–517, 2009.

[40] K. Fujimoto, T. Karuppuchamy, N. Takemura et al., "A new subset of CD103$^+$CD8α^+ dendritic cells in the small intestine expresses TLR3, TLR7, and TLR9 and induces Th1 response and CTL activity," *The Journal of Immunology*, vol. 186, no. 11, pp. 6287–6295, 2011.

[41] V. Cerovic, S. A. Houston, C. L. Scott et al., "Intestinal CD103$^-$ dendritic cells migrate in lymph and prime effector T cells," *Mucosal Immunology*, vol. 6, no. 1, pp. 104–113, 2013.

[42] C. L. Scott, T. F. P. Z. Murray, K. S. H. Beckham, G. Douce, and A. M. Mowat, "Signal regulatory protein alpha (SIRPα) regulates the homeostasis of CD103$^+$CD11b$^+$ DCs in the intestinal lamina propria," *European Journal of Immunology*, vol. 44, no. 12, pp. 3658–3668, 2014.

[43] E. K. Persson, C. L. Scott, A. M. Mowat, and W. W. Agace, "Dendritic cell subsets in the intestinal lamina propria: ontogeny and function," *European Journal of Immunology*, vol. 43, no. 12, pp. 3098–3107, 2013.

[44] S. Veenbergen, L. A. van Berkel, M. F. du Pré et al., "Colonic tolerance develops in the iliac lymph nodes and can be established independent of CD103$^+$ dendritic cells," *Mucosal Immunology*, 2015.

[45] N. E. Welty, C. Staley, N. Ghilardi, M. J. Sadowsky, B. Z. Igyártó, and D. H. Kaplan, "Intestinal lamina propria dendritic cells maintain T cell homeostasis but do not affect commensalism," *The Journal of Experimental Medicine*, vol. 210, no. 10, pp. 2011–2024, 2013.

[46] N. S. Wilson, L. J. Young, F. Kupresanin et al., "Normal proportion and expression of maturation markers in migratory dendritic cells in the absence of germs or Toll-like receptor signaling," *Immunology and Cell Biology*, vol. 86, no. 2, pp. 200–205, 2008.

[47] C. Qian, J. Liu, and X. Cao, "Innate signaling in the inflammatory immune disorders," *Cytokine and Growth Factor Reviews*, vol. 25, no. 6, pp. 731–738, 2014.

[48] O. Takeuchi and S. Akira, "Pattern recognition receptors and inflammation," *Cell*, vol. 140, no. 6, pp. 805–820, 2010.

[49] J. Brown, H. Wang, G. N. Hajishengallis, and M. Martin, "TLR-signaling networks: an integration of adaptor molecules, kinases, and cross-talk," *Journal of Dental Research*, vol. 90, no. 4, pp. 417–427, 2011.

[50] J. R. McDole, L. W. Wheeler, K. G. McDonald et al., "Goblet cells deliver luminal antigen to CD103$^+$ dendritic cells in the small intestine," *Nature*, vol. 483, no. 7389, pp. 345–349, 2012.

[51] E. Mazzini, L. Massimiliano, G. Penna, and M. Rescigno, "Oral tolerance can be established via gap junction transfer of fed antigens from CX3CR1$^+$ macrophages to CD103$^+$ dendritic cells," *Immunity*, vol. 40, no. 2, pp. 248–261, 2014.

[52] J. Farache, I. Koren, I. Milo et al., "Luminal bacteria recruit CD103$^+$ dendritic cells into the intestinal epithelium to sample bacterial antigens for presentation," *Immunity*, vol. 38, no. 3, pp. 581–595, 2013.

[53] A. Vallon-Eberhard, L. Landsman, N. Yogev, B. Verrier, and S. Jung, "Transepithelial pathogen uptake into the small intestinal lamina propria," *Journal of Immunology*, vol. 176, no. 4, pp. 2465–2469, 2006.

[54] N. Singh, A. Gurav, S. Sivaprakasam et al., "Activation of Gpr109a, receptor for niacin and the commensal metabolite butyrate, suppresses colonic inflammation and carcinogenesis," *Immunity*, vol. 40, no. 1, pp. 128–139, 2014.

[55] D. Han, M. C. Walsh, P. J. Cejas et al., "Dendritic cell expression of the signaling molecule TRAF6 is critical for gut microbiota-dependent immune tolerance," *Immunity*, vol. 38, no. 6, pp. 1211–1222, 2013.

[56] L. Delamarre, H. Holcombe, and I. Mellman, "Presentation of exogenous antigens on major histocompatibility complex (MHC) class I and MHC class II molecules is differentially regulated during dendritic cell maturation," *The Journal of Experimental Medicine*, vol. 198, no. 1, pp. 111–122, 2003.

[57] J. Liu and X. Cao, "Regulatory dendritic cells in autoimmunity: a comprehensive review," *Journal of Autoimmunity*, vol. 63, pp. 1–12, 2015.

[58] M. V. Dhodapkar, R. M. Steinman, J. Krasovsky, C. Munz, and N. Bhardwaj, "Antigen-specific inhibition of effector T cell function in humans after injection of immature dendritic cells," *Journal of Experimental Medicine*, vol. 193, no. 2, pp. 233–238, 2001.

[59] J. S. Frick, N. Zahir, M. Müller et al., "Colitogenic and non-colitogenic commensal bacteria differentially trigger DC maturation and Th cell polarization: an important role for IL-6," *European Journal of Immunology*, vol. 36, no. 6, pp. 1537–1547, 2006.

[60] M. B. Lutz, "Therapeutic potential of semi-mature dendritic cells for tolerance induction," *Frontiers in Immunology*, vol. 3, article 123, 2012.

[61] M. Menges, S. Rößner, C. Voigtländer et al., "Repetitive injections of dendritic cells matured with tumor necrosis factor α induce antigen-specific protection of mice from autoimmunity," *The Journal of Experimental Medicine*, vol. 195, no. 1, pp. 15–21, 2002.

[62] W. W. J. Unger, S. Laban, F. S. Kleijwegt, A. R. Van Der Slik, and B. O. Roep, "Induction of Treg by monocyte-derived DC modulated by vitamin D_3 or dexamethasone: differential role for PD-L1," *European Journal of Immunology*, vol. 39, no. 11, pp. 3147–3159, 2009.

[63] A. B. Addi, A. Lefort, X. Hua et al., "Modulation of murine dendritic cell function by adenine nucleotides and adenosine: involvement of the A_{2B} receptor," *European Journal of Immunology*, vol. 38, no. 6, pp. 1610–1620, 2008.

[64] J. Geisel, F. Kahl, M. Müller et al., "IL-6 and maturation govern TLR2 and TLR4 induced TLR agonist tolerance and cross-tolerance in dendritic cells," *The Journal of Immunology*, vol. 179, no. 9, pp. 5811–5818, 2007.

[65] E. Ozeri, M. Mizrahi, G. Shahaf, and E. C. Lewis, "α-1 antitrypsin promotes semimature, IL-10-producing and readily migrating tolerogenic dendritic cells," *Journal of Immunology*, vol. 189, no. 1, pp. 146–153, 2012.

[66] Y. Shen, M. L. G. Torchia, G. W. Lawson, C. L. Karp, J. D. Ashwell, and S. K. Mazmanian, "Outer membrane vesicles of a human commensal mediate immune regulation and disease protection," *Cell Host and Microbe*, vol. 12, no. 4, pp. 509–520, 2012.

[67] J. K. Nono, K. Pletinckx, M. B. Lutz, and K. Brehm, "Excretory/secretory-products of *Echinococcus multilocularis* larvae induce apoptosis and tolerogenic properties in dendritic cells in vitro," *PLoS Neglected Tropical Diseases*, vol. 6, no. 2, Article ID e1516, 2012.

[68] A. E. Morelli and A. W. Thomson, "Tolerogenic dendritic cells and the quest for transplant tolerance," *Nature Reviews Immunology*, vol. 7, no. 8, pp. 610–621, 2007.

[69] A. Iwasaki and R. Medzhitov, "Control of adaptive immunity by the innate immune system," *Nature Immunology*, vol. 16, no. 4, pp. 343–353, 2015.

[70] E. C. Steinbach and S. E. Plevy, "The role of macrophages and dendritic cells in the initiation of inflammation in IBD," *Inflammatory Bowel Diseases*, vol. 20, no. 1, pp. 166–175, 2014.

[71] R. B. Sartor, "Microbial influences in inflammatory bowel diseases," *Gastroenterology*, vol. 134, no. 2, pp. 577–594, 2008.

[72] J. L. Coombes and F. Powrie, "Dendritic cells in intestinal immune regulation," *Nature Reviews Immunology*, vol. 8, no. 6, pp. 435–446, 2008.

[73] S. Rakoff-Nahoum, L. Hao, and R. Medzhitov, "Role of toll-like receptors in spontaneous commensal-dependent colitis," *Immunity*, vol. 25, no. 2, pp. 319–329, 2006.

[74] J. M. Kim, J. P. Rasmussen, and A. Y. Rudensky, "Regulatory T cells prevent catastrophic autoimmunity throughout the lifespan of mice," *Nature Immunology*, vol. 8, no. 2, pp. 191–197, 2007.

[75] D. Haribhai, J. B. Williams, S. Jia et al., "A requisite role for induced regulatory T cells in tolerance based on expanding antigen receptor diversity," *Immunity*, vol. 35, no. 1, pp. 109–122, 2011.

[76] M. Kronenberg and A. Rudensky, "Regulation of immunity by self-reactive T cells," *Nature*, vol. 435, no. 7042, pp. 598–604, 2005.

[77] Q. Tang and J. A. Bluestone, "The $Foxp3^+$ regulatory T cell: a jack of all trades, master of regulation," *Nature Immunology*, vol. 9, no. 3, pp. 239–244, 2008.

[78] J. L. Coombes, K. R. R. Siddiqui, C. V. Arancibia-Cárcamo et al., "A functionally specialized population of mucosal $CD103^+$ DCs induces $Foxp3^+$ regulatory T cells via a TGF-β and retinoic acid-dependent mechanism," *Journal of Experimental Medicine*, vol. 204, no. 8, pp. 1757–1764, 2007.

[79] N. Toledano, D. Gur-Wahnon, A. Ben-Yehuda, and J. Rachmilewitz, "Novel CD47: SIRPα dependent mechanism for the activation of STAT3 in antigen-presenting cell," *PLoS ONE*, vol. 8, no. 9, Article ID e75595, 2013.

[80] F. Cheng, H.-W. Wang, A. Cuenca et al., "A critical role for Stat3 signaling in immune tolerance," *Immunity*, vol. 19, no. 3, pp. 425–436, 2003.

[81] V. Seiffart, J. Zoeller, R. Klopfleisch et al., "IL10-deficiency in $CD4^+$ T cells exacerbates the IFNγ and IL17 response during bacteria induced colitis," *Cellular Physiology and Biochemistry*, vol. 36, no. 4, pp. 1259–1273, 2015.

[82] M. Saraiva and A. O'Garra, "The regulation of IL-10 production by immune cells," *Nature Reviews Immunology*, vol. 10, no. 3, pp. 170–181, 2010.

[83] D. S. Shouval, J. Ouahed, A. Biswas et al., "Interleukin 10 receptor signaling: master regulator of intestinal mucosal homeostasis in mice and humans," *Advances in Immunology*, vol. 122, pp. 177–210, 2014.

[84] B. Begue, J. Verdier, F. Rieux-Laucat et al., "Defective IL10 signaling defining a subgroup of patients with inflammatory bowel disease," *American Journal of Gastroenterology*, vol. 106, no. 8, pp. 1544–1555, 2011.

[85] F. E. Buruiana, I. Sola, and P. Alonso-Coello, "Recombinant human interleukin 10 for induction of remission in Crohn's disease," *Cochrane Database of Systematic Reviews*, vol. 11, Article ID CD005109, 2010.

[86] J. Chang, S. L. Kunkel, and C.-H. Chang, "Negative regulation of MyD88-dependent signaling by IL-10 in dendritic cells," *Proceedings of the National Academy of Sciences of the United States of America*, vol. 106, no. 43, pp. 18327–18332, 2009.

[87] T. Kawai and S. Akira, "TLR signaling," *Cell Death and Differentiation*, vol. 13, no. 5, pp. 816–825, 2006.

[88] M. Rescigno and A. Di Sabatino, "Dendritic cells in intestinal homeostasis and disease," *Journal of Clinical Investigation*, vol. 119, no. 9, pp. 2441–2450, 2009.

[89] C. Porta, M. Rimoldi, G. Raes et al., "Tolerance and M2 (alternative) macrophage polarization are related processes orchestrated by p50 nuclear factor κB," *Proceedings of the National Academy of Sciences of the United States of America*, vol. 106, no. 35, pp. 14978–14983, 2009.

[90] G. Bonizzi and M. Karin, "The two NF-κB activation pathways and their role in innate and adaptive immunity," *Trends in Immunology*, vol. 25, no. 6, pp. 280–288, 2004.

[91] P. Larghi, C. Porta, E. Riboldi et al., "The p50 subunit of NF-κB orchestrates dendritic cell lifespan and activation of adaptive immunity," *PLoS ONE*, vol. 7, no. 9, Article ID e45279, 2012.

[92] E. M. Shevach, "Mechanisms of $foxp3^+$ T regulatory cell-mediated suppression," *Immunity*, vol. 30, no. 5, pp. 636–645, 2009.

[93] H. W. L. Ziegler-Heitbrock, I. Petersmann, and M. Frankenberger, "p50 (NF-κB1) is upregulated in LPS tolerant P388D1 murine macrophages," *Immunobiology*, vol. 198, no. 1–3, pp. 73–80, 1997.

[94] S. Manicassamy, B. Reizis, R. Ravindran et al., "Activation of β-catenin in dendritic cells regulates immunity versus tolerance in the intestine," *Science*, vol. 329, no. 5993, pp. 849–853, 2010.

[95] R. Liberman, S. Bond, M. G. Shainheit, M. J. Stadecker, and M. Forgac, "Regulated assembly of vacuolar ATPase is increased during cluster disruption-induced maturation of dendritic cells through a phosphatidylinositol 3-Kinase/mTOR-dependent pathway," *The Journal of Biological Chemistry*, vol. 289, no. 3, pp. 1355–1363, 2014.

[96] E. S. Trombetta, M. Ebersold, W. Garrett, M. Pypaert, and I. Mellman, "Activation of lysosomal function during dendritic cell maturation," *Science*, vol. 299, no. 5611, pp. 1400–1403, 2003.

[97] B. Vander Lugt, Z. T. Beck, R. C. Fuhlbrigge, N. Hacohen, J. J. Campbell, and M. Boes, "TGF-β suppresses β-catenin-dependent tolerogenic activation program in dendritic cells," *PLoS ONE*, vol. 6, no. 5, Article ID e20099, 2011.

[98] G. Huang, L. Z. Shi, and H. Chi, "Regulation of JNK and p38 MAPK in the immune system: signal integration, propagation and termination," *Cytokine*, vol. 48, no. 3, pp. 161–169, 2009.

[99] G. Huang, Y. Wang, P. Vogel, T.-D. Kanneganti, K. Otsu, and H. Chi, "Signaling via the kinase p38α programs dendritic cells to drive T_H17 differentiation and autoimmune inflammation," *Nature Immunology*, vol. 13, no. 2, pp. 152–161, 2012.

[100] J. Ochoa-Repáraz, D. W. Mielcarz, Y. Wang et al., "A polysaccharide from the human commensal *Bacteroides fragilis* protects against CNS demyelinating disease," *Mucosal Immunology*, vol. 3, no. 5, pp. 487–495, 2010.

[101] J. Ochoa-Repáraz, D. W. Mielcarz, L. E. Ditrio et al., "Central nervous system demyelinating disease protection by the human commensal *Bacteroides fragilis* depends on polysaccharide A expression," *Journal of Immunology*, vol. 185, no. 7, pp. 4101–4108, 2010.

[102] J. L. Round, S. M. Lee, J. Li et al., "The toll-like receptor 2 pathway establishes colonization by a commensal of the human microbiota," *Science*, vol. 332, no. 6032, pp. 974–977, 2011.

[103] J. M. Salvador, P. R. Mittelstadt, G. I. Belova, A. J. Fornace Jr., and J. D. Ashwell, "The autoimmune suppressor Gadd45α inhibits the T cell alternative p38 activation pathway," *Nature Immunology*, vol. 6, no. 4, pp. 396–402, 2005.

[104] M. Waidmann, O. Bechtold, J.-S. Frick et al., "Bacteroides vulgatus protects against *Escherichia coli*-induced colitis in gnotobiotic interleukin-2-deficient mice," *Gastroenterology*, vol. 125, no. 1, pp. 162–177, 2003.

[105] M. Müller, K. Fink, J. Geisel et al., "Intestinal colonization of IL-2 deficient mice with non-colitogenic *B. vulgatus* prevents DC maturation and T-cell polarization," *PLoS ONE*, vol. 3, no. 6, Article ID e2376, 2008.

[106] A.-M. Gerlach, A. Steimle, L. Krampen et al., "Role of CD40 ligation in dendritic cell semimaturation," *BMC Immunology*, vol. 13, article 22, 2012.

[107] K. Gronbach, I. Flade, O. Holst et al., "Endotoxicity of lipopolysaccharide as a determinant of T-cell-mediated colitis induction in mice," *Gastroenterology*, vol. 146, no. 3, pp. 765–775, 2014.

[108] S. Perruche, P. Zhang, Y. Liu, P. Saas, J. A. Bluestone, and W. Chen, "CD3-specific antibody-induced immune tolerance involves transforming growth factor-β from phagocytes digesting apoptotic T cells," *Nature Medicine*, vol. 14, no. 5, pp. 528–535, 2008.

[109] R. Kuang, S. Perruche, and W. Chen, "Apoptotic cell-linked immunoregulation: implications for promoting immune tolerance in transplantation," *Cell & Bioscience*, vol. 5, article 27, 2015.

[110] T. B. da Costa, L. R. Sardinha, R. Larocca, J. P. S. Peron, and L. V. Rizzo, "Allogeneic apoptotic thymocyte-stimulated dendritic cells expand functional regulatory T cells," *Immunology*, vol. 133, no. 1, pp. 123–132, 2011.

[111] M. A. Gleisner, M. Rosemblatt, J. A. Fierro, and M. R. Bono, "Delivery of alloantigens via apoptotic cells generates dendritic cells with an immature tolerogenic phenotype," *Transplantation Proceedings*, vol. 43, no. 6, pp. 2325–2333, 2011.

[112] F. Zhou, E. Lauretti, A. di Meco et al., "Intravenous transfer of apoptotic cell-treated dendritic cells leads to immune tolerance by blocking Th17 cell activity," *Immunobiology*, vol. 218, no. 8, pp. 1069–1076, 2013.

[113] M. J. Perone, S. Bertera, Z. S. Tawadrous et al., "Dendritic cells expressing transgenic galectin-1 delay onset of autoimmune diabetes in mice," *The Journal of Immunology*, vol. 177, no. 8, pp. 5278–5289, 2006.

[114] J. M. Ilarregui, D. O. Croci, G. A. Bianco et al., "Tolerogenic signals delivered by dendritic cells to T cells through a galectin-1-driven immunoregulatory circuit involving interleukin 27 and interleukin 10," *Nature Immunology*, vol. 10, no. 9, pp. 981–991, 2009.

[115] M. Xiang, J. Lu, C. Zhang et al., "Identification and quantification of total coumarins from Urtica dentata hand and its roles in promoting immune tolerance via TLR4-mediated dendritic cell immaturation," *Bioscience, Biotechnology and Biochemistry*, vol. 77, no. 6, pp. 1200–1206, 2013.

[116] H. R. Turnquist, G. Raimondi, A. F. Zahorchak, R. T. Fischer, Z. Wang, and A. W. Thomson, "Rapamycin-conditioned dendritic cells are poor stimulators of allogeneic $CD4^+$ T cells, but enrich for antigen-specific $Foxp3^+$ T regulatory cells and promote organ transplant tolerance," *The Journal of Immunology*, vol. 178, no. 11, pp. 7018–7031, 2007.

[117] S. Marin-Gallen, X. Clemente-Casares, R. Planas et al., "Dendritic cells pulsed with antigen-specific apoptotic bodies prevent experimental type 1 diabetes," *Clinical and Experimental Immunology*, vol. 160, no. 2, pp. 207–214, 2010.

[118] M. Knip and H. Siljander, "Autoimmune mechanisms in type 1 diabetes," *Autoimmunity Reviews*, vol. 7, no. 7, pp. 550–557, 2008.

[119] R. Cabezón, E. Ricart, C. España, J. Panés, and D. Benitez-Ribas, "Gram-negative enterobacteria induce tolerogenic maturation in dexamethasone conditioned dendritic cells," *PLoS ONE*, vol. 7, no. 12, Article ID e52456, 2012.

[120] S. Uematsu, K. Fujimoto, M. H. Jang et al., "Regulation of humoral and cellular gut immunity by lamina propria dendritic cells expressing Toll-like receptor 5," *Nature Immunology*, vol. 9, no. 7, pp. 769–776, 2008.

[121] R. Setoguchi, S. Hori, T. Takahashi, and S. Sakaguchi, "Homeostatic maintenance of natural $Foxp3^+$ $CD25^+$ $CD4^+$ regulatory T cells by interleukin (IL)-2 and induction of autoimmune disease by IL-2 neutralization," *Journal of Experimental Medicine*, vol. 201, no. 5, pp. 723–735, 2005.

Journal of Immunological Methods xxx (2016) xxx–xxx

Contents lists available at ScienceDirect

Journal of Immunological Methods

journal homepage: www.elsevier.com/locate/jim

A novel approach for reliable detection of cathepsin S activities in mouse antigen presenting cells

Alex Steimle [a], Hubert Kalbacher [b], Andreas Maurer [c], Brigitte Beifuss [a], Annika Bender [a], Andrea Schäfer [a], Ricarda Müller [a], Ingo B. Autenrieth [a], Julia-Stefanie Frick [a,*]

[a] Institute of Medical Microbiology and Hygiene, University of Tübingen, Germany
[b] Interfacultary Institute of Biochemistry, University of Tübingen, Germany
[c] Institute of Radiology, University of Tübingen, Germany

ARTICLE INFO

Article history:
Received 2 December 2015
Received in revised form 15 February 2016
Accepted 16 February 2016
Available online xxxx

Keywords:
Cathepsin S
Method
Enzyme activity
Autoimmune disease
Multiple sclerosis
IBD
Mouse

ABSTRACT

Cathepsin S (CTSS) is a eukaryotic protease mostly expressed in professional antigen presenting cells (APCs). Since CTSS activity regulation plays a role in the pathogenesis of various autoimmune diseases like multiple sclerosis, atherosclerosis, Sjögren's syndrome and psoriasis as well as in cancer progression, there is an ongoing interest in the reliable detection of cathepsin S activity. Various applications have been invented for specific detection of this enzyme. However, most of them have only been shown to be suitable for human samples, do not deliver quantitative results or the experimental procedure requires technical equipment that is not commonly available in a standard laboratory. We have tested a fluorogen substrate, Mca-GRWPPMGLPWE-Lys(Dnp)-DArg-NH_2, that has been described to specifically detect CTSS activities in human APCs for its potential use for mouse samples. We have modified the protocol and thereby offer a cheap, easy, reproducible and quick activity assay to detect CTSS activities in mouse APCs. Since most of basic research on CTSS is performed in mice, this method closes a gap and offers a possibility for reliable and quantitative CTSS activity detection that can be performed in almost every laboratory.

1. Introduction

Cathepsin S (CTSS) belongs to a group of eleven currently known human cysteine cathepsins (Turk et al., 2012). CTSS is a lysosomal and endosomal cysteine protease expressed in professional antigen presenting cells (APCs) such as macrophages, B cells and dendritic cells (Driessen et al., 1999). Though, also non-professional antigen presenting cells such as intestinal epithelial cells have been shown to express CTSS (Beers et al., 2005). Its main physiological role is the control of the maturation of MHC class II molecules by generating the class II-associated invariant chain peptide (CLIP) fragment through invariant chain (Ii) proteolysis. This proteolysis is a required step for the loading of antigenic peptide onto the MHC class II heterodimer and the subsequent transport to the cell surface where it is involved in T cell activation (Conus and Simon, 2010). This makes CTSS the main regulator for MHC class II surface expression in professional and non-professional APCs (Driessen et al., 1999). Therefore, CTSS is assigned to play a crucial role for the activation of MHC class II mediated immune responses. Hence, regulation of this protease seems to be of high importance for avoiding uncontrolled $CD4^+$ T cell activation. Indeed, enhanced CTSS protein expression, mRNA expression, protein secretion and activity dysregulation have an implication for the induction or progress of a variety of autoimmune diseases. CTSS dysregulation-associated autoimmune diseases are, i.e. atherosclerosis (Figueiredo et al., 2015), multiple sclerosis (Haves-Zburof et al., 2011; Fissolo et al., 2008), psoriasis (Schonefuss et al., 2010) and the Sjögren's syndrome (Hamm-Alvarez et al., 2014). Additionally, enhanced CTSS secretion into the intestinal lumen is reported to promote pain induction during inflammatory bowel disease (Cattaruzza et al., 2011). Furthermore, CTSS dysregulation is also involved in cancer progression (Sobotic et al., 2015). This involvement of CTSS in the pathogenesis of various diseases makes this protease an intensely studied drug target (Figueiredo et al., 2015; Kohl et al., 2015; Vazquez et al., 2015; Jadhav et al., 2014). In order to evaluate the precise role of CTSS function in this context, not only protein concentrations of CTSS should be detected but rather its catalytic activity as protein amount and enzymatic activity do not necessarily need to correlate. Cathepsins in general provide a broad and overall similar substrate specificity which makes it difficult to distinguish them in experimental settings (Choe et al., 2006).

Different methods have been used to detect specific CTSS activities in vitro or in vivo, all of them providing different advantages and

Abbreviations: APCs, antigen presenting cells; BMDCs, bone marrow derived dendritic cells; CTSB, cathepsin B; CTSD, cathepsin D; CTSL, cathepsin L; CTSS, cathepsin S; rh, recombinant human; PMGLP, Mca-GRWPPMGLPWE-Lys(Dnp)-DArg-NH_2; rm, recombinant mouse; RT, room temperature.

* Corresponding author at: Institute of Medical Microbiology and Hygiene, University of Tübingen, Elfriede-Aulhorn-Str. 6, D-72076 Tübingen, Germany.
E-mail address: julia-stefanie.frick@med.uni-tuebingen.de (J.-S. Frick).

http://dx.doi.org/10.1016/j.jim.2016.02.015
0022-1759/

disadvantages. Most of them focus on the detection of human CTSS. Here we present a method for in vitro detection of also mouse CTSS activities based on a fluorogen substrate that has previously been described to be exclusively cleaved by human CTSS (Lutzner and Kalbacher, 2008). This method is cheap, specific, reliable and easy to perform in a standard laboratory without the requirement of special technical equipment, besides the requisition of a fluorescence compatible photometer. We think this method could contribute to a progress in CTSS-related research.

2. Results

2.1. PMGLP is well recognized by recombinant mouse CTSS (rmCTSS)

The CTSS proteolysis activity detecting substrate Mca-GRWPPMGLPWE-Lys(Dnp)-DArg-NH_2 (PMGLP) was primarily designed for the detection of human CTSS activities (Lutzner and Kalbacher, 2008). Our aim was to determine whether PMGLP is also suitable for the detection of mouse CTSS. In a first step, we therefore tested several recombinant mouse cathepsins for their cleavage behavior towards PMGLP and compared them to recombinant human (rh) CTSS (Fig. 1). To assess the general enzymatic activity of the commercially purchased recombinant mouse (rm) cathepsins, we first looked for possible protein digestion in a Coomassie-stained 12% SDS gel (Fig. 1A, right panel). Since we could not detect any possible proteolysis-caused loss of function of rhCTSS, rmCTSS, rm cathepsin B (rmCTSB) and rm cathepsin D (rmCTSD), we next checked for their ability to cleave the substrate Z-FR-AMC. This substrate (Z-FR-AMC) is published as being recognized and cleaved by CTSS (Lutzner and Kalbacher, 2008), CTSB (Barrett, 1980) and CTSL (Malagon et al., 2010) and was used as a positive control to evaluate the proteolytic function and protein integrity of these cathepsins. However, rmCTSD integrity could not be checked by using Z-FR-AMC since this enzyme is not capable of cleavage this substrate. Both, PMGLP and Z-FR-AMC display fluorescent properties upon enzymatically catalyzed hydrolytic cleavage. The increase in detected fluorescence intensity change over time is therefore equivalent to the amount of proteolytically processed substrate. This enzymatically catalyzed substrate conversion into a fluorescent substance was monitored by measuring the fluorescence intensity change over time, therefore delivering substrate conversion curves (Fig. 1A, left panels). Fluorescence intensities are measured in dimensionless “arbitrary units” (AU). Absolute enzymatic activities were then calculated by performing a linear regression at the beginning of the substrate turnover curve (Fig. 1B). The slope magnitude of this linear regression delivers a value for the activity of the tested enzyme that can be expressed as the difference of fluorescence intensity in

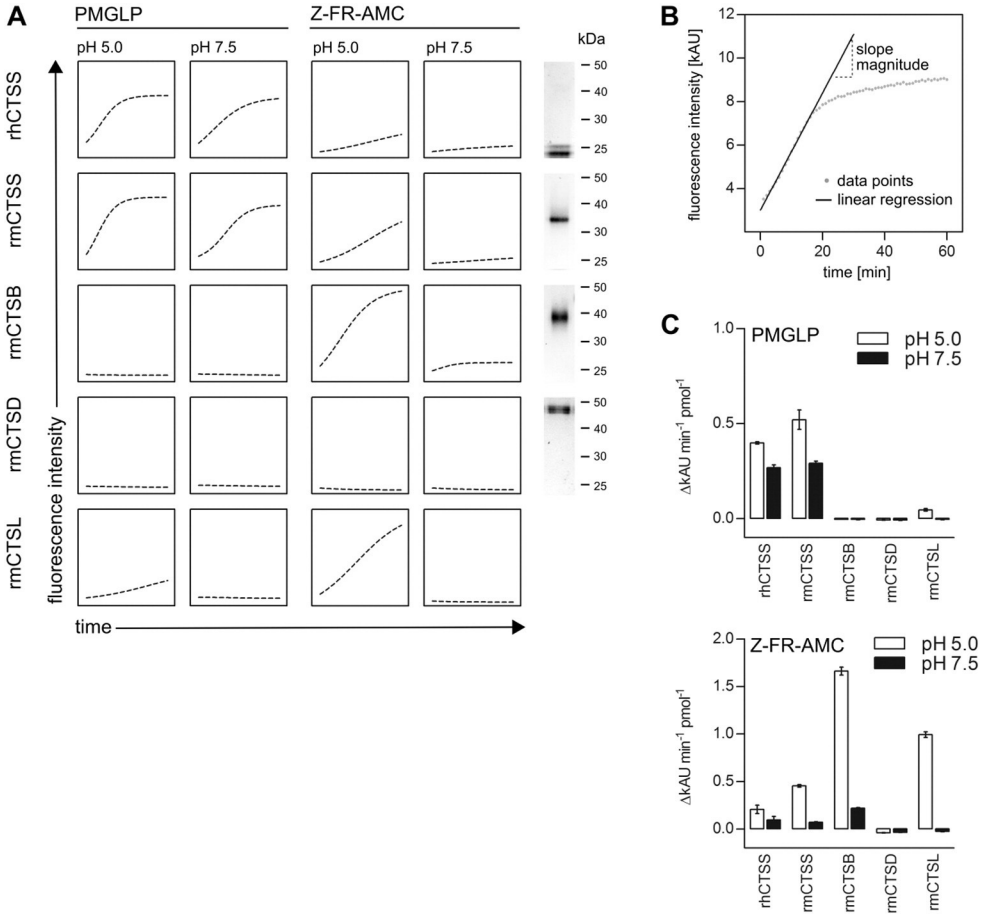

Fig. 1. Recombinant mouse CTSS efficiently cleaves PMGLP. Various recombinant mouse (rm) and human (rh) cathepsins (CTS) were tested for their cleavage behavior towards human cathepsin S (rhCTSS) substrate PMGLP. Z-FR-AMC was used as an activity control since it is efficiently cleaved by cathepsin B (CTSB), cathepsin S (CTSS) and cathepsin L (CTSL) but not cathepsin D (CTSD). Equimolar amounts of recombinant cathepsins were preincubated in either a phosphate buffer at pH 7.5 or a sodium citrate buffer at pH 5.0. After addition of the fluorogen substrates PMGLP or Z-FR-AMC, fluorescence increase due to substrate conversion was monitored for 60 min at 37 °C. (A) Monitoring of substrate conversion. Fluorescence increase was recorded for 60 min. Fluorescence intensities were adjusted to the conversion curve with the highest fluorescence increase. Illustrated conversion curves are averaged curves of three independent experiments. On the right, one representative Coomassie staining of each tested recombinant cathepsin that was separated on a 12% SDS gel. (B) Illustration of the way how enzymatic activities are calculated. Gray dots represent data points of the substrate conversion that results in an increase of fluorescence intensity. The solid line indicates the linear regression at the beginning of the enzymatic reaction. The broken line represents the slope magnitude of the linear regression. For details on how the linearization was performed, see the Materials and methods section. (C) Substrate conversion rates in $\Delta AU\ min^{-1}$ (pmol enzyme)$^{-1}$ were computed from the substrate conversion curves in (A) as described in (B) (see text for further information) (n = 3), error bars represent standard deviation (SD).

Please cite this article as: Steimle, A., et al., A novel approach for reliable detection of cathepsin S activities in mouse antigen presenting cells, J. Immunol. Methods (2016), http://dx.doi.org/10.1016/j.jim.2016.02.015

arbitrary units (AU) per time unit and per amount of applied enzyme, or briefly, as ΔAU min^{-1} pmol (enzyme)$^{-1}$ (Fig. 1B). All tested cathepsins, besides rmCTSD, provided remarkable Z-FR-AMC hydrolysis. Since, aside from CTSS (Turk et al., 2012), cathepsins generally exhibit stronger proteolysis activity at acidic pH values, we detected enhanced Z-FR-AMC cleavage at pH 5.0 compared to pH 7.5. The lysosomal location of cathepsins requires them to be active at acidic conditions, therefore adapting to the acidic environment in lysosomes providing pH values usually lower than pH 5 (Mindell, 2012). Hence, most cathepsins provide their pH optimum at acidic conditions. For example, CTSB requires a pH around 5.0 (Linebaugh et al., 1999), CTSD a pH around 4 (Cunningham and Tang, 1976) and CTSL, which is autocatalytically activated at pH 4 and provides maximum activity at pH 5.0 (Dolinar et al., 1995). Nevertheless, all tested cathepsins were catalytically active and therefore usable for testing PMGLP (Fig. 1A, left panel). We used 1.0 nmol PMGLP for the detection of 100 pmol recombinant enzyme. rmCTSB and rmCTSD did not provide any cleavage of PMGLP at both tested pH values. rmCTSL provided little PMGLP conversion at pH 5.0 but none at pH 7.5 (Fig. 1A and B). As expected, rhCTSS provided efficient PMGLP hydrolysis at both pH values, pH 5.0 and pH 7.5, respectively. rmCTSS also provided excellent cleavage of PMGLP at both of these pH values. The conversion rate per pmol enzyme at pH 5.0 was even higher than the conversion rate of the human recombinant CTSS. At a neutral pH of 7.5, both recombinant cathepsin S proteins, mouse and human, provided comparable PMGLP turnover (Fig. 1A and B).

2.2. PMGLP is efficiently cleaved by lysates of mouse bone marrow-derived dendritic cells

Recombinant mouse CTSL provided low, but measurable PMGLP conversion at pH 5. However, no rmCTSL-catalyzed PMGLP turnover could be detected at pH 7.5. Therefore, we performed further testing for PMGLP usability using a phosphate buffer system at pH 7.5, in order to exclude potential false positive results that might by generated by CTSL activity. rmCTSS has been shown to provide excellent cleavage behavior also at neutral pH values (Fig. 1A and B). PMGLP was designed to be used for the detection of enzymatic activities in human antigen presenting cells (Lutzner and Kalbacher, 2008). In order to verify the hypothesis that PMGLP is also suitable for the use in mouse-derived cells or cell lines, we first generated bone marrow derived dendritic cells (BMDCs) from the bone marrow of *wt* (*Ctss*$^{+/+}$) and CTSS-deficient (*Ctss*$^{-/-}$) mice. In order to lyse the cells efficiently without affecting cathepsin activity several lysing procedures have been tested. In general, hypotonic lysis was less harmful to cathepsins compared to lysing procedures using detergents (data not shown). Therefore, we performed all following experiments using hypotonic cell lysis as described in Materials and methods. The protein amount of the obtained cell lysate was determined in every case in order to equalize whole cell protein amount in each assay sample. In general, we used 25 μg whole cell protein in a 100 μL sample containing 10 μM PMGLP. DTT was added in relatively high concentrations (2.8 mM in the reaction assay) to ensure that the catalytic cysteine residue at the active site remains in a reduced state and therefore prevents from uncontrolled oxidation of the sulfhydryl group that might falsify obtained results. Besides DTT, the buffer contained EDTA to inhibit metalloproteases, pepstatin A for the inhibition of aspartyl proteases and Pefabloc for serine and threonine protease inhibition. Lysates from *Ctss*$^{+/+}$ (*wt*) BMDCs provided efficient PMGLP conversion (Fig. 2A). Addition of the CTSS-specific inhibitor LHVS was expected to completely anticipate substrate hydrolysis. However, aA remarkable substrate conversion was detected. This could also not be prevented by adding E-64, a highly selective cysteine protease inhibitor that inhibits all cathepsins. Next, we used cell lysates of CTSS-deficient (*Ctss*$^{-/-}$) BMDCs and checked for PMGLP hydrolysis (Fig. 2A). Again, we could observe certain background PMGLP cleavage in untreated as well as in LHVS- and E-64-treated samples. Surprisingly, we could show that E-64- and LHVS-treated *Ctss*$^{+/+}$ samples provided the same background PMGLP hydrolysis as did CTSS-deficient samples. We therefore concluded that this background PMGLP hydrolysis occurred independently of the presence of CTSS. Since inhibition of CTSS using either LHVS or E-64 in *Ctss*$^{+/+}$ samples reduced the detected conversion to the same level as in non-inhibited CTSS-deficient samples, we concluded that the difference is equal to the actual activity of mouse CTSS. From the obtained results shown in Fig. 2A, we hypothesized that background PMGLP hydrolysis might be caused by any other protease containing a cysteine residue at its active site that might not be inhibited by E-64. We therefore incubated cell lysates with Roche Complete Protease Inhibitor that is reported to efficiently inhibit all types of endogenous eukaryotic proteases (Fig. 2B). However, even the use of this inhibitor did not affect background cleavage and delivered the same PMGLP hydrolysis rates as did E-64- or LHVS-treated samples from *wt* BMDCs as well as samples from *Ctss*$^{-/-}$ BMDCs. We also checked for fluorogen behavior of BMDC lysates to evaluate any intrinsic cell component fluorescence and its putative contribution to the detected background turnover. Fig. 2C shows that we could not detect any fluorescence increase in non-PMGLP treated BMDC lysates. PMGLP itself is also not cleaved under measuring buffer conditions without adding cell lysates. We therefore conclude that a yet unidentified cell lysate component contributes to background PMGLP turnover.

2.3. Background turnover remains constant under different stimulation conditions

In order to prove that PMGLP is suitable for reliable detection of CTSS activities in mouse cell lysates despite the observed background hydrolysis, we differentially stimulated mouse BMDCs and tested for PMGLP cleavage with and without cathepsin inhibitor E-64.

Stimulation of BMDCs with TLR ligands like gram-negative bacteria results in a maturation process altering the phenotype of the dendritic cell. We have already shown that a commensal pathobiotic gut bacteria, *Escherichia coli* mpk, induces complete DC maturation in vitro as well in vivo (Muller et al., 2008; Frick et al., 2006). One of the most important maturation-associated proteins is MHC II, whose surface expression is drastically enhanced during DC maturation (Frick et al., 2006). Since CTSS is known to play a critical role in this process (Driessen et al., 1999), we stimulated BMDCs with maturation-inducing gram-negative *E. coli* mpk for 2 h or 18 h, respectively. Since the maturation process should be in a different stage after 18 h of bacterial stimulation compared to 2 h stimulation, we expected to detect different MHC II surface expression and therefore different CTSS activity.

We generated mouse BMDCs from three different individuals and first checked the maturation state of the respective cells after *E. coli* mpk stimulation. For this purpose, we defined the maturation state of CD11c^{+} BMDCs by their proportion of MHC II high positive (hi^{+}) cells, as published previously (Frick et al., 2006). Fig. 3A demonstrates that stimulation of immature CD11c^{+} BMDCs for 2 h with *E. coli* mpk led to slight enhancement of the proportion of MHC II hi^{+} CD11c^{+} BDMCs. However, the proportion of MHC II hi^{+} cells among all CD11c^{+} BMDCs rose up to about 61% after 18 h of *E. coli* mpk stimulation compared to only about only 31% MHC II hi^{+} CD11c^{+} BMDCs in the unstimulated mock control (Fig. 3A).

Additionally, we checked for PMGLP hydrolysis efficiency in BMDCs that were stimulated with *E. coli* mpk for either 2 h or 18 h, respectively. Fig. 3B shows that PMGLP hydrolysis 2 h after *E. coli* mpk stimulation was significantly higher compared to PMGLP conversion in BMDCs that were stimulated for 18 h. We used E-64 to check for background PMGLP conversion (Fig. 3C). Although not being a selective CTSS inhibitor, we consider E-64 to be suitable for final specific CTSS activity computation, since we demonstrated that the use of E-64 and the specific CTSS inhibitor LHVS resulted in the detection of the same background activity (Fig. 2A). E-64 has the advantage of being cheap and easily commercially available without being disadvantageous for reliable background activity detection. Although we could observe

Please cite this article as: Steimle, A., et al., A novel approach for reliable detection of cathepsin S activities in mouse antigen presenting cells, J. Immunol. Methods (2016), http://dx.doi.org/10.1016/j.jim.2016.02.015

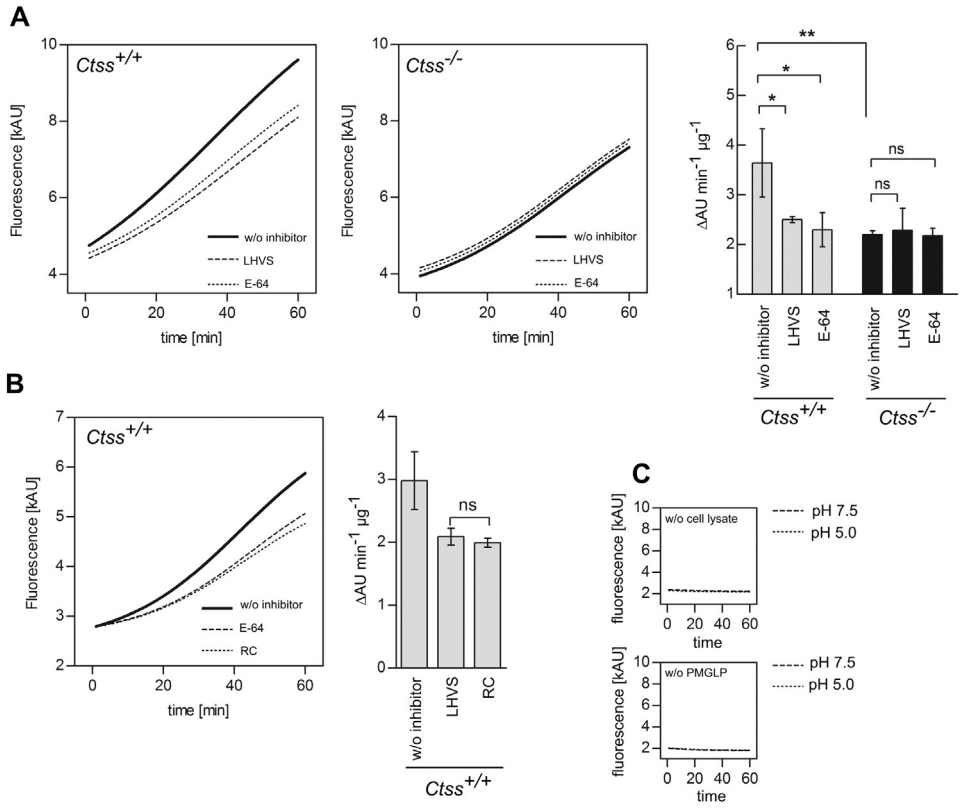

Fig. 2. *Ctss*$^{+/+}$ BMDCs fail to specifically cleave PMGLP. Bone marrow derived dendritic cells (BMDCs) from wildtype (*Ctss*$^{+/+}$) and cathepsin S-deficient (*Ctss*$^{-/-}$) mice were generated and lysed as described. 25 µg whole BMDC lysate protein was tested for PMGLP cleavage behavior at pH 7.5. Substrate cleavage was monitored by observing fluorescence increase at 405 nm. (A) *Ctss*$^{+/+}$ and *Ctss*$^{-/-}$ BMDC lysates were pre-incubated with all-cathepsin-inhibitor E-64, specific CTSS inhibitor LHVS or without any inhibitor before PMGLP addition. PMGLP cleavage was monitored for 60 min at 37 °C. Conversion curves are shown on the left. Specific substrate conversion rates in ΔAU per minute and µg whole BMDC lysate protein (ΔAU min^{-1} µg^{-1}) were computed as described in the Materials and methods section and are shown on the right. (B) Pre-incubation of *Ctss*$^{+/+}$ BMDC lysate with LHVS was compared to Roche Complete Protease Inhibitor (RC). Conversion curves are shown on the left, specific conversion rates on the right. (C) Top: conversion curve of PMGLP at 405 nm in pH 7.5 and pH 5.0 measuring buffer without addition of BMDC lysates, bottom: conversion curve of BMDC lysates without addition of PMGLP at 405 nm in pH 7.5 and pH 5.0 measuring buffer. (A–C) Illustrated conversion curves are averaged curves of three independent experiments. Statistical analyses were performed using Student's t-test. $^{*}p < 0.05$, $^{**}p < 0.01$, n = 3, error bars represent standard deviation (SD).

slight differences in PMGLP hydrolysis under E-64 treatment between BMDCs generated from different individuals (Fig. 3C), there was no significant difference between BMDCs that were stimulated for 2 h and 18 h with *E. coli* mpk (Fig. 3D). Final CTSS activity has been determined by subtracting the slope magnitude of a linear regression at the beginning of the enzymatically catalyzed PMGLP hydrolysis in inhibitor-treated samples from the slope magnitude of non-inhibitor-treated samples of BMDCs generated from the same individual. This resulted in a significantly enhanced CTSS activity for 2 h *E. coli* mpk treated BMDCs compared to 18 h stimulated BMDCs (Fig. 3D). This correlates well with the detected surface expression of MHC II (Fig. 3A), since 2 h after TLR-induced maturation of BMDCs, CTSS activity is upregulated to start the maturation of the MHC II complex through invariant chain processing, finally resulting in enhanced MHC II surface expression 18 h after *E. coli* mpk stimulation. At this point, CTSS activity seems to be downregulated since no further MHC II transport to the cell surface is required for BMDC maturation.

2.4. Recommended experimental workflow for the detection of CTSS activities in mouse antigen presenting cells

In summary, we recommend the following workflow using PMGLP as a fluorogen substrate for the detection of cathepsin S activities from mouse derived cells (Fig. 4). Cells are harvested as carefully as possible followed by hypotonic lysis as described in the Materials and methods section. In order to compare cathepsin S activities in different samples, equal protein amounts should be used in all tested samples. Each sample is then divided into two: one sample is pre-incubated with cathepsin inhibitor E-64, whereas the other one is not. PMGLP is added into both samples followed by measuring fluorescence intensity increase as a function of time. PMGLP turnover rates are computed as described in Fig. 1B and the Materials and methods section. The mathematical difference between the PMGLP turnover rates in the E-64 pre-incubated sample and the non-inhibited sample is directly equivalent to the activity of mouse cathepsin S. We want to underline that it is crucial for a successful CTSS activity detection to keep the samples on ice throughout the entire experiment. Unfortunately, after blast freezing in liquid nitrogen, samples cannot be frozen again for longtime storage since this leads to a dramatic loss of enzymatic activity (data not shown). Additionally, long time storage in liquid nitrogen, starting directly after adding deionized water for the hypotonic lysis, also leads to a remarkable, yet not complete, reduction of enzymatic activity (data not shown). Hence, the whole experimental setup should be performed in one go in order to obtain the best possible results.

3. Discussion

Altered cathepsin S (CTSS) activities have been published to play crucial roles in the pathology of several ailments, especially autoimmune diseases (Figueiredo et al., 2015; Haves-Zburof et al., 2011; Fissolo et al., 2008; Schonefuss et al., 2010; Hamm-Alvarez et al., 2014; Cattaruzza et al., 2011). In light of these findings, the interest in reliable methods of detecting the activity of CTSS in human and mouse samples has grown, especially in the context of investigations into intrinsic CTSS regulation mechanisms. Several new applications for CTSS activity detection have been published within the last few years. Most of them,

Please cite this article as: Steimle, A., et al., A novel approach for reliable detection of cathepsin S activities in mouse antigen presenting cells, J. Immunol. Methods (2016), http://dx.doi.org/10.1016/j.jim.2016.02.015

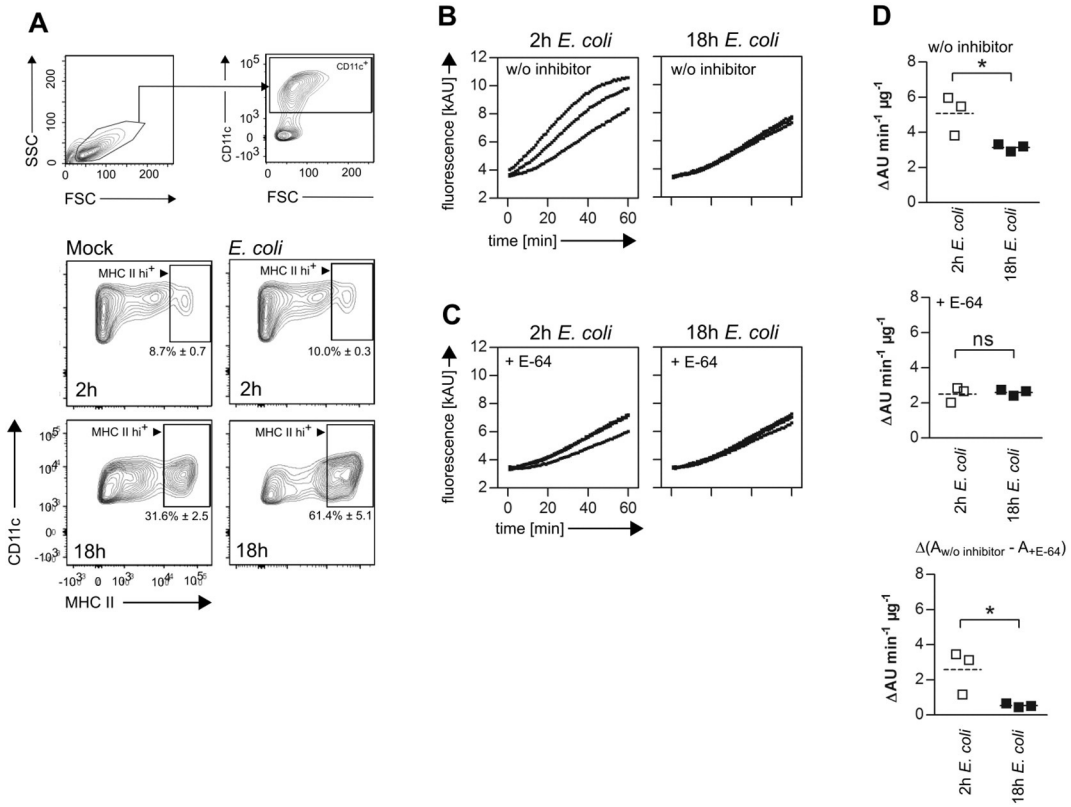

Fig. 3. Background PMGLP conversion remains constant in samples with different CTSS activity. Bone marrow derived dendritic cells from wildtype (*Ctss*$^{+/+}$) mice were generated as described. At day 7 after bone marrow isolation, differentiated BMDCs were stimulated with *E. coli* mpk for 2 h or 18 h respectively. (A) *E. coli* mpk stimulated and non-stimulated (mock) control BMDCs were stained with antibodies against CD11c and MHC II for flow cytometrical analysis. Only CD11c^{+} cells were analyzed for MHC II surface expression (lower panel). Each contour blot is representative for 3 independent experiments. Mean proportions (±SEM) of MHC IIhi^{+} cells among all CD11c^{+} cells are indicated inside the contour blots. (B, C, D) After stimulation, BMDCs were lysed and 25 µg whole BMDC lysate protein was tested for PMGLP cleavage behavior at pH 7.5. Substrate cleavage was monitored by observing fluorescence increase at 405 nm. (B) Conversion curves of PMGLP without addition of inhibitor. Each curve represents one of three independent experiments. (C) Conversion curves of the same samples as in (A), but with the addition of 10 µM E-64. (D) Specific substrate conversion rates in ΔAU per minute and µg whole BMDC lysate protein (ΔAU min^{-1} µg^{-1}) were computed as described in Fig. 1B. Lower panel: result of the mathematical subtraction of the obtained conversion rates in (B)($A_{w/o\ inhibitor}$) and (C) ($A_{+\ E\text{-}64}$). Each dot represents data from BMDCs generated from a different individual. Statistical analyses were performed using Student's t-test. *$p < 0.05$, **$p < 0.01$, $n = 3$. Error bars represent standard deviation (SD).

however, provide distinct disadvantages for high-throughput usage. Four criteria should be fulfilled to deliver an adequate substrate or detection method: First, since most basic research is performed using mouse models or mouse cell lines, an application must not only be suitable for human samples but also for mouse-derived samples. Second, high specificity has to be guaranteed. Cathepsins in general provide a broad range of potential endogenous or exogenous substrates (Choe et al., 2006). This physiologically valuable property makes them poor targets for specific detection. Other cathepsins than CTSS, especially abundant and highly expressed cathepsins like cathepsin B (CTSB), need to be prevented from interfering with the detection method, as they might otherwise falsify obtained results. Third, the application should be able to be performed in a standard laboratory without requiring specialized and expensive equipment. Fourth, the results should be quantitative and reproducible. For the in vitro detection of mouse CTSS activities, several oligopeptide substrates have been used. A commercially available aminomethylcoumarine coupled pentapeptide Ac-KQKLR-AMC is described as detecting specific mouse CTSS activities (Balce et al., 2014). However, this substrate has also been shown to be efficiently cleaved by CTSB (O'Brien et al., 2008). The dipeptide substrate Z-FR-AMC has been widely used to detect the activities of CTSB, CTSS and CTSL in one experimental setting. Since the substrate is cleaved by all three cathepsins, the main discrimination between CTSS on the one side and CTSL and CTSB on the other side was performed by measuring at different pH values. In contrast to CTSB and CTSL, CTSS shows efficient protease activity even at neutral pH values. The activity optimum of cathepsins B and L at acidic pH values is due to their location in acidified lysosomes where they have to fulfill their biological role in degrading proteins (Turk et al., 2012), but CTSS retains activity at pH 7.0 to 7.5 (Kirschke et al., 1989). However, as demonstrated here, slight Z-FR-AMC hydrolysis caused by CTSB can even occur at neutral pH and therefore makes reliable CTSS activity detection using this method unlikely. Activity probes of different chemical structures are widely used for activity detection of one or more cathepsins in one single assay. DCG-04 and DCG-0N are probably the most prominent ones (Hoogendoorn et al., 2011). Garenne et al. have recently published a diazomethylketone probe for the detection of extra- and intracellular human CTSS activities (Garenne et al., 2015). However, it has not been demonstrated to be suitable for the detection of mouse CTSS. Like all activity based probes, DCG-04 and the diazomethylketone probe only deliver semi-quantitative results based on normalized band intensities on an electrophoresis-assisted gel. For the generation of quantitative results, the use of a fluorogen substrate provides advantages over activity probes. A certain fluorogen substrate, Mca-GRWPPMGLPWE-Lys(Dnp)-DArg-NH_2 (PMGLP), has been shown to be cleaved specifically by CTSS in human antigen presenting cells (Lutzner and Kalbacher, 2008). We showed that the use of this substrate is also suitable for the quantitative detection of CTSS in mouse antigen presenting cells. The experimental procedure is easy, fast, cheap, and delivers reliable and highly reproducible results. Besides the substrate itself, all other components and chemicals are easily available and the detection of substrate conversion merely requires the availability of a heatable fluorescence compatible photometer and no further expensive or special technical equipment. We strongly recommend performing the entire experiment,

Please cite this article as: Steimle, A., et al., A novel approach for reliable detection of cathepsin S activities in mouse antigen presenting cells, J. Immunol. Methods (2016), http://dx.doi.org/10.1016/j.jim.2016.02.015

beginning with cell lysis and ending with fluorometer-based detection of substrate conversion, in one go. Unfortunately, this means that samples cannot be stored at temperatures of −80 °C or below since this results in remarkable loss of CTSS activity in cell lysates therefore making reliable detection impossible.

In contrast to the cleavage behavior in human APC (Lutzner and Kalbacher, 2008), mouse bone marrow-derived dendritic cells provide a certain background cleavage of this substrate that is not caused by CTSS or any other protease that can be inhibited by E-64 or the Roche Complete Protease Inhibitor. We still do not know what the cause for this background hydrolysis of PMGLP is. However, our recommended workflow (Fig. 4) offers a possibility to detect specific mouse CTSS activities besides background substrate hydrolysis. After hypotonic lysis of the cells, we recommend to create two different reaction samples out of one sample of interest. The first sample contains the substrate, the second both, the substrate and E-64, an inhibitor against all cysteine cathepsins to detect the background activity. CTSS activity is therefore equivalent to the difference in PMGLP conversion between the reaction sample containing no inhibitor and the sample containing E-64.

Since CTSS is exclusively expressed in professional antigen presenting cells, we recommend using cell populations which are as homogenous as possible for CTSS activity detection. Otherwise the cell amount of CTSS expressing cells can fall below a critical level for reliable CTSS activity detection.

In summary, we have shown (I) that a specific CTSS inhibitor is not necessary for the detection of background activity, therefore the easily commercially available E-64 can be used and (II) that the background activity is not different between differentially stimulated APC. Therefore, this PMGLP-assisted CTSS activity assay is also useable for high-throughput experiments within a short period of time and we think that this experimental assay contributes to simplify CTSS related research.

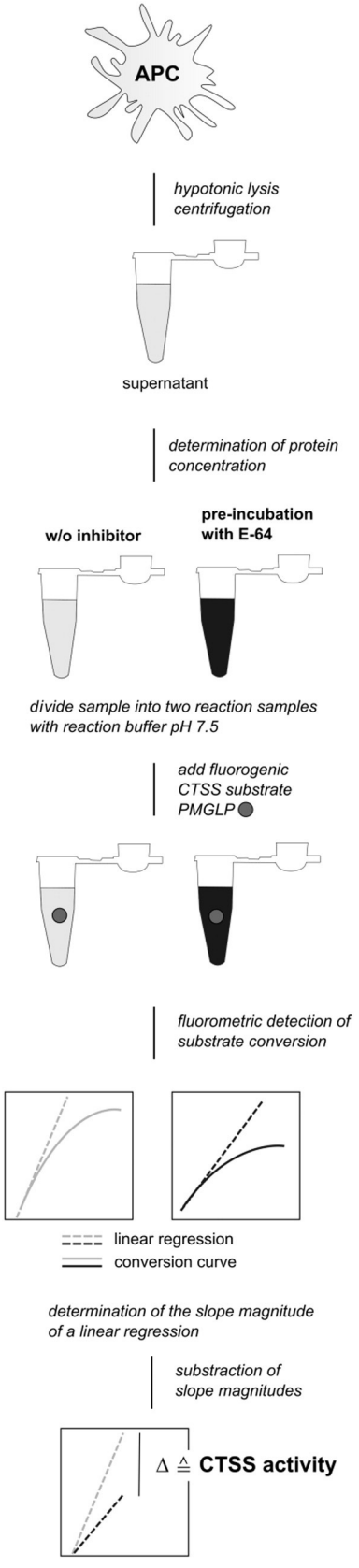

4. Materials and methods

4.1. Mice

Cathepsin S-deficient ($Ctss^{-/-}$) and wildtype ($Ctss^{+/+}$) mice have been generated by mating $Ctss^{+/-}$ mice. $Ctss^{+/-}$ mice were kindly provided by the lab of Thomas Reinheckel, University of Freiburg, Germany. All animal experiments were reviewed and approved by the responsible Institutional Review Board.

4.2. Bacteria

E. coli mpk was used for stimulation of mouse bone marrow dendritic cells (BMDCs). This *E. coli* mpk strain was grown in Luria-Bertani (LB) medium under aerobic conditions at 37 °C. At the day of BMDC stimulation, 200 μL of a 5 mL overnight culture was subcultured and added to 20 mL of fresh LB medium. Bacteria were then cultivated for another 1.5 h until reaching an OD_{600} of about 2–3. This guaranteed using bacteria in the exponential growth phase. Quantification of bacteria was performed by measuring OD at 600 nm. An OD_{600} of 1.0 is equal to a concentration of 5×10^8 bacteria per mL. This OD-to-

Fig. 4. Experimental workflow for the detection of CTSS activities in mouse APC. Cells of interest are lysed hypotonically followed by blast freezing in liquid nitrogen as described in Materials and methods section. Supernatant is used for CTSS activity detection. Out of each sample, two reaction samples containing the same amount of whole cell protein are created. The first sample contains the fluorogen substrate, the second both, the substrate and the cathepsin inhibitor E-64. Reaction buffer provides a pH of 7.5 to minimize false positive substrate conversion caused by other cathepsins. Substrate conversion is monitored for 60 min at 37 °C. A linear regression at the very beginning of the sigmoidal conversion curve is performed for both reaction samples. The slope magnitude of this linear regression is equivalent to the substrate conversion per time unit. The difference in the slope magnitude of both reaction samples is equivalent to the CTSS activity in the sample the lysate was taken from. CTSS activities can therefore be expressed as the difference of fluorescence intensity per μg cell protein and time unit, i.e. $\Delta AU\ min^{-1}\ \mu g^{-1}$.

Please cite this article as: Steimle, A., et al., A novel approach for reliable detection of cathepsin S activities in mouse antigen presenting cells, J. Immunol. Methods (2016), http://dx.doi.org/10.1016/j.jim.2016.02.015

concentration correlation was confirmed by plating *E. coli* mpk on LB agar plates.

4.3. Recombinant cathepsins

The recombinant mouse (rm) cathepsins cathepsin S (rmCTSS) and cathepsin B (rmCTSB) were purchased from Sino Biological. Recombinant mouse cathepsin D (rmCTSD) and recombinant mouse cathepsin L (rmCTSL) were purchased from R&D. Recombinant human CTSS (rhCTSS) was kindly provided by the lab of Hubert Kalbacher, University of Tübingen.

4.4. Fluorogen cathepsin activity substrates

The substrate for specific detection of human CTSS activities, Mca-GRWPPMGLPWE-Lys(Dnp)-DArg-NH_2 (PMGLP), was provided by the lab of Hubert Kalbacher, University of Tübingen, Germany. The substrate Z-FR-AMC was purchased from Peptide Institute, Rep. of Korea.

4.5. Generation of bone marrow-derived dendritic cells

Bone marrow cells were isolated from *wt* ($Ctss^{+/+}$) and $Ctss^{-/-}$ mice and differentiated to bone marrow derived dendritic cells (BMDCs) as described previously (Lutz et al., 1999).

4.6. Stimulation of bone marrow-derived dendritic cells

At day 7 after bone marrow isolation, resulting $CD11c^+$ bone marrow derived dendritic cells were stimulated for 2 h or 18 h with *E. coli* mpk. BMDCs were harvested, counted and 2×10^6 BMDCs were incubated with *E. coli* mpk using MOI 1 for 2 h and 18 h respectively at 37 °C and 5% CO_2. MOI stands for "multiplicity of infection" and refers to the number of bacteria used per cell for stimulation. The used MOI of 1.0 is known to efficiently induce maturation of BMDCs (Frick et al., 2006). As cell purity controls, a part of each sample was analyzed by flow cytometry to determine CD11c surface expression. All samples contained at least 80% $CD11c^+$ cells and were therefore named BMDCs.

4.7. SDS gel electrophoresis and Coomassie staining of recombinant cathepsins

500 ng of each recombinant cathepsin were loaded on a 12% polyacrylamide gel. Proteins were then separated via SDS-PAGE. Afterwards, gels were transferred into a staining solution consisting of 10% (*v*/*v*) glacial acetic acid, 40% (*v*/*v*) MeOH, 0.1% (*w*/*v*) Coomassie R250 dye. Gels were incubated in this staining solution at room temperature overnight followed by destaining in 10% (*v*/*v*) glacial acetic acid and 20% (*v*/*v*) MeOH for approximately 2 h.

4.8. Hypotonic lysis of bone marrow derived dendritic cells

BMDCs were harvested and centrifuged for 5 min at 400 ×*g*. Cells were then lysed hypotonically using 100 μL de-ionized sterile water per one million cells. After incubation for 30 min on ice, cell suspensions were shock frozen at −170 °C and thawed carefully immediately afterwards, followed by centrifugation for 10 min at 1000 ×*g* and 4 °C. Supernatants were taken for CTSS activity determination.

4.9. Determination of protein concentrations in BMDC lysates

Protein concentrations of BMDC lysates were determined using a commercially available BCA kit (ThermoScientific).

4.10. Detection of CTSS activities using PMGLP or Z-FR-AMC as fluorogen substrates

25 μL de-ionized water containing 25 μg whole cell protein of lysed BMDCs or 25 μL deionized water containing 0.5 pmol recombinant cathepsin were added to 70 μL pH 7.5 reaction buffer (0.1 M phosphate buffer pH 7.5, 4 mM DTT, 4 mM EDTA, 1 mM Pefabloc (Sigma) and 1 μM pepstatin A) or pH 5.0 reaction buffer (0.1 M sodium citrate buffer pH 5.0, 4 mM DTT, 4 mM EDTA, 1 mM Pefabloc (Sigma, Germany) and 1 μM pepstatin A), respectively. After 10 min pre-incubation at RT, PMGLP was added at a final concentration of 10 μM or Z-FR-AMC at a final concentration of 10 μg mL^{-1}. Hydrolysis of PMGLP was tracked by observing the fluorescence increase of the fluorophore at 405 nm when excited at 340 nm using a Tecan Infinite 200 Fluororeader. Z-FR-AMC hydrolysis was observed at 441 nm when excited at 342 nm. For the determination of substrate conversion rates and therefore enzymatic activities, a linearization of the substrate conversion curve was performed. For this purpose, fluorescence increase as a function of time was detected for 60 min at 37 °C. At the very beginning of the enzymatically catalyzed substrate conversion leading to an increase in fluorescence intensity, the fluorescence intensity increases linearly before reaching a plateau. Fifteen to twenty pairs of variates of the linear fluorescence progression at the very beginning of the substrate conversion were taken for mathematical linearization. This was performed using GraphPad Prism 5.0. This program was used to (Turk et al., 2012) determine the R2 value in order to assess the quality of fit of the linear curve and (Driessen et al., 1999) to determine the slope of the linear regression. Only linear curves providing R2 values greater than 0.99 were further analyzed. The obtained slopes from the linear curves directly correspond to the fluorescence increase per time unit usually expressed as $\Delta AU\ min^{-1}$. AU stands for "arbitrary units" in order to refer to the dimensionless measurements of fluorescence intensities. If protein amounts or concentrations are known, this information can be included into the unit, leading to $\Delta AU\ min^{-1}\ \mu g^{-1}$ or $\Delta AU\ min^{-1}\ nmol^{-1}$.

4.11. Inhibition of proteases

In order to inhibit all cathepsins or CTSS alone in the reaction sample (2.10), E-64 and LHVS were added 10 min before substrate addition to the reaction buffer at final concentrations of 500 nM or 10 nM, respectively. Roche Complete Protease Inhibitor (RC) was added according to the manufacturer's instructions.

Conflict of interest

The authors disclose all commercial affiliations and competing financial interests.

Acknowledgments

We thank Prof. Thomas Reinheckel, University of Freiburg, Germany for kindly handing over $CTSS^{-/-}$ mice.

Work was supported by the DFG (DFG FR 2087/6-1, DFG FR 2087/8-1, CRC685, SPP1656, SFB685), the DFG Research Training Group 1708 and the German Centre for Infection Research (DZIF) (TTU 06.707).

References

Balce, D.R., Allan, E.R., McKenna, N., Yates, R.M., 2014. Gamma-interferon-inducible lysosomal thiol reductase (GILT) maintains phagosomal proteolysis in alternatively activated macrophages. J. Biol. Chem. 289 (46), 31891–31904.

Barrett, A.J., 1980. Fluorimetric assays for cathepsin B and cathepsin H with methylcoumarylamide substrates. Biochem. J. 187 (3), 909–912.

Beers, C., Burich, A., Kleijmeer, M.J., Griffith, J.M., Wong, P., Rudensky, A.Y., 2005. Cathepsin S controls MHC class II-mediated antigen presentation by epithelial cells in vivo. J. Immunol. 174 (3), 1205–1212.

Please cite this article as: Steimle, A., et al., A novel approach for reliable detection of cathepsin S activities in mouse antigen presenting cells, J. Immunol. Methods (2016), http://dx.doi.org/10.1016/j.jim.2016.02.015

Cattaruzza, F., Lyo, V., Jones, E., Pham, D., Hawkins, J., Kirkwood, K., et al., 2011. Cathepsin S is activated during colitis and causes visceral hyperalgesia by a PAR2-dependent mechanism in mice. Gastroenterology 141 (5), 1864–1874 (e1–3).

Choe, Y., Leonetti, F., Greenbaum, D.C., Lecaille, F., Bogyo, M., Bromme, D., et al., 2006. Substrate profiling of cysteine proteases using a combinatorial peptide library identifies functionally unique specificities. J. Biol. Chem. 281 (18), 12824–12832.

Conus, S., Simon, H.U., 2010. Cathepsins and their involvement in immune responses. Swiss Med. Wkly. 140, w13042.

Cunningham, M., Tang, J., 1976. Purification and properties of cathepsin D from porcine spleen. J. Biol. Chem. 251 (15), 4528–4536.

Dolinar, M., Maganja, D.B., Turk, V., 1995. Expression of full-length human procathepsin L cDNA in *Escherichia coli* and refolding of the expression product. Biol. Chem. Hoppe Seyler 376 (6), 385–388.

Driessen, C., Bryant, R.A., Lennon-Dumenil, A.M., Villadangos, J.A., Bryant, P.W., Shi, G.P., et al., 1999. Cathepsin S controls the trafficking and maturation of MHC class II molecules in dendritic cells. J. Cell Biol. 147 (4), 775–790.

Figueiredo, J.L., Aikawa, M., Zheng, C., Aaron, J., Lax, L., Libby, P., et al., 2015. Selective cathepsin S inhibition attenuates atherosclerosis in apolipoprotein E-deficient mice with chronic renal disease. Am. J. Pathol. 185 (4), 1156–1166.

Fissolo, N., Kraus, M., Reich, M., Ayturan, M., Overkleeft, H., Driessen, C., et al., 2008. Dual inhibition of proteasomal and lysosomal proteolysis ameliorates autoimmune central nervous system inflammation. Eur. J. Immunol. 38 (9), 2401–2411.

Frick, J.S., Zahir, N., Muller, M., Kahl, F., Bechtold, O., Lutz, M.B., et al., 2006. Colitogenic and non-colitogenic commensal bacteria differentially trigger DC maturation and Th cell polarization: an important role for IL-6. Eur. J. Immunol. 36 (6), 1537–1547.

Garenne, T., Saidi, A., Gilmore, B.F., Niemiec, E., Roy, V., Agrofoglio, L.A., et al., 2015. Active site labeling of cysteine cathepsins by a straightforward diazomethylketone probe derived from the N-terminus of human cystatin C. Biochem. Biophys. Res. Commun. 460 (2), 250–254.

Hamm-Alvarez, S.F., Janga, S.R., Edman, M.C., Madrigal, S., Shah, M., Frousiakis, S.E., et al., 2014. Tear cathepsin S as a candidate biomarker for Sjogren's syndrome. Arthritis Rheum. 66 (7), 1872–1881.

Haves-Zburof, D., Paperna, T., Gour-Lavie, A., Mandel, I., Glass-Marmor, L., Miller, A., 2011. Cathepsins and their endogenous inhibitors cystatins: expression and modulation in multiple sclerosis. J. Cell. Mol. Med. 15 (11), 2421–2429.

Hoogendoorn, S., Habets, K.L., Passemard, S., Kuiper, J., van der Marel, G.A., Florea, B.I., et al., 2011. Targeted pH-dependent fluorescent activity-based cathepsin probes. Chem. Commun. 47 (33), 9363–9365.

Jadhav, P.K., Schiffler, M.A., Gavardinas, K., Kim, E.J., Matthews, D.P., Staszak, M.A., et al., 2014. Discovery of cathepsin S inhibitor LY3000328 for the treatment of abdominal aortic aneurysm. ACS Med. Chem. Lett. 5 (10), 1138–1142.

Kirschke, H., Wiederanders, B., Bromme, D., Rinne, A., 1989. Cathepsin S from bovine spleen. Purification, distribution, intracellular localization and action on proteins. Biochem. J. 264 (2), 467–473.

Kohl, F., Schmitz, J., Furtmann, N., Schulz-Fincke, A.C., Mertens, M.D., Kuppers, J., et al., 2015. Design, characterization and cellular uptake studies of fluorescence-labeled prototypic cathepsin inhibitors. Org. Biomol. Chem.

Linebaugh, B.E., Sameni, M., Day, N.A., Sloane, B.F., Keppler, D., 1999. Exocytosis of active cathepsin B enzyme activity at pH 7.0, inhibition and molecular mass. Eur. J. Biochem. 264 (1), 100–109.

Lutz, M.B., Kukutsch, N., Ogilvie, A.L., Rossner, S., Koch, F., Romani, N., et al., 1999. An advanced culture method for generating large quantities of highly pure dendritic cells from mouse bone marrow. J. Immunol. Methods 223 (1), 77–92.

Lutzner, N., Kalbacher, H., 2008. Quantifying cathepsin S activity in antigen presenting cells using a novel specific substrate. J. Biol. Chem. 283 (52), 36185–36194.

Malagon, D., Diaz-Lopez, M., Benitez, R., Adroher, F.J., 2010. Cathepsin B- and L-like cysteine protease activities during the in vitro development of *Hysterothylacium aduncum* (Nematoda: Anisakidae), a worldwide fish parasite. Parasitol. Int. 59 (1), 89–92.

Mindell, J.A., 2012. Lysosomal acidification mechanisms. Annu. Rev. Physiol. 74, 69–86.

Muller, M., Fink, K., Geisel, J., Kahl, F., Jilge, B., Reimann, J., et al., 2008. Intestinal colonization of IL-2 deficient mice with non-colitogenic *B. vulgatus* prevents DC maturation and T-cell polarization. PLoS ONE 3 (6), e2376.

O'Brien, T.C., Mackey, Z.B., Fetter, R.D., Choe, Y., O'Donoghue, A.J., Zhou, M., et al., 2008. A parasite cysteine protease is key to host protein degradation and iron acquisition. J. Biol. Chem. 283 (43), 28934–28943.

Schonefuss, A., Wendt, W., Schattling, B., Schulten, R., Hoffmann, K., Stuecker, M., et al., 2010. Upregulation of cathepsin S in psoriatic keratinocytes. Exp. Dermatol. 19 (8), e80–e88.

Sobotic, B., Vizovisek, M., Vidmar, R., Van Damme, P., Gocheva, V., Joyce, J.A., et al., 2015. Proteomic identification of cysteine cathepsin substrates shed from the surface of cancer cells. Mol. Cell. Proteomics 14 (8), 2213–2228.

Turk, V., Stoka, V., Vasiljeva, O., Renko, M., Sun, T., Turk, B., et al., 2012. Cysteine cathepsins: from structure, function and regulation to new frontiers. Biochim. Biophys. Acta 1824 (1), 68–88.

Vazquez, R., Astorgues-Xerri, L., Bekradda, M., Gormley, J., Buick, R., Kerr, P., et al., 2015. Fsn0503h antibody-mediated blockade of cathepsin S as a potential therapeutic strategy for the treatment of solid tumors. Biochimie 108, 101–107.

Please cite this article as: Steimle, A., et al., A novel approach for reliable detection of cathepsin S activities in mouse antigen presenting cells, J. Immunol. Methods (2016), http://dx.doi.org/10.1016/j.jim.2016.02.015

J Neurology Neuromedicine
www.jneurology.com
Journal of Neurology & Neuromedicine

Mini Review Open Access

The challenge of specific Cathepsin S activity detection in experimental settings

Alex Steimle and Julia-Stefanie Frick*

Institute of Medical Microbiology and Hygiene, University of Tuebingen, Tübingen, Germany

Article Info

Article Notes
Received: May 04, 2016
Accepted: June 01, 2016

***Correspondence:**
Dr. Julia-Stefanie Frick
Institute of Medical Microbiology and Hygiene
University of Tübingen
Elfriede-Aulhorn-Str. 6, D-72076 Tübingen, Germany
Telephone: +49 7071 29 82352
Fax: +49 7071 29 5440
Email: Julia-stefanie.frick@med.uni-tuebingen.de

Keywords
Cathepsin S
Multiple Sclerosis
Alzheimer's Disease
Enzyme
Method

ABSTRACT

In recent years, a growing interest in pathophysiological processes that are associated with the endosomal and lysosomal protease cathepsin S (CTSS) results in an increasing number of various published methods for CTSS activity detection. CTSS has been reported to be involved in the pathology of autoimmune diseases like multiple sclerosis as well as in tumor growth and Alzheimer's disease. These implications make this enzyme a first class drug target. In order to fully understand the involvement of CTSS in the formation of pathological processes, gene and protein expression analysis is not sufficient. Rather, one should focus on the regulation of its enzymatic activity. Different approaches for CTSS activity detection are available and described. However, some of these approaches are not suitable for a standard laboratory without special equipment or technical expertise or provide other limitations. We have recently published an easy-to-perform protocol for reliable, quantifiable and reproducible CTSS activity detection. In this review we want to discuss our application and compare it with other published methods and protocols. This might help researchers who are interested in CTSS research to decide which application fits best to their technical or personal facilities.

Text

Cathepsin S (CTSS) is a protease located in lysosomes or endosomes of professional antigen presenting cells (APC), such as macrophages, dendritic cells and B cells[1]. Dysregulated CTSS expression and/or activity has been reported to be involved in the pathogenesis of various diseases. CTSS is the major regulator of major histocompatibility complex (MHC) II surface expression. Therefore, especially autoimmune diseases which are caused by (or which are associated with) pathologically enhanced $CD4^+$ T cell activation are part of this disease portfolio. In this context, the Sjögren's syndrome[2], atherosclerosis[3], psoriasis[4] and an animal model of rheumatic arthritis[5] play dominant roles. But not only autoimmune diseases are associated with CTSS dysregulation. Enhanced CTSS activity could also be detected in the bronchoalveolar lavage of cystic fibrosis patients[6]. Neurologists might focus on the role of CTSS in the development of multiple sclerosis (MS) and experimental autoimmune encephalomyelitis (EAE), the corresponding mouse model of MS[7]. Indeed, it could already been shown that CTSS is capable of myelin basic protein proteolysis[8] which might contribute to the observed phenotypes in MS patients. In fact, enhanced CTSS levels could be found in peripheral blood mononuclear cells, serum and the cerebrospinal fluid of MS patients[9-12]. In line with these observations, chemical inhibition of CTSS led to a reduction of phenotypical severity in the EAE mouse model[5,13]. Besides MS

patients, enhanced CTSS activity at the primary site in breast cancer patients correlated with an increased frequency of the appearance of brain metastases[14]. The implication of CTSS concerning cancer was linked with with tumor-associated APCs, namely macrophages[15]. Alzheimer's disease (AD) was already reported to be associated with a malfunctioning Cathepsin B (CTSB) activity regulation[16,17]. But also human Cathepsin S seems to be involved in the manifestation of the disease phenotype since also CTSS provides β-secretase activity[18] which leads to the AD phenotype causing agent Aβ peptide through amyloid precursor protein proteolysis[19]. One important feature of CTSS, distinguishing it from other cysteine cathepsins, is the retention of its proteolytic activity at neutral pH. Being part of the endosomal and lysosomal compartment, CTSS can be secreted into the extracellular space providing neutral pH where it can cause additional pathologies. Extracellular CTSS activity has already been shown to be involved in activating protease-activated receptors (PAR) like PAR_2 as well as G-protein coupled receptors like Mrgprs leading to the promotion of itch and pain sensation in both cases[20-23].

All the above mentioned implications for CTSS activity dysregulation which are linked with manifestation of various pathologies makes this enzyme an attractive and intensely studied drug target. Some studies just refer to enhanced *Ctss* gene expression rates or increased protein amounts inside or outside of target cells. However, mRNA expression levels of a protease-encoding gene or expression of the corresponding protein does not necessarily correlate with the overall detected activity of the respective enzyme. This is due to several possible posttranscriptional regulation mechanisms that can occur inside or outside a eukaryotic cell. Proteases can be (i) translated as inactive zymogens requiring proteolytic activation, (ii) activated by co-factors, (iii) separated from their substrates by localization in distinct intra- or extracellular compartments or (iv) inhibited by binding of endogenous inhibitors to the active site of the protease[24]. All these examples illustrate that focusing on mRNA or protein expression is not sufficient to reliably investigate the role of proteases in biological or pathophysiological processes. Therefore, specific detection of the activity of a certain protease has to be guaranteed in order to exclude false positive detection of one or more other proteases with a similar substrate specifity. This is a grave problem concerning the protease group "cathepsins", which consists of currently eleven known members[25], since cathepsins in general provide a broad and overall similar substrate specifity[26]. This makes CTSS activity detection a challenge, in vitro, ex vivo and especially in vivo.

But how can an experimentator achieve the goal to reliably detect CTSS activity in the biological system of choice? There are several possibilities how CTSS activity can be detected, all of them with their characteristic advantages and limitations. A suitable CTSS activity detection method should match the following four criteria: (i) high specifity, (ii) high sensitivity since CTSS expression is restricted to APC, (iii) the experimental workflow should be able to be performed in a more or less standard laboratory without the requirement of highly special technical equipment and (iv) the method should deliver reproducible and quantifiable results. We summarize some available techniques for CTSS activity detection with their characteristic pros and cons in table 1.

Popular approaches include activity based probes (ABPs). These are small reporters of proteolytic activity which bind covalently and irreversibly to the active site of the target enzymes[27] leading to a loss of enzymatic activity. This irreversible CTSS inhibition should be kept in mind if in vivo monitoring shall be performed. ABPs usually consist of three distinct functionalities (Fig. 1A): (1) The so-called warhead functionality leads the probe to enzymes sharing a common catalytic mechanism, (2) the recognition element that enhances specificity for one or more specific enzymes and (3) a tag for a later detection of the tagged enzymes. Such ABPs exist for the detection of human and mouse CTSS. General disadvantages of such ABPs include a lack of specificity for CTSS for some of these ABPs. This has then to be compensated by further time-consuming experimental approaches like western blotting, immunoprecipitations etc. Additionally, CTSS activity can often only be determined in a semi-quantitative manner like measuring band intensities on a gel or a detection of overall fluorescence intensity. However, the potential labelling of proteolytically active CTSS in live cells due to cell permeability is a big advantage of some ABPs. Veilleux et al. developed radioiodinated ABPs to selectively label active CTSS in human whole blood[28]. Ben-Aderet et al.[29] and Oresic Bender et al.[30] used fluorogenic ABPs to monitor enzymatically active CTSS in human cells or live mice, respectively. Other examples of recent ABPs development for CTSS activity detection include the publications of Barlow et al.[31], Hughes et al.[32], Mertens et al.[33] and Garenne et al[34]. However, some of them provide a lack of specificity for CTSS and also label other cathepsins[29,32-35] while other ABPs selectively label human or mouse CTSS[28,30,36]. Another general disadvantage of ABPs include the requirement of more specialized detection techniques that a non-specialized lab could tentatively not afford.

Recently, commercially available CTSS activity detection kits have been developed and are sold. Experiences made by our group revealed, however, that these kits are far less specific than they are advertised to be and we strongly recommend to use alternative techniques for reliable CTSS activity detection. If this is not possible, a strict validation of the claimed specificity for CTSS should be performed, i.e. using recombinant enzymes or knock-out cells for various

Application category	Characteristic	Example	target	Year published	Quantification method	Limitation	Outstanding advantage
Activity based probe (ABPs)	covalent binding to CTSS active site leading to enzyme inhibition	GB123[29]	Human CTSS and CTSB	2015	Fluorescent label	Binds also to CTSB. Gel-assisted enzyme separation or IP needed	Non invasive in vivo imaging possible
		Probe 7[36]	Human CTSS	2015	Fluorescent label	Not cell permeable	Specificity for CTSS
		Z-PraVG-DMG[32]	Human CTSS, CTSB and CTSL	2016	Rhodamine azide labelling	Similar K_i values for CTSS, CTSB and CTSL	Cell-permeability of the substrate
		CM-279[35]	Human CTSS and CTSL	2013	Luciferase assisted light detection	Also labels CTSL	Reliable detection of combined CTSS and CTSL activity
		BMV157[30]	Mouse CTSS	2015	Fluorescent label	availability	Highly specific, in vivo and in vitro application possible
		BIL-DMK[28]	Human CTSS	2011	Radioactive label	Radioactivity	Specificity for CTSS
		Probe 10[33]	Human CTSS, CTSL, CTSB and CTSK	2014	Fluorescent label	Not specific for CTSS	Suitable for complex protein mixtures
		Biot-$(PEG)_2$-Ahx-LeuValGly-DMK[34]	Human CTSS, CTSL, CTSB and CTSL	2015	SDS Page assisted chemi-luminescence	Not specific for CTSS	Easy to perform
Substrate based probes (SBP)	Substrate turnover; enzyme is not inhibited and remains proteolytically active	**PMGLP**	**Human CTSS[43] and mouse CTSS[42]**	**2016**	**Fluorescence increase**	**Requires cell lysis and inhibition control**	**Simple enzymatic assay, easy-to-perform, time saving.**
		Ac-KQKLR-AMC	Mouse CTSS	2014	Fluorescence increase	Requires cell lysis and inhibition control	Simple enzymatic assay
		NB200[31]	Mouse CTSS, CTSK and CTSB	2015	Fluorescence increase	Detects also CTSK at pH7.5 and CTSB at pH 5.5	Simple enzymatic assay
		Z-FR-AMC	Mouse CTSS, CTSB and CTSL	2002	Fluorescence increase	Unspecificity, requires extensive experimental setting	Simple enzymatic assay
Indirect detection methods	Does not directly interact with CTSS	Detection of CTSS substrate accumulation by western blotting[3]	Mouse invariant chain p10 detection	2015	Western blot band intensity of Iip10	Does not detect CTSS activity directly	Simple to perform
		Western blotting of 24 kDa CTSS[37]	Human CTSS	2014	Western blot band intensity of 24 kDa CTSS	Does not consider potential binding of endogenous inhibitors and does not refer to activity	Simple to perform

Table 1: Summary of various CTSS activity detection techniques. The techniques are grouped into the major functional classes.

cysteine cathepsins.

Other approaches include an indirect method to determine CTSS proteolytic (table 1) activity by not directly assessing the enzymatic activity but rather determining the intracellular amount of the MHC II-bound invariant chain fragment (Iip10), which is a substrate for CTSS. Therefore, decreased amounts of Iip10 is stated to correlate with enhanced CTSS activity[5]. Since CTSS is translated into an inactive pro-enzyme requiring proteolytical cleaving which results in a 24 kDa active enzyme, some publications refer to the band intensities of this 24 kDa band when making statements on CTSS activity[37]. However this does not

take the potential binding of endogenous inhibitors into account.

Another possibility for direct CTSS activity determination is to use substrate-based probes (SBP) like i.e. fluorochrome-coupled peptidyl substrates. The principle mechanism includes a detection in the increase of a peptidyl-coupled and later proteolytically liberated fluorochrome (Figure 1B). SBPs provide the advantage of not inhibiting the target enzyme. Prominent examples are Z-VVR-AMC[38] , Z-FR-AMC[36,39] or Ac-KQKLR-AMC[20,40]. All of them share the aminomethyl coumarin group as a fluorogen tag. Coumarins are popular fluorescent labels due to their large stoke's shifts[41] and their small size allowing for incorporation into small peptides[33] . These peptidyl substrates generally provide the disadvantage to be usable only in cell lysates and not in living cells or organisms. The major potential problem with most peptidyl substrates is the unsatisfactory specificity for CTSS. Due to the already mentioned similar substrate specificity among cysteine cathepsins, other cathepsins than CTSS can deliver false positive results due to unspecific cleavage of the substrate. However, we have recently reported on a CTSS activity detection method using a coumarin-coupled peptidyl substrate (PMGLP) that allows for highly specific CTSS activity detection in mouse samples[42]. This method is a simple standard enzymatic assay detecting a time-dependent increase in fluorescence intensity caused by cleaving of the peptidyl sequence. It is easy-to-perform, time-saving and can be used for high-throughput applications. Additionally, a standard curve using free aminomethyl coumarin can be created allowing for the detection of specific enzymatic activities within a tested sample which is a big advantage over ABPs. The oligopeptidyl substrate we use was initially published as being suitable for highly specific detection of CTSS activity in human antigen presenting cells[43]. However, we could demonstrate that is also suitable for mouse samples. The substrate, Mca-GRWPPMGLPWE-Lys(Dnp)-DArg-NH_2 (PMGLP) was shown to be cleaved specifically by murine CTSS at a pH of 7.5 with no other murine cathepsin contributing to substrate cleaving in cell lysates[42]. The obtained results were easily quantifiable and highly reproducible as demonstrated in mouse bone marrow derived dendritic cells that were differentiated from the bone marrow of different individuals. The presented method therefore delivers specific CTSS activities and only requires a phosphate buffer system and a fluorescence compatible heatable photometer making the application attractive for less specialized laboratories.

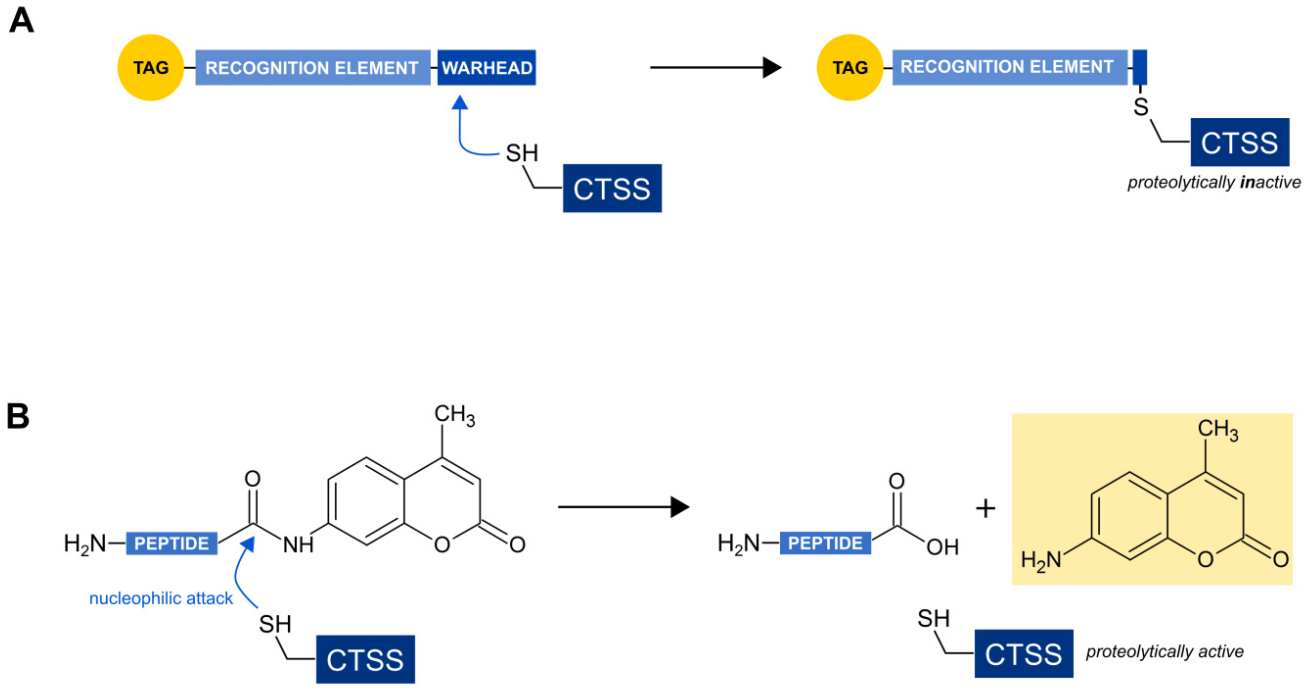

Figure 1: Functional comparison of the two major classes of probes for direct CTSS activity detection

(a) activity based probes (ABPs): The so-called warhead covalently links the probe with CTSS, leading to the inhibition of its enzymatic activity. The recognition element supports the specificity for CTSS alone or some related cysteine cathepsins. The tag allows for later detection of the tagged enzymes.

(b) substrate based probes (SBPs): The thiol group at the active site of CTSS nucleophilically attacks the peptide bond of the peptidyl substrate leading to a deliberation of the aminomethylcoumarin. The resulting change in the fluorogenic behaviour of free aminomethylcoumarin can then be detected in a fluorescent compatible photometer.

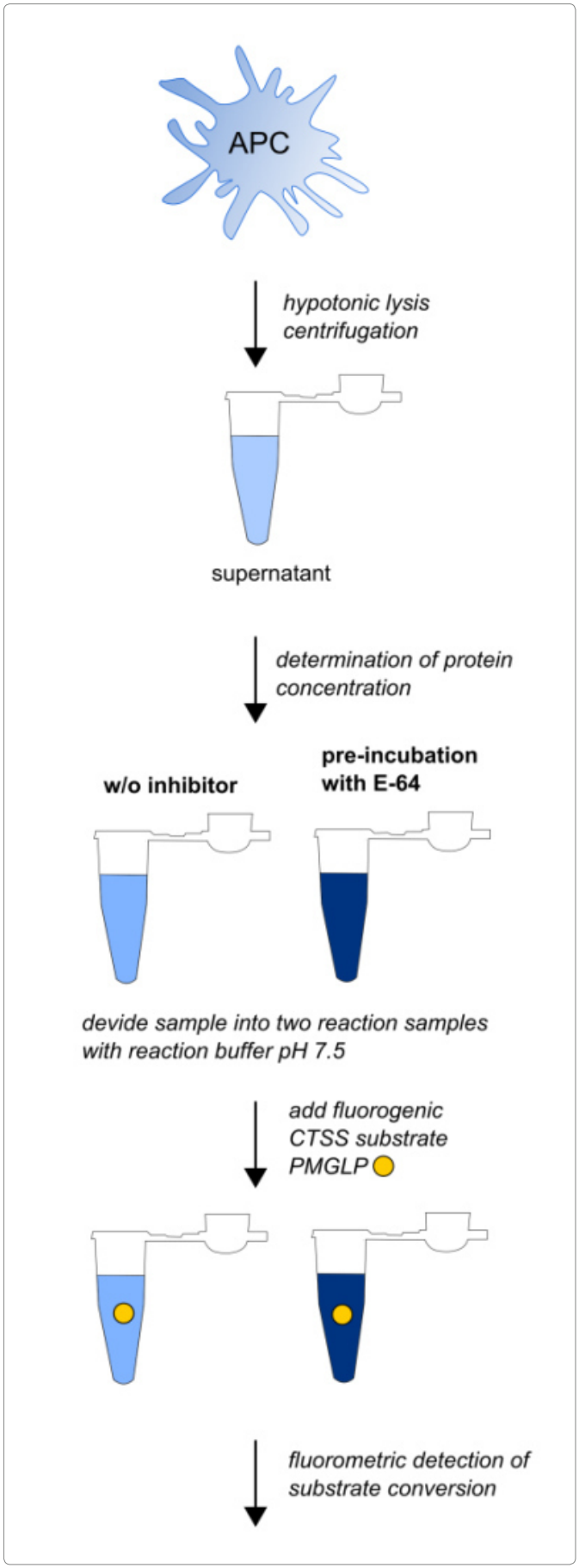

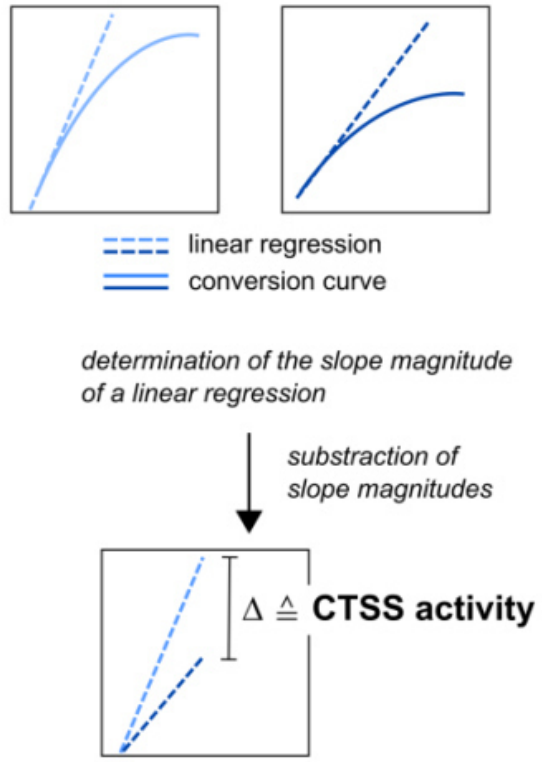

Figure 2: Experimental workflow for the detection of CTSS activities in mouse APC[42] (adapted from Steimle et al., 2016)

Cells of interest are lysed hypotonically followed by blast freezing in liquid nitrogen as described in materials and methods section. Supernatant is used for CTSS activity detection. Out of each sample, two reaction samples containing the same amount of whole cell protein are created. The first sample contains the fluorogen substrate, the second both, the substrate and the cathepsin inhibitor E-64. Reaction buffer provides a pH of 7.5 to minimize false positive substrate conversion caused by other cathepsins. Substrate conversion is monitored for 60 min at 37 °C. A linear regression at the very beginning of the sigmoidal conversion curve is performed for both reaction samples. The slope magnitude of this linear regression is equivalent to the substrate conversion per time unit. The difference in the slope magnitude of both reaction samples is equivalent to the CTSS activity in the sample the lysate was taken from. CTSS activities can therefore be expressed as the difference of fluorescence intensity per µg cell protein and time unit, i.e. ΔAU min-1 µg-1.

We recommend the following simple workflow (Figure 2): the target cells are lysed hypotonically with the support of freezing in liquid nitrogen. This guarantees a minimal loss of CTSS activity due to cell lysis. Protein concentrations of the lysates are determined afterwards and each sample is separated into two samples. The first one contains the substrate, PMGLP, and the second one PMGLP and E-64, a cysteine cathepsin inhibitor that is easily commercially available and cheap. The latter sample is used as a negative control. Substrate conversion is detected for at least 20 min at 37°C by detection of fluorescence increase at 405 nm after excitation at 340 nm. Conversion rates are computed

by determination of the slopes of the linear fluorescence increase and the slope of the inhibitor treated negative control is substracted from the slope of the non-inhibitor treated sample. This workflow is fast and the obtained results are highly specific for murine CTSS as demonstrated in our published protocol[42]. We therefore hope to contribute to a progress in CTSS related research.

Acknowledgements

Work was supported by the DFG (DFG FR 2087/6-1, DFG FR 2087/8-1, CRC685, SPP1656), the Bundesministerium für Bildung and Forschung (BMBF) and the German Centre for Infection Research (DZIF)

References

1. Beers C, Burich A, Kleijmeer MJ, Griffith JM, Wong P, Rudensky AY. Cathepsin S controls MHC class II-mediated antigen presentation by epithelial cells in vivo. J Immunol. 2005;174(3):1205-12.
2. Hamm-alvarez SF, Janga SR, Edman MC, et al. Tear cathepsin S as a candidate biomarker for Sjögren's syndrome. Arthritis Rheumatol. 2014;66(7):1872-81.
3. Figueiredo JL, Aikawa M, Zheng C, et al. Selective cathepsin S inhibition attenuates atherosclerosis in apolipoprotein E-deficient mice with chronic renal disease. Am J Pathol. 2015;185(4):1156-66.
4. Schönefuss A, Wendt W, Schattling B, et al. Upregulation of cathepsin S in psoriatic keratinocytes. Exp Dermatol. 2010;19(8):e80-8.
5. Baugh M, Black D, Westwood P, et al. Therapeutic dosing of an orally active, selective cathepsin S inhibitor suppresses disease in models of autoimmunity. J Autoimmun. 2011;36(3-4):201-9.
6. Weldon S, Mcnally P, Mcauley DF, et al. miR-31 dysregulation in cystic fibrosis airways contributes to increased pulmonary cathepsin S production. Am J Respir Crit Care Med. 2014;190(2):165-74.
7. Baxter AG. The origin and application of experimental autoimmune encephalomyelitis. Nat Rev Immunol. 2007;7(11):904-12.
8. Beck H, Schwarz G, Schröter CJ, et al. Cathepsin S and an asparagine-specific endoprotease dominate the proteolytic processing of human myelin basic protein in vitro. Eur J Immunol. 2001;31(12):3726-36.
9. Nagai A, Murakawa Y, Terashima M, et al. Cystatin C and cathepsin B in CSF from patients with inflammatory neurologic diseases. Neurology. 2000;55(12):1828-32.
10. Staun-ram E, Miller A. Cathepsins (S and B) and their inhibitor Cystatin C in immune cells: modulation by interferon-β and role played in cell migration. J Neuroimmunol. 2011;232(1-2):200-6.
11. Bever CT, Garver DW. Increased cathepsin B activity in multiple sclerosis brain. J Neurol Sci. 1995;131(1):71-3.
12. Haves-zburof D, Paperna T, Gour-lavie A, Mandel I, Glass-marmor L, Miller A. Cathepsins and their endogenous inhibitors cystatins: expression and modulation in multiple sclerosis. J Cell Mol Med. 2011;15(11):2421-9.
13. Fissolo N, Kraus M, Reich M, et al. Dual inhibition of proteasomal and lysosomal proteolysis ameliorates autoimmune central nervous system inflammation. Eur J Immunol. 2008;38(9):2401-11.
14. Sevenich L, Bowman RL, Mason SD, et al. Analysis of tumour- and stroma-supplied proteolytic networks reveals a brain-metastasis-promoting role for cathepsin S. Nat Cell Biol. 2014;16(9):876-88.
15. Verdoes M, Edgington LE, Scheeren FA, et al. A nonpeptidic cathepsin S activity-based probe for noninvasive optical imaging of tumor-associated macrophages. Chem Biol. 2012;19(5):619-28.
16. Hook V, Toneff T, Bogyo M, et al. Inhibition of cathepsin B reduces beta-amyloid production in regulated secretory vesicles of neuronal chromaffin cells: evidence for cathepsin B as a candidate beta-secretase of Alzheimer's disease. Biol Chem. 2005;386(9):931-40.
17. Hook V, Schechter I, Demuth HU, Hook G. Alternative pathways for production of beta-amyloid peptides of Alzheimer's disease. Biol Chem. 2008;389(8):993-1006.
18. Schechter I, Ziv E. Cathepsins S, B and L with aminopeptidases display β-secretase activity associated with the pathogenesis of Alzheimer's disease. Biol Chem. 2011;392(6):555-69.
19. Poeck B, Strauss R, Kretzschmar D. Analysis of amyloid precursor protein function in Drosophila melanogaster. Exp Brain Res. 2012;217(3-4):413-21.
20. Zhao P, Lieu T, Barlow N, et al. Cathepsin S causes inflammatory pain via biased agonism of PAR2 and TRPV4. J Biol Chem. 2014;289(39):27215-34.
21. Cattaruzza F, Lyo V, Jones E, et al. Cathepsin S is activated during colitis and causes visceral hyperalgesia by a PAR2-dependent mechanism in mice. Gastroenterology. 2011;141(5):1864-74.e1-3.
22. Reddy VB, Sun S, Azimi E, Elmariah SB, Dong X, Lerner EA. Redefining the concept of protease-activated receptors: cathepsin S evokes itch via activation of Mrgprs. Nat Commun. 2015;6:7864.
23. Reddy VB, Shimada SG, Sikand P, Lamotte RH, Lerner EA. Cathepsin S elicits itch and signals via protease-activated receptors. J Invest Dermatol. 2010;130(5):1468-70.
24. Turk B. Targeting proteases: successes, failures and future prospects. Nat Rev Drug Discov. 2006;5(9):785-99.
25. Turk V, Stoka V, Vasiljeva O, et al. Cysteine cathepsins: from structure, function and regulation to new frontiers. Biochim Biophys Acta. 2012;1824(1):68-88.
26. Choe Y, Leonetti F, Greenbaum DC, et al. Substrate profiling of cysteine proteases using a combinatorial peptide library identifies functionally unique specificities. J Biol Chem. 2006;281(18):12824-32.
27. Serim S, Haedke U, Verhelst SH. Activity-based probes for the study of proteases: recent advances and developments. ChemMedChem. 2012;7(7):1146-59.
28. Veilleux A, Black WC, Gauthier JY, et al. Probing cathepsin S activity in whole blood by the activity-based probe BIL-DMK: cellular distribution in human leukocyte populations and evidence of diurnal modulation. Anal Biochem. 2011;411(1):43-9.
29. Ben-aderet L, Merquiol E, Fahham D, et al. Detecting cathepsin activity in human osteoarthritis via activity-based probes. Arthritis Res Ther. 2015;17:69.
30. Oresic bender K, Ofori L, Van der linden WA, et al. Design of a highly selective quenched activity-based probe and its application in dual color imaging studies of cathepsin S activity localization. J Am Chem Soc. 2015;137(14):4771-7.
31. Barlow N, Nasser Y, Zhao P, et al. Demonstration of elevated levels of active cathepsin S in dextran sulfate sodium colitis using a new activatable probe. Neurogastroenterol Motil. 2015;27(11):1675-80.
32. Hughes CS, Shaw G, Burden RE, Scott CJ, Gilmore BF. The application of a novel, cell permeable activity-based probe for the detection of cysteine cathepsins. Biochem Biophys Res Commun. 2016;472(3):444-50.
33. Mertens MD, Schmitz J, Horn M, et al. A coumarin-labeled vinyl sulfone as tripeptidomimetic activity-based probe for cysteine cathepsins. Chembiochem. 2014;15(7):955-9.
34. Garenne T, Saidi A, Gilmore BF, et al. Active site labeling of cysteine cathepsins by a straightforward diazomethylketone probe derived from the N-terminus of human cystatin C. Biochem Biophys Res Commun. 2015;460(2):250-4.

35. Caglič D, Repnik U, Jedeszko C, et al. The proinflammatory cytokines interleukin-1α and tumor necrosis factor α promote the expression and secretion of proteolytically active cathepsin S from human chondrocytes. Biol Chem. 2013;394(2):307-16.

36. Kohl F, Schmitz J, Furtmann N, et al. Design, characterization and cellular uptake studies of fluorescence-labeled prototypic cathepsin inhibitors. Org Biomol Chem. 2015;13(41):10310-23.

37. Castellano J, Badimon L, Llorente-cortés V. Amyloid-β increases metallo- and cysteine protease activities in human macrophages. J Vasc Res. 2014;51(1):58-67.

38. Magister S, Obermajer N, Mirković B, et al. Regulation of cathepsins S and L by cystatin F during maturation of dendritic cells. Eur J Cell Biol. 2012;91(5):391-401.

39. Schwarz G, Boehncke WH, Braun M, et al. Cathepsin S activity is detectable in human keratinocytes and is selectively upregulated upon stimulation with interferon-gamma. J Invest Dermatol. 2002;119(1):44-9.

40. Balce DR, Allan ER, Mckenna N, Yates RM. γ-Interferon-inducible lysosomal thiol reductase (GILT) maintains phagosomal proteolysis in alternatively activated macrophages. J Biol Chem. 2014;289(46):31891-904.

41. Katritzky AR, Cusido J, Narindoshvili T. Monosaccharide-based water-soluble fluorescent tags. Bioconjug Chem. 2008;19(7):1471-5.

42. Steimle A, Kalbacher H, Maurer A, et al. A novel approach for reliable detection of cathepsin S activities in mouse antigen presenting cells. J Immunol Methods. 2016;432:87-94.

43. Lützner N, Kalbacher H. Quantifying cathepsin S activity in antigen presenting cells using a novel specific substrate. J Biol Chem. 2008;283(52):36185-94.

Journal of Autoimmunity xxx (2016) 1–14

Contents lists available at ScienceDirect

Journal of Autoimmunity

journal homepage: www.elsevier.com/locate/jautimm

Symbiotic gut commensal bacteria act as host cathepsin S activity regulators

Alex Steimle [a, 1], Kerstin Gronbach [a, 1], Brigitte Beifuss [a], Andrea Schäfer [a], Robin Harmening [a], Annika Bender [a], Jan Kevin Maerz [a], Anna Lange [a], Lena Michaelis [a], Andreas Maurer [c], Sarah Menz [a], Kathy McCoy [d], Ingo B. Autenrieth [a], Hubert Kalbacher [b], Julia-Stefanie Frick [a, *]

[a] Institute of Medical Microbiology and Hygiene, University of Tübingen, Tübingen, Germany
[b] Interfacultary Institute of Biochemistry, Universitiy of Tübingen, Tübingen, Germany
[c] Institute of Radiology, Werner Siemens Imaging Center, Department of Preclinical Imaging and Radiopharmacy, University of Tübingen, Tübingen, Germany
[d] Department of Clinical Reasearch, Gastroenterology, University of Bern, Bern, Switzerland

ARTICLE INFO

Article history:
Received 7 January 2016
Received in revised form
14 July 2016
Accepted 21 July 2016
Available online xxx

Keywords:
Inflammatory bowel disease
Cathepsin S
Microbiota
Immunotherapy
Protease regulation
Autoimmune disease

ABSTRACT

Cathepsin S (CTSS) is a lysosomal protease whose activity regulation is important for MHC-II signaling and subsequent activation of $CD4^+$ T cell mediated immune responses. Dysregulation of its enzymatic activity or enhanced secretion into extracellular environments is associated with the induction or progression of several autoimmune diseases. Here we demonstrate that commensal intestinal bacteria influence secretion rates and intracellular activity of host CTSS and that symbiotic bacteria, i.e. *Bacteroides vulgatus* mpk, may actively regulate this process and help to maintain physiological levels of CTSS activities in order to prevent from induction of pathological inflammation. The symbiont-controlled regulation of CTSS activity is mediated by anticipating reactive oxygen species induction in dendritic cells which, in turn, maintains cystatin C (CysC) monomer binding to CTSS. CysC monomers are potent endogenous CTSS inhibitors. This *Bacteroides vulgatus* caused and CysC dependent CTSS activity regulation is involved in the generation of tolerant intestinal dendritic cells contributing to prevention of T-cell mediated induction of colonic inflammation. Taken together, we demonstrate that symbionts of the intestinal microbiota regulate host CTSS activity and secretion and might therefore be an attractive approach to deal with CTSS associated autoimmune diseases.

1. Introduction

Cathepsin S (CTSS) is a lysosomal single-chain protease that is expressed in professional antigen-presenting cells (APC) like macrophages, dendritic cells (DC) [1] and B cells as well as in non-professional APC like intestinal epithelial cells [2]. It belongs to the papain-like cysteine protease family that comprises eleven members in humans [3]. It is mainly involved in the stepwise degradation of the MHC-II associated chaperone invariant chain (Ii) [4]. These proteolytic events are crucial for the loading of antigen-derived peptides on MHC-II and the subsequent transport of this MHC-II-peptide complex to the APC surface where it promotes $CD4^+$ T cell activation [5]. CTSS activity can be influenced by transcriptional and post-translational regulation or by protein-protein-interaction with endogenous inhibitors, mainly cystatins [6]. However, there are contradictory reports on cystatin-mediated CTSS activity regulation [7–10]. Though, adequate regulation of CTSS is necessary to retain the steady state of $CD4^+$ T cell dependent immune responses. In fact, dysregulation of CTSS activity, expression or secretion into the extracellular space is associated with the pathogenesis of various autoimmune diseases (AID), i.e. arthritis [11,12], type-I-diabetes [13], Sjögren's syndrome [14,15], multiple sclerosis [8,16] and atherosclerosis [17,18]. Furthermore, CTSS secretion contributes to pain induction during inflammatory bowel disease (IBD) [19], another example of AID.

* Corresponding author. Institute of Medical Microbiology and Hygiene, University of Tübingen, Elfriede-Aulhorn-Str.6, D-72076 Tübingen, Germany.
E-mail address: julia-stefanie.frick@med.uni-tuebingen.de (J.-S. Frick).
[1] Both authors contributed equally to this work.

http://dx.doi.org/10.1016/j.jaut.2016.07.009
0896-8411/

Due to the implications of CTSS dysregulation for the pathogenesis of AID, there is an intense search ongoing for the development of drugs that are able to specifically inhibit CTSS proteolytic activity [20]. Eventually, we demonstrate that an alteration of the gut microbiota composition can contribute to host CTSS regulation and that the microbiota composition itself could be decisive to control host CTSS secretion and activity, hence chemical treatment might not be necessary. As most autoimmune diseases are associated with dysbiosis of the intestinal microbiota [21], we compared effects of symbiotic or pathobiotic commensals on host CTSS activities and protein levels *in vivo* and *in vitro*. *Bacteroides vulgatus* mpk could already be demonstrated to be a symbiotic bacteria, mediating anti-inflammatory effects [22–24] which are directly associated with the induction of a tolerant DC phenotype termed semi-mature [23–25].

Here we demonstrate that in an experimental mouse model for $CD4^+$ T cell mediated colitis, *B. vulgatus* mpk promotes maintenance of the immune equilibrium via regulation of CTSS activity and secretion. We further provide evidence, that this regulation is mediated by altering cystatin C binding behaviour to CTSS through controlling intracellular levels of reactive oxygen species. This intestinal microbiota triggered CTSS regulation might deliver new possibilities for the treatment of other CTSS dysregulation-associated AID in general.

2. Materials and methods

2.1. T cell mediated induction of chronic colitis in *Rag1*$^{-/-}$ mice

Germfree (GF) or conventionally colonized (CV) C57BL/6J-Rag1^{tm1Mom} (*Rag1*$^{-/-}$) mice were transplanted with 5×10^5 splenic $CD4^+CD62L^+CD45RB^{hi}$ *wt* T cells at 8–10 weeks of age. The conventional microbiota (CV) was free of Norovirus, Rotavirus and *Helicobacter hepaticus*. *Rag1*$^{-/-}$ mice were kept under SPF conditions and analyzed after 4–8 weeks after T cell transplantation as indicated in the results section.

2.2. Administration of cathepsin S inhibitor into *Rag1*$^{-/-}$ mice

Cathepsin S Inhibitor LY3000328 was purchased from ApexBio. The lyophilized powder was reconstituted in 83% (v/v) NaCl (0.9%), 12% (v/v) DMSO and 5% (v/v) Tween-20 to obtain a concentration of 0.5 mg mL^{-1}200 μL suspension was administered daily by intraperitoneal injection in order to obtain an amount of 100 μg Cathepsin S inhibitor per dose. The inhibitor was started to be administered three days before T cell transplantation and was continued to be administered for 21 days after T cell transplantation.

2.3. Determination of cathepsin S activities in BMDC lysates

Cathepsin S activity assays of differentially stimulated bone marrow derived dendritic cells were performed as described previously [26,27]. using the fluorogenic substrate Mca-GRWPPMGLPWEK (Dnp)-D-Arg-NH_2 (abbreviated as PMGLP). Determined activities in stimulated samples were normalized to the activities detected in unstimulated control samples generated from the same individual.

2.4. Cultivation of bone marrow derived dendritic cells (BMDCs)

Bone marrow cells were isolated and cultivated as described previously [28]. At day 7 after isolation, resulting CD11c positive bone marrow derived dendritic cells (BMDCs) were used for *in vitro* experiments.

2.5. Stimulation of bone marrow derived dendritic cells

2×10^6 BMDCs were stimulated with either PBS or *B. vulgatus* mpk or *E. coli* mpk at a MOI of 1. Cells were stimulated for a maximum of 24 h. If a second challenge was used, cells were stimulated with bacteria followed by exchanging used for fresh medium and by challenging the cells with a second stimulus for a maximum of 16 h. PBS was used as mock stimulation control.

2.6. Cytokine analysis by ELISA

For analysis of cathepsin S concentrations in cell culture supernatants or blood serum of mice, the CTSS ELISA Kit purchased from Cusabio Biotech was used according to the manufacturer's instructions.

2.7. Flow cytometrical analysis

Multi-color FCM analyses were performed on a FACS Calibur or FACS LSRII (BD Biosciences). All fluorochrome-coupled antibodies were purchased from BD Biosciences. Data were analyzed using the FlowJo software (Tree Star Inc., USA).

2.8. Western blotting

For western blot analysis of MHC class II bound invariant chain and, cystatin C, cathepsin S and the MHC-II bound CLIP fragment, cells were lysed using 10 μL lysis buffer (50 mM Tris/HCl pH 7.6, 150 mM NaCl, 0.5% (v/v) NP40, 1× Roche Complete Protease Inhibitor, 0.4 mM DTT) per 10^6 cells. Non lysed cell components were removed by centrifugation at 12'000*g*. Concentration of solubilized proteins in the resulting supernatant was measured using a commercial BCA Kit (ThermoScientific). A total of 50 μg was transferred on polyacrylamide gels containing 8%–12% polyacrylamide depending on the protein to be detected. Since MHC-II-invariant chain heterotrimers are stable in SDS solutions but sensitive towards heating, samples were usually not heated before electrophoretic separation. Proteins were separated via SDS-PAGE gels and transferred to nitrocellulose membranes. Membranes were blocked subsequently for 1 h at room temperature in a BSA containing blocking buffer (LiCor) followed by incubation with primary Abs diluted 1:1000 in blocking buffer over night at 4 °C. After incubation the membranes were washed three times in PBS/T (PBS pH 7.4 + 0.1% Tween-20) and were subsequently incubated with fluorochrome coupled secondary antibodies (LiCor) according to the manufacturer's instruction for 2 h at room temperature. After repeating the washing step with PBS/T the membranes were washed twice with PBS to remove detergent from the membranes. Proteins were detected using the LiCor visualization system. Before using β-actin (mouse anti-mouse β-actin; Sigma) as a control for protein loading, the blots were stripped for 20 min with 10 mL stripping solution (10 mM NaOH, 250 mM guanidinium chloride).

2.9. Purification of RNA and quantitative real-time PCR

Purification of RNA from BMDCs lysates was performed using Qiagen's RNeasy Mini Kit according to the manufacturer's instructions. Additional DNA digestion was conducted by using 4 U rDNase I and 40 U rRNasin for a RNA solution of 0.1 μg μL^{-1}. After 30 min of incubation at RT, DNase was inactivated using Ambion DNase inactivation reagent which was later removed by centrifugation for 1 min at 10'000*g*. SybrGreen based quantitative RT-PCR was performed on a Roche LightCycler480 using QiagenSybrGreen RT-PCR Kit. Primer annealing occured at 60 °C. 10–100 ng

Please cite this article in press as: A. Steimle, et al., Symbiotic gut commensal bacteria act as host cathepsin S activity regulators, Journal of Autoimmunity (2016), http://dx.doi.org/10.1016/j.jaut.2016.07.009

DNA-digested RNA was used for qRT-PCR. Relative mRNA expression in BMDCs stimulated with bacteria to unstimulated BMDCs was determined with using β-actin as housekeeping gene using the ΔΔCp-method that included the specific amplification efficiency of every used primer pair and each PCR run.

2.10. Co-immunoprecipitation and mass spectrometrical analysis

For immunoprecipitation assays we used between 2 and 3×10^7 BMDCs and stimulated them with either PBS, *B. vulgatus* mpk MOI1 or *E. coli* mpk MOI1. Cells were harvested after 16 h of stimulation, counted and lysed using 200 μL lysis buffer (50 mM Tris/HCl pH 7.4, 150 mM NaCl, 1 mM EDTA, 1% Nonident P-40, Roche Complete Protease Inhibitor and Phosphatase Inhibitor) for 1×10^7 cells. Non-lysed structures were then separated by centrifugation for 10 min at 1000*g*. Protein concentration was measured in each lysate and the same protein amount was used for IPs in all samples that were directly compared to each other. 10 μg anti-mouse cystatin C antibody (R&D) was coupled to Protein-G coupled Sepharose magnetic beads (Dynabeads, Invitrogen) that were diluted in 600 μL PBS + 0.1% Tween-20 and incubated for 10 min at RT. After washing steps, cell lysate was added and incubated for another 10 min at RT. After additional washing steps using PBS +0.1% Tween-20, bound proteins were removed from the beads using 0.1 M glycine pH 2.5 and afterwards neutralized using 1 M Tris/HCl pH 8.0. MS analysis was performed at the Proteome Center, Tübingen, Germany. CoIP samples were loaded on an SDS gel using a non-reducing loading buffer. After electrophoretic separation, SDS gels were silver stained using SilverStain Plus Kit from BioRad. Each lane of a silver stained SDS gel was cut into 7 pieces and subsequently tryptically digested. Following analysis was performed using a LTQ-Oribitrap XL mass spectrometer.

2.11. Isolation of lamina propria (LP) dendritic cells (DC) and T cells and adoptive transfer of T cells

Isolation of LP cells was performed as published previously [29]. For adoptive transfer, splenic $CD4^+$ T cells from C57BL/6 mice were purified using a MACS-based negative selection kit (Miltenyi) according to the manufacturer's instructions. The isolated cells were stained for CD3ε, CD4 and CD62 for reanalysis, purity was generally >90% with >80% being $CD4^+CD62L^+CD45RB^{hi}$. 5×10^5 $CD4^+$ T cells were injected into the peritoneum (i.p.) of *Rag1*$^{-/-}$ mice as described previously [30].

2.12. Detection of intracellular ROS formation

Intracellular formation of ROS was measured using a kit purchased by Enzo LifeScience and was performed according to manufacturer's instruction. ROS formation was detected by flow cytometry, in which fluorescence intensity in the FITC channel is directly proportional to the amount of intracellular ROS. Median fluorescence intensities (MFI) of bacterially stimulated cells were normalized to MFIs of unstimulated control cells derived from the same individual.

2.13. Histology

Colonic tissues were fixed in neutral buffered 4% formalin. Formalin-fixed tissues were embedded in paraffin and cut into 2 μm sections. They were stained with hematoxylin (Merck) and eosin (Merck) for histological scoring. Scoring was conducted in a blinded fashion on a validated scale of 0–3, weith 0 representing no inflammation and 3 representing severe inflammation characterized by infiltration with inflammatory cells, crypt hyperplasia, loss of goblet cells and distortion of architecture [31].

2.14. Statistics

Statistical analyses were performed using the unpaired student's *t*-test to compare two groups with each other. For comparing *in vitro* results, samples were considered to be biologically independent if the samples were generated from BMDCs from different mice. Differences were considered to be statistically significant if $p < 0.05$. Error bars, if shown, represent ± standard deviation (SD).

2.15. Bacteria

The bacteria used for stimulation of the murine dendritic cells were *Escherichia coli* mpk and *Bacteroides vulgatus* mpk. The *E. coli* mpk strain was grown in Luria-Bertani (LB) medium under aerobic conditions at 37 °C. *Bacteroides vulgatus* was grown in Brain-Heart-Infusion (BHI) medium and anaerobic conditions at 37 °C.

2.16. Mice

C57BL/6J mice were purchased from Charles River Laboratories. Cathepsin S-deficient (*Ctss*$^{-/-}$) mice were provided by the lab of Thomas Reinheckel, University of Freiburg, Germany. Cystatin C-deficient (*Cst3*$^{-/-}$) mice were handed over by the lab of Mathias Jucker, Hertie Institute Tübingen, Germany and had initially been created in the lab of Anders Grubb, University of Lund, Sweden. *Ctss*$^{-/-}$ mice were obtained by mating *Ctss*$^{+/-}$ animal parents. Resulting *Ctss*$^{+/+}$ pups were used as *wt* controls. *Cst3*$^{-/-}$ mice were paired with wt 129S2/SvPasCrl mice purchased from Charles River Laboratories. Resulting *Cst3*$^{+/-}$ pups were mated and resulting *Cst3*$^{-/-}$ mice from the F2 generation were used for the experiments. *Cst3*$^{+/+}$ littermates served as *wt* controls. All animals were kept and bred under SPF conditions. For isolation of bone marrow, only female mice aged 6–12 weeks were used. Animal experiments were reviewed and approved by the responsible institutional review committee and the local authorities in Germany and Switzerland.

3. Results

Monocolonization with *B. vulgatus* mpk induces DC tolerance and does not promote proliferation of transplanted T cells in *Rag1*$^{-/-}$ mice.

It is known that apathogenic commensal bacteria can have either symbiotic or pathobiotic properties concerning the activation of the immune system. In previous work, we identified symbiotic *B. vulgatus* mpk which protects *Il2*$^{-/-}$ mice from induction of colitis, hence promoting the immunological equilibrium, whereas pathobiont *E. coli* mpk promotes induction of colitis, thus featuring pathobiotic effects [23,24]. Likewise, in IBD patients, *Bacteroidetes* proportions in the intestine are decreased while *Enterobactericeae* proportions are enhanced [32,33]. Therefore, we consider *B. vulgatus* mpk and *E. coli* mpk to represent adequate symbiotic and pathobiotic model organisms. Thus, we wanted to elucidate the distinct T cell activation potential of these two model organisms. In order to investigate the microbiota dependent maturation of intestinal dendritic cells and the resulting activation and proliferation of naïve *wt* $CD4^+CD62L^+CD45RB^{hi}$ T cells, we used germfree (GF) *Rag1*$^{-/-}$ mice, lacking functional T cells and B cells, for monocolonization with either symbiotic *B. vulgatus* mpk or pathobiotic *E. coli* mpk and for cocolonization with both bacteria. Cocolonization resulted in efficient colonization with both *B. vulgatus* and *E. coli* in an almost 1:1 ratio (data not shown).

4 weeks after start of colonization 5×10^5 naïve wt

$CD4^+CD62L+CD45RBhi$ T cells were transplanted by i. p. injection. Eight weeks after T cell transfer, the phenotype and maturation state of lamina propria (LP) $CD11c^+$ cells and the proliferation of transplanted *wt* T cells were determined by flow cytometry (Fig. 1a). In earlier studies we could demonstrate that *B. vulgatus* mpk converts immature dendritic cells into a tolerant semi-mature phenotype *in vitro* as well as *in vivo* which prevents from T cell activation and induction of inflammation [22–24]. Here, we show that monocolonization of *Rag1*$^{-/-}$ mice with *B. vulgatus* mpk was associated with differentiation of LP $CD11c^+$ cells into a semi-mature phenotype as indicated by a low to intermediate expression of MHC-II and a low positive expression of CD40 (Fig. 1c and d). The presence of semi-mature cLP $CD11c^+$ cells in *B. vulgatus* mpk monocolonized *Rag1*$^{-/-}$ mice was associated with a reduced absolute cell count of $CD3^+CD4^+$ T cells in the cLP as compared to *E. coli* mpk monocolonized mice (Fig. 1b). The monocolonization of *Rag1*$^{-/-}$ mice with *E. coli* mpk resulted in an increased expression of MHC-II and CD40 on $CD11c^+$ cells in the cLP (Fig. 1c and d) and was associated with a higher amount of T cells in the cLP (Fig. 1b).

Cocolonization resulted in higher amounts of $CD3^+CD4^+$ T cells as well as in higher MHC-II and CD40 surface expression on colonic $CD11c^+$ cells compared to *B. vulgatus* monocolonized mice. However, all three parameters were significantly reduced compared to *E. coli* monocolonized mice, indicating an active immune regulating mechanism that prevents from *E. coli* mpk induced proliferation of $CD3^+CD4^+$ T cells.

In summary, it can be concluded that monocolonization with symbiotic *B. vulgatus* mpk induces tolerant semi-mature cLP DCs and does not promote T cell proliferation whereas monocolonization with pathobiotic *E. coli* mpk induces DC maturation and clearly promotes proliferation of transplanted T cells.

3.1. Cathepsin S regulation is crucial for tolerance of DCs in terms of MHC-II surface expression

Since the semi-mature phenotype of LP DCs, especially the MHC-II surface expression, plays a pivotal role for the observed prevention of T cell activation in *B. vulgatus* mpk monocolonized and *B. vulgatus* mpk and *E. coli* mpk cocolonized gnotobiotic mice, we had a closer look on the molecular mechanisms of semi-maturation *in vitro*. We generated bone marrow derived DCs which were stimulated with either *B. vulgatus* mpk or *E. coli* mpk with a MOI of 1. As published previously, the stimulation of BMDCs with *B. vulgatus* mpk resulted in a lower proportion of MHC-II high positive (MHC-II hi$^+$) $CD11c^+$ cells compared to stimulation with *E. coli* mpk. *B. vulgatus* mpk stimulation generally leads to a lower expression of CD40, CD80 and CD86 as well as lower expression of pro-inflammatory cytokines [22]. We generally consider PBS (mock) treated BMDCs to be immature (iDCs), *E. coli* mpk treated ones to be fully mature (mDCs) and *B. vulgatus* mpk stimulated BMDCs to be semi-mature (smDCs) with mDCs and smDCs reaching the maximum expression level after 16 h of stimulation (Fig. 2b). A characteristic feature of smDCs is the non-responsiveness towards further bacterial stimuli in terms of surface MHC-II expression [22] (Fig. 2c and d). This means, *B. vulgatus* mpk primed semi-mature BMDCs that were subsequently challenged with maturation-inducing *E. coli* mpk do not further upregulate MHC-II surface expression (Fig. 2d). The lysosomal protease cathepsin S (CTSS) is known to be crucial for the regulation of MHC-II transport from intracellular vesicles to the cell surface. In order figure out the role of CTSS on DC semi-maturation, especially on the non-responsiveness in terms of MHC-II surface expression, we used *Ctss*$^{-/-}$ BMDCs, primed them with either PBS, *B. vulgatus* mpk or

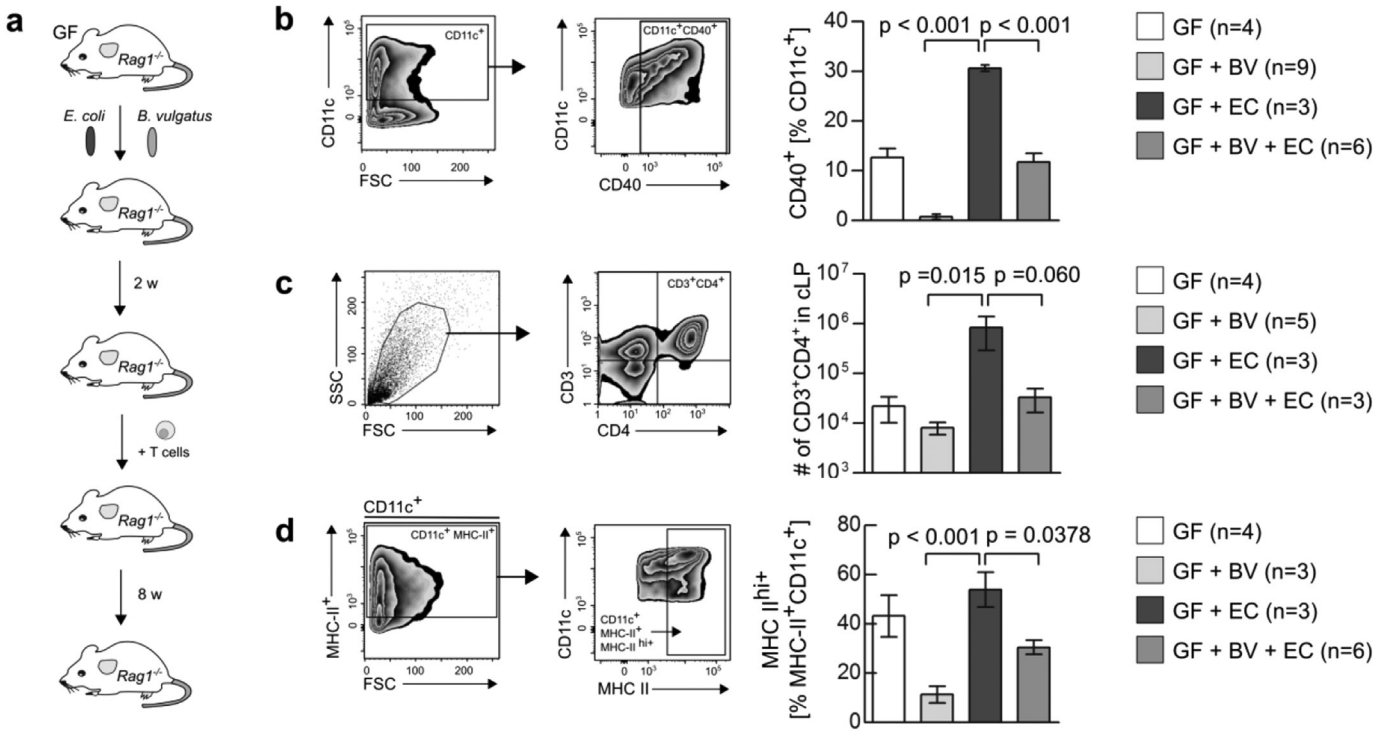

Fig. 1. *Bacteroides vulgatus* monocolonization of GF *Rag1*$^{-/-}$ mice protects from T cell activation. Germfree (GF) *Rag1*$^{-/-}$ mice were colonized with either *B. vulgatus* mpk (GF + BV), *E. coli* mpk (GF + EC) or a combination of *B. vulgatus* mpk and *E. coli* mpk (GF + BV + EC). After 2 weeks of colonization, *wt* $CD4^+CD62L^+CD45RB^{hi}$ T cells were transplanted. 8 weeks after T cell transplantation, mice were analyzed. (a) Overview over experimental setting (b + c + d) flow cytometry based analysis of T cells and $CD11c^+$ cells in the colonic lamina propria (cLP). Left panels demonstrate the used gating strategies. (b) proportion of $CD40^+$ cells of cLP $CD11c^+$ cells. (c) absolute cell count of repopulated $CD3^+CD4^+$ T cells in the cLP. (d) proportion of MHC II high positive (MHC II^{hi+}) cells among all MHC II^+CD11c^+ cLP cells. Statistical analysis was performed using student's *t*-test. Error bars represent SD. The number of replicates per group is indicated in the figure.

Please cite this article in press as: A. Steimle, et al., Symbiotic gut commensal bacteria act as host cathepsin S activity regulators, Journal of Autoimmunity (2016), http://dx.doi.org/10.1016/j.jaut.2016.07.009

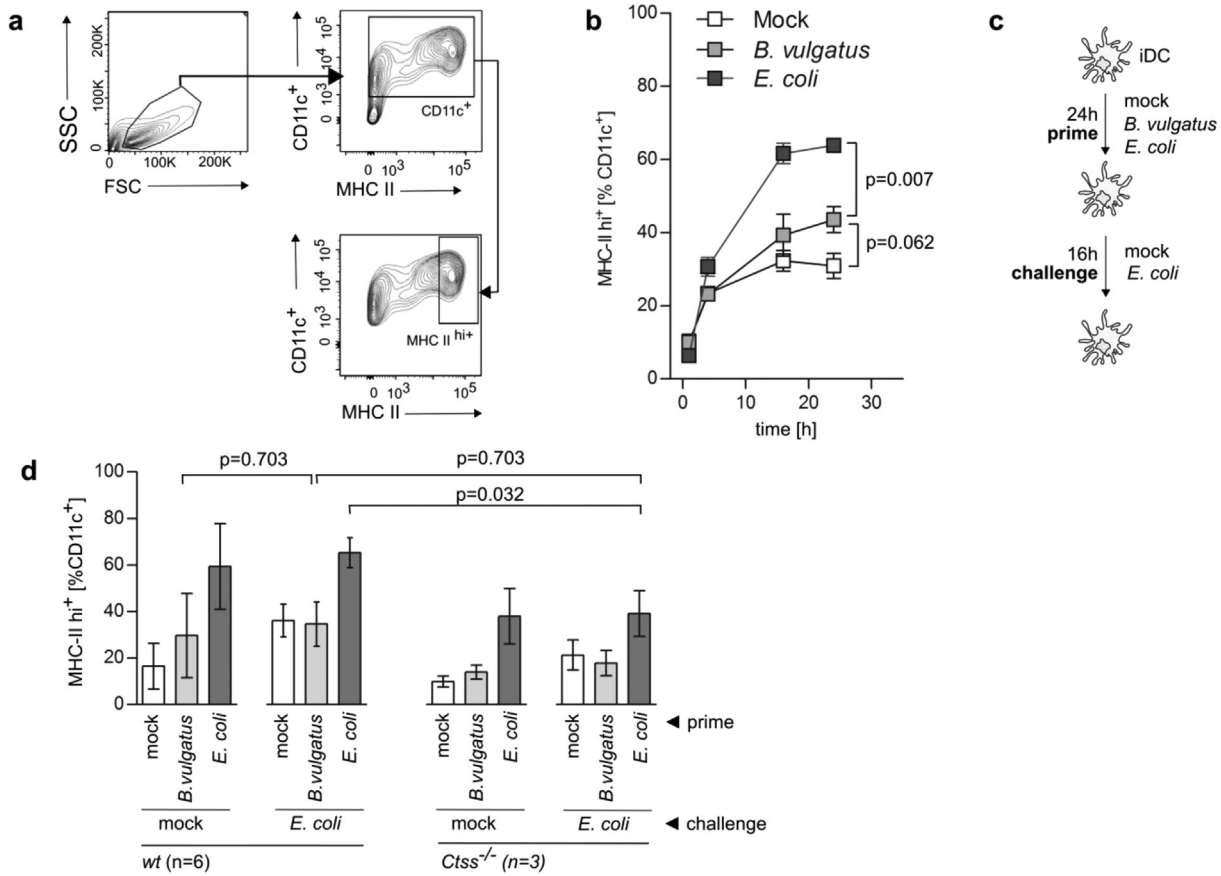

Fig. 2. Induction of dendritic cell semi-maturation is cathepsin S dependent. (a) Gating strategy for the determination of MHC class II high positive (MHC-II hi$^+$) bone marrow derived dendritic cells (BMDCs). CD11c-negative cells were outgated and the proportion of MHC-II hi$^+$ DCs within the population of CD11c$^+$ cells was determined as shown. (b) MHC class II hi$^+$ population of CD11c$^+$ BMDCs that were stimulated with PBS, *B. vulgatus* mpk or *E. coli* mpk for 1 h–24 h (n = 3 for each group). (c) Experimental setting for investigation of dendritic cell tolerance after induction of semi-maturation. BMDCs are primed for 24 h with either PBS (mock) to preserve an immature phenotype, *B. vulgatus* mpk to induce semi-maturation or *E. coli* mpk to induce BMDC maturation. After medium change, these cells were challenged for 16 h with either PBS (mock) as controls or *E. coli* mpk to investigate possible tolerance mechanisms. (d) MHC class II hi$^+$ population of *wt* and CTSS-deficient (*Ctss*$^{-/-}$) CD11c$^+$ BMDCs that were primed with PBS (mock), *B. vulgatus* mpk or *E. coli* mpk for 24 h and challenged with either PBS (mock) or *E. coli* mpk for 16 h. Number of replicates are indicated in the figure. All statistical analyses were performed using student's *t*-test. Error bars represent SD.

E. coli mpk for 24 h and challenged them afterwards with either PBS or *E. coli* mpk for 16 h (see experimental design in Fig. 2c). Final MHC-II surface expression was analyzed by flow cytometry and compared to MHC-II surface expression of equally treated *wt* BMDCs (Fig. 2d). *Ctss*$^{-/-}$ BMDCs generally provided decreased MHC-II surface expression compared to equally treated *wt* BMDCs. Though, *E. coli* mpk primed *Ctss*$^{-/-}$ BMDCs provide slightly enhanced surface MHC-II expression despite the loss of CTSS (Fig. 2d), indicating other possible MHC-II surface expression regulation mechanisms in these *Ctss*$^{-/-}$ BMDCs. However and importantly, the MHC-II surface expression level of these *E. coli* mpk primed and *E. coli* mpk challenged *Ctss*$^{-/-}$ BMDCs rather resembles the MHC-II expression level of *B. vulgatus* mpk primed and *E. coli* mpk challenged *wt* semi-mature BMDCs ($p = 0.703$). This clearly demonstrates the significance of CTSS activity control for the induction of tolerant semi-mature DCs. The CTSS deficiency did not influence other immunomodulatory mechanisms of dendritic cells since expression of pro-inflammatory cytokines and T cell co-stimulatory factors were not affected (see Supplementary Fig. S1).

3.2. Semi-mature DC show non-responsiveness concerning CTSS activity upon E. coli mpk challenge

The cleavage of the MHC-II bound Invariant chain (Ii) is one required event for the subsequent transport of the MHC-II protein complex to the cell surface, where MHC-II is essential for T cell activation. The invariant chain is expressed as two different splicing variants (Ii p31 and Ii p41) and is associated with the MHC-II heterodimer. The Ii cleavage includes several subsequent protease-catalyzed hydrolysis events. The last proteolytic cleavage generates CLIP out of the MHC-II bound invariant chain p10 fragment (MHC-II-Ii p10) and CLIP can then be replaced by exogenous protein-derived peptide fragments. This last hydrolysis event is a major regulation step for MHC-II transport to the surface of the cell. Since we detected different MHC-II surface expression in *B. vulgatus* mpk and *E. coli* mpk treated BMDCs, we also compared the amount of the intracellular MHC-II-Ii p10 heterotrimer as well as the Ii p31 and Ii p41 expression between *B. vulgatus* mpk and *E. coli* mpk stimulated bone marrow derived dendritic cells (BMDCs). *B. vulgatus* mpk stimulated smDCs displayed greater band intensity of MHC-II-Ii p10 than *E. coli* mpk-stimulated mDCs (Fig. 3a) suggesting less efficient MHC-II-Ii p10 cleaving in *B. vulgatus* mpk stimulated DC compared to *E. coli* mpk stimulated DC. This is in line with the observation that the amount of MHC-II-CLIP is also decreasing in *E. coli* mpk simulated BMDCs (Fig. 3b). The amount of non-cleaved Ii p31 was constant among all DC phenotypes (Fig. 3a) indicating that no differential protein expression of Ii occurs. We could also not detect any differences in mRNA expression of the *Cd74* gene, which encodes for the invariant chain (Ii) (Fig. 3c). Additionally, only the band ratio between the MHC-II-Ii p10

Please cite this article in press as: A. Steimle, et al., Symbiotic gut commensal bacteria act as host cathepsin S activity regulators, Journal of Autoimmunity (2016), http://dx.doi.org/10.1016/j.jaut.2016.07.009

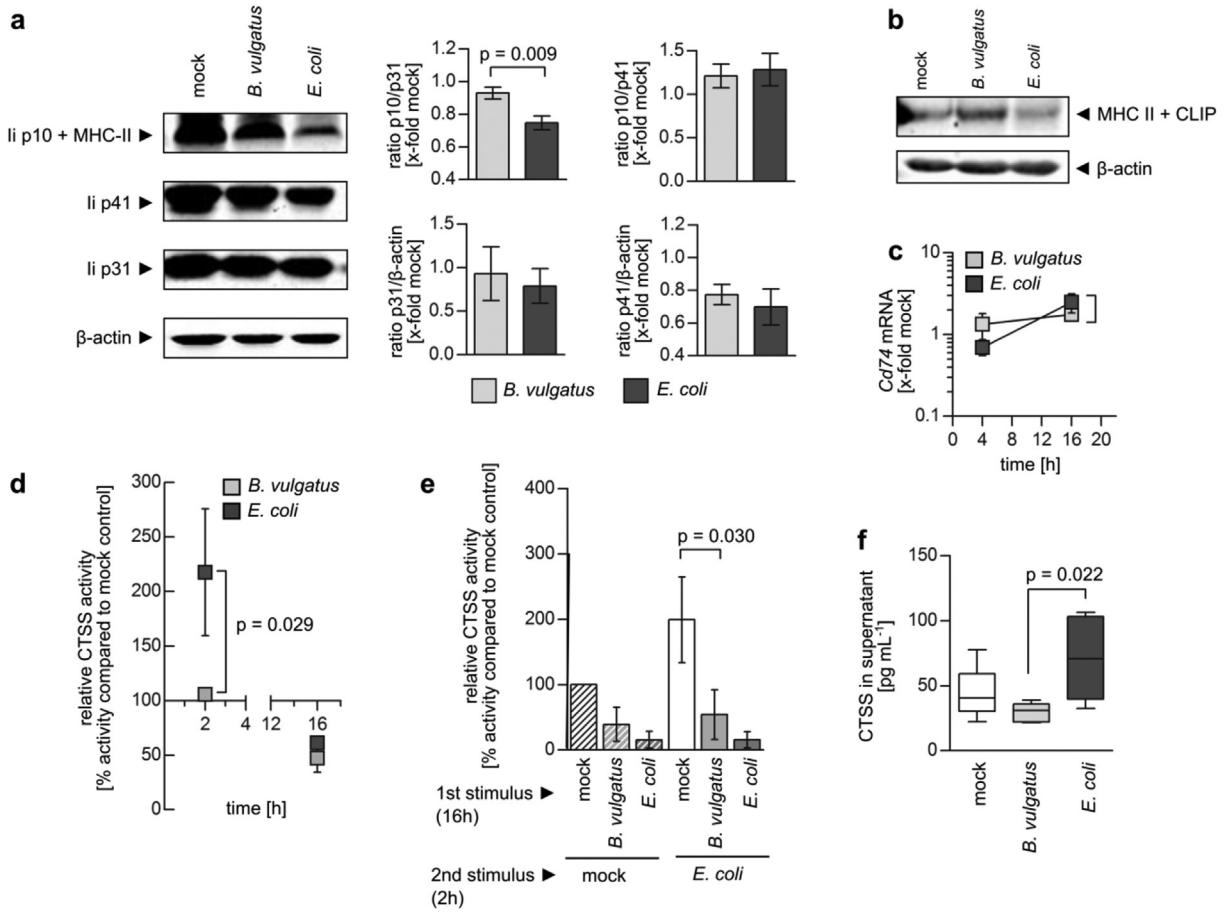

Fig. 3. *B. vulgatus* mpk prevents from CTSS activity increase in BMDCs. (a) *wt* BMDCs were stimulated for 20 h with either PBS (mock), *B. vulgatus* mpk or *E. coli* mpk. The amount of the MHC-II bound invariant chain p10 fragment (Ii p10 + MHC-II) was determined by western blotting (n = 8). One representative blot is shown in the left panel. The uncleaved invariant chain splicing variants Ii p31 and Ii p41 are also depicted. For validation of the assigned bands see Supplementary Fig. S3. Right panel: Quantification of the Western Blot Band using LiCor ImageStudio. The band intensities of p10 were normalized to p31 and p41, p31 and p41 band intensities were normalized to β-actin. The ratios were then normalized to the mock stimulated band ratios of BMDCs derived from the same individual (b) Western Blot of CLIP-loaded MHC-II of BMDCs that were stimulated for 20 h with either PBS (mock), *B. vulgatus* mpk or *E. coli* mpk. (c) mRNA expression of the *Cd74* gene encoding for the invariant chain in BMDCs that were stimulated with *B. vulgatus* mpk or *E. coli* mpk for 4 h and 16 h were determined and normalized on the expression of the PBS-stimulated mock control in BMDCs generated from the same individual (n = 3), (d) BMDCs were stimulated with either *B. vulgatus* mpk, *E. coli* mpk or PBS (mock) for 2 h and 16 h. CTSS activities were determined using PMGLP as a fluorogenic CTSS specific substrate as described. CTSS activities were normalized to the activity of the PBS-stimulated mock control in BMDCs generated from the same individual (n = 4). (e) CTSS activity determination of BMDCs that were primed (1st stimulus) with PBS (mock), *B. vulgatus* mpk or *E. coli* mpk for 16 h and challenged (2nd stimulus) with either PBS or *E. coli* mpk for 2 h (n = 4). (f) CTSS secretion into the cell supernatant of BMDCs that were stimulated for 16 h with *B. vulgatus* mpk, *E. coli* mpk or PBS (mock) was determined by ELISA (n = 5). The boxes represent the 25th to the 75th percentile, the whiskers indicate the lowest and highest single value. The line within the boxes represents the statistical median. All statistical analyses were performed using student's *t*-test. Error bars represent SD.

fragment compared to constantly expressed uncleaved monomeric Ii p31 is different (Fig. 3a). Therefore we suggested that the observed differences in MHC-II-Ii p10 amount is exclusively due to altered cathepsin S (CTSS) activity since CTSS is the only protease in dendritic cells that can generate the CLIP fragment out of Ii p10 [1]. Therefore we wanted to check if CTSS activity is also differentially regulated in *B. vulgatus* mpk stimulated smDCs compared to *E. coli* mpk stimulated mDCs which would explain the reduced cleaving of the invariant chain as well as the decreased expression of surface MHC-II (Fig. 2b and d). Furthermore, we wanted to elucidate if CTSS activity regulation contributes to non-responsiveness of *B. vulgatus* primed smDCs in terms of surface MHC-II expression. We could demonstrate that stimulation of BMDCs with *E. coli* mpk leads to a 2.2-fold increase of CTSS activity 2 h after bacterial encounter compared to stimulation with PBS (Fig. 3d). This increase in protease activity is followed by a decrease to about 50% of the activity of PBS treated BMDCs 16 h after stimulation (Fig. 3d). However, *B. vulgatus* mpk stimulated BMDCs do not provide a protease activity upregulation 2 h after stimulation. But, after 16 h of stimulation, the activity also decreases to about 50% activity of the PBS stimulated control sample (Fig. 3d). The loss of proteolytic activity after 16 h of *E. coli* mpk stimulation can – at least in part – be explained by the detected secretion of CTSS protein into the cell culture supernatant (Fig. 3f) after 16 h of stimulation. However, this could not be confirmed in *B. vulgatus* mpk treated samples and *B. vulgatus* mpk stimulation does not lead to increased CTSS secretion from BMDCs (Fig. 3f). Since the non-responsiveness towards subsequent bacterial stimuli is one of the key features of smDCs it was necessary to check for CTSS activities in *B. vulgatus* mpk primed and *E. coli* mpk challenged BMDCs. Therefore, we primed BMDCs with PBS, *B. vulgatus* mpk and *E. coli* mpk for 24 h to induce iDCs, smDCs and mDCs, respectively. These BMDCs were subsequently challenged with either PBS or *E. coli* mpk for 2 h followed by cell lysis and CTSS activity detection. Fig. 3e shows that PBS-primed (iDCs) and *E. coli* mpk challenged BMDCs provide a CTSS activity increase of about 100% compared to PBS (mock) primed and PBS (mock) challenged control BMDCs. *E. coli* mpk primed and *E. coli* mpk challenged mDCs provided very low CTSS

Please cite this article in press as: A. Steimle, et al., Symbiotic gut commensal bacteria act as host cathepsin S activity regulators, Journal of Autoimmunity (2016), http://dx.doi.org/10.1016/j.jaut.2016.07.009

activity rates (Fig. 3e), which might also be due to the high secretion rates of CTSS in *E. coli* mpk primed cells (Fig. 3f). *B. vulgatus* mpk primed smDCs which were subsequently challenged with *E. coli* mpk did not show any increase in CTSS activity compared to untreated PBS (mock) primed and PBS (mock) challenged control cells (Fig. 3e). Thus, we demonstrate that *B. vulgatus* mpk stimulated, semi-mature DC also provide non-responsiveness in terms of CTSS activity which therefore seems to be part of the tolerant semi-mature DC phenotype.

3.3. *B. vulgatus mpk mediates CTSS activity regulation via cystatin C*

Since we detected different CTSS activities in BMDCs that were stimulated with either *B. vulgatus* mpk or *E. coli* mpk finally resulting in different MHC-II surface expression and T cell activation, the question of the underlying regulation mechanism arised. First, we checked for a transcriptional regulation of the *Ctss* gene, encoding for CTSS protein. *Ctss* mRNA expression in both, *E. coli* mpk and *B. vulgatus* mpk treated samples were not significantly different from those of PBS treated controls after 1 h, 2 h, 4 h and 16 h of bacterial stimulation (Fig. 4a). Therefore we assume that transcriptional regulation does not contribute to the observed changes in CTSS activity. Another possible regulation mechanism would be endogenous inhibition by a regulatory protein. Cystatins have been widely discussed to be such endogenous cathepsin inhibitors. For CTSS, cystatin C (CysC) [7–9] was proposed to be the

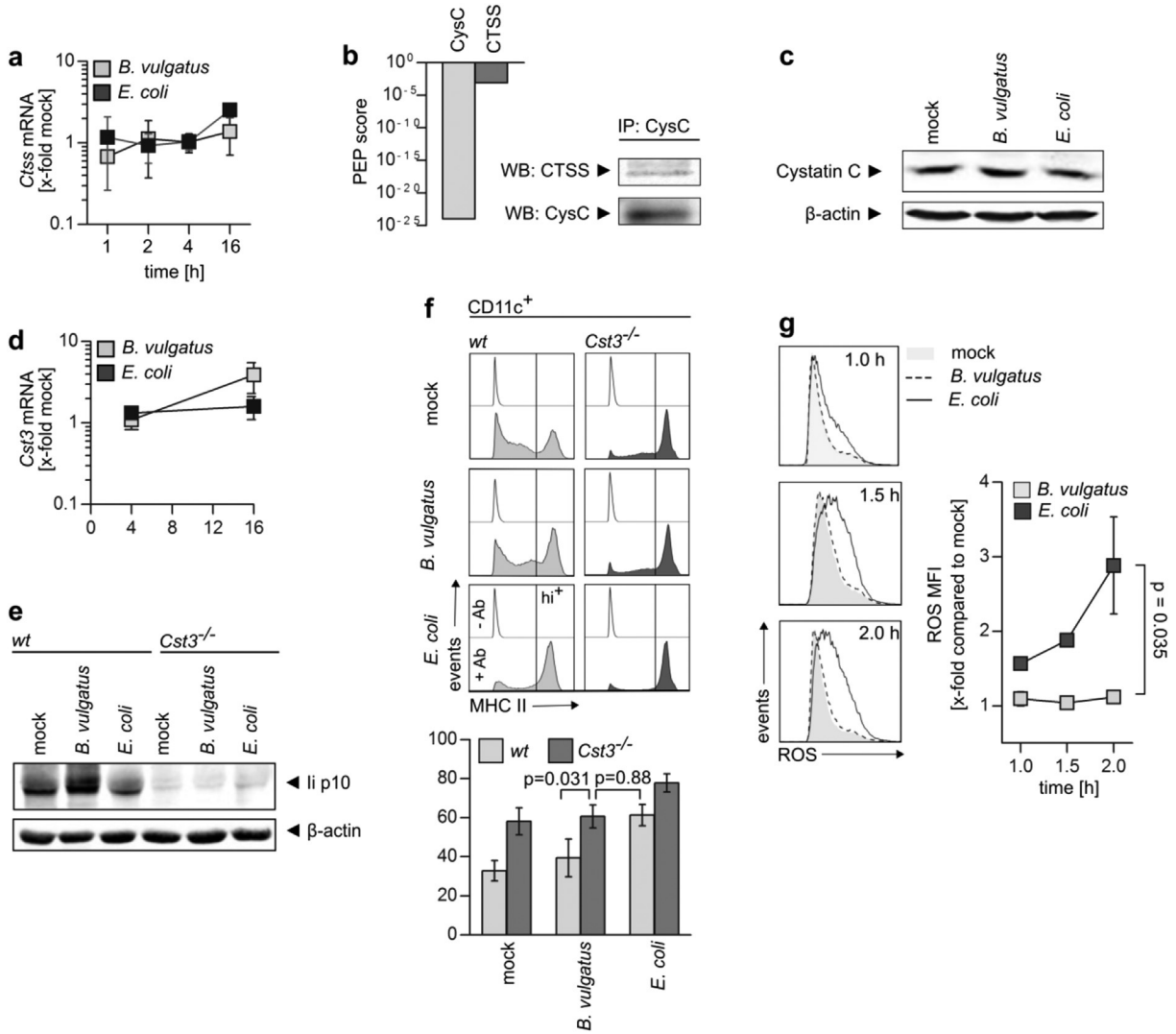

Fig. 4. *B. vulgatus* mpk mediates CTSS activity regulation via intracellular ROS amounts and binding behaviour of cystatin C. (a) *Ctss* mRNA expression of *wt* (*Cst3*$^{+/+}$) BMDCs that were stimulated with *B. vulgatus* mpk or *E. coli* mpk for 1 h, 2 h, 4 h and 16 h were determined and normalized on the expression of the PBS-stimulated mock control in BMDCs generated from the same individual (n = 4). (b) CoIPs using α-cystatin C antibodies were performed with cell lysates of immature *wt* (*Cst3*$^{+/+}$) BMDCs. Potential interaction partners were identified using MS. CTSS was detected with a reliably low PEP score, with PEP indicating the probability of a false positive detection result. Western Blots against CTSS and Cystatin C (CysC) in α-CysC CoIPs were performed to verify these results (n = 3). (c) *wt* (*Cst3*$^{+/+}$) BMDCs were stimulated for 20 h with either PBS (mock), *B. vulgatus* mpk or *E. coli* mpk. CysC protein amount was detected by western blotting (n = 4). (d) *Cst3* mRNA expression (encoding for CysC) of *wt* (*Cst3*$^{+/+}$) BMDCs that were stimulated with *B. vulgatus* mpk or *E. coli* mpk for 4 h and 16 h were determined and normalized on the expression of the mock control in BMDCs generated from the same individual (n = 4), (e) *wt* (*Cst3*$^{+/+}$) and Cystatin C-deficient *Cst3*$^{-/-}$ BMDCs were stimulated for 20 h with either PBS (mock), *B. vulgatus* mpk or *E. coli* mpk. The amount of the MHC-II bound invariant chain p10 fragment (Ii p10) was determined by western blotting (n = 3). One representative blot is shown. (f) Flow cytometrical determination of the MHC class II hi^{+} population among *Cst3*$^{+/+}$ (*wt*) and Cystatin C-deficient (*Cst3*$^{-/-}$) CD11c^{+} BMDCs that were stimulated with PBS, *B. vulgatus* mpk or *E. coli* mpk for 16 h (=3), (G) *wt* (*Cst3*$^{+/+}$) BMDCs were stimulated for either 1 h, 1.5 h or 2 h with PBS (mock), *B. vulgatus* mpk or *E. coli* mpk. ROS formation was detected by using flow cytometry as described. Relative Median Fluorescence intensities (MFI) were determined and normalized to the MFI of the unstimulated mock control derived from cells of the same mouse (n = 4). All statistical analyses were performed using student's *t*-test. Error bars represent SD.

Please cite this article in press as: A. Steimle, et al., Symbiotic gut commensal bacteria act as host cathepsin S activity regulators, Journal of Autoimmunity (2016), http://dx.doi.org/10.1016/j.jaut.2016.07.009

major regulatory protein. First, we wanted to know if cystatin C actually binds to CTSS. Thus, we performed immunoprecipitation assays in immature BMDCs using an antibody against cystatin C and checked for interaction partners by using mass spectrometric approaches. As a negative control, IPs from cystatin C-deficient BMDCs were used (data not shown) to exclude false positive potential interaction partners. We could identify CTSS as cystatin C interaction partner in immature DC with a reliable PEP score of 1.3×10^{-3} (Fig. 4b). Interestingly, the total amount of CysC protein and the mRNA expression of the *Cst3* gene, encoding for CysC, was not altered between iDCs, smDCs and mDCs (Fig. 4c and d). In order to prove CysC dependent CTSS regulation, we used BMDCs from *Cst3*$^{-/-}$ mice, lacking cystatin C, for *in vitro* experiments. Like in *Ctss*$^{-/-}$ DCs, the cystatin C deficiency did not influence other immunomodulatory mechanisms of dendritic cells since expression of pro-inflammatory cytokines and T cell costimulatory factors were not affected (see Supplementary Fig. S2). *B. vulgatus* mpk stimulation in *Cst3*$^{-/-}$ BMDCs led to fully mature DC in terms of MHC-II expression and therefore failed to induce semi-maturation as indicated by a proportion of MHC-II hi^{+} DC that is comparable to *E. coli* mpk stimulated *wt* DCs (Fig. 4f). Even if CysC might not be the only regulator or repressor of MHC-II expression, CysC seems to be essential for the induction of *B. vulgatus* mpk caused DC semi-maturation (Fig. 4f). These results are in line with the obtained high cleaving rates of the MHC-II bound invariant chain (MHC-II-Ii p10) in *Cst3*$^{-/-}$ BMDCs. In contrast to *wt* BMDCs, neither *B. vulgatus* mpk, nor *E. coli* mpk stimulated *Cst3*$^{-/-}$ BMDCs showed any clearly visible band for the MHC-II-Ii p10 heterotrimer, indicating efficient cleaving probably due to generally enhanced CTSS activity (Fig. 4e). Since we could prove a cystatin C-dependent regulation of invariant chain cleaving and MHC-II surface expression, which both seemed to be independent from *Cst3* gene expression or intracellular cystatin C protein amounts, we suggested that the protein-protein-interaction between cystatin C and its target protease CTSS might be affected by bacterial stimulation. In order to prove this hypothesis we checked for intracellular levels of reactive oxygen species (ROS) in *B. vulgatus* mpk and *E. coli* mpk stimulated DCs. It is known that upon increase of intracellular ROS amounts, cystatin C monomers preferentially form protein homodimers leading to a loss of the inhibitory potential [34]. Since only CysC monomers can bind to CTSS, ROS-dependent CysC dimer formation would lead to dissociation of cystatin C monomers from CTSS, therefore promoting CTSS activity increase. We could demonstrate that *B. vulgatus* mpk stimulation of BMDCs does not induce ROS production (Fig. 4g). This would, in turn, promote maintenance of cystatin C monomers that are able to bind to CTSS, therefore inhibiting CTSS proteolytic activity. *E. coli* mpk stimulation, however, leads to significantly higher intracellular ROS amounts compared to *B. vulgatus* mpk stimulated cells (Fig. 4g). *E. coli* mpk induced higher ROS levels would favour homodimerization of cystatin C which would subsequently lead to a loss of CTSS inhibition, resulting in CTSS activity increase. Therefore we conclude that lower intracellular ROS amounts are, at least in part, responsible for CTSS activity control in semi-mature DC.

3.4. Administration of *B. vulgatus* mpk protects mice from induction of *CD4*$^{+}$ *T cell driven transfer colitis*

In vitro and *in vivo* experiments (Figs. 2–4) revealed that DCs primed with *B. vulgatus* mpk differentiate to tolerant semi-mature DCs which prevent from T cell activation (Fig. 1). *Rag1*$^{-/-}$ mice harbouring a conventional (CV) microbiota with high levels of pathobiotic *Enterobactericeae* develop chronic colitis upon transfer of naïve CD4^{+} *wt* T cells. In this experiment, we tried to protect these mice from colitis induction and promotion by applying *B. vulgatus* mpk via drinking water and thus shifting the microbiota composition in favour of *Bacteroides sp*. We started *B. vulgatus* mpk application 3 days before T cell transplantation and continued bacterial application until the end of the experiment (Fig. 5a). 6 weeks after T cell transplantation, *B. vulgatus* mpk colonization anticipated induction of colonic mucosal inflammation and *Rag1*$^{-/-}$ mice harbouring CV microbiota stayed without any colitis symptoms as indicated by the histological colitis score (Fig. 5e). This was associated with the detection of semi-mature dendritic cells in the colonic LP as indicated by low MHC-II (Fig. 5b) and CD40 surface expression (Fig. 5c), as well as by a lower relative proportion of CD3^{+}CD4^{+} T cells in the cLP (Fig. 5d).

3.5. *B. vulgatus* mpk dependent prevention of colitis is associated with prevention of CTSS secretion into blood serum

Enhanced CTSS serum levels have been reported to be associated with several T cell mediated autoimmune diseases. We therefore compared the CTSS serum levels in T cell transplanted CV *Rag1*$^{-/-}$ mice suffering from chronic colitis with *B. vulgatus* mpk treated CV *Rag1*$^{-/-}$ mice, which stayed healthy. As negative controls, we used germfree (GF) T cell transplanted *Rag1*$^{-/-}$ mice. Germfree *Rag1*$^{-/-}$ mice, as well as *B. vulgatus* mpk treated CV *Rag1*$^{-/-}$ mice provided significantly lower CTSS secretion into the serum compared to non-*B. vulgatus* mpk treated CV *Rag1*$^{-/-}$ mice (Fig. 5f). A clear correlation between the histological colitis score, representing the severity of disease, of each individual mouse and its respective CTSS serum level was detectable (Fig. 5f).

3.6. Feeding symbiont *B. vulgatus mpk* is equally effective in prevention of colitis induction as administration of a chemical CTSS inhibitor

The data presented above support the hypothesis that CTSS activity regulation is an important feature for the prevention of pathological inflammatory reactions and that *B. vulgatus* mpk might act as a CTSS regulatory agent. In order to prove that a hypothesized CTSS activity regulation *in vivo* is the cause for the *B. vulgatus* mpk mediated prevention of colitis induction in *Rag1*$^{-/-}$ mice (Fig. 5), we compared the anti-colitogenic properties of *B. vulgatus* mpk with the properties of a chemical CTSS inhibitor. Therefore, we again used *Rag1*$^{-/-}$ mice harbouring a highly colitogenic CV microbiota and treated them with either *B. vulgatus* mpk in the drinking water, a chemical CTSS inhibitor or a vehicle, representing the solvent mixture in which the inhibitor was dissolved. The CTSS inhibitor and the vehicle were administered intraperitoneally daily, starting three days before T cell transplantation. *B. vulgatus* mpk administration via drinking water was also started three days before T cell transplantation and continued throughout the experiment. Since we were focused on the induction of an inflammatory reaction, mice were analyzed already 21 days after T cell transplantation. We could detect a lower colonic inflammation in the *B. vulgatus* mpk and CTSS inhibitor treated animals compared to vehicle treated controls as indicated by a lower histological colitis score (Fig. 6b and c). This observation was in line with the detected increased weight loss of the vehicle treated animals compared to both other groups (Fig. 6d). The reduced inflammation of the colon of *B. vulgatus* mpk and CTSS inhibitor treated animals in this CD4^{+} T cell mediated experimental mouse model for colitis was associated with a lower number of CD3^{+}CD4^{+} T cells in the colon (Fig. 6f) as well as with a lower number of MHC-II^{hi+} CD11c^{+} cells in the colon (Fig. 6e) as compared to the inflamed vehicle treated control animals. These findings demonstrate that a chemical CTSS inhibitor and *B. vulgatus* mpk have similar effects on prevention of colitis induction and that

Please cite this article in press as: A. Steimle, et al., Symbiotic gut commensal bacteria act as host cathepsin S activity regulators, Journal of Autoimmunity (2016), http://dx.doi.org/10.1016/j.jaut.2016.07.009

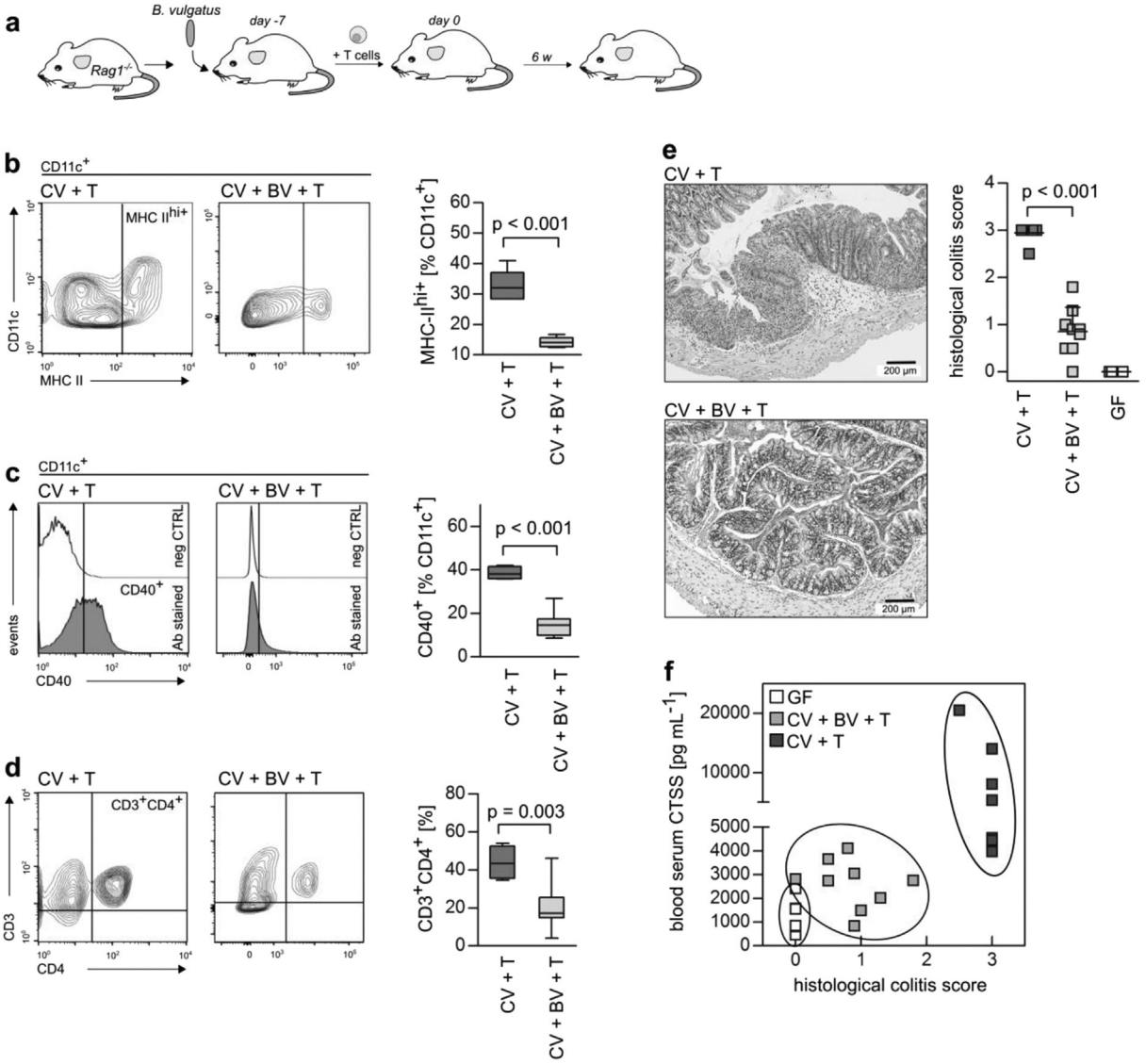

Fig. 5. *B. vulgatus* mpk protects from CD4$^+$ T cell mediated colitis in *Rag1*$^{-/-}$ mice. (a) experimental setting. *Rag1*$^{-/-}$ mice harbouring conventional microbiota (CV) were either fed *B. vulgatus* mpk (CV + BV + T) or not (CV + T) and transplanted with CD4$^+$CD62L$^+$CD45RB^{hi} *wt* T cells. (b + c) Flow cytometrical determination of the MHC-II hi$^+$ (b) and CD40 (c) population among CD11c$^+$ DC isolated from the colonic lamina propria (cLP). (b) sample size: CV + T: n = 6, CV + BV + T: n = 7; (c) sample size: CV + T: n = 4, CV + BV + T: n = 10 (d) Flow cytometrical determination of CD3$^+$CD4$^+$ T cells from cLP. Samples sizes: CV + T: n = 4, CV + BV + T: n = 10 (b + c + d) The boxes represent the 25th to the 75th percentile, the whiskers indicate the lowest and highest single value. The line within the boxes represent the statistical median. (e) representative H&E stained colonic sections and histological colitis score. Each dot represents one individual. As controls, non-inflamed germfree (GF) mice were used (f) Correlation between CTSS serum level and histological colitis score. Each dot represents one individual. All statistical analyses were performed using student's *t*-test. Error bars, if shown, represent SD.

the *B. vulgatus* caused prohibition of a CD4$^+$ T cell mediated immune response in this animal model is mediated by CTSS activity regulation (Fig. 5f). Furthermore, the data support the hypothesis that the enhanced CTSS secretion that can be detected in mice with colonic inflammation may not only be a simple consequence of inflammatory processes but might rather be a feature of disease-inducing mechanisms. However, we are aware that this is highly speculative at the moment and further data acquisition is necessary to define the role of secreted CTSS in colitis pathology. So far, we cannot state any information on the activity of the secreted CTSS since the method we used for intracellular CTSS activity detection is not suitable for the detection of extracellular soluble CTSS in biological fluids. Summing up, *B. vulgatus* mediated regulation of intracellular CTSS activity, and MHC-II signaling in consequence, is one crucial component in the prevention of colitis induction but it might not be the only one due to the potential pathological effects of secreted extracellular CTSS.

In summary, we demonstrate that the symbiotic commensal *B. vulgatus* mpk induces a tolerant semi-mature DC phenotype via ROS and cystatin C-dependent regulation of the lysosomal protease CTSS. This, in turn, prevents from MHC-II associated pathophysiological activation of CD4$^+$ T cells. Fig. 7 summarizes the postulated mechanism how *B. vulgatus* mpk regulates CTSS activities and therefore prevents from colitis induction. *B. vulgatus* mpk, located in the intestinal lumen, interacts with DC underlying the intestinal epithelium and induces DC semi-maturation. This is accompanied by low intracellular levels of ROS, which, in turn, favour the maintenance of cystatin C monomers that can subsequently bind to CTSS, inhibiting its proteolytical activity. This leads to less efficient cleaving of the MHC-II bound invariant chain, resulting in low MHC-II surface expression preventing from CD4$^+$ T cell activation. As a characteristic of semi-maturation, this DC phenotype is

Please cite this article in press as: A. Steimle, et al., Symbiotic gut commensal bacteria act as host cathepsin S activity regulators, Journal of Autoimmunity (2016), http://dx.doi.org/10.1016/j.jaut.2016.07.009

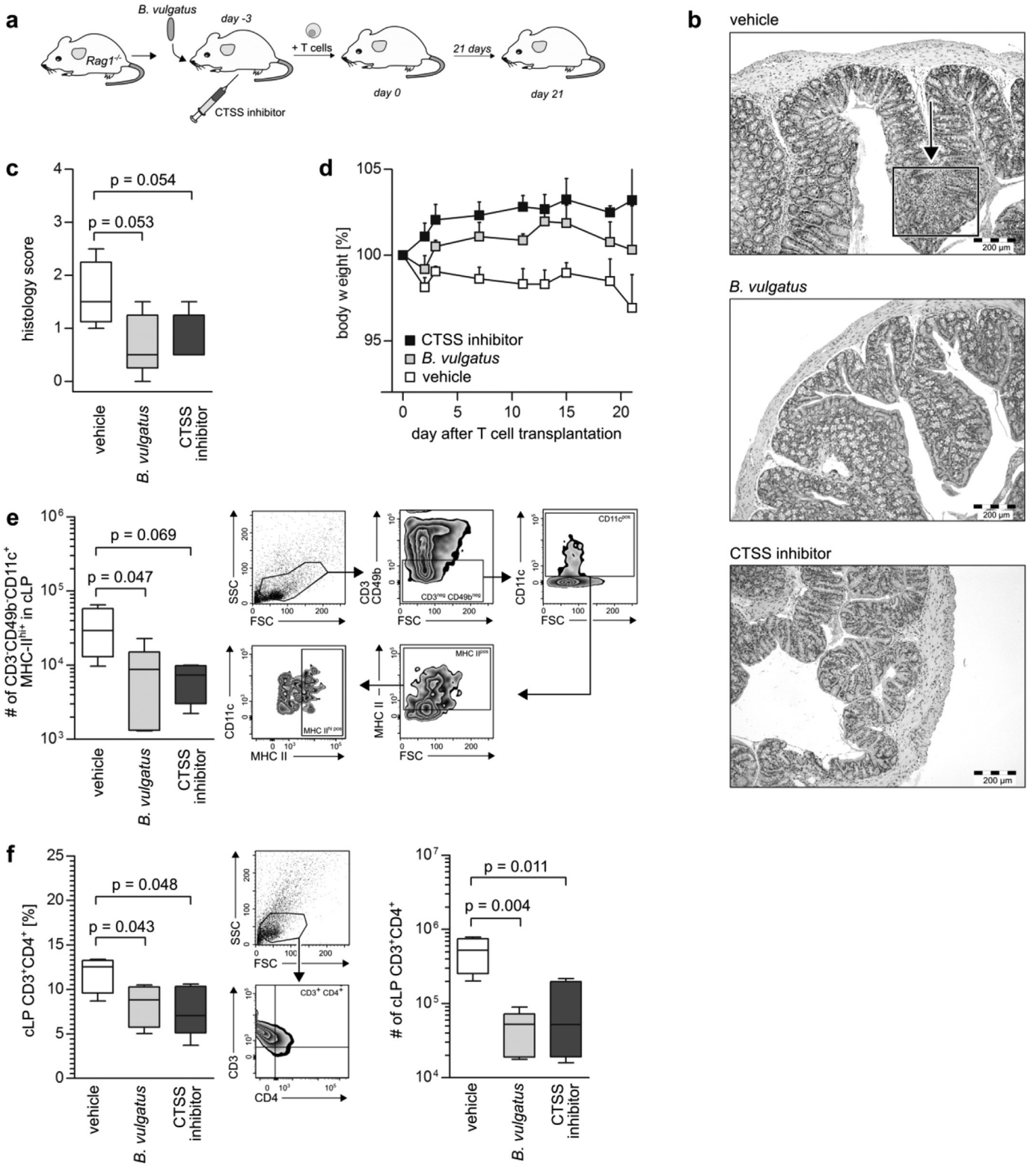

Fig. 6. Chemical CTSS inhibition protects from induction of a $CD4^+$ T cell mediated colitis in $Rag1^{-/-}$ mice. (a) experimental setting. $Rag1^{-/-}$ mice harbouring conventional microbiota (CV) were either fed *B. vulgatus* mpk or administered daily a chemical CTSS inhibitor or a vehicle, respectively. Three days after start of CTSS inhibitor and vehicle treatment, mice were transplanted with $CD4^+CD62L^+CD45RB^{hi}$ *wt* T cells. (n = 5 per group) Analysis of the animals was performed 21 days after T cell transplantation. (b) Representative H&E stained colonic sections. The arrow and the box highlight the influx of lymphocytes into the colonic epithelium indicating inflammatory processes. (c) Histological colitis score, (d) Weight curve. Weight was determined every 2–3 days and normalized to the weight at the day of T cell transplantation. Error bars represent SD. (e) Flow cytometrical determination of the cell number of $CD3^{neg}CD48b^{neg}CD11c^+MHC\text{-}II^+MHC\text{-}II^{hi+}$ cells in the colonic lamina propria (cLP) Right panel: gating strategy; (f) Flow cytometrical determination of the percentage (left panel) and the total cell number (right panel) of $CD3^+CD4^+$ T cells from the cLP. (c + e + f) box and whiskers: the boxes represent the 25th to the 75th percentile, the whiskers indicate the lowest and highest single value. The line within the boxes represents the statistical median. All statistical analyses were performed using student's *t*-test.

Please cite this article in press as: A. Steimle, et al., Symbiotic gut commensal bacteria act as host cathepsin S activity regulators, Journal of Autoimmunity (2016), http://dx.doi.org/10.1016/j.jaut.2016.07.009

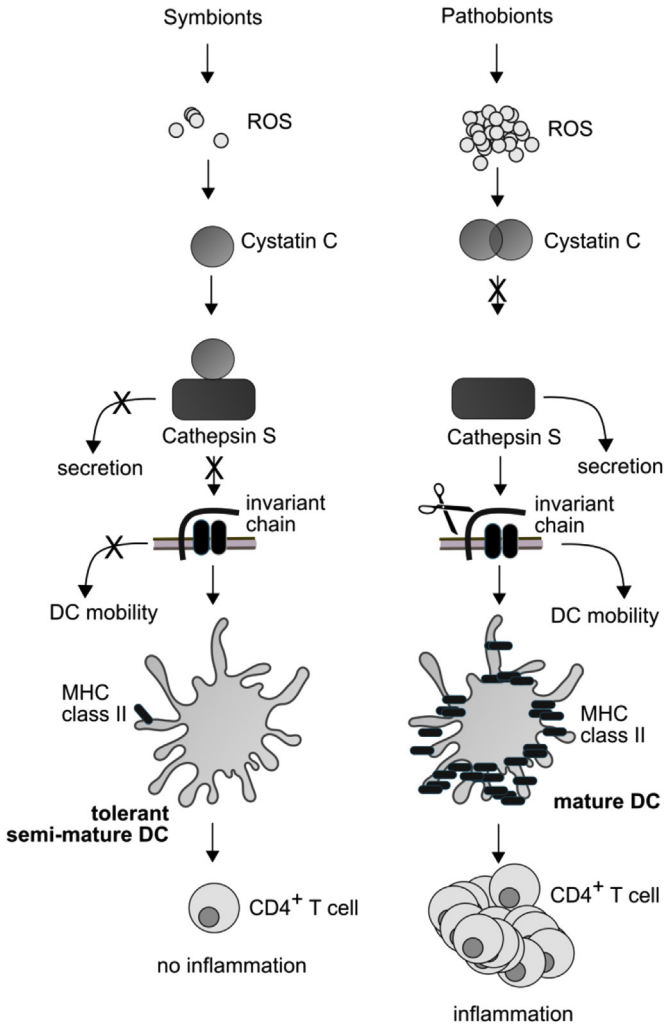

Fig. 7. Postulated mechanism how commensal symbiont *Bacteroides vulgatus* mpk prevents from inflammation induction via cathepsin S activity regulation. Left panel: *B. vulgatus* mpk is suspected to promote only a weak immunological signal in dendritic cells resulting in low amounts of reactive oxygen species (ROS). These low ROS amounts favour cystatin C monomers which can therefore efficiently bind to cathepsin S (CTSS) and thus cause inhibition of CTSS proteolytic activity. This results in less efficient cleaving of the invariant chain (Ii) and therefore in lower amounts of surface MHC-II and reduced DC mobility. Additionally, CTSS secretion into the extracellular space is omitted. These events lead to the conversion of immature DC into tolerant semi-mature DC that fail to induce a $CD4^+$ T cell mediated immune response and therefore protect from inflammatory reactions. Right panel: In contrast to symbiont commensals, pathobionts like *E. coli* mpk induce intracellular ROS formation promoting homodimerization of Cystatin C leading to a loss of its inhibitory capacity towards CTSS. This leads to enhanced invariant chain cleaving, high MHC-II expression, increased DC mobility and high CTSS secretion. These events characterize a mature DC which are finally capable to induce a $CD4^+$ T cell mediated immune response.

ultimate and cannot be overcome by a subsequent maturating stimulus.

4. Discussion

Here we demonstrate that regulation of cathepsin S (CTSS) activity importantly contributes to the maintenance of the intestinal immune equilibrium. CTSS activity can be regulated by the intestinal microbiota with symbionts triggering physiological CTSS activity and pathobionts inducing pathological CTSS activity increase, the latter resulting in T cell activation and proliferation which, in turn, supports pro-inflammatory host immune responses. The microbiota dependent regulation of CTSS activity is mediated by the induction of reactive oxygen species (ROS). Pathobionts, but not symbionts, induced high intracellular ROS levels in DCs, allowing for homodimerization of cystatin C (CysC) and resulting in an abrogation of the CysC-mediated inhibition of CTSS activity. This promotes intestinal inflammatory host responses, in our mouse model resulting in induction of colitis. The symbiont induced low intracellular ROS levels lead to a preservation of CysC monomers, mediating inhibition of CTSS via direct protein-protein-interactions, which therefore results in physiological CTSS activity levels and maintenance of intestinal homeostasis.

CTSS is a physiologically required lysosomal cysteine protease that is mainly expressed in professional antigen presenting cells like macrophages, dendritic cells (DC) and B cells [1,35]. It is mainly involved in regulation of the MHC-II associated antigen presenting pathway. This underlines its crucial role in the activation of MHC-II dependent immune responses. Pathogenesis of most autoimmune diseases (AID), and of IBD in particular, is associated with an induction of a $CD4^+$ T cell mediated immune response, highlighting the importance of the MHC-II mediated antigen presenting pathway for the onset of AID. Therefore a strict regulation of the CTSS activity is important to retain a balanced immune system. CTSS exerts its physiological functions intracellularly. However, secretion can occur since CTSS is part of the lysosomal compartment. This might cause additional pathophysiological processes in the extracellular space. Upon secretion, cathepsins end in extracellular environments whose pH values strongly affect their proteolytical activity. Among all cathepsins, CTSS is the only enzyme with significant activity within a broader pH range since it is also capable of catalysing peptide bond cleavage at neutral pH [36]. All other cathepsins provide their maximum activity at acidic pH values [37]. Since in extracellular environments a neutral pH is dominant, CTSS is not automatically inactivated like other cathepsins. Extracellular or, in other words, secreted CTSS is involved in the pathology of a variety of autoimmune diseases. For example, increased CTSS levels in the serum or cerebrospinal fluid can be found in multiple sclerosis patients [8]. In the mouse model of experimental autoimmune encephalomyelitis (EAE), resembling the multiple sclerosis phenotype in humans, increased extracellular CTSS levels could be detected [38]. Its extracellular pathological function might be proteolysis of the myelin basic protein which could be observed *in vitro* [39]. In Sjögren's syndrome patients, enhanced CTSS activity could be detected in tear fluid [14], therefore making CTSS activity in tears an appropriate biomarker for the diagnosis of this disease [15]. Especially the atheriosclerosis phenotype is affected by extracellular CTSS. Secreted CTSS cleaves proteins of the extracellular matrix (ECM) like laminin, collagen or elastin [40]. Resulting elastin peptides are able to incite inflammation and stimulate macrophage chemotaxis [41]. Concerning inflammatory bowel disease, general ECM degradation therefore could promote epithelial damage or relieve bacterial contact to APC leading to accelerated T cell responses and IBD promotion. CTSS secretion into the colonic lumen might cause damage of the epithelial barrier leading to intensified colitis symptoms as enhanced encounter of gut bacteria with immune cells on the basolateral side of the epithelium would be possible. We could now show in a mouse model for T cell mediated colitis using *Rag1*$^{-/-}$ mice, that feeding symbiotic *B. vulgatus* mpk via drinking water protects mice from colitis induction and we provide evidence that this is due to a strict regulation of intracellular CTSS activity and possibly also due to a prevention of secretion from DCs into extracellular environments. There is a clear correlation between the CTSS concentration in blood serum and severity of colonic damage and we could demonstrate that administration of a chemical CTSS inhibitor prevents from colitis induction in a $CD4^+$ T cell mediated

Please cite this article in press as: A. Steimle, et al., Symbiotic gut commensal bacteria act as host cathepsin S activity regulators, Journal of Autoimmunity (2016), http://dx.doi.org/10.1016/j.jaut.2016.07.009

mouse model for experiment colitis using *Rag1*$^{-/-}$ mice. We could confirm this observation *in vitro* by detecting low CTSS secretion rates in *B. vulgatus* mpk stimulated bone marrow derived dendritic cells (BMDCs). It has already been shown that CTSS secretion promotes pain induction during colitis via cleaving of the PAR-2 receptor [19]. However, our data support the idea that CTSS activity dysregulation and enhanced secretion is the decisive trigger for colitis induction.

Intracellular CTSS activity also requires precise regulation. CTSS is the main protease in DCs that is responsible for cleaving the MHC-II associated chaperone invariant chain (Ii). This cleaving event is the major regulation step for loading antigen-derived peptides onto the MHC-II binding groove and the subsequent transport of peptide-loaded MHC-II to the cell surface. We could show that DC maturation induced by the pathobiotic commensal *E. coli* mpk results in strong intracellular CTSS activity increase and therefore enhanced MHC-II surface expression which is required for a powerful CD4^{+} T cell mediated immune response. Symbiotic commensal *B. vulgatus* mpk priming of DC, however, prevents from *E. coli* mpk induced CTSS activity increase and therefore from Ii cleaving and enhanced MHC-II surface expression. We have previously shown that *B. vulgatus* mpk converts DC into a tolerant semi-mature phenotype [22,24]. These tolerant semi-mature DCs are non-responsive to further stimuli, they fail to activate CD4^{+} T cells and they are associated with the prevention of colitis in various mouse models [22,24]. We now demonstrate that CTSS activity regulation is one of the most important reasons for induction of DC semi-maturation and the circumvention of T cell activation. Prevention of CTSS activity increase results in less efficient Ii cleaving. It was shown that CTSS deficiency significantly impairs DC mobility since Ii seems to interact with cellular myosin II [42] and efficient Ii cleaving therefore seems to be required for adequate interaction of Ii with myosin II and thus for DC mobility. Therefore, reduced Ii cleaving might contribute to impaired mobility of semi-mature DC [24]. Furthermore, CTSS catalyzed Ii cleaving leads to NFκB activation resulting in enhanced secretion of pro-inflammatory cytokines [43]. In fact, smDCs express only low amounts of pro-inflammatory cytokines [22] and this might be, at least in part, due to reduced cleaving of MHC-II bound Ii in smDCs.

The question emerges which intracellular regulation mechanisms are involved in *B. vulgatus* mpk mediated CTSS activity regulation. In principle, CTSS activity can be regulated by various mechanisms. Possible regulation via transcriptional control, i.e. induced by IL-10 binding and STAT3 dimerisation [44] can be excluded in this case since we could not detect any transcriptional regulation of the *Ctss* gene. Another potential regulation mechanism is control of the lysosomal pH, but this might not be of importance in case of CTSS due to the broad pH range in which CTSS provides remarkable activity. Possible post-translational regulation might occur through inhibition by chondroitin-4-sulfate [3] or the creation of an oxidizing environment by NADPH oxidase NOX2 [45,46]. A prominently discussed endogenous CTSS inhibitor is cystatin C (CysC). However, there are contradictory reports about the role of CysC for CTSS activity regulation. Although some groups claim CysC to be the major CTSS activity regulator [7–9], Magister et al. published that CysF might be the more important regulator protein [10]. In order to elucidate the role of CysC during *B. vulgatus* mpk induced DC semi-maturation and the effect on CTSS activity, we first performed immunoprecipitations against CysC that proved convincing interaction between CysC and CTSS. We could further demonstrate that *B. vulgatus* mpk fails to induce DC semi-maturation in Cystatin C-deficient *Cst3*$^{-/-}$ DCs indicating a central role for CysC in the semi-maturation process. We conclude that *B. vulgatus* mpk mediates its CTSS regulating functions via Cystatin C. There are different possibilities how a bacterial stimulus on DCs might affect the interaction between CysC and CTSS. Transcriptional regulation of the CysC gene might be the first possibility since it could be shown that transcription factors like IRF-8 and PU.1 enhance CysC mRNA transcription [47]. However, we could not detect any alteration in CysC gene transcription during the DC maturation or semi-maturation process. In line with this, we could also not detect any differences in the amount of CysC protein in DCs of different maturation states. CysC inhibits target proteases like CTSS by forming tight and non-covalent complexes [48]. Complex forming with CTSS is limited to CysC monomers. However, CysC protein expression in the endoplasmatic reticulum (ER) does not only yield in the formation of monomers but also in dimers that do not form inhibitory complexes with target proteases [49]. Xu et al. demonstrated that the formation of non-inhibitory CysC dimers is dependent on the amount of ROS inside the cell, whereupon ROS presence promotes dimer formation [34]. Since bacterial lipopolysaccharide (LPS) induced DC maturation leads to an increase in intracellular ROS concentrations [50], we hypothesized that a weaker *B. vulgatus* mpk LPS signalling (data not shown) leads to less ROS formation and therefore enhanced levels of monomeric CysC compared to completely mature DC. In fact, *B. vulgatus* mpk stimulation does not lead to an increase of intracellular ROS amounts, in contrast to *E. coli* mpk stimulation which efficiently enhances ROS production. We therefore assume that *B. vulgatus* mpk stimulation leads to less CysC dimer formation, thus resulting in increased proportions of monomeric cystatin C. These enhanced amounts of monomeric CysC can subsequently form inhibitory complexes with CTSS, which we could prove via immunoprecipitation, resulting in permanently low CTSS activities. In line with this, we could detect a CysC-regulation dependent MHC-II surface expression of DCs supporting the findings of Pierre et al. [35] but opposing findings of El-Sukkari et al. [51]. In line with this, we detected extremely efficient Ii cleavage in *Cst3*$^{-/-}$ BMDCs, with Ii cleaving being the precondition for MHC-II translocation to the cell surface.

There is an intense ongoing research for adequate CTSS inhibitors for the use as potential drugs in order to treat autoimmune diseases. Some groups developed chemical CTSS inhibitors and chemical CTSS inhibition could attenuate atherosclerosis in mice [18] and T cell mediated inflammation in the murine central nervous system [52]. However, a non site-directed complete inhibition of CTSS might have severe side effects on the host organism. Furthermore, the effectiveness of chemical substances is dependent on bioavailability and membrane passage behaviour if inhibitors are supposed to act intracellularly. In contrast to a chemical inhibitor, *B. vulgatus* mpk does not lead to a completely inhibited CTSS as demonstrated in our experiments. This is a strong advantage over a chemical inhibitor that usually leads to a complete inhibition of its target enzyme. Therefore, *B. vulgatus* mpk treatment still allows for CTSS to achieve its physiological role and only prevents from pathophysiological activation.

We could show that *B. vulgatus* mpk prevents from pathological reactions of the immune system via regulation of intracellular host CTSS activity and therefore contributes to the maintenance of the intestinal homeostasis. This could be underlined by the observation that the *B. vulgatus* mpk associated protection of *Rag1*$^{-/-}$ mice from colitis induction is accompanied by inducing DC semi-maturation and inhibition of CTSS secretion. This makes *B. vulgatus* mpk a promising candidate for the treatment for IBD and other CTSS-associated AID. We think that *B. vulgatus* mpk might be an even better tool than a chemical inhibitor to treat CTSS-associated AID since (i) it is easily administrable, (ii) it does not completely suppress physiological functions of CTSS but only suppresses pathological activities and (iii) it acts as a commensal symbiont. It does not influence a normal immune response due to acute infections

Please cite this article in press as: A. Steimle, et al., Symbiotic gut commensal bacteria act as host cathepsin S activity regulators, Journal of Autoimmunity (2016), http://dx.doi.org/10.1016/j.jaut.2016.07.009

but strongly inhibits pathological gut microbiota associated immune responses. Therefore severe side effects of symbiont-mediated CTSS activity regulation should not occur and could not be observed in the used mouse model, another advantage over a chemical inhibitor.

Acknowledgements

We thank Prof. Thomas Reinheckel, University of Freiburg, Germany for kindly handing over *Ctss*$^{-/-}$ mice. Work was supported by the DFG (DFG FR 2087/6-1, DFG FR 2087/8-1, CRC685, SPP1656, SFB685) the DFG research training group 1708 and the German Center for Infection Research.

Appendix A. Supplementary data

Supplementary data related to this article can be found at http://dx.doi.org/10.1016/j.jaut.2016.07.009.

References

[1] C. Driessen, R.A. Bryant, A.M. Lennon-Dumenil, J.A. Villadangos, P.W. Bryant, G.P. Shi, et al., Cathepsin S controls the trafficking and maturation of MHC class II molecules in dendritic cells, J. Cell Biol. 147 (1999) 775–790.
[2] C. Beers, A. Burich, M.J. Kleijmeer, J.M. Griffith, P. Wong, A.Y. Rudensky, Cathepsin S controls MHC class II-mediated antigen presentation by epithelial cells *in vivo*, J. Immunol. 174 (2005) 1205–1212.
[3] J. Sage, F. Mallevre, F. Barbarin-Costes, S.A. Samsonov, J.P. Gehrcke, M.T. Pisabarro, et al., Binding of chondroitin 4-sulfate to cathepsin S regulates its enzymatic activity, Biochemistry 52 (2013) 6487–6498.
[4] L.C. Hsing, A.Y. Rudensky, The lysosomal cysteine proteases in MHC class II antigen presentation, Immunol. Rev. 207 (2005) 229–241.
[5] S. Conus, H.U. Simon, Cathepsins and their involvement in immune responses, Swiss Med. Wkly. 140 (2010) w13042.
[6] G. Lalmanach, A. Saidi, S. Marchand-Adam, F. Lecaille, M. Kasabova, Cysteine cathepsins and cystatins: from ancillary tasks to prominent status in lung diseases, Biol. Chem. 396 (2015) 111–130.
[7] J.M. Cox, J.S. Troutt, M.D. Knierman, R.W. Siegel, Y.W. Qian, B.L. Ackermann, et al., Determination of cathepsin S abundance and activity in human plasma and implications for clinical investigation, Anal. Biochem. 430 (2012) 130–137.
[8] D. Haves-Zburof, T. Paperna, A. Gour-Lavie, I. Mandel, L. Glass-Marmor, A. Miller, Cathepsins and their endogenous inhibitors cystatins: expression and modulation in multiple sclerosis, J. Cell Mol. Med. 15 (2011) 2421–2429.
[9] E. Staun-Ram, A. Miller, Cathepsins (S and B) and their inhibitor Cystatin C in immune cells: modulation by interferon-beta and role played in cell migration, J. Neuroimmunol. 232 (2011) 200–206.
[10] S. Magister, N. Obermajer, B. Mirkovic, U. Svajger, M. Renko, A. Softic, et al., Regulation of cathepsins S and L by cystatin F during maturation of dendritic cells, Eur. J. Cell Biol. 91 (2012) 391–401.
[11] H. Vogel, B. Altincicek, G. Glockner, A. Vilcinskas, A comprehensive transcriptome and immune-gene repertoire of the lepidopteran model host Galleria mellonella, BMC genomics 12 (2011) 308.
[12] M.F. Alghoribi, T.M. Gibreel, A.R. Dodgson, S.A. Beatson, M. Upton, Galleria mellonella infection model demonstrates high lethality of ST69 and ST127 uropathogenic E. coli, PLoS One 9 (2014) e101547.
[13] L.C. Hsing, E.A. Kirk, T.S. McMillen, S.H. Hsiao, M. Caldwell, B. Houston, et al., Roles for cathepsins S, L, and B in insulitis and diabetes in the NOD mouse, J. Autoimmun. 34 (2010) 96–104.
[14] X. Li, K. Wu, M. Edman, K. Schenke-Layland, M. MacVeigh-Aloni, S.R. Janga, et al., Increased expression of cathepsins and obesity-induced proinflammatory cytokines in lacrimal glands of male NOD mouse, Investig. Ophthalmol. Vis. Sci. 51 (2010) 5019–5029.
[15] S.F. Hamm-Alvarez, S.R. Janga, M.C. Edman, S. Madrigal, M. Shah, S.E. Frousiakis, et al., Tear cathepsin S as a candidate biomarker for Sjogren's syndrome, Arthritis Rheumatol. 66 (2014) 1872–1881.
[16] M. Giannouli, A.T. Palatucci, V. Rubino, G. Ruggiero, M. Romano, M. Triassi, et al., Use of larvae of the wax moth Galleria mellonella as an *in vivo* model to study the virulence of helicobacter pylori, BMC Microbiol. 14 (2014) 228.
[17] A.O. Samokhin, P.A. Lythgo, J.Y. Gauthier, M.D. Percival, D. Bromme, Pharmacological inhibition of cathepsin S decreases atherosclerotic lesions in Apoe-/- mice, J. Cardiovasc. Pharmacol. 56 (2010) 98–105.
[18] J.L. Figueiredo, M. Aikawa, C. Zheng, J. Aaron, L. Lax, P. Libby, et al., Selective cathepsin S inhibition attenuates atherosclerosis in apolipoprotein E-deficient mice with chronic renal disease, Am. J. Pathol. 185 (2015) 1156–1166.
[19] F. Cattaruzza, V. Lyo, E. Jones, D. Pham, J. Hawkins, K. Kirkwood, et al., Cathepsin S is activated during colitis and causes visceral hyperalgesia by a PAR2-dependent mechanism in mice, Gastroenterology 141 (2011) 1864–1874 e1–3.
[20] S. Gupta, R.K. Singh, S. Dastidar, A. Ray, Cysteine cathepsin S as an immunomodulatory target: present and future trends, Expert Opin. Ther. Targets 12 (2008) 291–299.
[21] M.H. McLean, D. Dieguez Jr., L.M. Miller, H.A. Young, Does the microbiota play a role in the pathogenesis of autoimmune diseases? Gut 64 (2015) 332–341.
[22] J.S. Frick, N. Zahir, M. Muller, F. Kahl, O. Bechtold, M.B. Lutz, et al., Colitogenic and non-colitogenic commensal bacteria differentially trigger DC maturation and Th cell polarization: an important role for IL-6, Eur. J. Immunol. 36 (2006) 1537–1547.
[23] M. Waidmann, O. Bechtold, J.S. Frick, H.A. Lehr, S. Schubert, U. Dobrindt, et al., Bacteroides vulgatus protects against Escherichia coli-induced colitis in gnotobiotic interleukin-2-deficient mice, Gastroenterology 125 (2003) 162–177.
[24] M. Muller, K. Fink, J. Geisel, F. Kahl, B. Jilge, J. Reimann, et al., Intestinal colonization of IL-2 deficient mice with non-colitogenic B. vulgatus prevents DC maturation and T-cell polarization, PLoS One 3 (2008) e2376.
[25] K. Gronbach, I. Flade, O. Holst, B. Lindner, H.J. Ruscheweyh, A. Wittmann, et al., Endotoxicity of lipopolysaccharide as a determinant of T-cell-mediated colitis induction in mice, Gastroenterology 146 (2014) 765–775.
[26] N. Lutzner, H. Kalbacher, Quantifying cathepsin S activity in antigen presenting cells using a novel specific substrate, J. Biol. Chem. 283 (2008) 36185–36194.
[27] A. Steimle, H. Kalbacher, A. Maurer, B. Beifuss, A. Bender, A. Schafer, et al., A novel approach for reliable detection of cathepsin S activities in mouse antigen presenting cells, J. Immunol. methods 432 (2016) 87–94.
[28] M.B. Lutz, N. Kukutsch, A.L. Ogilvie, S. Rossner, F. Koch, N. Romani, et al., An advanced culture method for generating large quantities of highly pure dendritic cells from mouse bone marrow, J. Immunol. methods 223 (1999) 77–92.
[29] S.G. Jeon, H. Kayama, Y. Ueda, T. Takahashi, T. Asahara, H. Tsuji, et al., Probiotic Bifidobacterium breve induces IL-10-producing Tr1 cells in the colon, PLoS Pathog. 8 (2012) e1002714.
[30] S. Rakoff-Nahoum, J. Paglino, F. Eslami-Varzaneh, S. Edberg, R. Medzhitov, Recognition of commensal microflora by toll-like receptors is required for intestinal homeostasis, Cell 118 (2004) 229–241.
[31] J. Chow, S.K. Mazmanian, A pathobiont of the microbiota balances host colonization and intestinal inflammation, Cell host microbe 7 (2010) 265–276.
[32] A.D. Kostic, R.J. Xavier, D. Gevers, The microbiome in inflammatory bowel disease: current status and the future ahead, Gastroenterology 146 (2014) 1489–1499.
[33] C.R. Harding, G.N. Schroeder, S. Reynolds, A. Kosta, J.W. Collins, A. Mousnier, et al., Legionella pneumophila pathogenesis in the Galleria mellonella infection model, Infect. Immun. 80 (2012) 2780–2790.
[34] Y. Xu, P. Lindemann, J. Vega-Ramos, J.G. Zhang, J.A. Villadangos, Developmental regulation of synthesis and dimerization of the amyloidogenic protease inhibitor cystatin C in the hematopoietic system, J. Biol. Chem. 289 (2014) 9730–9740.
[35] J.K. Bender, T. Wille, K. Blank, A. Lange, R.G. Gerlach, LPS structure and PhoQ activity are important for Salmonella Typhimurium virulence in the Galleria mellonella infection model [corrected], PLoS One 8 (2013) e73287.
[36] F. Qian, S.J. Chan, Q.M. Gong, A.S. Bajkowski, D.F. Steiner, A. Frankfater, The expression of cathepsin B and other lysosomal proteinases in normal tissues and in tumors, Biomed. Biochim. Acta 50 (1991) 531–540.
[37] B. Turk, D. Turk, V. Turk, Lysosomal cysteine proteases: more than scavengers, Biochim. Biophys. Acta 1477 (2000) 98–111.
[38] A.K. Clark, M. Malcangio, Microglial signalling mechanisms: cathepsin S and fractalkine, Exp. Neurol. 234 (2012) 283–292.
[39] H. Beck, G. Schwarz, C.J. Schroter, M. Deeg, D. Baier, S. Stevanovic, et al., Cathepsin S and an asparagine-specific endoprotease dominate the proteolytic processing of human myelin basic protein *in vitro*, Eur. J. Immunol. 31 (2001) 3726–3736.
[40] F. Lohoefer, C. Reeps, C. Lipp, M. Rudelius, A. Zimmermann, S. Ockert, et al., Histopathological analysis of cellular localization of cathepsins in abdominal aortic aneurysm wall, Int. J. Exp. Pathol. 93 (2012) 252–258.
[41] C.L. Simpson, S. Lindley, C. Eisenberg, D.M. Basalyga, B.C. Starcher, D.T. Simionescu, et al., Toward cell therapy for vascular calcification: osteoclast-mediated demineralization of calcified elastin. Cardiovascular pathology, Off. J. Soc. Cardiovasc. Pathol. 16 (2007) 29–37.
[42] G. Faure-Andre, P. Vargas, M.I. Yuseff, M. Heuze, J. Diaz, D. Lankar, et al., Regulation of dendritic cell migration by CD74, the MHC class II-associated invariant chain, Science 322 (2008) 1705–1710.
[43] R.D. Wilkinson, S.M. Magorrian, R. Williams, A. Young, D.M. Small, C.J. Scott, et al., CCL2 is transcriptionally controlled by the lysosomal protease cathepsin S in a CD74-dependent manner, Oncotarget 6 (30) (2015) 29725–29739.
[44] L.L. Chan, B.K. Cheung, J.C. Li, A.S. Lau, A role for STAT3 and cathepsin S in IL-10 down-regulation of IFN-gamma-induced MHC class II molecule on primary human blood macrophages, J. Leukoc. Biol. 88 (2010) 303–311.
[45] J.M. Rybicka, D.R. Balce, S. Chaudhuri, E.R. Allan, R.M. Yates, Phagosomal proteolysis in dendritic cells is modulated by NADPH oxidase in a pH-independent manner, EMBO J. 31 (2012) 932–944.
[46] E.R. Allan, P. Tailor, D.R. Balce, P. Pirzadeh, N.T. McKenna, B. Renaux, et al., NADPH oxidase modifies patterns of MHC class II-restricted epitopic repertoires through redox control of antigen processing, J. Immunol. 192 (2014) 4989–5001.

[47] Y. Xu, P. Schnorrer, A. Proietto, G. Kowalski, M.A. Febbraio, H. Acha-Orbea, et al., IL-10 controls cystatin C synthesis and blood concentration in response to inflammation through regulation of IFN regulatory factor 8 expression, J. Immunol. 186 (2011) 3666–3673.
[48] Y. Xu, Y. Ding, X. Li, X. Wu, Cystatin C is a disease-associated protein subject to multiple regulation, Immunol. Cell Biol. 93 (2015) 442–451.
[49] R. Janowski, M. Kozak, E. Jankowska, Z. Grzonka, A. Grubb, M. Abrahamson, et al., Human cystatin C, an amyloidogenic protein, dimerizes through three-dimensional domain swapping, Nat. Struct. Biol. 8 (2001) 316–320.
[50] S.L. Jiang, Z.M. Liu, Z.R. Sun, Y. Cao, L.B. Liu, [A method for registration of stomach movement of rabbits in chronic experiments]. Sheng li xue bao, Acta physiol. Sin. 38 (1986) 102–106.
[51] D. El-Sukkari, N.S. Wilson, K. Hakansson, R.J. Steptoe, A. Grubb, K. Shortman, et al., The protease inhibitor cystatin C is differentially expressed among dendritic cell populations, but does not control antigen presentation, J. Immunol. 171 (2003) 5003–5011.
[52] N. Fissolo, M. Kraus, M. Reich, M. Ayturan, H. Overkleeft, C. Driessen, et al., Dual inhibition of proteasomal and lysosomal proteolysis ameliorates autoimmune central nervous system inflammation, Eur. J. Immunol. 38 (2008) 2401–2411.

Please cite this article in press as: A. Steimle, et al., Symbiotic gut commensal bacteria act as host cathepsin S activity regulators, Journal of Autoimmunity (2016), http://dx.doi.org/10.1016/j.jaut.2016.07.009

International Journal of Medical Microbiology xxx (2016) xxx–xxx

Contents lists available at ScienceDirect

International Journal of Medical Microbiology

journal homepage: www.elsevier.com/locate/ijmm

Structure and function: Lipid A modifications in commensals and pathogens

Alex Steimle, Ingo B. Autenrieth, Julia-Stefanie Frick*

Institute of Medical Microbiology and Hygiene, University of Tübingen, Elfriede-Aulhorn-Str. 6, D-72076 Tübingen, Germany

ARTICLE INFO

Article history:
Received 2 February 2016
Received in revised form 1 March 2016
Accepted 2 March 2016

Keywords:
Lipid A
Homoeostasis
Inflammation

ABSTRACT

Lipopolysaccharides (LPS) of Gram negative bacteria are one of the most potent stimulators of the host innate immune system and LPS recognition is essential for the host organism to clear infections of invading bacterial pathogens. Here we review on the latest research on how LPS is sensed by host cells and how distinct LPS structures differentially modulate the strength of the host immune response. Much is known about host immunological reactions towards pathogens via recognition of their LPS, as well as strategies of pathogens to modulate their LPS structure in order to evade the immune system. However, less is known about differential sensing of lipopolysaccharides of commensal bacteria in the intestine and how this contributes to manifestation or destruction of the intestinal homeostasis. LPS sensing is necessary to fight pathogens. However, sensing of LPS of gut commensal bacteria can simultaneously be disadvantageous for the genetically predisposed host, since this might lead to damage of the intestinal homeostasis and therefore to chronic intestinal inflammation. However, less immunogenic LPS could also serve as therapeutics to antagonize an overreacting innate immune system. Therefore, commensal gut bacteria-derived LPS could prevent from uncontrolled intestinal immune response in the intestine which makes LPS an attractive therapeutical approach to treat e.g. IBD.

1. Introduction

Lipopolysaccharides fulfil two major functions. First, the LPS anchored in the outer bacterial membrane provides a protective function for Gram negative bacteria and therefore acts as a defence mechanism against harsh environmental conditions. It provides a barrier against surrounding stress factors which therefore makes LPS indispensable for bacterial viability in various distinct ecosystems (Silipo et al., 2012). By substituting the lipid A sugar moieties with phosphate groups, the bacterium achieves to create a negatively charged outer membrane which can therefore interact with divalent cations present in the surrounding milieu. This plays an important role for the rigidity and the tightness of the outer membrane and hence mediates bacterial resistance to external stress factors (Alexander and Rietschel, 2001). Second, LPS is one of the most conserved structures within all Gram negative bacterial species. This makes LPS an important pathogen associated molecular pattern (PAMP) to be recognized by the mammalian innate immune system which can subsequently initiate the clearance of a bacterial infection. This important immunological reaction contributes to the manifestation of relatively conserved molecular structures in mammals for the recognition of this PAMP (Akira and Takeda, 2004). A timely recognition and sensing of LPS of invading Gram negative bacteria strongly accounts for host immune system activation (Netea et al., 2002). However, the initiated immune response has to be balanced. Uncontrolled bacterial overgrowth within the mammalian body usually leads to the release of large amounts of non-membrane bound LPS which can, in turn, result in exaggerated systemic host immune responses. In severe cases, this leads to septic shock with fatal consequences for the host (Bone, 1991; Bone et al., 1997).

2. Structure of lipopolysaccharides

LPS consists of three genetically, biologically and chemically distinct domains (Alexander and Rietschel, 2001) (Fig. 1): (I) the more or less acylated and phosphorylated lipid A being anchored in the bacterial outer membrane, (II) the core oligosaccharide linked by 3-deoxy-D-*manno*-oct-ulosonic acid (Kdo) with lipid A and (III) the so-called O-antigen or O-specific polysaccharide, with the latter two pointing to the aqueous environment. Lipopolysaccharides that comprise all three regions are called smooth (S)-form LPS, while LPS lacking the O-antigen are named rough (R)-form LPS or lipooligosaccharide (LOS) (Fig. 1). The lipid A structure in

* Corresponding author. Tel.: +49 70712982351.
E-mail address: julia-stefanie.frick@med.uni-tuebingen.de (J.-S. Frick).

http://dx.doi.org/10.1016/j.ijmm.2016.03.001

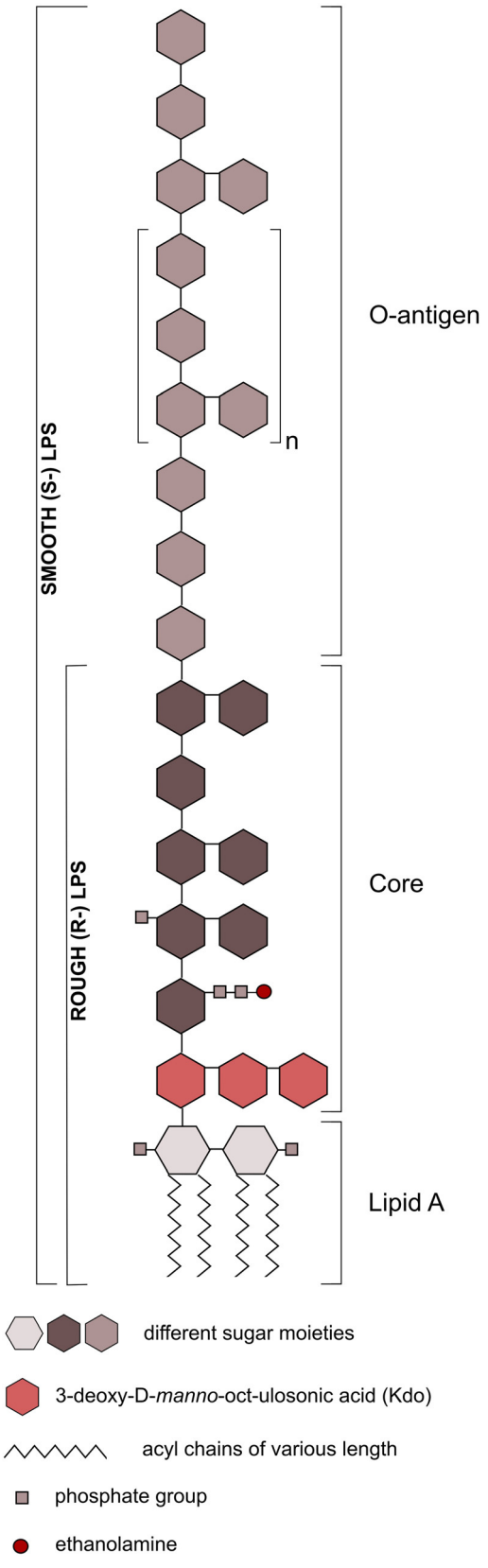

Fig. 1. *Schematic diagram of the general structure of lipopolysaccharides of Gram negative bacteria.* Lipolysaccharides of Gram negative bacteria consist of three main subunits (from bottom to top): lipid A, the core region and the O-antigen. Lipid A and the core-region form rough (R)-type LPS. Lipid A, the core-region and the O-antigen together form smooth (S)-type LPS. The number and chemical structure of the acyl chains can vary. Sugar moieties are depticted as hexagons in different colours. The number and chemical structure of these sugar moieties can vary.

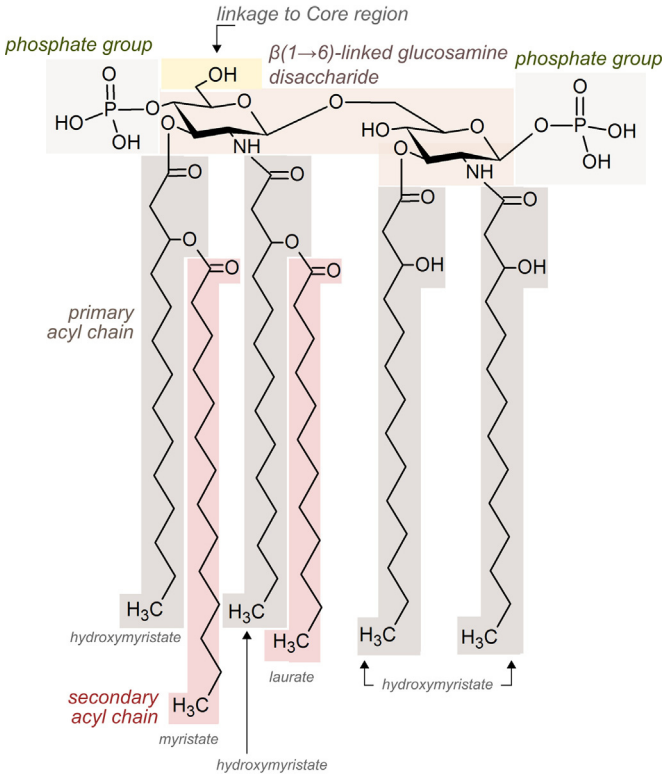

Fig. 2. *Detailed Structure of E. coli lipid A. E. coli* lipid A contains a β(1 → 6)-linked glucosamine disaccharide backbone (light brown). The hydroxyl group (light yellow) of the distal glucosamine links lipid A to the Core region. The two phosphate groups are depicted in light green. Primary acyl chains (light grey) are directly linked to the sugar moieties, secondary acyl chains (light red) are esterified with the hydroxyl groups of primary acyl chains. All primary acyl chains of *E. coli* lipid are hydroxymyristates, one of the two secondary acyl chains is myristate while the other one being laurate.

general is highly conserved, which is important for host receptor recognition.

3. Lipid A

Basically, lipid A is made up of a $\beta(1 \rightarrow 6)$-linked glucosamine disaccharide backbone which is mostly phosphorylated at position 1 and 4′ of the saccharides and acylated at positions 2 and 3 of each monosaccharide portion (Galanos and Freudenberg, 1993; Homma et al., 1985; Kotani et al., 1985).

Usually, lipid A is hexaacetylated, meaning that six acyl chains of variable length are esterified with the disaccharide backbone. Primary acyl chains are directly esterified with the sugar moiety while so-called secondary acyl chains form ester bonds with hydroxyl groups of primary acyl chains. “Symmetrically” acetylated lipid A means that each glucosamine moiety carries the same number of acyl chains. *Escherichia coli* LPS is an example for containing an “asymmetrically” acetylated lipid A, since 4 of its 6 acyl chains are carried by the first glucosamine. Lipid A is embedded in the outer leaflet of the bacterial outer membrane through electrostatic and mainly hydrophobic interactions. Here, the diglucosamine part of the lipid A is orientated towards the exterior environment while the lipid A acyl chains point to the hydrophilic interior of the membrane (Raetz and Whitfield, 2002). Fig. 2 illustrates the detailed structure of *E. coli* lipid A which is considered to be the prototype form of all lipid A structures. Its two glucosamine residues are each substituted by a phosphate residue at positions 1 and 4′, respectively. The hydroxyl groups at positions 2 and 3 of each monosaccharide are

Please cite this article in press as: Steimle, A., et al., Structure and function: Lipid A modifications in commensals and pathogens. Int. J. Med. Microbiol. (2016), http://dx.doi.org/10.1016/j.ijmm.2016.03.001

esterified with hydroxymyristate, a saturated acyl chain with 14 carbon atoms, as primary acyl chain. Two additional secondary acyl chains, laurate (C_{12}) and myristate (C_{14}), are coupled to hydroxymyristates at positions 2′ and 3′ (Raetz and Whitfield, 2002) (Fig. 2).

However, Lipid A structures widely vary among the different bacterial species. Sometimes there are even more than one different lipid A structure within a single species (Raetz and Whitfield, 2002). The sugar moieties of the saccharide backbone are mostly 2-amino-2-deoxy-D-glucopyranoses (D-GlcpN) like in *E. coli* lipid A, but can also be, i.e. 2,3-diamino-2,3-dideoxy-D-glucopyranose (D-GlcpN3N) containing an additional amino group (Molinaro et al., 2015; Roppel and Mayer, 1975). Other potential differences refer to the number, position and length of the esterified acyl chains, the presence of charged groups on the polar heads as well as the number of phosphate groups coupled to the disaccharide backbone (Raetz et al., 2007). The lipid A part of LPS is coupled to the core region through linkage via the non-reducing distal amino sugar of lipid A (Molinaro et al., 2015) (Fig. 2).

In *E. coli* lipid A, C12 and C14 acyl chains are the only ones being esterified with the disaccharide backbone (Fig. 2). However, other bacteria can provide differentially acylated lipid A which is supposed to be mediated by other enzymes than the ones in *E. coli* which are specific for substituting C14 and C12. However, it could be demonstrated that in *Bacteroides fragilis* and *Bordetella pertussis*, the enzymes catalysing the acylation of the sugar moieties seem to be multifunctional, therefore being able to recognize more than one specific acyl chain as a substrate (Bainbridge et al., 2008; Sweet et al., 2002).

The number of acyl chains esterified with the disaccharide backbone varies among the lipid A of different bacterial species. As mentioned above, the prototype hexaacylated lipid A contains six acyl chains. However, certain bacterial species can provide "underacylated" lipid A structures, like tetraacylated *Helicobacter pylori* lipid A (Mattsby-Baltzer et al., 1992; Moran et al., 1997) (Fig. 4), or even "overacylated" structures like heptaacylated *Acinetobacter* spp. lipid A (Leone et al., 2006, 2007).

The phosphorylation pattern of the disaccharide backbone is also not conserved among different bacterial species. As phosphate groups are negatively charged, a more or less phosphorylated lipid A allows bacteria to change the net charge of their surface. This surface net charge may vary considerably dependent on environmental factors like temperature, pH value or, important for immune evasion, the presence of antibiotics and antimicrobial peptides (AMPs). The phosphate groups can mediate interactions with neighbouring phosphorylated lipid A structures via divalent cations being present in the surrounding environment. These interactions considerably increase the stability of the bacterial outer membrane and reduce the permeability of the cell wall (Molinaro et al., 2015).

4. Core and O-antigen

The core moiety of LPS starts with at least one residue of 3-deoxy-D-manno-oct-ulosonic acid (Kdo) which is directly linked to one of the sugar moieties of lipid A (Figs. 1 and 2). The core contains up to 15 sugar residues and provides antigenic properties in the case of a missing O-antigen (rough-type LPS) (Caroff and Karibian, 2003). The O-antigen, sometimes also named O-specific polysaccharide or simply "glycan" consists of repeating units of usually not more than five sugar units. The O-antigen can only be found in smooth type LPS where it determines its antigenic properties (Raetz and Whitfield, 2002).

5. Molecular weight and micelle formation of isolated LPS

Usually, LPS is anchored in the bacterial outer membrane. However, for immunological sensing by the host immune system it has to be released from the bacterial membrane. The exact conformation of isolated, non-bacterially attached, LPS is not easy to determine. However, this is an important issue for in vitro experiments using isolated LPS in aqueous solutions. Due to its amphiphilic structure, with the acyl chains of the lipid A forming the hydrophobic part and the sugar residues of lipid A, the core and the O-antigen building up the hydrophilic part, isolated LPS rarely forms monomers in any solvent. Therefore, molecular weight determination of either smooth or rough LPS is not trivial. Dependent on the presence of divalent cations, detergents or the pH value of the solvent, these large amphiphilic molecules form either monomers, micelles or even vesicles. The critical LPS concentration in aqueous solutions for micelle formation is stated to be 11 μg/mL (Aurell and Wistrom, 1998). Additionally, micelle formation capacity is dependent on the structure of LPS, especially if it consists of the S- or R- form. These micelles usually provide low solubility in any solvent (Molinaro et al., 2015). However, the typical molecular weight of monomeric S-form LPS of *E. coli* is reported to be between 11.8 and 18 kDa.

6. Biosynthesis of lipopolysaccharides of Gram negative bacteria

The biosynthesis of hexaacetylated *E. coli* LPS has been described in detail in 2002 by Raetz and Whitfield (Raetz and Whitfield, 2002). Briefly, the formation of Kdo2-substituted lipid A includes nine enzymatic steps catalyzed by the enzymes LpxA, LpxB, LpxC, LpxD, LpxH, LpxK, LpxL, LpxM and WaaA. This Kdo2 substituted lipid A is synthesized in the bacterial cytosol and acyl chain substitution involves the aid of bacterial acyl carrier proteins. Lipid A-Kdo2 is completely synthesized in the cytosol either by soluble cytosolic proteins or enzymes that are associated with the cytosolic part of the inner bacterial membrane (Carty et al., 1999; Clementz et al., 1996, 1997; Garrett et al., 1997; Vorachek-Warren et al., 2002). The LPS core region is also synthesized in the cytosol. Lipid A-Kdo2 and the core region together form the rough-type (R-) LPS which is transported across the inner membrane into the periplasmatic space. Once located there, R-type LPS can either be directly inserted into the outer leaflet of the outer bacterial membrane or it can be converted into the S-(smooth) type LPS in the periplasmatic space before being shuttled to the outer membrane. The flipping of the lipid A coupled LPS core is carried out by MsbA, an ATP-binding cassette (ABC) transporter protein (Karow and Georgopoulos, 1993; Zhou et al., 1998).

Although this describes only the events during biosynthesis of LPS in *E. coli*, the general mechanisms seem to be conserved among most Gram negative bacteria. Bioinformatics-based studies revealed that many Gram negative bacteria share enzymes like the ones that are used in *E. coli* for LPS biosynthesis. But since lipid A structures differ between distinct bacteria, alterations in the structure are supposed to be due to genetic and/or environmental differences or influences (Molinaro et al., 2015; Raetz et al., 2007).

7. Extracellular sensing of LPS through recognition by the MD-2/TLR4 receptor complex

Long time, Toll-like receptor 4 (TLR4) was supposed to be the sole LPS sensor in mammalian organisms. TLR4 is a transmembrane protein composed of 22 leucine-rich repeats (LRRs), one transmembrane domain and a cytosolic Toll/IL-1 receptor (TIR) domain, the latter being a common feature in all TLRs. LPS is anchored in the

Please cite this article in press as: Steimle, A., et al., Structure and function: Lipid A modifications in commensals and pathogens. Int. J. Med. Microbiol. (2016), http://dx.doi.org/10.1016/j.ijmm.2016.03.001

bacterial outer membrane. However, for being recognized by the host immune system, LPS has to be removed from the membrane or membranous structures. This can either happen indirectly by bacterial cell death leading to a release of LPS or directly by the soluble host protein lipid A-binding protein (LBP), a lipid transferase that is able to remove LPS molecules from the bacterial membrane (Miyake, 2006). LBP is present in the serum to sense bacterial presence in the blood. Additionally, LBP is secreted into the intestinal lumen where it is involved in sensing not only invading pathogens, but also commensal-derived LPS (Hansen et al., 2009) (Vreugdenhil et al., 2000). In general, commensal intestinal bacteria can be subdivided into two distinct groups, dependent on their potential to induce disease under certain circumstances: (1) symbiotic bacteria that never induce disease and (2) pathobiontic bacteria which are potentially able to induce pathological immune reactions. Sensing of LPS molecules from these two different bacterial subgroups is important for a balanced intestinal immune system. This fact makes LBP essential for the maintenance of the intestinal homeostasis. LBP transports monomeric lipid A molecules to CD14. CD14 can either be a membrane-anchored protein of TLR4-expressing cells or can be secreted into the environment as a soluble protein. The presence of CD14 is important for LPS sensing, since it increases the susceptibility of TLR4-expressing cells to LPS by factor 10^2 to 10^3 (Wright et al., 1990). CD14-associated monomeric LPS is then shuttled to MD-2 (Fig. 3A). Like CD14, MD-2 can be a soluble protein secreted into the cell exterior or it can be permanently attached to a TLR4 monomer via hydrogen bonds (Kim et al., 2007; Visintin et al., 2003). Binding of LPS to MD-2 leads to formation of a heterooligomeric protein complex consisting of two MD-2 and two TLR4 molecules (Fig. 3A). This protein complex formation is initially induced through interaction at the extracellular domains. These extracellular protein-protein-interactions, in turn, result in dimerization of TIR-domain containing intracellular cytosolic parts of the TLR4 receptors leading to Myeloid differentiation primary response gene 88 (MyD88)- or TIR-domain-containing adapter-inducing interferon-β (TRIF)-dependent downstream signalling (Molinaro et al., 2015) (Fig. 3A). Binding of LPS to MD-2 leads to conformational changes within MD-2 therefore promoting MD-2 binding to the ectodomain of TLR4 (Ohto et al., 2007, 2012). In 2009, Park et al. (2009) revealed interesting detailed informations on the binding conditions within a crystallized hexaacylated LPS-MD-2-TLR4 complex with both, murine and human TLR4 ectodomains. In general, five of the six acyl chains of hexaacylated LPS are buried inside a binding grove in the interior of MD-2. The sixth acyl chain is located on the surface of MD-2 and partially exposed to the surrounding solvent. In combination with hydrophobic residues of MD-2, this 6th acyl chain promotes intermolecular interactions with TLR4 (Jin and Lee, 2008; Ohto et al., 2012). Taken together, the initial binding of LPS to MD-2 creates a new binding interface for MD-2 and therefore promotes MD-2 binding to TLR4 (Park et al., 2009). The resulting conformational changes within this complex lead to dimerization of the C-termini of the TLR4 ectodomaines. This event is supposed to mediate the dimerization also of the cytosolic TIR domains of the TLR4 which initializes intracellular downstream signalling (Jin and Lee, 2008; Kim et al., 2007; Ohto et al., 2012) (Fig. 3A). Taken together, MD-2 binding of lipid A is essential for TLR4-mediated LPS recognition. However, LBP and CD14 are supposed to be important for LPS sensing at low LPS concentration whereas they seem to be dispensable at high concentrations (Wurfel et al., 1995; Wurfel and Wright, 1997). Activation of the TLR4-receptor complex results in an activation of more than 10^3 genes (Bjorkbacka et al., 2004) and promotes, i.e. the secretion of pro-inflammatory cytokines like TNF, IL-6, IL-1β as well as in enhanced production of the superoxide anion O_2^-, hydroxyl radicals, NO and antimicrobial peptides (AMPs) (Ohto et al., 2007; Poltorak et al., 2000) (Fig. 3A).

8. Intracellular sensing of LPS through recognition by cytosolic caspase-11

Caspases are intracellular cysteine proteases. The so-called "inflammatory caspases" comprise a certain subset of these enzymes which are critical for clearance of microbial infections and initiation of the host immune system to fight pathogens (Lamkanfi et al., 2002; Martinon and Tschopp, 2004). Among others, murine caspases 1, 4, 5 and 11 as well as human caspases 4 and 5 are considered to be such inflammatory caspases. They all have in common that they are synthesized as proteolytically inactive zymogens, needing proteolytic cleavage to induce enzymatic activity. Furthermore, they share an *N*-terminal domain responsible for protein-protein interactions called caspase activation and recruitment domain (CARD). All genes of inflammatory caspases are encoded in an inflammatory gene cluster. Once activated, inflammatory caspases lead to the maturation of the pro-inflammatory cytokines IL-1β and IL-18 and induce a special kind of cell death, pyroptosis. Both mechanisms are mediated by activation of cytosolic inflammasomes. Inflammasome activation can be carried out through two different mechanisms: the canonical and non-canonical way. The classical, or "canonical" way to activate inflammasomes in a caspase-dependent manner, involves proteins like Nod-like receptor protein 3 (NLRP3) or NLR family CARD domain-containing protein 4 (NLRC4) engaging the intracellular adaptor protein NLR family CARD domain-containing protein 4 (ASC) resulting in an activation of caspase-1 (Casp1) which leads to a Casp1-catalyzed cleavage of IL-1β and IL-18 followed by secretion of the mature cytokines (Mariathasan et al., 2006; Martinon et al., 2006; Schroder and Tschopp, 2010). The non-canonical way includes Casp1 activation with the requirement of Casp11 (Wang et al., 1996). Interestingly, Casp11 can directly sense the presence of cytosolic lipid A independently from TLR4 recognition but also leading to inflammasome activation and consequently to IL-1β and IL-18 secretion as well as pyroptosis (Fig. 3B).

The non-canonical inflammasome activation requires two independent activation steps: First, a priming signal that leads to an increase in intracellular expression of inflammasome components like Casp1, NLRP3, ASC and Casp11. This initial event can be lipid A binding to TLR4 (Raetz and Whitfield, 2002) which efficiently enhances Casp11 gene transcription (Hagar et al., 2013; Kayagaki et al., 2013; Wang et al., 1996). However, the priming event is not restricted to TLR4 recognition of lipid A. In fact, activation of TLR2 and/or TLR7 by other bacterial components is sufficient to act as such a priming signal (Takeuchi and Akira, 2010). Second, after the priming event, intracellularly located LPS can directly bind to Casp11 leading to its activation which subsequently results in inflammasome activation. It could already be shown that this Casp11-mediated non-canonical inflammasome activation, independent of TLR4 activation, plays an important role during bacterial challenge of the host with pathogens like *Shigella flexneri* (Rathinam et al., 2012), *Salmonella typhimurium* (Broz et al., 2012a), *Legionella pneumophila* (Case et al., 2013) or *Burkholderia thailandiensis* (Aachoui et al., 2013) but is also important for sensing the LPS of gut commensals like *E. coli* (Kayagaki et al., 2013). Furthermore, it seems that Casp11-mediated sensing of Gram negative bacteria is not just an alternative to the TLR4-mediated way but rather seems to be critical for an adequate response of the immune system to these bacteria (Aachoui et al., 2013; Broz et al., 2012b; Kayagaki et al., 2011; Rathinam et al., 2012).

But how can lipid A of non-invading bacteria like *E. coli* be sensed intracellularly by cytosolic inflammasome components? As known so far, Casp11 non-canonical inflammasome activation mostly occurs in macrophages in mice, although a recent publications reports on Casp11 expression in mouse epithelial cells (Knodler et al., 2014). Macrophages are phagocytes which can include

Please cite this article in press as: Steimle, A., et al., Structure and function: Lipid A modifications in commensals and pathogens. Int. J. Med. Microbiol. (2016), http://dx.doi.org/10.1016/j.ijmm.2016.03.001

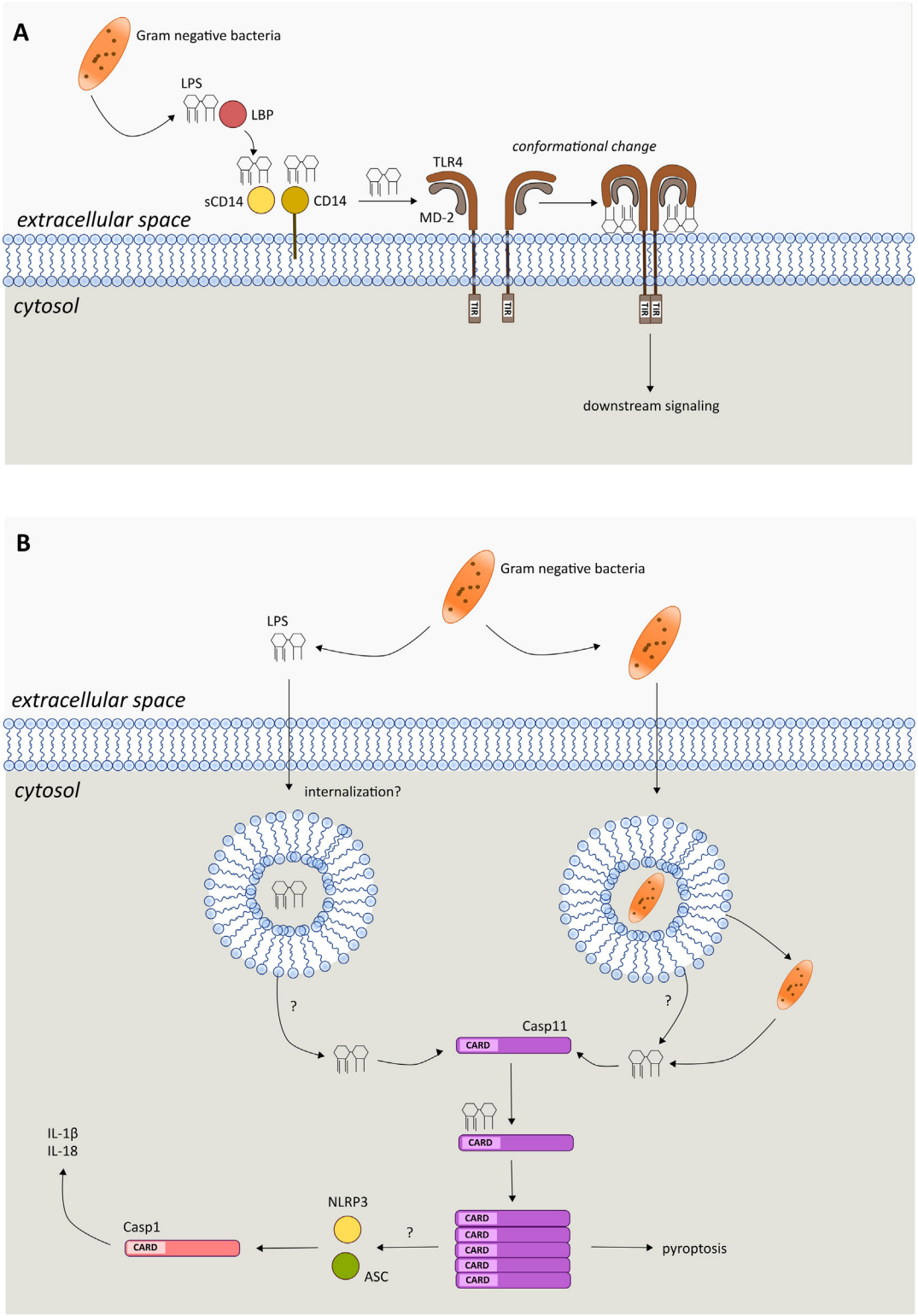

Fig. 3. *Molecular mechanisms of extracellular and intracellular sensing of bacterial LPS.* (A) Extracellular LPS sensing. The host lipid binding protein (LBP) samples LPS from the outer membrane of Gram negative bacteria and mediates its transport to host CD14. CD14 can either be soluble (sCD14) or anchored in the membrane of TLR4 expressing cells. CD14 shuttles LPS to the TLR4 coreceptor protein MD-2 which initiates a conformational change in MD-2 and TLR4, resulting in dimerization of the extracellular and subsequently of the intracellular TIR domains. TIR domain dimerization mediates downstream signaling leading to enhanced expression of more than 1000 different genes. (B) Intracellular LPS sensing. Left side: LPS that is present in the extracellular space can enter (for example by, but not exclusively due to, receptor-mediated endocytosis) the vacuoles of caspase-11 (Casp11) expressing cells. LPS escapes the vacuoles via a yet unidentified mechanism. Right side: Gram negative bacteria can be sampled by phagocytotic cells like Casp11 expressing macrophages. The LPS of non-cell invading bacteria or whole cell invading bacteria are relieved into the cytosol. Both: LPS present in the cytosol actively binds to the CARD domain of Casp11 leading to Casp11 oligomerization that results in Casp11 activation. By a yet unknown mechanism, this Casp11 activation results in inflammasome assembly resulting in Caspase-1 (Casp1) mediated secretion of the pro-inflammatory cytokines IL-1β and IL-18. Casp11 oligomerization can also lead to pyroptosis, a special kind of cell death.

Please cite this article in press as: Steimle, A., et al., Structure and function: Lipid A modifications in commensals and pathogens. Int. J. Med. Microbiol. (2016), http://dx.doi.org/10.1016/j.ijmm.2016.03.001

extracellular bacteria into vacuolar phagolysosomes. Some bacteria, which are specialized in intracellular replication, like *Burkholderia* spp. can actively escape the phagosomes into the cytosol of host macrophages where they can trigger LPS-dependent Casp11 activation (Aachoui et al., 2013). *Salmonella typhimurium* is able to rupture the membrane of the bacteria-containing vacuole with the use of Guanine-binding protein 2 (GBP2). However, the presence of GBP2 is obviously dispensable for Casp11-mediated sensing of *S. typhimurium* LPS (Kayagaki et al., 2013), although other studies report GBPs to be critical for the release of vacuole content (Meunier et al., 2014; Pilla et al., 2014). How LPS of other Gram negative bacteria which are not specialized in host cell invasion like *E. coli* or *Citrobacter rodentium* (Kayagaki et al., 2013; Meunier et al., 2014) can be translocated from the vacuole to the cytosol of host macrophages in order to be sensed by Casp11 is unknown so far (Fig. 3B). Most in vitro studies therefore used methods like electroporation or transfection to make cytosolic Casp11 capable of LPS sensing.

It is already clear that, lipid A is the decisive part for intracellular Casp11-mediated LPS sensing (Hagar et al., 2013; Kayagaki et al., 2013), just like it is the case for TLR4-mediated recognition of LPS. It could also be shown that the categories "antagonistic" and "agonistic" in terms of LPS endotoxicity can also be referred to lipid A-induced Casp11 activation, since lipid A structures that are weakly agonistic or antagonistic for TLR4 activation also fail to induce Casp11 activation (Hagar et al., 2013; Kayagaki et al., 2013). This is not due to a lower affinity for lipid A to Casp11 since it could be demonstrated that these less agonistic lipid A structures efficiently bind to Casp11 (Shi et al., 2014). However, it is not known if the same structural criteria for being agonistic or antagonistic, which are valid in case of MD-2/TLR4-mediated lipid A sensing, also counts for Casp11. When lipid A is located in the cytosol, it is able to directly bind to Casp11 with the help of the Casp11- intrinsic CARD domain subsequently leading to Casp11 oligomerization (Shi et al., 2014). The exact mechanisms behind these findings are not understood so far. However, it is clear that this lipid A- induced Casp11 oligomerization leads to proteolytical activation of Casp11 within the oligomer (Shi et al., 2014; Shin et al., 2007). Lipid A binding to Casp11 is highly specific, since no other LPS component could be shown to interact with Casp11 and, inversely, no other caspase interacts with lipid A (Shi et al., 2014). Caspase-11 (Casp11) was initially discovered by Wang et al (Wang et al., 1996) and two corresponding orthologues of murine Casp11 could be discovered in humans: caspase-4 (Casp4) and caspase-5 (Casp5) (Stowe et al., 2015).

9. Other host proteins being involved in LPS sensing

Apolipoprotein CI (ApoCI) is a small apolipoprotein which is present in the serum. It has been shown to provide an LPS-binding motif with which it is able to bind to bacterial LPS, finally enhancing an LPS induced inflammatory host response (Berbee et al., 2006). It seems to act in a comparable way like LBP and promotes CD14/MD-2/TLR4-mediated LPS signalling (Berbee et al., 2010). By its strong affinity to bacterial LPS it enhances the residence time of LPS in the circulation (Berbee et al., 2006). This makes ApoCI an important feature to protect from fatal sepsis, since the prolonged residence time enhanced the access for LPS-sensing blood cells in order to fight invading pathogens, as demonstrated in a *Klebsiella pneumoniae* sepsis model (Berbee et al., 2006). Acyloxyacyl hydrolase (AOAH) is an enzyme, expressed in host antigen presenting cells, that renders agonistic lipid A into non-TLR4 signaling structures by removing acyl chains from the lipid A disaccharide backbone (Munford and Hall, 1986). AOAH is a critical enzyme when it comes to inactivation of agonistic LPS of pathogens and endotoxin tolerance. Such a tolerance towards pathogen-derived lipid A diminishes the immune response of the host to fight these invading microbes (Lu et al., 2008). The restoration of a powerful immune response is dependent on the inactivation of the pathogen's lipid A, making AOAH crucial in this context (Lu et al., 2008). The impact of AOAH on inactivation of commensal lipid A is less clear. It could be shown that AOAH is preferentially expressed in a Th17-immune response mediating dendritic cell subpopulation and that AOAH deficiency favours induction of T_{reg} cells over induction of Th17 cells (Janelsins et al., 2014). However, the correlation between AOAH activity, microbiota composition (and therefore lipid A structures) and the outcome of inflammatory bowel disease still needs to be elucidated.

10. Immunogenicity of lipopolysaccharide

As already mentioned, LPS structure, especially its lipid A chemistry, differs among distinct bacterial species. Indeed, the exact LPS structure, and in this context mainly the lipid A structure, determines LPS immunogenicity and is therefore decisive for its function (Brandenburg et al., 1993; Seydel et al., 2000). LPS which triggers a strong pro-inflammatory reactions of host cells are named "agonistic" lipolysaccharides. In contrast, structurally different lipid A can also result in weak inflammatory host responses, hence being called "weak agonistic" or it can even completely block any pro-inflammatory reactions by binding to corresponding host receptors. The latter lipopolysaccharides are therefore called "antagonistic". Most Gram negative bacteria express agonistic hexaacylated LPS like *E. coli* LPS, which is one of the most potent agonists of the human innate immune system (Beutler and Rietschel, 2003; Raetz and Whitfield, 2002; Zahringer et al., 1994) (Fig. 4A). Usually the number of lipid A acyl chains directly correlates with the ability to induce cytokine production whereas the hexaacylated forms usually are the most immunostimulating ones (Munford and Varley, 2006). Within a biological system, distinct lipid A structures compete for binding to host receptors. Antagonistic lipid A might therefore compete with agonistic LPS for host receptor binding. Hexaacylated lipid A seems to promote the strongest proinflammatory immune reactions after binding to TLR4. This is due to the fact that the first five acyl chains are buried in a hydrophobic cavity of the TLR4 adaptor molecule MD-2 while the sixth chain mediates the binding to TLR4, the precondition for TLR4-mediated intracellular signalling (Maeshima and Fernandez, 2013; Park et al., 2009). Therefore, TLR4-mediated signalling usually is drastically reduced if this sixth acyl chain is missing. However, due to the already mentioned differences in the structures of the lipid A binding cavity of the TLR4 receptor between different mammal species, distinct lipid A structures can provide a different immunogenic potential between these species. Fig. 4 summarizes different lipid A structures and their corresponding agonistic or antagonistic properties.

Not only acyl chains contribute to the immunogenic properties of lipid A, but also the number of phosphate groups. A deletion of a phosphate group can result in a loss of the endotoxic activity (Rietschel et al., 1994). Most lipid A structures contain two phosphate residues, one on each sugar moiety. However, some bacterial lipid As lack one or even both of them, therefore altering its immunogenic potential. For example, *Francisella tularensis* lacks one or both phosphate groups and this is considered to be, at least in part, the reason for its weak agonistic property (Molinaro et al., 2015) (Fig. 4E). Furthermore, the non-phosphorylation might also be seen as an immune evasion strategy for certain bacteria since some antimicrobial peptides (AMPs) specifically target negative charges on bacterial surfaces and a loss of negatively charged phosphate residues therefore renders bacteria to be invisible for these AMPs.

Please cite this article in press as: Steimle, A., et al., Structure and function: Lipid A modifications in commensals and pathogens. Int. J. Med. Microbiol. (2016), http://dx.doi.org/10.1016/j.ijmm.2016.03.001

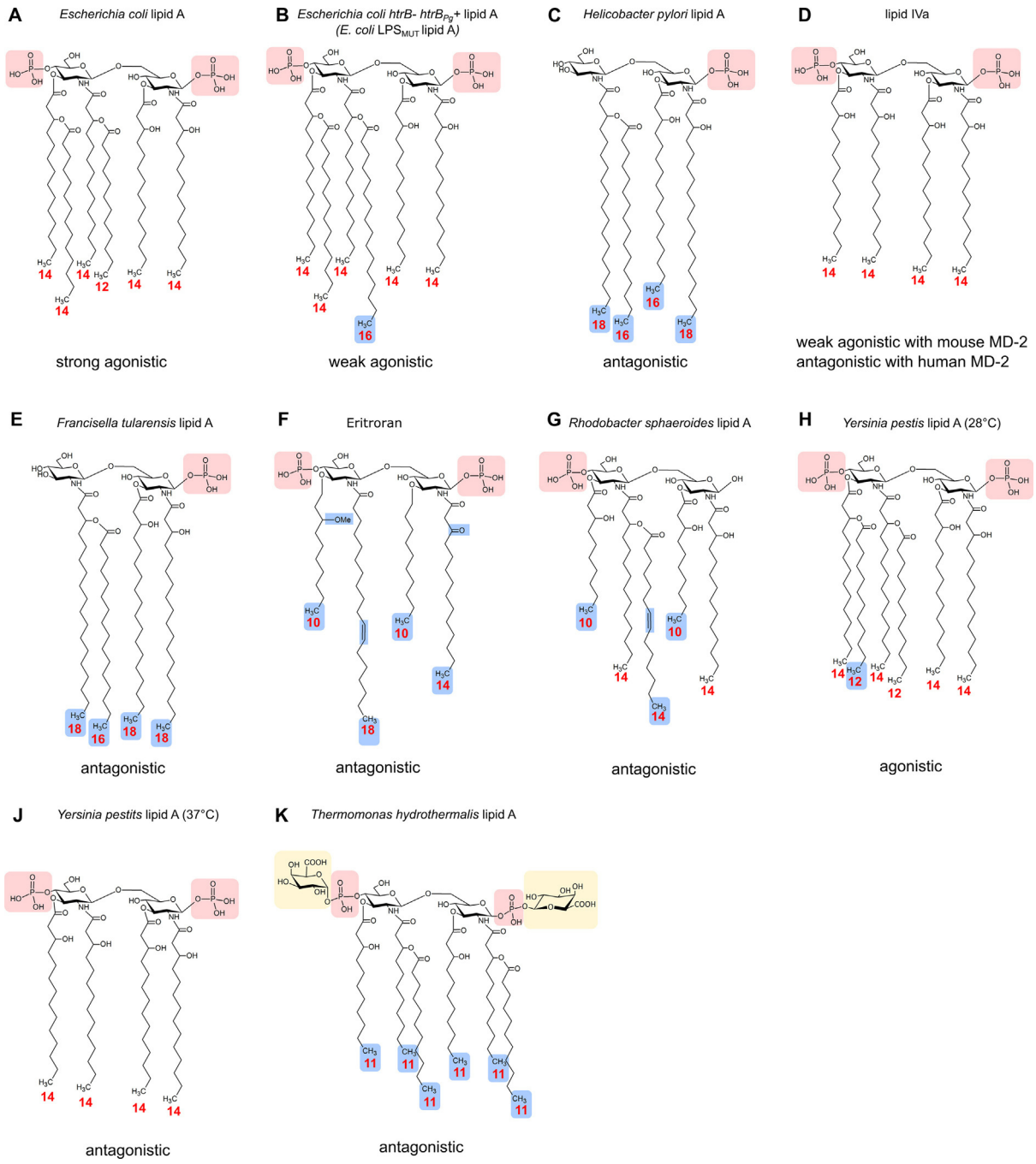

Fig. 4. *Different lipid A structures of various bacteria and their immunogenic potential.* (A) prototype E. coli lipid A. (B–C, E, G–K) lipid A structures of other bacteria. (D) structure of antagonistic lipid IVa. (F) structure of the chemically synthesized TLR4 antagonist Eritroran. Immunogenic phosphate groups are highlighted in light red. The bold red numbers below each acyl chain refers to the number of carbon atoms of the respective chain. Structural differences of the acyl chains compared to prototype agonistic *E. coli* lipid A are highlighted in light blue. Structural differences of the disaccharide backbone compared to prototype agonistic *E. coli* lipid A are highlighted in light yellow. The classification of each lipid A structure as agonistic or antagonistic refers to its immunogenic behaviour due to TLR4 binding. See text for details.

11. Immune-evasion

Induction of antibacterial defence by triggering inflammatory host responses is a crucial function of the innate immune system in response to invading bacteria. This reaction prevents the spreading of bacteria and suppresses the bacterial growth. In many infections with pathogens, the innate immune responses slow the progress of infection and allow for the adaptive immune responses to develop (Montminy et al., 2006). Suppressing or evading the host immune responses is a successful strategy of pathogenic bacteria, known as immune-evasion (Montminy et al., 2006). Immune evasion strategies based on lipid A modification help to promote the survival of Gram negative bacteria by evading host immune responses that are directed against bacterial invasion, chronic persistence or susceptibility to cationic antimicrobial peptides (CAMP) (Needham and Trent, 2013).

As mentioned above, the acylation pattern of lipid A varies between species and is heterogeneous even within a single species (Dixon and Darveau, 2005; Raetz and Whitfield, 2002; Zähringer and Rietschel, 1999). Environmental conditions are known to influence the lipid A structure by modulating for example the number, composition and location of acyl chains

thereby affecting the biological activity of lipid A. The production of weak stimulatory lipid A is thought to be involved in the virulence of several Gram negative pathogens (Dixon and Darveau, 2005).

An impressive and well-characterized example of lipid A modification as immune evasion mechanism represents *Yersinia pestis* (Montminy et al., 2006). *Y. pestis* grown at 21–28 °C (flea temperature) expresses hexaacylated lipid A structures (Fig. 4H), but these lipid A structures are mainly tetraacylated at 37 °C (host temperature) (Kawahara et al., 2002; Knirel et al., 2005; Rebeil et al., 2004) (Fig. 4J). Although hexaacylated lipid A is normally a strong activator of human TLR4, tetraacylated lipid A has a significantly lower activity (Golenbock et al., 1991; Kawahara et al., 2002; Lien et al., 2000; Loppnow et al., 1989; Rebeil et al., 2004) and is thought to act as a TLR4 antagonist (Needham and Trent, 2013). To suppress local inflammatory immune responses, *Y. pestis* uses several parallel mechanisms that individually are necessary for virulence like e.g. a type 3 secretion system (T3SS), releasing immunosuppressive proteins (Nakajima et al., 1995). However, evading activation of TLR4 was shown to be an essential part of the *Y. pestis* immune evasion. The ability of a *Y. pestis* mutant strain expressing lipid A with an increased capacity to activate TLR4 at 37 °C was dominant over the anti-host bacterial defences provided by the T3SS and other *Y. pestis* activities (Montminy et al., 2006). Hence, despite retention of multiple immune evasive proteins used by *Y. pestis* to suppress host responses, a strain producing hexaacylated lipid A and thus being quickly detectable by means of TLR4-MD-2 failed to cause disease (Montminy et al., 2006).

Similar to *Y. pestis, F. tularensis* (Fig. 4E) shows a dynamic regulation of lipid A acyl chain length according to temperature (Okan and Kasper, 2013; Needham and Trent, 2013). *F. tularensis* has two homologues of the essential lipid A biosytheses acyl transferase LpxD, LpxD1/LpxD2, (Valentin-Hansen et al., 2007). LpxD1 has its optimum activity at 37 °C and consistent with this the lpxD1 mutant is unable to express the modified lipid A with longer acyl groups and is severely attenuated in mice (Okan and Kasper, 2013; Li et al., 2012) and is also more susceptible to antibiotics and CAMP by reason of an increased membrane permeability (Li et al., 2012; Needham and Trent, 2013).

Another example of evading the recognition of the host's immune system by modifying the lipid A component of LPS is *H. pylori*. Despite a robust host immune response, *H. pylori* persists within the gastric niche and promotes a chronic infection for the duration of the host's life (Gaddy et al., 2015). *H. pylori* uses two lipid A based immune evasion strategies, evasion of detection by TLR4 and resistance to CAMP. The lipid A *of H. pylori* has a unique structure and lower biological activity as compared to lipid A from other bacteria, e.g. *E. coli* (Chmiela et al., 2014; Moran and Aspinall, 1998; Muotiala et al., 1992). Interestingly *H. pylori* synthesizes a hexaacylated lipid A but exhibits a tetraacylated lipid A lacking phosphate groups at its surface (Needham and Trent, 2013) (Fig. 4C). The structural differences are generated by the action of several enzymes including deacylation by LpxR and dephosphorylation by LpxE and LpxF (Gaddy et al., 2015; Needham and Trent, 2013). Hence *H. pylori* provides a tetraacetylated antagonistic lipid A structure (Fig. 4C) that not only prevents TLR4-mediated activation of the innate immune system (Moran et al., 1997; Ogawa et al., 2003; Raetz et al., 2007), but also from Casp11-mediated inflammasome activation (Kayagaki et al., 2013) (Fig. 3B). Other examples for underacetylated antagonistic lipid A are *Rhodobacter sphaeroides* (Fig. 4G) and *Rhodobacter capsulatus* lipid A structures (Rose et al., 1995).

Many Gram-negative bacteria utilize lipid A modifications to survive the antimicrobial peptide response imposed by the vertebrate host. Altering the bacterial surface charge by e.g. adding positively charged moieties reduces the binding affinity of cationic antimicrobial peptides with the bacterial outer membrane. An important antimicrobial factor is calprotectin. It is a critical component of the host nutrient withholding process, termed nutritional immunity (Gaddy et al., 2015; Gebhardt et al., 2006; Urban et al., 2009). One mechanism of nutritional immunity is the host induced restricted access for bacteria to essential metals (Hood and Skaar, 2012). Calprotectin binds Zn^{2+} and Mn^{2+} with high affinity which starves bacteria of these essential metals, creating a Zn^{2+} and Mn^{2+} limited environment. Additionally, calprotectin exhibits antimicrobial activity against numerous Gram-positive and Gram-negative bacteria (Corbin et al., 2008; Damo et al., 2013; Hood et al., 2012; Liu et al., 2012; Lusitani et al., 2003; Sohnle et al., 2000; Steinbakk et al., 1990). Moreover calprotectin has been demonstrated to inhibit *H. pylori* growth and has the capacity to modify the activity of the cag type IV secretion system. However *H. pylori* is able to persist in the gastric niche despite this robust immune response. One mechanism allowing for persistence is the modification of the *H. pylori* lipid A in response to calprotectin. Thereby the lipid A modification pathway is influenced by the host nutritional immune response as the calprotectin dependent restricted access to essential metals like Zn^{2+} and Mn^{2+} perturbs the function of *H. pylori* enzymes involved in the lipid A modification pathway, resulting in increased bacterial fitness and increased biofilm formation.

Salmonella enterica subsp. enterica serovar Typhimurium is an intracellular pathogen which causes gastroenteritis in humans. In *S. typhimurium* the modification of lipid A is controlled by the PhoPQ system which is activated by low Mg^{2+} concentrations or CAMPs (Guo et al., 1997; Guo et al., 1998; Raetz et al., 2007), e.g. by growing cells under Mg^{2+} limitation or during growth within macrophage phagosomal vacuoles (Martin-Orozco et al., 2006). The activation of the PhoPQ and the PmrAB systems results in an addition of phosphoethanolamine and aminoarabinose and to a PagP and PagL dependent acyl chain remodelling (Richards et al., 2012). In addition LpxO hydrolates *S. typhimurium* lipid A as part of a coordinated stress response (Moreira et al., 2013; Needham and Trent, 2013).

Porphyromonas gingivalis which is considered to be an important agent in human periodontal disease exhibits a very large degree of flexibility in the structure of its lipid A (Curtis et al., 2011). It harbours di-and monophosphorylated and penta- and tetraacylated moieties (Kumada et al., 1995) and in addition a spectrum of nonphosphorylated lipid A species (Rangarajan et al., 2008). Dependent on the temperature *P. gingivalis* shifts the lipid A from an inert nonphosphorylated and antagonizing, monophosphorylated, tetra-acylated structure at 37 °C to a monophosphorylated, penta-acylated higher-potency TLR4 agonistic structure at 41 °C (Curtis et al., 2011). In addition, the lipid A structure of the tetra-acylated nonphosphorylated *P. gingivalis* grown at 37 °C contributes to the resistance to CAMPs (Coats et al., 2009).

12. Other antagonistic lipid A structures

Usually, pathogenic bacteria naturally provide antagonistic lipid A structures as a strategy of immune evasion, since a non-response towards their LPS renders them less visible for the host immune system. One of the most known antagonistic lipid A structures for the human TLR4 receptor complex is the so-called lipid Iva (Fig. 4D). Its backbone structure strongly resembles the structure of agonistic *E. coli* LPS. In fact, it constitutes a precursor form of mature *E. coli* lipid A. However, due to a lack of both secondary acyl chains (Fig. 4D) that are present in *E. coli* lipid A (Fig. 4A), it provides strong antagonistic properties with simultaneous high affinity binding to MD-2 and therefore TLR4

Please cite this article in press as: Steimle, A., et al., Structure and function: Lipid A modifications in commensals and pathogens. Int. J. Med. Microbiol. (2016), http://dx.doi.org/10.1016/j.ijmm.2016.03.001

(Beutler and Rietschel, 2003; Raetz and Whitfield, 2002; Zahringer et al., 1994). Although being a strong antagonist for the human TLR4 receptor complex, lipid IVa is a weak agonist for the murine TLR4 receptor complex. This is based in minor structural differences between human and murine MD-2. Whereas lipid IVa binding to human MD-2 results in an upward shift of the phosphorylated disaccharide backbone mediating antagonistic properties, the binding of lipid IVa to the murine MD-2 leads to a similar conformation compared to agonistic hexaacylated lipid A (Ohto et al., 2012).

13. Endotoxicity of LPS as a determinant of intestinal inflammation or homoeostasis

It is well accepted that in inflammatory bowel diseases (IBD), chronic inflammatory disorders of the intestine, the mucosal immune system reacts inappropriately towards the intestinal commensal microbiota (Vijay-Kumar and Gewirtz, 2009). However no particular microbial species has been consistently linked to IBD pathogenesis, but some symbiotic bacteria species have been shown to prevent inflammatory host responses (Chassaing and Darfeuille-Michaud, 2011; Chow and Mazmanian, 2010; Devkota et al., 2012; Jeon et al., 2012; Round and Mazmanian, 2009).

The mono-colonization of *Il2*$^{-/-}$ mice with *E. coli* is reported to induce severe colitis, whereas monocolonization with *Bacteroides vulgatus* does not and *B. vulgatus* even inhibits the *E. coli* induced inflammation in co-colonized *Il2*$^{-/-}$ mice (Waidmann et al., 2003). Recently we showed that a low endotoxicity of the intestinal microbiota was associated with mucosal immune homeostasis in a mouse model of chronic intestinal inflammation (Gronbach et al., 2014). T cell transplanted *Rag1*$^{-/-}$ harboring a low endotoxic complex intestinal microbiota, characterized by high numbers of *Bacteroidetes* and low numbers of *Enterobacteriaceae* did not develop colitis, whereas T cell transplanted *Rag1*$^{-/-}$ mice harboring a high endotoxic complex intestinal microbiota, characterized by high numbers of *Enterobacteriaceae* and low numbers of *Bacteroidetes* developed severe intestinal inflammation (Gronbach et al., 2014). In line with this, feeding of *Rag1*$^{-/-}$ mice, harboring the low endotoxic microbiota with commensal but pathobiontic *E. coli* JM83 resulted in intestinal inflammation, whereas the administration of an *E. coli* JM83 mutant containing an acyltransferase from *P. gingivalis* (*E. coli*$_{MUT}$) protected *Rag1*$^{-/-}$ mice harboring the high endotoxic microbiota from induction of disease (Bainbridge et al., 2006). We isolated and purified LPS from both *E. coli*$_{WT}$ and *E. coli*$_{MUT}$ and characterized its fatty acid composition. Investigations by high-resolution electrospray ionization Fourier transform ion cyclotron mass spectrometry revealed the same hexaacetylated lipid A molecules in both strains. In addition, *E. coli*$_{MUT}$ contained a major portion of lipid A, in which a 12 carbon atom laurate acyl chain is replaced by a 16 carbon atom palmitate acyl chain (Gronbach et al., 2014) (Fig. 4A and B). This minor modification in *E. coli* JM83 is reported to significantly affect host cell signaling (Bainbridge et al., 2006). To verify the altered stimulatory capacity of LPS$_{MUT}$ compared with LPS$_{WT}$, we used TLR4-overexpressing human embryonic kidney cells (HEK293). Stimulation of cells with the modified LPS$_{MUT}$ resulted in a significantly reduced IL-8 secretion 4 h after stimulation, as compared with LPS$_{WT}$ indicating a reduced endotoxicity but not TLR4 antagonism of the altered LPS$_{MUT}$. Feeding of *Rag1*$^{-/-}$ mice harboring the low endotoxic microbiota with LPS$_{WT}$ resulted in severe intestinal inflammation, however challenging mice which were colonized with the high endotoxic microbiota protected these animal from induction of colitis (Gronbach et al., 2014). This data suggest that the ratio of high endotoxic and low endotoxic LPS is crucial for the regulation of the intestinal immune balance. A predominance of high endotoxic LPS might promote a TH1/TH17 response, subsequently supporting intestinal inflammation, and a predominance of low endotoxic LPS might induce an altered activation of the innate immune system, and either induction of regulatory T cells or prevention of a TH1/TH17 response, associated with intestinal immune homeostasis (Gronbach et al., 2014). Therefore LPS might act as a key microbial symbiosis factor that, depending on its structure, can induce or prevent bowel inflammation by shaping the innate immunity via TLR4-dependent signaling mechanisms (Gronbach et al., 2014; Yamamoto and Akira, 2009).

14. LPS as a potential drug for the treatment of inflammatory bowel disease?

The role of LPS for the host immune system provides ambivalent features. While LPS is essential for the host organism to sense infections of bacterial pathogens at an early stage, therefore helping to clear the infection, an imbalanced LPS sensing can have severe effects for the host organism with fatal sepsis being the most severe consequence. Blocking TLR4 mediated downstream signaling has been implicated to be useful as a drug to prevent from septic shock (O'Neill et al., 2009). Therefore, synthetic antagonistic lipid A structures were invented in order to block TLR4 receptor signaling, such as Eritroran (Fig. 4F). Eritroran strongly prevents from binding of agonistic lipid A to MD-2 and therefore terminates MD-2/TLR4-mediated signaling in vitro, ex vivo and in vivo (Mullarkey et al., 2003; Rossignol and Lynn, 2002; Rossignol et al., 2004). Despite these findings, Eritroran failed to improve survival in a phase III trial in patients with severe sepsis (Opal et al., 2013). Until now, it is not known why Eritroran gavage failed to prevent from fatal sepsis. Possible explanations might be the delayed administration of this strong TLR4 agonist or a failure in trial design (Opal et al., 2013; Tse, 2013). Nevertheless, antagonistic lipid A structures still seem to be a promising tool for the treatment of bacterially induced sepsis. This strategy to prevent from an uncontrolled, or "imbalanced", TLR4 signaling-mediated immune response might also be an attractive approach to deal with inflammatory disorders of the gut. Inflammatory bowel disease develops from an uncontrolled immune response directed towards the intrinsic microbiota. In this case, not pathogens are the target of the immune system, but rather commensal bacteria located in the intestine. It might therefore be possible that antagonistic or weakly agonistic lipid A structures could prevent from uncontrolled TLR4-mediated immune responses towards the own microbiota. In fact, we could already show that the lipid A structure of commensal bacteria is a decisive trigger for the induction of colitis in a genetically predisposed host (Gronbach et al., 2014).

Two main questions remain concerning the administration of isolated LPS (or lipid A) for the treatment of IBD. (I) Which lipid A structure might provide the best results and (II) is TLR4 blocking really "the method of choice"?

The specific structure of lipid A can have profound and even unpredictable effects upon TLR4 signaling. Although detailed studies about the interaction of lipid A with its corresponding MD-2 co-receptors are available (Ohto et al., 2012; Park et al., 2009), the precise immunogenicity cannot be predicted from knowing the structure alone. However, a recent report by Paramo et al. (2015) means a major advance concerning this issue, since they manage to predict the binding behaviour of lipid A structures to MD-2 by measuring their potentials of mean force. The second question is even more complicated to answer. It is possible that TLR4 blocking might not restore homeostasis in every case, since TLR4 signaling

Please cite this article in press as: Steimle, A., et al., Structure and function: Lipid A modifications in commensals and pathogens. Int. J. Med. Microbiol. (2016), http://dx.doi.org/10.1016/j.ijmm.2016.03.001

seems to be important for the prevention of dextran sodium sulfate (DSS)- induced colitis in mice (Rakoff-Nahoum et al., 2006; Wittmann et al., 2015). Therefore, an antagonistic lipid A structure, completely preventing from TLR4 signaling, might not be the lipid A of choice. Possibly, a rather weakly agonistic lipid A structure, allowing basic TLR4-mediated signaling, but preventing from uncontrolled TLR4 activation might be a better tool. Additionally, the recent discovery of caspase-11 as an intracellular lipid A binding LPS sensor (Kayagaki et al., 2011, 2013; Shi et al., 2014) leads to the question, if blocking the TLR4 binding cavity is sufficient to influence LPS-mediated induction of the host immune system. As described above, a block of TLR4 is not sufficient to prevent from LPS induced Casp11-mediated inflammasome activation. Other bacterial components, largely present in the intestine, can activate other TLRs than TLR4 to induce an increase in cytosolic amounts of Casp11 being a precondition for intracellular lipid A sensing. Therefore, a potential lipid A-derived drug needs to have access to the cytosol of host target cells. Although being highly speculative, this might be another explanation why Eritroran failed in the clinical study since it was not granted access to the cytosolic compartment. This fact rises drug development to a severe challenge and strategies need to be developed to target therapeutic lipid A to the cytosolic compartment. Since it could be shown that lipid A structures that act antagonistically in TLR4-signaling also prevent from Casp11 oligomerization and activation despite efficient binding (Shi et al., 2014). Therefore, it seems that the immunogenicity of lipid A structure concerning TLR4 activation, described by the terms agonistic and antagonistic, also accounts for intracellular lipid A induced intracellular inflammasome activation.

There is an ongoing research for new lipid A structures in order to be used as therapeutic. Although most research on this topic focuses on the treatment of sepsis, the idea behind it can easily be transferred to the treatment of chronic inflammatory intestinal disorders. Besides synthetic or chemical development of lipid A structure-related TLR4 antagonists, there is an ongoing interest also on LPS structures of more "exotic" bacteria and how they might contribute to a research progress on this topic. For example, Di Lorenzo et al. (2014) identified a lipid A structure with strong antagonistic activity in a bacterium living in hot springs: *Thermomonas hydrothermalis* (Fig. 4K). However, a closer and more detailed look on the lipid A structures of symbiotic commensal bacteria might be helpful for the development of a lipid A structure providing weak agonistic activity to prevent from both, TLR4- and Casp11-mediated, uncontrolled immune responses of the host organism towards its own microbiota.

Disclosures

The authors disclose all commercial affiliations and competing financial interests and the authors declare that there is no conflict of interest regarding the publication of this paper.

Acknowledgement

Work by J.S.F was supported by the DFG (DFG FR 2087/6-1, DFG FR 2087/8-1, CRC685, SPP1656) the DFG research training group 1708 and the German Centre for Infection Research (DZIF).

References

Aachoui, Y., Leaf, I.A., Hagar, J.A., Fontana, M.F., Campos, C.G., Zak, D.E., Tan, M.H., Cotter, P.A., Vance, R.E., Aderem, A., Miao, E.A., 2013. Caspase-11 protects against bacteria that escape the vacuole. Science 339, 975–978.
Akira, S., Takeda, K., 2004. Toll-like receptor signalling. Nat. Rev. Immunol. 4, 499–511.
Alexander, C., Rietschel, E.T., 2001. Bacterial lipopolysaccharides and innate immunity. J. Endotoxin Res. 7, 167–202.
Aurell, C.A., Wistrom, A.O., 1998. Critical aggregation concentrations of gram-negative bacterial lipopolysaccharides (LPS). Biochem. Biophys. Res. Commun. 253, 119–123.
Bainbridge, B.W., Coats, S.R., Pham, T.T., Reife, R.A., Darveau, R.P., 2006. Expression of a *Porphyromonas gingivalis* lipid A palmitylacyltransferase in *Escherichia coli* yields a chimeric lipid A with altered ability to stimulate interleukin-8 secretion. Cell. Microbiol. 8, 120–129.
Bainbridge, B.W., Karimi-Naser, L., Reife, R., Blethen, F., Ernst, R.K., Darveau, R.P., 2008. Acyl chain specificity of the acyltransferases LpxA and LpxD and substrate availability contribute to lipid A fatty acid heterogeneity in *Porphyromonas gingivalis*. J. Bacteriol. 190, 4549–4558.
Berbee, J.F., Coomans, C.P., Westerterp, M., Romijn, J.A., Havekes, L.M., Rensen, P.C., 2010. Apolipoprotein CI enhances the biological response to LPS via the CD14/TLR4 pathway by LPS-binding elements in both its N- and C-terminal helix. J. Lipid Res. 51, 1943–1952.
Berbee, J.F., van der Hoogt, C.C., Kleemann, R., Schippers, E.F., Kitchens, R.L., van Dissel, J.T., Bakker-Woudenberg, I.A., Havekes, L.M., Rensen, P.C., 2006. Apolipoprotein CI stimulates the response to lipopolysaccharide and reduces mortality in gram-negative sepsis. FASEB J. 20, 2162–2164.
Beutler, B., Rietschel, E.T., 2003. Innate immune sensing and its roots: the story of endotoxin. Nat. Rev. Immunol. 3, 169–176.
Bjorkbacka, H., Fitzgerald, K.A., Huet, F., Li, X., Gregory, J.A., Lee, M.A., Ordija, C.M., Dowley, N.E., Golenbock, D.T., Freeman, M.W., 2004. The induction of macrophage gene expression by LPS predominantly utilizes Myd88-independent signaling cascades. Physiol. Genomics 19, 319–330.
Bone, R.C., 1991. The pathogenesis of sepsis. Ann. Intern. Med. 115, 457–469.
Bone, R.C., Grodzin, C.J., Balk, R.A., 1997. Sepsis: a new hypothesis for pathogenesis of the disease process. Chest 112, 235–243.
Brandenburg, K., Mayer, H., Koch, M.H., Weckesser, J., Rietschel, E.T., Seydel, U., 1993. Influence of the supramolecular structure of free lipid A on its biological activity. Eur. J. Biochem. 218, 555–563.
Broz, P., Ohlson, M.B., Monack, D.M., 2012a. Innate immune response to *Salmonella typhimurium*, a model enteric pathogen. Gut Microbes 3, 62–70.
Broz, P., Ruby, T., Belhocine, K., Bouley, D.M., Kayagaki, N., Dixit, V.M., Monack, D.M., 2012b. Caspase-11 increases susceptibility to Salmonella infection in the absence of caspase-1. Nature 490, 288–291.
Caroff, M., Karibian, D., 2003. Structure of bacterial lipopolysaccharides. Carbohydr. Res. 338, 2431–2447.
Carty, S.M., Sreekumar, K.R., Raetz, C.R., 1999. Effect of cold shock on lipid A biosynthesis in *Escherichia coli*. Induction At 12 degrees C of an acyltransferase specific for palmitoleoyl-acyl carrier protein. J. Biol. Chem. 274, 9677–9685.
Case, C.L., Kohler, L.J., Lima, J.B., Strowig, T., de Zoete, M.R., Flavell, R.A., Zamboni, D.S., Roy, C.R., 2013. Caspase-11 stimulates rapid flagellin-independent pyroptosis in response to *Legionella pneumophila*. Proc. Natl. Acad. Sci. U.S.A. 110, 1851–1856.
Chassaing, B., Darfeuille-Michaud, A., 2011. The commensal microbiota and enteropathogens in the pathogenesis of inflammatory bowel diseases. Gastroenterology 140, 1720–1728.
Chmiela, M., Miszczyk, E., Rudnicka, K., 2014. Structural modifications of Helicobacter pylori lipopolysaccharide: an idea for how to live in peace. World J. Gastroenterol. 20, 9882–9897.
Chow, J., Mazmanian, S.K., 2010. A pathobiont of the microbiota balances host colonization and intestinal inflammation. Cell Host Microbe 7, 265–276.
Clementz, T., Bednarski, J.J., Raetz, C.R., 1996. Function of the htrB high temperature requirement gene of *Escherichia coli* in the acylation of lipid A: HtrB catalyzed incorporation of laurate. J. Biol. Chem. 271, 12095–12102.
Clementz, T., Zhou, Z., Raetz, C.R., 1997. Function of the *Escherichia coli* msbB gene, a multicopy suppressor of htrB knockouts, in the acylation of lipid A: acylation by MsbB follows laurate incorporation by HtrB. J. Biol. Chem. 272, 10353–10360.
Coats, S.R., Jones, J.W., Do, C.T., Braham, P.H., Bainbridge, B.W., To, T.T., Goodlett, D.R., Ernst, R.K., Darveau, R.P., 2009. Human toll-like receptor 4 responses to *P. gingivalis* are regulated by lipid A 1- and 4′-phosphatase activities. Cell. Microbiol. 11, 1587–1599.
Corbin, B.D., Seeley, E.H., Raab, A., Feldmann, J., Miller, M.R., Torres, V.J., Anderson, K.L., Dattilo, B.M., Dunman, P.M., Gerads, R., Caprioli, R.M., Nacken, W., Chazin, W.J., Skaar, E.P., 2008. Metal chelation and inhibition of bacterial growth in tissue abscesses. Science 319, 962–965.
Curtis, M.A., Percival, R.S., Devine, D., Darveau, R.P., Coats, S.R., Rangarajan, M., Tarelli, E., Marsh, P.D., 2011. Temperature-dependent modulation of *Porphyromonas gingivalis* lipid A structure and interaction with the innate host defenses. Infect. Immun. 79, 1187–1193.
Damo, S.M., Kehl-Fie, T.E., Sugitani, N., Holt, M.E., Rathi, S., Murphy, W.J., Zhang, Y., Betz, C., Hench, L., Fritz, G., Skaar, E.P., Chazin, W.J., 2013. Molecular basis for manganese sequestration by calprotectin and roles in the innate immune response to invading bacterial pathogens. Proc. Natl. Acad. Sci. U.S.A. 110, 3841–3846.
Devkota, S., Wang, Y., Musch, M.W., Leone, V., Fehlner-Peach, H., Nadimpalli, A., Antonopoulos, D.A., Jabri, B., Chang, E.B., 2012. Dietary-fat-induced taurocholic acid promotes pathobiont expansion and colitis in Il10$^{-/-}$ mice. Nature 487, 104–108.
Di Lorenzo, F., Paciello, I., Fazio, L.L., Albuquerque, L., Sturiale, L., da Costa, M.S., Lanzetta, R., Parrilli, M., Garozzo, D., Bernardini, M.L., Silipo, D.A., Molinaro, A., 2014. Thermophiles as potential source of novel endotoxin antagonists: the

full structure and bioactivity of the lipo-oligosaccharide from *Thermomonas hydrothermalis*. ChemBioChem: Eur. J. Chem. Biol. 15, 2146–2155.
Dixon, D.R., Darveau, R.P., 2005. Lipopolysaccharide heterogeneity: innate host responses to bacterial modification of lipid a structure. J. Dent. Res. 84, 584–595.
Gaddy, J.A., Radin, J.N., Cullen, T.W., Chazin, W.J., Skaar, E.P., Trent, M.S., Algood, H.M., 2015. *Helicobacter pylori* resists the antimicrobial activity of calprotectin via lipid A modification and associated biofilm formation. mBio 6, e01349–01315.
Galanos, C., Freudenberg, M.A., 1993. Bacterial endotoxins: biological properties and mechanisms of action. Mediators Inflamm. 2, S11–S16.
Garrett, T.A., Kadrmas, J.L., Raetz, C.R., 1997. Identification of the gene encoding the *Escherichia coli* lipid A 4′-kinase. Facile phosphorylation of endotoxin analogs with recombinant LpxK. J. Biol. Chem. 272, 21855–21864.
Gebhardt, C., Nemeth, J., Angel, P., Hess, J., 2006. S100A8 and S100A9 in inflammation and cancer. Biochem. Pharmacol. 72, 1622–1631.
Golenbock, D.T., Hampton, R.Y., Qureshi, N., Takayama, K., Raetz, C.R., 1991. Lipid A-like molecules that antagonize the effects of endotoxins on human monocytes. J. Biol. Chem. 266, 19490–19498.
Gronbach, K., Flade, I., Holst, O., Lindner, B., Ruscheweyh, H.J., Wittmann, A., Menz, S., Schwiertz, A., Adam, P., Stecher, B., Josenhans, C., Suerbaum, S., Gruber, A.D., Kulik, A., Huson, D., Autenrieth, I.B., Frick, J.S., 2014. Endotoxicity of lipopolysaccharide as a determinant of T-cell-mediated colitis induction in mice. Gastroenterology 146, 765–775.
Guo, L., Lim, K.B., Gunn, J.S., Bainbridge, B., Darveau, R.P., Hackett, M., Miller, S.I., 1997. Regulation of lipid A modifications by *Salmonella typhimurium* virulence genes phoP-phoQ. Science 276, 250–253.
Guo, L., Lim, K.B., Poduje, C.M., Daniel, M., Gunn, J.S., Hackett, M., Miller, S.I., 1998. Lipid A acylation and bacterial resistance against vertebrate antimicrobial peptides. Cell 95, 189–198.
Hagar, J.A., Powell, D.A., Aachoui, Y., Ernst, R.K., Miao, E.A., 2013. Cytoplasmic LPS activates caspase-11: implications in TLR4-independent endotoxic shock. Science 341, 1250–1253.
Hansen, G.H., Rasmussen, K., Niels-Christiansen, L.L., Danielsen, E.M., 2009. Lipopolysaccharide-binding protein: localization in secretory granules of Paneth cells in the mouse small intestine. Histochem. Cell Biol. 131, 727–732.
Homma, J.Y., Matsuura, M., Kanegasaki, S., Kawakubo, Y., Kojima, Y., Shibukawa, N., Kumazawa, Y., Yamamoto, A., Tanamoto, K., Yasuda, T., et al., 1985. Structural requirements of lipid A responsible for the functions: a study with chemically synthesized lipid A and its analogues. J. Biochem. 98, 395–406.
Hood, M.I., Mortensen, B.L., Moore, J.L., Zhang, Y., Kehl-Fie, T.E., Sugitani, N., Chazin, W.J., Caprioli, R.M., Skaar, E.P., 2012. Identification of an *Acinetobacter baumannii* zinc acquisition system that facilitates resistance to calprotectin-mediated zinc sequestration. PLoS Pathog. 8, e1003068.
Hood, M.I., Skaar, E.P., 2012. Nutritional immunity: transition metals at the pathogen-host interface. Nat. Rev. Microbiol. 10, 525–537.
Janelsins, B.M., Lu, M., Datta, S.K., 2014. Altered inactivation of commensal LPS due to acyloxyacyl hydrolase deficiency in colonic dendritic cells impairs mucosal Th17 immunity. Proc. Natl. Acad. Sci. U.S.A. 111, 373–378.
Jeon, S.G., Kayama, H., Ueda, Y., Takahashi, T., Asahara, T., Tsuji, H., Tsuji, N.M., Kiyono, H., Ma, J.S., Kusu, T., Okumura, R., Hara, H., Yoshida, H., Yamamoto, M., Nomoto, K., Takeda, K., 2012. Probiotic *Bifidobacterium breve* induces IL-10-producing Tr1 cells in the colon. PLoS Pathog. 8, e1002714.
Jin, M.S., Lee, J.O., 2008. Structures of TLR-ligand complexes. Curr. Opin. Immunol. 20, 414–419.
Karow, M., Georgopoulos, C., 1993. The essential *Escherichia coli* msbA gene, a multicopy suppressor of null mutations in the htrB gene, is related to the universally conserved family of ATP-dependent translocators. Mol. Microbiol. 7, 69–79.
Kawahara, K., Tsukano, H., Watanabe, H., Lindner, B., Matsuura, M., 2002. Modification of the structure and activity of lipid A in *Yersinia pestis* lipopolysaccharide by growth temperature. Infect. Immun. 70, 4092–4098.
Kayagaki, N., Warming, S., Lamkanfi, M., Vande Walle, L., Louie, S., Dong, J., Newton, K., Qu, Y., Liu, J., Heldens, S., Zhang, J., Lee, W.P., Roose-Girma, M., Dixit, V.M., 2011. Non-canonical inflammasome activation targets caspase-11. Nature 479, 117–121.
Kayagaki, N., Wong, M.T., Stowe, I.B., Ramani, S.R., Gonzalez, L.C., Akashi-Takamura, S., Miyake, K., Zhang, J., Lee, W.P., Muszynski, A., Forsberg, L.S., Carlson, R.W., Dixit, V.M., 2013. Noncanonical inflammasome activation by intracellular LPS independent of TLR4. Science 341, 1246–1249.
Kim, H.M., Park, B.S., Kim, J.I., Kim, S.E., Lee, J., Oh, S.C., Enkhbayar, P., Matsushima, N., Lee, H., Yoo, O.J., Lee, J.O., 2007. Crystal structure of the TLR4-MD-2 complex with bound endotoxin antagonist Eritoran. Cell 130, 906–917.
Knirel, Y.A., Lindner, B., Vinogradov, E.V., Kocharova, N.A., Senchenkova, S.N., Shaikhutdinova, R.Z., Dentovskaya, S.V., Fursova, N.K., Bakhteeva, I.V., Titareva, G.M., Balakhonov, S.V., Holst, O., Gremyakova, T.A., Pier, G.B., Anisimov, A.P., 2005. Temperature-dependent variations and intraspecies diversity of the structure of the lipopolysaccharide of *Yersinia pestis*. Biochemistry 44, 1731–1743.
Knodler, L.A., Crowley, S.M., Sham, H.P., Yang, H., Wrande, M., Ma, C., Ernst, R.K., Steele-Mortimer, O., Celli, J., Vallance, B.A., 2014. Noncanonical inflammasome activation of caspase-4/caspase-11 mediates epithelial defenses against enteric bacterial pathogens. Cell Host Microbe 16, 249–256.
Kotani, S., Takada, H., Tsujimoto, M., Ogawa, T., Takahashi, I., Ikeda, T., Otsuka, K., Shimauchi, H., Kasai, N., Mashimo, J., et al., 1985. Synthetic lipid A with endotoxic and related biological activities comparable to those of a natural lipid A from an *Escherichia coli* re-mutant. Infect. Immun. 49, 225–237.
Kumada, H., Haishima, Y., Umemoto, T., Tanamoto, K., 1995. Structural study on the free lipid A isolated from lipopolysaccharide of *Porphyromonas gingivalis*. J. Bacteriol. 177, 2098–2106.
Lamkanfi, M., Declercq, W., Kalai, M., Saelens, X., Vandenabeele, P., 2002. Alice in caspase land. A phylogenetic analysis of caspases from worm to man. Cell Death Differ. 9, 358–361.
Leone, S., Molinaro, A., Pessione, E., Mazzoli, R., Giunta, C., Sturiale, L., Garozzo, D., Lanzetta, R., Parrilli, M., 2006. Structural elucidation of the core-lipid A backbone from the lipopolysaccharide of *Acinetobacter radioresistens* S13, an organic solvent tolerant Gram-negative bacterium. Carbohydr. Res. 341, 582–590.
Leone, S., Sturiale, L., Pessione, E., Mazzoli, R., Giunta, C., Lanzetta, R., Garozzo, D., Molinaro, A., Parrilli, M., 2007. Detailed characterization of the lipid A fraction from the nonpathogen *Acinetobacter radioresistens* strain S13. J. Lipid Res. 48, 1045–1051.
Li, Y., Powell, D.A., Shaffer, S.A., Rasko, D.A., Pelletier, M.R., Leszyk, J.D., Scott, A.J., Masoudi, A., Goodlett, D.R., Wang, X., Raetz, C.R., Ernst, R.K., 2012. LPS remodeling is an evolved survival strategy for bacteria. Proc. Natl. Acad. Sci. U.S.A. 109, 8716–8721.
Lien, E., Means, T.K., Heine, H., Yoshimura, A., Kusumoto, S., Fukase, K., Fenton, M.J., Oikawa, M., Qureshi, N., Monks, B., Finberg, R.W., Ingalls, R.R., Golenbock, D.T., 2000. Toll-like receptor 4 imparts ligand-specific recognition of bacterial lipopolysaccharide. J. Clin. Invest. 105, 497–504.
Liu, J.Z., Jellbauer, S., Poe, A.J., Ton, V., Pesciaroli, M., Kehl-Fie, T.E., Restrepo, N.A., Hosking, M.P., Edwards, R.A., Battistoni, A., Pasquali, P., Lane, T.E., Chazin, W.J., Vogl, T., Roth, J., Skaar, E.P., Raffatellu, M., 2012. Zinc sequestration by the neutrophil protein calprotectin enhances Salmonella growth in the inflamed gut. Cell Host Microbe 11, 227–239.
Loppnow, H., Brade, H., Durrbaum, I., Dinarello, C.A., Kusumoto, S., Rietschel, E.T., Flad, H.D., 1989. IL-1 induction-capacity of defined lipopolysaccharide partial structures. J. Immunol. 142, 3229–3238.
Lu, M., Varley, A.W., Ohta, S., Hardwick, J., Munford, R.S., 2008. Host inactivation of bacterial lipopolysaccharide prevents prolonged tolerance following gram-negative bacterial infection. Cell Host Microbe 4, 293–302.
Lusitani, D., Malawista, S.E., Montgomery, R.R., 2003. Calprotectin, an abundant cytosolic protein from human polymorphonuclear leukocytes, inhibits the growth of *Borrelia burgdorferi*. Infect. Immun. 71, 4711–4716.
Maeshima, N., Fernandez, R.C., 2013. Recognition of lipid A variants by the TLR4-MD-2 receptor complex. Front. Cell. Infect. Microbiol. 3, 3.
Mariathasan, S., Weiss, D.S., Newton, K., McBride, J., O'Rourke, K., Roose-Girma, M., Lee, W.P., Weinrauch, Y., Monack, D.M., Dixit, V.M., 2006. Cryopyrin activates the inflammasome in response to toxins and ATP. Nature 440, 228–232.
Martin-Orozco, N., Touret, N., Zaharik, M.L., Park, E., Kopelman, R., Miller, S., Finlay, B.B., Gros, P., Grinstein, S., 2006. Visualization of vacuolar acidification-induced transcription of genes of pathogens inside macrophages. Mol. Biol. Cell 17, 498–510.
Martinon, F., Petrilli, V., Mayor, A., Tardivel, A., Tschopp, J., 2006. Gout-associated uric acid crystals activate the NALP3 inflammasome. Nature 440, 237–241.
Martinon, F., Tschopp, J., 2004. Inflammatory caspases: linking an intracellular innate immune system to autoinflammatory diseases. Cell 117, 561–574.
Mattsby-Baltzer, I., Mielniczuk, Z., Larsson, L., Lindgren, K., Goodwin, S., 1992. Lipid A in *Helicobacter pylori*. Infect. Immun. 60, 4383–4387.
Meunier, E., Dick, M.S., Dreier, R.F., Schurmann, N., Kenzelmann Broz, D., Warming, S., Roose-Girma, M., Bumann, D., Kayagaki, N., Takeda, K., Yamamoto, M., Broz, P., 2014. Caspase-11 activation requires lysis of pathogen-containing vacuoles by IFN-induced GTPases. Nature 509, 366–370.
Miyake, K., 2006. Roles for accessory molecules in microbial recognition by toll-like receptors. J. Endotoxin Res. 12, 195–204.
Molinaro, A., Holst, O., Di Lorenzo, F., Callaghan, M., Nurisso, A., D'Errico, G., Zamyatina, A., Peri, F., Berisio, R., Jerala, R., Jimenez-Barbero, J., Silipo, A., Martin-Santamaria, S., 2015. Chemistry of lipid A: at the heart of innate immunity. Chemistry 21, 500–519.
Montminy, S.W., Khan, N., McGrath, S., Walkowicz, M.J., Sharp, F., Conlon, J.E., Fukase, K., Kusumoto, S., Sweet, C., Miyake, K., Akira, S., Cotter, R.J., Goguen, J.D., Lien, E., 2006. Virulence factors of *Yersinia pestis* are overcome by a strong lipopolysaccharide response. Nat. Immunol. 7, 1066–1073.
Moran, A.P., Aspinall, G.O., 1998. Unique structural and biological features of *Helicobacter pylori* lipopolysaccharides. Prog. Clin. Biol. Res. 397, 37–49.
Moran, A.P., Lindner, B., Walsh, E.J., 1997. Structural characterization of the lipid A component of *Helicobacter pylori* rough- and smooth-form lipopolysaccharides. J. Bacteriol. 179, 6453–6463.
Moreira, C.G., Herrera, C.M., Needham, B.D., Parker, C.T., Libby, S.J., Fang, F.C., Trent, M.S., Sperandio, V., 2013. Virulence and stress-related periplasmic protein (VisP) in bacterial/host associations. Proc. Natl. Acad. Sci. U.S.A. 110, 1470–1475.
Mullarkey, M., Rose, J.R., Bristol, J., Kawata, T., Kimura, A., Kobayashi, S., Przetak, M., Chow, J., Gusovsky, F., Christ, W.J., Rossignol, D.P., 2003. Inhibition of endotoxin response by e5564, a novel toll-like receptor 4-directed endotoxin antagonist. J. Pharmacol. Exp. Ther. 304, 1093–1102.
Munford, R.S., Hall, C.L., 1986. Detoxification of bacterial lipopolysaccharides (endotoxins) by a human neutrophil enzyme. Science 234, 203–205.
Munford, R.S., Varley, A.W., 2006. Shield as signal: lipopolysaccharides and the evolution of immunity to gram-negative bacteria. PLoS Pathog. 2, e67.

Please cite this article in press as: Steimle, A., et al., Structure and function: Lipid A modifications in commensals and pathogens. Int. J. Med. Microbiol. (2016), http://dx.doi.org/10.1016/j.ijmm.2016.03.001

Muotiala, A., Helander, I.M., Pyhala, L., Kosunen, T.U., Moran, A.P., 1992. Low biological activity of *Helicobacter pylori* lipopolysaccharide. Infect. Immun. 60, 1714–1716.
Nakajima, R., Motin, V.L., Brubaker, R.R., 1995. Suppression of cytokines in mice by protein A-V antigen fusion peptide and restoration of synthesis by active immunization. Infect. Immun. 63, 3021–3029.
Needham, B.D., Trent, M.S., 2013. Fortifying the barrier: the impact of lipid A remodelling on bacterial pathogenesis. Nat. Rev. Microbiol. 11, 467–481.
Netea, M.G., van, D.M., Kullberg, B.J., Cavaillon, J.M., Van der Meer, J.W., 2002. Does the shape of lipid A determine the interaction of LPS with toll-like receptors? Trends Immunol. 23, 135–139.
O'Neill, L.A., Bryant, C.E., Doyle, S.L., 2009. Therapeutic targeting of toll-like receptors for infectious and inflammatory diseases and cancer. Pharmacol. Rev. 61, 177–197.
Ogawa, T., Asai, Y., Sakai, Y., Oikawa, M., Fukase, K., Suda, Y., Kusumoto, S., Tamura, T., 2003. Endotoxic and immunobiological activities of a chemically synthesized lipid A of Helicobacter pylori strain 206-1. FEMS Immunol. Med. Microbiol. 36, 1–7.
Ohto, U., Fukase, K., Miyake, K., Satow, Y., 2007. Crystal structures of human MD-2 and its complex with antiendotoxic lipid IVa. Science 316, 1632–1634.
Ohto, U., Fukase, K., Miyake, K., Shimizu, T., 2012. Structural basis of species-specific endotoxin sensing by innate immune receptor TLR4/MD-2. Proc. Natl. Acad. Sci. U.S.A. 109, 7421–7426.
Okan, N.A., Kasper, D.L., 2013. The atypical lipopolysaccharide of Francisella. Carbohydr. Res. 378, 79–83.
Opal, S.M., Laterre, P.F., Francois, B., LaRosa, S.P., Angus, D.C., Mira, J.P., Wittebole, X., Dugernier, T., Perrotin, D., Tidswell, M., Jauregui, L., Krell, K., Pachl, J., Takahashi, T., Peckelsen, C., Cordasco, E., Chang, C.S., Oeyen, S., Aikawa, N., Maruyama, T., Schein, R., Kalil, A.C., Van Nuffelen, M., Lynn, M., Rossignol, D.P., Gogate, J., Roberts, M.B., Wheeler, J.L., Vincent, J.L., Group, A.S., 2013. Effect of eritoran, an antagonist of MD2-TLR4, on mortality in patients with severe sepsis: the ACCESS randomized trial. JAMA 309, 1154–1162.
Paramo, T., Tomasio, S.M., Irvine, K.L., Bryant, C.E., Bond, P.J., 2015. Energetics of endotoxin recognition in the toll-like receptor 4 innate immune response. Sci. Rep. 5, 17997.
Park, B.S., Song, D.H., Kim, H.M., Choi, B.S., Lee, H., Lee, J.O., 2009. The structural basis of lipopolysaccharide recognition by the TLR4-MD-2 complex. Nature 458, 1191–1195.
Pilla, D.M., Hagar, J.A., Haldar, A.K., Mason, A.K., Degrandi, D., Pfeffer, K., Ernst, R.K., Yamamoto, M., Miao, E.A., Coers, J., 2014. Guanylate binding proteins promote caspase-11-dependent pyroptosis in response to cytoplasmic LPS. Proc. Natl. Acad. Sci. U.S.A. 111, 6046–6051.
Poltorak, A., Ricciardi-Castagnoli, P., Citterio, S., Beutler, B., 2000. Physical contact between lipopolysaccharide and toll-like receptor 4 revealed by genetic complementation. Proc. Natl. Acad. Sci. U.S.A. 97, 2163–2167.
Raetz, C.R., Reynolds, C.M., Trent, M.S., Bishop, R.E., 2007. Lipid A modification systems in gram-negative bacteria. Annu. Rev. Biochem. 76, 295–329.
Raetz, C.R., Whitfield, C., 2002. Lipopolysaccharide endotoxins. Annu. Rev. Biochem. 71, 635–700.
Rakoff-Nahoum, S., Hao, L., Medzhitov, R., 2006. Role of toll-like receptors in spontaneous commensal-dependent colitis. Immunity 25, 319–329.
Rangarajan, M., Aduse-Opoku, J., Paramonov, N., Hashim, A., Bostanci, N., Fraser, O.P., Tarelli, E., Curtis, M.A., 2008. Identification of a second lipopolysaccharide in *Porphyromonas gingivalis* W50. J. Bacteriol. 190, 2920–2932.
Rathinam, V.A., Vanaja, S.K., Waggoner, L., Sokolovska, A., Becker, C., Stuart, L.M., Leong, J.M., Fitzgerald, K.A., 2012. TRIF licenses caspase-11-dependent NLRP3 inflammasome activation by gram-negative bacteria. Cell 150, 606–619.
Rebeil, R., Ernst, R.K., Gowen, B.B., Miller, S.I., Hinnebusch, B.J., 2004. Variation in lipid A structure in the pathogenic yersiniae. Mol. Microbiol. 52, 1363–1373.
Richards, S.M., Strandberg, K.L., Conroy, M., Gunn, J.S., 2012. Cationic antimicrobial peptides serve as activation signals for the *Salmonella typhimurium* PhoPQ and PmrAB regulons in vitro and in vivo. Front. Cell. Infect. Microbiol. 2, 102.
Rietschel, E.T., Kirikae, T., Schade, F.U., Mamat, U., Schmidt, G., Loppnow, H., Ulmer, A.J., Zahringer, U., Seydel, U., Di, P.F., 1994. Bacterial endotoxin: molecular relationships of structure to activity and function. FASEB J. 8, 217–225.
Roppel, J., Mayer, H., 1975. Identification of a 2,3-diamino-2,3-dideoxyhexose in the lipid A component of lipopolysaccharides of *Rhodopseudomonas viridis* and *Rhodopseudomonas palustris*. Carbohydr. Res. 40, 31–40.
Rose, J.R., Christ, W.J., Bristol, J.R., Kawata, T., Rossignol, D.P., 1995. Agonistic and antagonistic activities of bacterially derived *Rhodobacter sphaeroides* lipid A: comparison with activities of synthetic material of the proposed structure and analogs. Infect. Immun. 63, 833–839.
Rossignol, D.P., Lynn, M., 2002. Antagonism of in vivo and ex vivo response to endotoxin by E5564, a synthetic lipid A analogue. J. Endotoxin Res. 8, 483–488.
Rossignol, D.P., Wasan, K.M., Choo, E., Yau, E., Wong, N., Rose, J., Moran, J., Lynn, M., 2004. Safety, pharmacokinetics, pharmacodynamics, and plasma lipoprotein distribution of eritoran (E5564) during continuous intravenous infusion into healthy volunteers. Antimicrob. Agents Chemother. 48, 3233–3240.
Round, J.L., Mazmanian, S.K., 2009. The gut microbiota shapes intestinal immune responses during health and disease. Nat. Rev. Immunol. 9, 313–323.
Schroder, K., Tschopp, J., 2010. The inflammasomes. Cell 140, 821–832.
Seydel, U., Oikawa, M., Fukase, K., Kusumoto, S., Brandenburg, K., 2000. Intrinsic conformation of lipid A is responsible for agonistic and antagonistic activity. Eur. J. Biochem. 267, 3032–3039.
Shi, J., Zhao, Y., Wang, Y., Gao, W., Ding, J., Li, P., Hu, L., Shao, F., 2014. Inflammatory caspases are innate immune receptors for intracellular LPS. Nature 514, 187–192.
Shin, H.J., Lee, H., Park, J.D., Hyun, H.C., Sohn, H.O., Lee, D.W., Kim, Y.S., 2007. Kinetics of binding of LPS to recombinant CD14, TLR4, and MD-2 proteins. Mol. Cells 24, 119–124.
Silipo, A., Leone, M.R., Lanzetta, R., Parrilli, M., Lackner, G., Busch, B., Hertweck, C., Molinaro, A., 2012. Structural characterization of two lipopolysaccharide O-antigens produced by the endofungal bacterium *Burkholderia* sp. HKI-402 (B4). Carbohydr. Res. 347, 95–98.
Sohnle, P.G., Hunter, M.J., Hahn, B., Chazin, W.J., 2000. Zinc-reversible antimicrobial activity of recombinant calprotectin (migration inhibitory factor-related proteins 8 and 14). J. Infect. Dis. 182, 1272–1275.
Steinbakk, M., Naess-Andresen, C.F., Lingaas, E., Dale, I., Brandtzaeg, P., Fagerhol, M.K., 1990. Antimicrobial actions of calcium binding leucocyte L1 protein, calprotectin. Lancet 336, 763–765.
Stowe, I., Lee, B., Kayagaki, N., 2015. Caspase-11: arming the guards against bacterial infection. Immunol. Rev. 265, 75–84.
Sweet, C.R., Preston, A., Toland, E., Ramirez, S.M., Cotter, R.J., Maskell, D.J., Raetz, C.R., 2002. Relaxed acyl chain specificity of Bordetella UDP-*N*-acetylglucosamine acyltransferases. J. Biol. Chem. 277, 18281–18290.
Takeuchi, O., Akira, S., 2010. Pattern recognition receptors and inflammation. Cell 140, 805–820.
Tse, M.T., 2013. Trial watch: sepsis study failure highlights need for trial design rethink. Nat. Rev. Drug Discovery 12, 334.
Urban, C.F., Ermert, D., Schmid, M., Abu-Abed, U., Goosmann, C., Nacken, W., Brinkmann, V., Jungblut, P.R., Zychlinsky, A., 2009. Neutrophil extracellular traps contain calprotectin, a cytosolic protein complex involved in host defense against *Candida albicans*. PLoS Pathog. 5, e1000639.
Valentin-Hansen, P., Johansen, J., Rasmussen, A.A., 2007. Small RNAs controlling outer membrane porins. Curr. Opin. Microbiol. 10, 152–155.
Vijay-Kumar, M., Gewirtz, A.T., 2009. Flagellin: key target of mucosal innate immunity. Mucosal Immunol. 2, 197–205.
Visintin, A., Latz, E., Monks, B.G., Espevik, T., Golenbock, D.T., 2003. Lysines 128 and 132 enable lipopolysaccharide binding to MD-2, leading to Toll-like receptor-4 aggregation and signal transduction. J. Biol. Chem. 278, 48313–48320.
Vorachek-Warren, M.K., Ramirez, S., Cotter, R.J., Raetz, C.R., 2002. A triple mutant of *Escherichia coli* lacking secondary acyl chains on lipid A. J. Biol. Chem. 277, 14194–14205.
Vreugdenhil, A.C., Snoek, A.M., Greve, J.W., Buurman, W.A., 2000. Lipopolysaccharide-binding protein is vectorially secreted and transported by cultured intestinal epithelial cells and is present in the intestinal mucus of mice. J. Immunol. 165, 4561–4566.
Waidmann, M., Bechtold, O., Frick, J.S., Lehr, H.A., Schubert, S., Dobrindt, U., Loeffler, J., Bohn, E., Autenrieth, I.B., 2003. *Bacteroides vulgatus* protects against *Escherichia coli*-induced colitis in gnotobiotic interleukin-2-deficient mice. Gastroenterology 125, 162–177.
Wang, S., Miura, M., Jung, Y., Zhu, H., Gagliardini, V., Shi, L., Greenberg, A.H., Yuan, J., 1996. Identification and characterization of Ich-3, a member of the interleukin-1beta converting enzyme (ICE)/Ced-3 family and an upstream regulator of ICE. J. Biol. Chem. 271, 20580–20587.
Wittmann, A., Bron, P.A., van II, S.S., Kleerebezem, M., Adam, P., Gronbach, K., Menz, S., Flade, I., Bender, A., Schafer, A., Korkmaz, A.G., Parusel, R., Autenrieth, I.B., Frick, J.S., 2015. TLR signaling-induced CD103-expressing cells protect against intestinal inflammation. Inflamm. Bowel Dis. 21 (3), 507–519.
Wright, S.D., Ramos, R.A., Tobias, P.S., Ulevitch, R.J., Mathison, J.C., 1990. CD14, a receptor for complexes of lipopolysaccharide (LPS) and LPS binding protein. Science 249, 1431–1433.
Wurfel, M.M., Hailman, E., Wright, S.D., 1995. Soluble CD14 acts as a shuttle in the neutralization of lipopolysaccharide (LPS) by LPS-binding protein and reconstituted high density lipoprotein. J. Exp. Med. 181, 1743–1754.
Wurfel, M.M., Wright, S.D., 1997. Lipopolysaccharide-binding protein and soluble CD14 transfer lipopolysaccharide to phospholipid bilayers: preferential interaction with particular classes of lipid. J. Immunol. 158, 3925–3934.
Yamamoto, M., Akira, S., 2009. Lipid A receptor TLR4-mediated signaling pathways. Adv. Exp. Med. Biol. 667, 59–68.
Zahringer, U., Lindner, B., Rietschel, E.T., 1994. Molecular structure of lipid A, the endotoxic center of bacterial lipopolysaccharides. Adv. Carbohydr. Chem. Biochem. 50, 211–276.
Zähringer, U.L.B., Rietschel, E.T., 1999. Endotoxin in Health and Disease. Marcel Dekker, New York, NY.
Zhou, Z., White, K.A., Polissi, A., Georgopoulos, C., Raetz, C.R., 1998. Function of *Escherichia coli* MsbA, an essential ABC family transporter, in lipid A and phospholipid biosynthesis. J. Biol. Chem. 273, 12466–12475.

Please cite this article in press as: Steimle, A., et al., Structure and function: Lipid A modifications in commensals and pathogens. Int. J. Med. Microbiol. (2016), http://dx.doi.org/10.1016/j.ijmm.2016.03.001

Bacteroides vulgatus mpk lipopolysaccharide acts as inflammation-silencing agent for the treatment of intestinal inflammatory disorders

Alex Steimle[1,*], Flaviana Di Lorenzo[2,*], Kerstin Gronbach[1], Thorsten Kliem[1], Kerstin Fuchs[3], Hasan Halit Öz[4], Andrea Schäfer[1], Annika Bender[1], Anna Lange[1], Jan Kevin Maerz[1], Sarah Menz[1], Ingo B. Autenrieth[1], Bernd J. Pichler[3], Hans Bisswanger[5], Ewelina Łakomiec[6], Wojciech Jachymek[6], Alba Silipo[2], Antonio Molinaro[2,#] and Julia-Stefanie Frick[1,#]

[1] Institute of Medical Microbiology and Hygiene, University of Tübingen, Tübingen, Germany

[2] Department of Chemical Sciences, University of Naples Federico II, Naples, Italy

[3] Institute of Radiology, Werner Siemens Imaging Center, Department of Preclinical Imaging and Radiopharmacy, University of Tübingen, Tübingen, Germany

[4] Children's Hospital, University of Tübingen, Tübingen, Germany

[5] Interfacultary Institute of Biochemistry, University of Tübingen, Tübingen, Germany

[6] Hirszfeld Institute of Immunology and Experimental Therapy, Polish Academy of Sciences, Wrocław, Poland

[*] Both authors contributed equally to this work

[#] Both authors share last authorship

Corresponding authors:

Prof. Dr. Julia-Stefanie Frick, University of Tübingen, Institute of Medical Microbiology and Hygiene, Elfriede-Aulhorn-Straße 6, D-72076 Tübingen, Germany, Tel.: +49 7071 29 82352, E-Mail: Julia-stefanie.frick@med.uni-tuebingen.de

Prof. Antonio Molinaro, University of Napoli Federico II, Department of Chemical Sciences, Complesso Universitario Monte S. Angelo, Via Cintia 4, I-80126 Napoli, Italy, Tel.: +39 081 674 123, E-Mail: molinaro@unina.it

Abstract

Bacteroides vulgatus mpk is a symbiotic gut commensal from the mouse intestine. It is known that administration of this bacterium protects from colonic inflammation in various mouse models for experimental colitis. Here, we demonstrate that *B. vulgatus* mpk even restores gut homeostasis in an already inflamed intestine. This effect is mainly mediated by the unique structure of its lipopolysaccharide (LPS). Although the binding affinity to the host MD-2/TLR4 receptor complex is similar to a strong agonistic LPS, it exhibits only weakly agonistic activity. Such activity converts intestinal dendritic cells into a tolerant and tolerogenic phenotype that mediates the intestinal homeostasis-restoring properties of *B. vulgatus* mpk LPS. Thus, we promote symbiotic *B. vulgatus* mpk LPS, as a potential alternative therapeutic approach for the treatment of Inflammatory Bowel Diseases. Furthermore, insights gained from the structural analysis of *B. vulgatus* mpk LPS might help to chemically design novel potent inflammation-silencing drugs.

Introduction

Inflammatory Bowel Diseases (IBD) are characterized by chronic relapsing intestinal inflammation with Crohn's Disease (CD) and Ulcerative Colitis (UC) being the most frequent and clinically relevant forms of this disease complex[1]. IBD is considered to be a multifactorial disease with genetics[2], environmental factors[3] and intestinal microbiota composition[4] contributing to the pathology. Therapy of IBD in humans is currently focused on symptomatic treatment, often by means of immunosuppression[5]. Additionally, fecal transplantation or bacteriotherapy is recently discussed as a potential therapy[6], though sometimes offering more questions than answers.

It is widely accepted that the composition of the intestinal microbiota can strongly influence the progress and outcome of IBD. However, we recently reported that not only the presence, abundance or proportion of certain live microbial species contribute to such microbiota-mediated effects. Indeed, the structure, and consequently the endotoxicity, of lipopolysaccharides from Gram-negative bacteria determines the outcome of inflammation in a mouse model for experimental colitis[7]. Lipopolysaccharides (LPS), in their smooth form, consist of three distinct domains: (1) an O-specific polysaccharide, (2) a core oligosaccharide (core OS) and (3) the lipid A which anchors LPS to the outer leaflet of the bacterial cell wall[8]. With its highly conserved overall structure and composition, LPS represents an important microbe-associated molecular pattern (MAMP) playing an essential role for the recognition of bacterial invasion by the host innate immune system[9, 10] through recognition by the host myeloid-differentiation-2/Toll-like receptor 4 (MD-2/TLR4) receptor complex. Importantly, the fine structure of LPS, primarily the detailed composition of lipid A, drastically influences its biological activity, ranging from strong activation of the innate immune system, in case of agonistic LPS, to a complete block of immune responses, in case of antagonists[9, 11]. This different behaviour is reflected in diverse binding modes of such lipid A structures to the MD-2/TLR4 receptor complex[12].

A prominent intestinal commensal Gram-negative and, therefore, LPS-producing bacterial phylum in humans is *Bacteroidetes*[13, 14]. We have previously characterized a member of this phylum, namely *Bacteroides vulgatus* mpk, as a symbiotic commensal of the mouse intestine providing high genome plasticity[15] and exhibiting strong immune-modulating properties leading to a prevention of colitis induction

in several mouse models for experimental colitis[16, 17, 18]. Here, we demonstrate that this commensal symbiont, *B. vulgatus* mpk, drastically reduced an already established intestinal inflammation in mice leading to a complete healing of damaged intestinal tissue. Intriguingly, this effect was mirrored by only using its purified LPS. Detailed determination of the *B. vulgatus* mpk LPS structure revealed a hypoacylated and *mono*-phosphorylated lipid A species and a unique core OS structure which does not result in an antagonistic, but rather in a weakly agonistic activity. These weakly agonistic properties are responsible for its active inflammation silencing characteristics. Hence, this specific LPS structure might be a novel and effective therapeutic agent for the treatment of IBD. Furthermore, revealing its detailed molecular structure might therefore contribute to IBD therapy-related drug design.

Results

B. vulgatus mpk actively silences established inflammatory reactions in a mouse model for experimental colitis as confirmed by non-invasive *in vivo* PET imaging

We have demonstrated that mouse gut-associated symbiotic commensal *B. vulgatus* mpk exhibits anti-inflammatory properties in various mouse models for experimental colitis[16, 17, 18]. These anti-inflammatory properties were exhibited when *B. vulgatus* mpk was administered before onset of disease resulting in prevention of intestinal inflammation. This prompted us to verify whether this symbiont was also capable of reducing inflammatory reactions in an already inflamed environment thus making such a symbiotic commensal a therapeutic tool for treatment of colitis in mice. Therefore, we used *Rag1*$^{-/-}$ mice harbouring a highly colitogenic microbiota containing high proportions of *Enterobactericeae*[7] and transplanted them with 5 x 10^5 naïve *wt* $CD4^+CD62L^+CD45Rb^{hi}$ T-cells. Four weeks after T-cell transplantation, mice were administered 5 x 10^8 live *B. vulgatus* mpk per mL of drinking water until the end of the experiment, 8 weeks after T-cell transplantation. As controls, non-transplanted and transplanted but not live *B. vulgatus* mpk-treated *Rag1*$^{-/-}$ mice were used (Fig. 1a). In order to monitor the actual degree of colonic inflammation, all mice were injected with [^{18}F]FDG and non-invasive *in vivo* PET imaging was performed. [^{18}F]FDG is suitable for the detection of ongoing inflammatory processes in living animals, since sites of inflammation are depicted as regions with higher [^{18}F]FDG uptake in PET scans compared to non-inflamed surrounding environments[19]. However, some organs as heart and bladder generally provide a basic tracer uptake signal

independent from their inflammatory status. We monitored the colonic [^{18}F]FDG uptake over time from all mice used for this experiment. Therefore each mouse was injected with [^{18}F]FDG and PET-imaging was performed at the day of T-cell transplantation (week 0) as well as 4, 6 and 8 weeks after T-cell transplantation (Fig. 1b). The obtained data were corrected for decay, due to the half life time of [^{18}F], and normalized to the injected activity per animal. As demonstrated in the upper panel of Fig. 1b, non-transplanted *Rag1*$^{-/-}$ mice provided low [^{18}F]FDG uptake during the whole observation period, indicating no ongoing inflammatory processes in the colon. However, *Rag1*$^{-/-}$ mice transplanted with T-cells provided

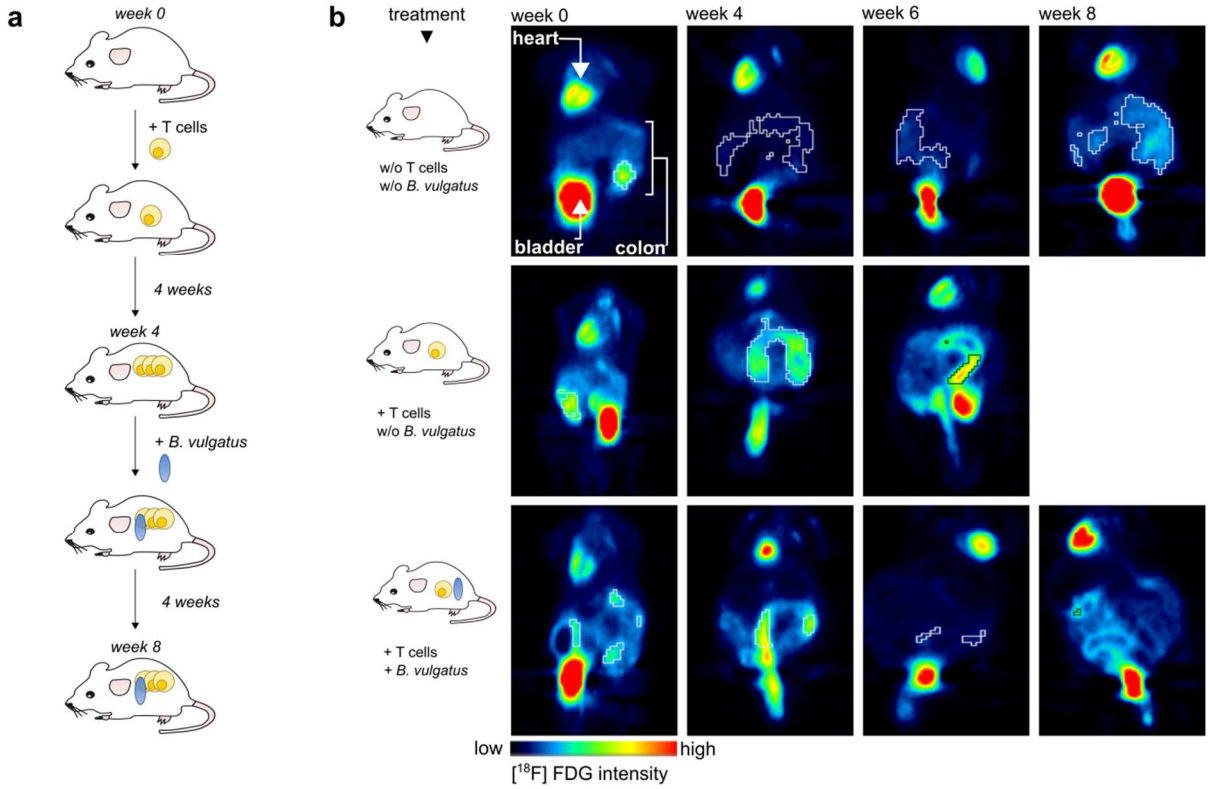

Figure 1: Administration of live *B. vulgatus* mpk reduces intestinal inflammation in *Rag1*$^{-/-}$ mice with established colonic inflammation as confirmed by non-invasive *in vivo* PET imaging.

a. Experimental setup: *Rag1*$^{-/-}$ mice harboring a highly colitogenic microbiota were transplanted with CD4^{+} T-cells to induce intestinal inflammation as described. 4 weeks after T-cell transplantation, mice were started to be administered live *B. vulgatus* mpk in the drinking water at a concentration of 5 x 10^{8} mL^{-1}. *B. vulgatus* mpk treatment was continued for 4 more weeks. 8 weeks after T-cell transplantation mice were sacrificed and analyzed. As controls, one group was transplanted without following *B. vulgatus* administration and one group was not T-cell transplanted.

b. High resolution non-invasive small animal *in vivo* PET imaging. 8.3 ± 1.3 MBq [^{18}F]FDG was injected into the tail vein of each mouse. Static PET scans were performed at the day of T-cell transplantation and repeated 4, 6 and 8 weeks after T-cell transplantation. Data was corrected for decay and normalized to the injected activity. PET images of one representative individual per group are depicted. Organs providing high intensity signals (heart, bladder and inflamed colon) are labelled in the upper left panel.

138 severe colonic inflammation as illustrated by a high colonic [^{18}F]FDG uptake at weeks 4 and 6 (Fig 1b,
139 middle panel). Since the inflammation in these animals exceeded an ethically maintainable level, we had to
140 sacrifice the animals at week 6. As another group, T-cell transplanted *Rag1*$^{-/-}$ mice, displaying severe signs of
141 intestinal inflammation at week 4 (Fig. 1b, lower panel) were administered *B. vulgatus* mpk via drinking
142 water.In these mice, we observed a considerable reduction of colonic [^{18}F]FDG uptake already after two
143 weeks. Another PET scan at week 8 revealed comparably low [^{18}F]FDG uptake indicating that the
144 inflammatory processes, visible at week 4, were cleared by *B. vulgatus* mpk administration.

145 This considerably demonstrated that the anti-inflammatory properties of the commensal symbiont *B.*
146 *vulgatus* mpk did not only prevent from induction of inflammation. It also actively silenced already
147 established colonic inflammation, alleviating symptoms of colitis in *Rag1*$^{-/-}$ mice.

148

149 ***B. vulgatus* mpk LPS mimics the anti-inflammatory activity exerted by live *B. vulgatus* mpk**
150 Since one of the major immunoreactive compounds of Gram-negative bacteria is LPS, we investigated
151 whether the administration of pure *B. vulgatus* mpk LPS (LPS_{BV}) exhibits the same anti-inflammatory and
152 inflammation-silencing properties as the live bacterium. Therefore, we isolated LPS_{BV} and used it for *in vivo*
153 administration. Again, we used *Rag1*$^{-/-}$ mice harbouring a highly colitogenic microbiota and induced colonic
154 inflammation through transplantation of 5 x 10^5 naïve *wt* $CD4^+CD62L^+CD45RB^{hi}$ T-cells. At week 4,
155 transplanted mice showed clear signs of colonic inflammation such as bloody feces and diarrhea, which is in
156 line with the PET imaging that was performed to monitor intestinal inflammation (Fig. 1b). At this point, we
157 administered live *B. vulgatus* mpk, as described above, and LPS_{BV} at a concentration of 160 µg mL^{-1} in the
158 drinking water from week 4 until the end of the experiment (8 weeks after T-cell transplantation) (Fig. 2a).
159 Figure 2b illustrates representative H&E stained colonic sections from each group. Non-treated T-cell
160 transplanted animals showed severe signs of colonic inflammation (Fig. 2b, left panel). However, the LPS_{BV}-
161 and live bacteria-treated animals provided significantly lower intestinal inflammation (Fig. 2b, middle and
162 right panel) compared to non-treated mice (Fig. 2c). $CD3^+CD4^+$ T-cells isolated from the colonic lamina
163 propria (cLP) of live *B. vulgatus* mpk-treated *Rag1*$^{-/-}$ mice expressed significantly lower amounts of IL-17
164 (Fig. 2e), thus providing a clearly reduced Th17 response[20]. Furthermore, qRT-PCRs from colonic scrapings

revealed that live *B. vulgatus* mpk-treated animals expressed significantly higher amounts of aldehyde dehydrogenase (ALDH) mRNA, which triggers the induction of immune response silencing Foxp3$^+$ regulatory T-cells (Tregs) by metabolizing vitamin A-derived retinol into retinoic acid (RA). RA has been shown to be a crucial mediator for the induction of Tregs and ALDH$^+$ intestinal dendritic cells are considered to be important mediators for immune homeostasis[21, 22, 23]. LPS$_{BV}$-treated T-cell transplanted *Rag1*$^{-/-}$ mice

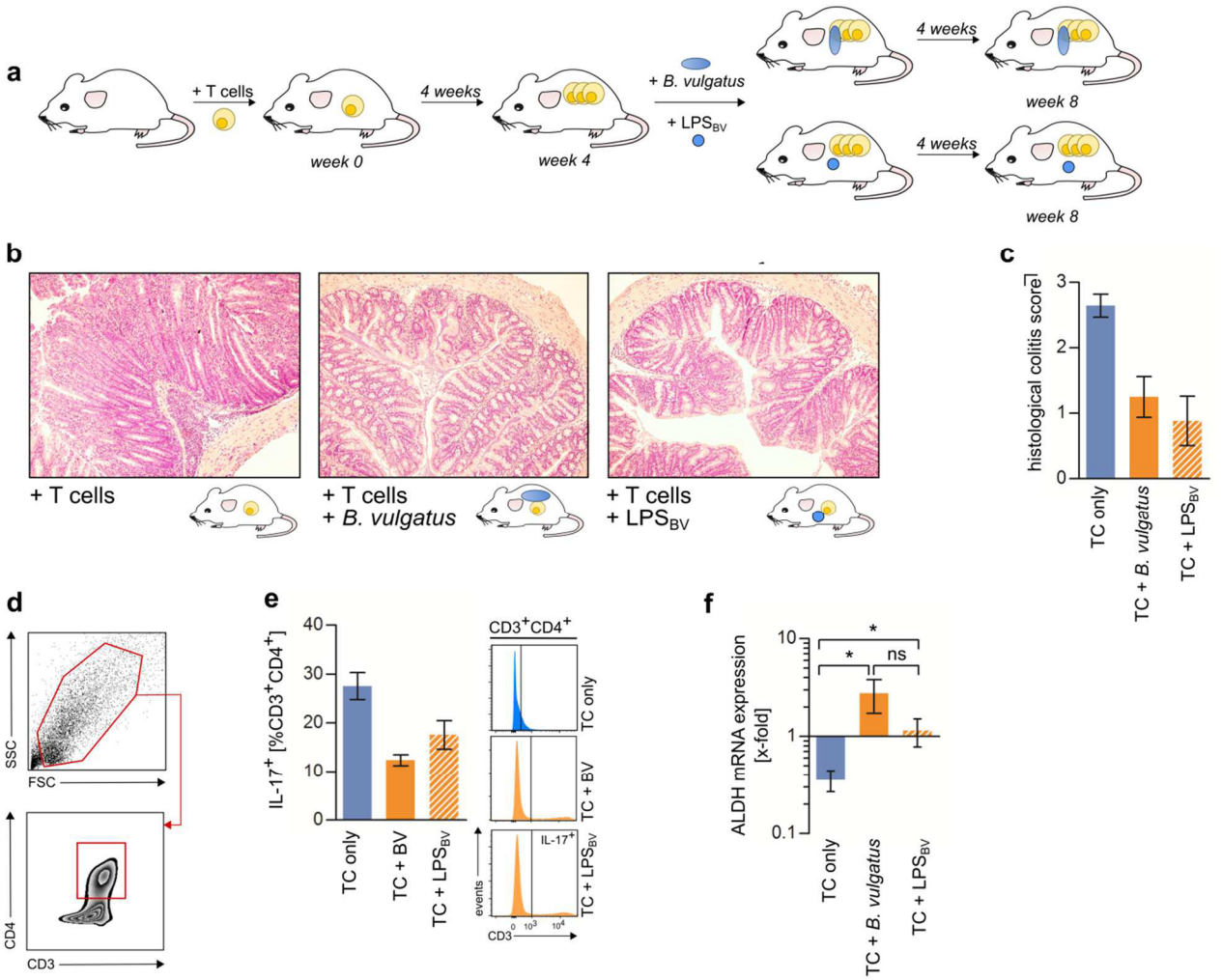

Figure 2: Isolated LPS$_{BV}$ provides the same capability to reduce intestinal inflammation in *Rag1*$^{-/-}$ mice with established colonic inflammation as live *B. vulgatus* mpk.

a. Experimental setup: *Rag1*$^{-/-}$ mice harbouring a highly colitogenic microbiota were transplanted with CD4+ T-cells to induce intestinal inflammation as described. 4 weeks after T-cell transplantation, mice were either non-treated, treated with live *B. vulgatus* mpk by administration of 5 x 10^8 bacteria mL^{-1} in the drinking water or treated with isolated LPS$_{BV}$ in the drinking water at a concentration of 160 µg mL^{-1}. Mice were sacrificed and analysed 8 weeks after T-cell transplantation.

b. Representative H&E stained colonic sections at week 8.

c. Histological colitis score at week 8, ranging from 0 to a maximum of 3.

d. gating strategy to determine the CD3$^+$CD4$^+$ T-cell population in the colonic lamina propria (cLP) at week 8.

e. Proportion of IL-17$^+$ cells among the population of cLP CD3$^+$CD4$^+$ T-cells, determined by flow cytometry.

f. Relative *Aldh* mRNA expression in colonic scrapings at week 8, determined by qRT-PCR. Data were normalized to *Aldh2* mRNA expression in colonic scrapings of non-inflamed non-T-cell-transplanted *Rag1*$^{-/-}$ mice.

also provided significantly lower proportions of IL-17 expressing $CD3^+CD4^+$ cLP T-cells as well as higher *Aldh* mRNA expression in colonic scrapings. These data indicated that both, live *B. vulgatus* mpk bacteria and isolated LPS_{BV} are equally able to silence established inflammatory processes in the large intestine by downregulation of Th17 immune response promoting cytokines and by favoring Treg inducing environmental conditions.

B. vulgatus mpk LPS contains tetra- and pentaacylated lipid A and provides a unique composition of its core structure

Due to the immune response silencing properties of isolated LPS_{BV}, we characterized its structure in detail. After extraction and purification of LPS_{BV}, a mild acid hydrolysis allowed to isolate lipid A which was investigated by chemical analyses and MALDI mass spectrometry revealing a heterogeneous mixture of tetra- and pentaacylated species (Fig. 3a,b). Nature and distribution of the fatty acids were similar to the previously reported lipid A structure from *B. dorei*[24], a close relative of *B. vulgatus*.

Likewise, the lipid A blend resulted to be phosphorylated only at the reducing glucosamine (α-GlcN), as also observed in *B. dorei*[24]; the occurrence of a minor *bis*-phosphorylated lipid A species was also detected. Furthermore, NMR-based studies, in parallel to ESI MS analyses, on both the core OS and the O-chain polysaccharide (Fig. 3c,d) disclosed a novel structure of the LPS core region. Briefly, the core region was built up of a hexasaccharide bearing a phosphorylated Kdo unit, in turn, substituted at position O-5 by a rhamnose residue. This latter was found to be a branched monosaccharide bearing a β-galactofuranose unit (Gal*f*) at its position O-3 and, at position O-4, a β-galactopyranose unit. This latter was, in turn, disubstituted by α-fucose and β-glucose. The O-chain polysaccharide was built up of repeating units of α-rhamnose and β-mannose which is in full agreement with the O-chain of *B. vulgatus* IMCJ1204 previously characterized by Hashimoto *et al.*[25] (Fig. 3d). Full characterization details are presented in the Supplementary Notes. Interestingly, only the Kdo sugar unit carried at O-4 a negatively charged group, namely a phosphate group. From the carbohydrate and LPS chemistry point of view, it is very important to underline the unusual presence of Gal*f* in the core region. Indeed, to the best of our knowledge, it has only been found in an environmental *Shewanella* strain[26] as well as in the thermophilic bacterium *Thermomonas hydrothermalis*[27]. This finding is even more interesting taking into account that the presence of five membered rings in the LPS core OS is very rare[28] and that Gal*f* is a major constituent of fungal and mycobacterial cell walls in which a

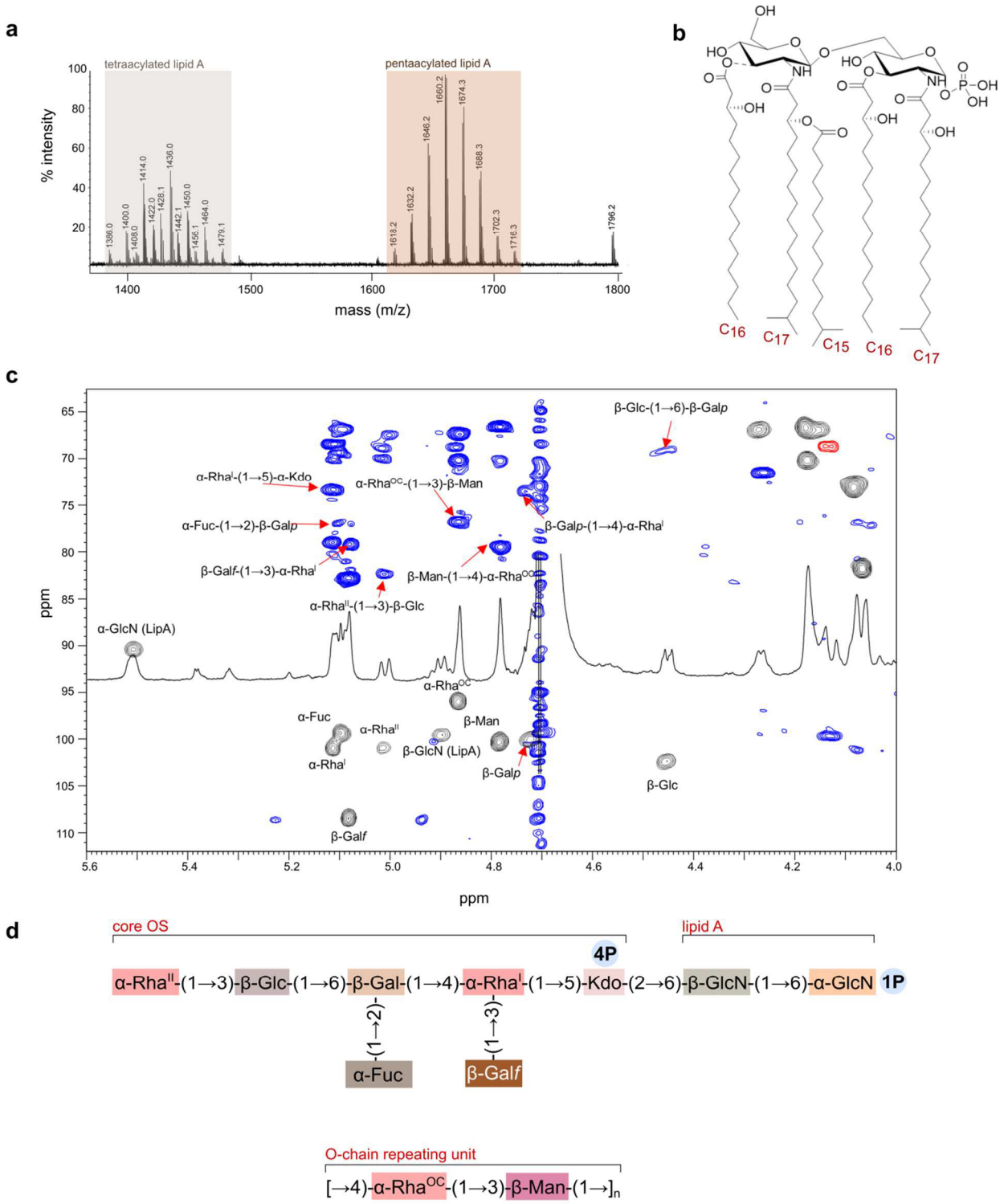

Figure 3: MS and NMR based structural analysis of LPS$_{BV}$.

a. Reflectron MALDI TOF mass spectrum (MS), acquired in negative polarity, of purified *B. vulgatus* mpk lipid A. Spectrum shows two intense groups of ions around *m/z* 1420.5 and *m/z* 1660.8. Each group is characterized by the presence of mass differences of 14 kDa indicative of lipid A species differing in their acyl chain length. Assignment of the lipid A species is depicted as tetraacylated lipid A and pentaacylated lipid A.

b. Structure of a representative lipid A species relative to ion peak at *m/z* 1688.8.

c. Zoom of the overlapped ^{1}H, ^{13}C HSQC (black/red) and ^{1}H, ^{13}C HMBC (blue) spectra of the fully deacylated LPS from *B. vulgatus* mpk. The most relevant long-range correlations that allowed the complete structural characterization of the LPS saccharide moiety are reported.

d. Structure of the core OS and the O-chain (biological repeating unit) moieties from LPS_{BV} derived from the combination of chemical, NMR and MALDI MS and MS/MS analyses.

linear chain of alternating β-(1→5)- and β-(1→6)-linked Gal*f* residues is attached to a disaccharide containing rhamnose and *N*-acetylglucosamine.

B. vulgatus mpk LPS exhibits weakly agonistic immunogenicity and is sufficient to render dendritic cells tolerant and semi-mature

It is known that apathogenic commensal bacteria can have either symbiotic or pathobiotic properties concerning the activation of the immune system. As mentioned previously, we identified *B. vulgatus* mpk as such a symbiotic commensal and *E. coli* mpk as a representative apathogenic pathobiotic commensal. We confirmed that pure LPS was able to mimic the immunogenic properties of both commensal bacteria with LPS_{BV} providing low and LPS_{EC} exhibiting strong immuno-stimulating properties (Supplementary Fig. 1). Hence, LPS_{BV} is not a MD-2/TLR4 receptor complex antagonist since it provided weakly agonistic activity as demonstrated by low, but still detectable amounts of secreted cytokines and by slight enhancement of T-cell stimulatory surface proteins as MHC-II, CD40, CD80 and CD86 (Supplementary Figure 1). We have previously reported on the crucial role of semi-mature dendritic cells (smDCs) for the maintenance of intestinal homeostasis and the prevention of intestinal inflammation[7, 17, 18, 29]. A peculiar feature of *B. vulgatus* mpk induced smDCs is the non-responsiveness towards further bacterial stimuli in terms of surface expression of MHC-II, CD40, CD80 and CD86 as well as secretion of cytokines such as TNF and IL-12p40 but not IL-6[29]. Supplementary Fig. 1 indicates that LPS_{BV} stimulated BMDCs might be semi-mature since they strongly resembled the phenotype caused by *B. vulgatus* mpk stimulation. However, in order to determine whether LPS_{BV} stimulation effectively renders BMDCs semi-mature they need to be challenged with a maturating stimulus, such as *E. coli* mpk, checking for immunoreactivity in case of immature DCs or tolerance in case of smDCs. As controls, we primed BMDCs for 24 h with PBS to keep them immature, with *B. vulgatus* mpk to render them semi-mature and with *E. coli* mpk to induce complete BMDC maturation (Fig. 4a). Additionally, we primed BMDCs with LPS_{BV} and LPS_{EC} to verify their respective maturation phenotype. 24 h after priming, medium was changed for fresh medium and the cells were challenged with either PBS or *E. coli* mpk for further 16 h (Fig. 4a,b). As demonstrated in Fig. 4a and 4b, LPS_{BV}-primed and

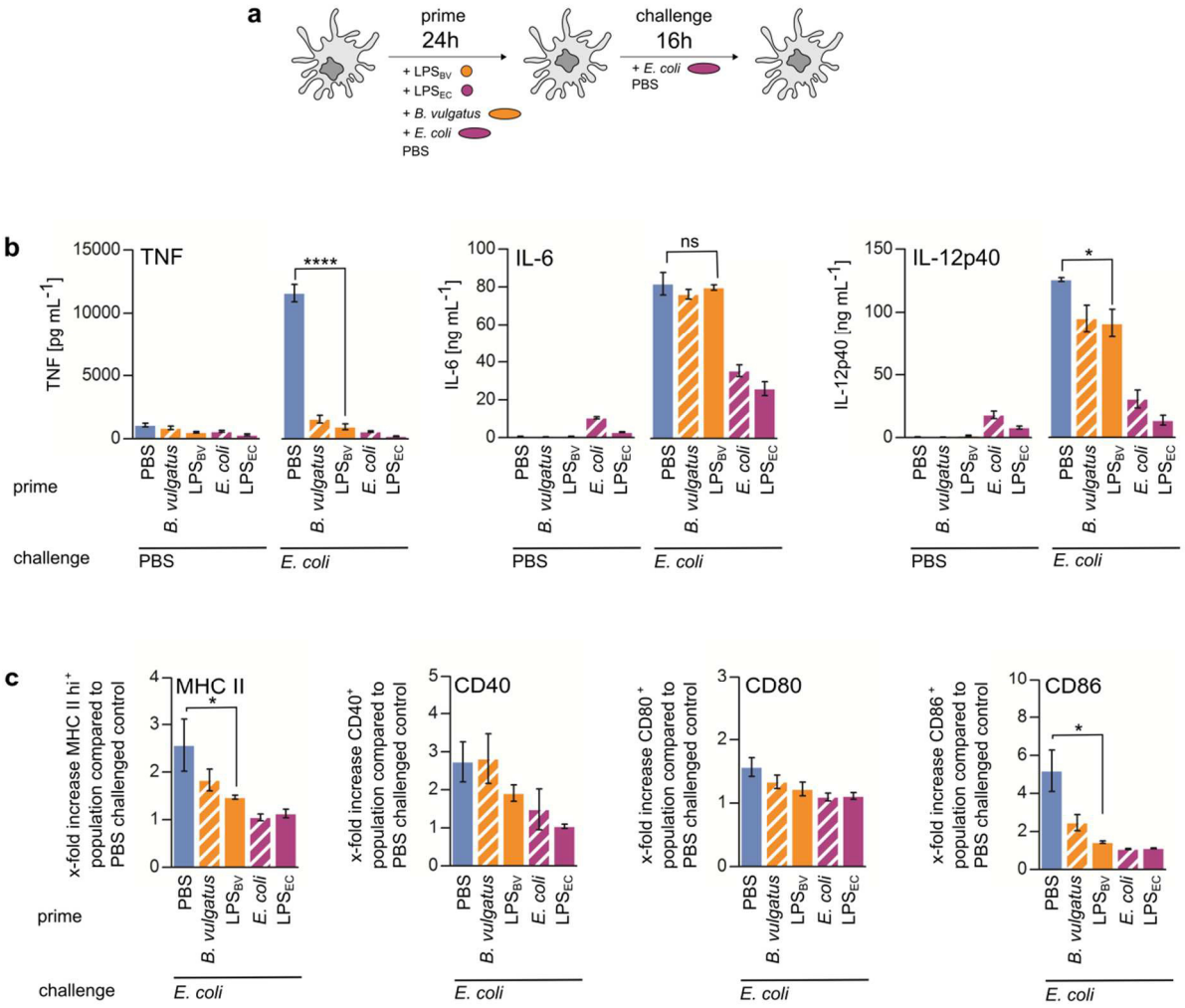

Figure 4: LPS$_{BV}$ converts bone marrow derived dendritic cells into a tolerant semi-mature state.
a. Experimental setting: Bone marrow derived dendritic cells (BMDCs) from wt mice were generated as described and primed with either PBS (mock control), *B. vulgatus* mpk (MOI 1), *E. coli* mpk (MOI 1), LPS$_{BV}$ (50 ng per 10^6 BMDCs) or *E. coli* mpk LPS (LPS$_{EC}$) (50 ng per 10^6 BMDCs) for 24 h. Medium was changed and primed BMDCs were challenged with either PBS (mock control) or *E. coli* mpk for another 16 h.
b. Secretion of TNF, IL-12p40 and IL-6 into cell supernatant after medium change followed by PBS- or *E. coli* mpk-challenge, determined by ELISA.
c. Flow cytometric analyses of BMDC surface expression of the CD4$^+$ T-cell activating surface proteins MHC-II, CD40, CD80 and CD86 among the population of CD11c$^+$ cells. The proportion MHC-IIhi$^+$, CD40$^+$, CD80$^+$ and CD86$^+$ cells among the population of differentially primed and *E. coli* mpk challenged CD11c$^+$ BMDCs was determined by flow cytometry and normalized to the proportion of MHC-IIhi$^+$, CD40$^+$, CD80$^+$ and CD86$^+$ CD11c$^+$ BMDCs of equally primed, but PBS challenged controls. Statistical analyses were performed using student's t-test. Error bars represent SD.

E. coli mpk-challenged BMDCs provided significantly lower secretion of IL-12p40 and TNF, as well as MHC-II and CD86 surface expression compared to PBS-primed and *E. coli* mpk-challenged BMDCs. All above features are typical for tolerant smDCs. Additionally, priming with either LPS$_{BV}$ or *B. vulgatus* mpk had the same effect on DCs, since in both cases DCs became semi-mature. As previously published, priming

with *E. coli* mpk leads to full DC maturation (mDCs)[18, 29], an effect that can be mimicked by priming with LPS_{EC} alone.

In summary, differential maturation of DCs by commensal bacteria was highly dependent on their LPS structure. Moreover, live *B. vulgatus* mpk bacteria were not necessary to induce smDCs providing immune homeostasis maintaining properties, as the usage of the isolated LPS_{BV} was sufficient to induce DC semi-maturation.

LPS_{BV} and LPS_{EC} provide similar binding affinity to the MD-2/TLR4 receptor complex

The observation that both, LPS_{BV} and LPS_{EC}, showed different immunological effects on DCs *in vitro*, prompted us to define and compare their binding affinity to the MD-2/TLR4 receptor complex. We established an experimental setting to determine *quasi* dissociation constants (K_D) of both LPS structures using biotinylated LPS_{BV} ($bioLPS_{BV}$). We are aware of the fact that we cannot determine real K_D-values since we do not know the exact molarity of the used LPS solutions. The assembly of amphiphilic LPS monomers into micelles, vesicles or even more complicated structures is highly dependent on the buffer and ionic strength and is therefore hardly predictable. This exacerbated the determination of the molarity of LPS monomers which effectively have access to the receptor, rendering them "active ligands" thus contributing to K_D values. However, assuming that (1) $bioLPS_{BV}$ and LPS_{EC} provide a comparable monomeric molecular weight, (2) $bioLPS_{BV}$ and LPS_{EC} behave in a similar chemical manner under the experimental conditions and (3) all experiments were carried out incubating both LPS at the same time, we can speculate that a qualitative comparison using K_D-values in the unit [g L^{-1}] instead of [mol L^{-1}] is qualifiable for a comparison of their binding affinity. In order to determine K_D values for both LPS, we used human embryonic kidney (HEK) cells which were stably transfected with a plasmid encoding for murine CD14, MD-2 and TLR4 (HEK-mTLR4). These latter were expressed by HEK-mTLR4 cells in excess and in equal amount, representing a fundamental prerequisite for K_D determination. Since $bioLPS_{BV}$ did not show any difference in the immunological behaviour compared to LPS_{BV} (data not shown), we concluded that biotinylation did not affect the interaction with the receptor complex. We incubated HEK-mTLR4 cells with various concentrations of $bioLPS_{BV}$ and we then visualized bound $bioLPS_{BV}$ by adding PE-coupled streptavidin

followed by flow cytometric analysis of the resulting PE fluorescence. As shown in Fig. 5a, non-biotinylated LPS and cells without addition of any LPS did not contribute to the PE fluorescence signal. The resulting PE-fluorescence in $bioLPS_{BV}$-treated samples was dependent on $bioLPS_{BV}$ concentration and showed a classical perpendicular hyperbola binding curve of a ligand to its respective receptor (Fig. 5a, right panel). In order to determine K_D of $bioLPS_{BV}$ and LPS_{EC}, we simultaneously incubated HEK-mTLR4 cells with different concentrations of both LPS for 1 h and detected resulting PE fluorescence, which is directly proportional to the amount of bound $bioLPS_{BV}$ (Fig. 5b). In order to define the K_D value of $bioLPS_{BV}$, various concentrations of this LPS alone without addition of LPS_{EC} were used. The K_D equalled the concentration of $bioLPS_{BV}$ corresponding to the half maximal MFI PE intensity, which could be determined as 0.412 mg L^{-1}. In other words, adding 0.412 mg L^{-1} to the used 1 x 10^5 HEK-mTLR4 cells led to occupation of half of the available MD-2/TLR4 binding sites (Fig. 5c). In order to determine K_D of LPS_{EC}, several concentrations of LPS_{EC} were co-incubated with different concentrations of $bioLPS_{BV}$, resulting in 4 different binding curves representing the 4 employed LPS_{EC} concentrations (Fig. 5d). The resulting binding curves follow the equation

$$(1)\ MFI\ PE = \frac{n[bioLPS_{BV}]}{[bioLPS_{BV}]+K_D(bioLPS_{BV})\times\left(1+\frac{[LPS_{EC}]}{K_D(LPS_{EC})}\right)}$$

with n being the number of different binding sites (which was assumed to be 1 in our case). The binding curves shown in Fig. 5d were then plotted into a double reciprocal form resulting in 4 different straight lines whose slopes were determined using GraphPad Prism (Fig. 5e). The slopes obtained from Fig. 5e were afterwards plotted against the respective LPS_{EC} concentration resulting in a straight line whose intersection with the x-axis represented the negative value of the LPS_{EC} binding constant which was determined to be 0.304 mg L^{-1}, being in the same biologically relevant range as $bioLPS_{BV}$ K_D.

These data allowed us to conclude that LPS_{BV} and LPS_{EC} provide similar binding affinity to the MD-2/TLR4 receptor complex.

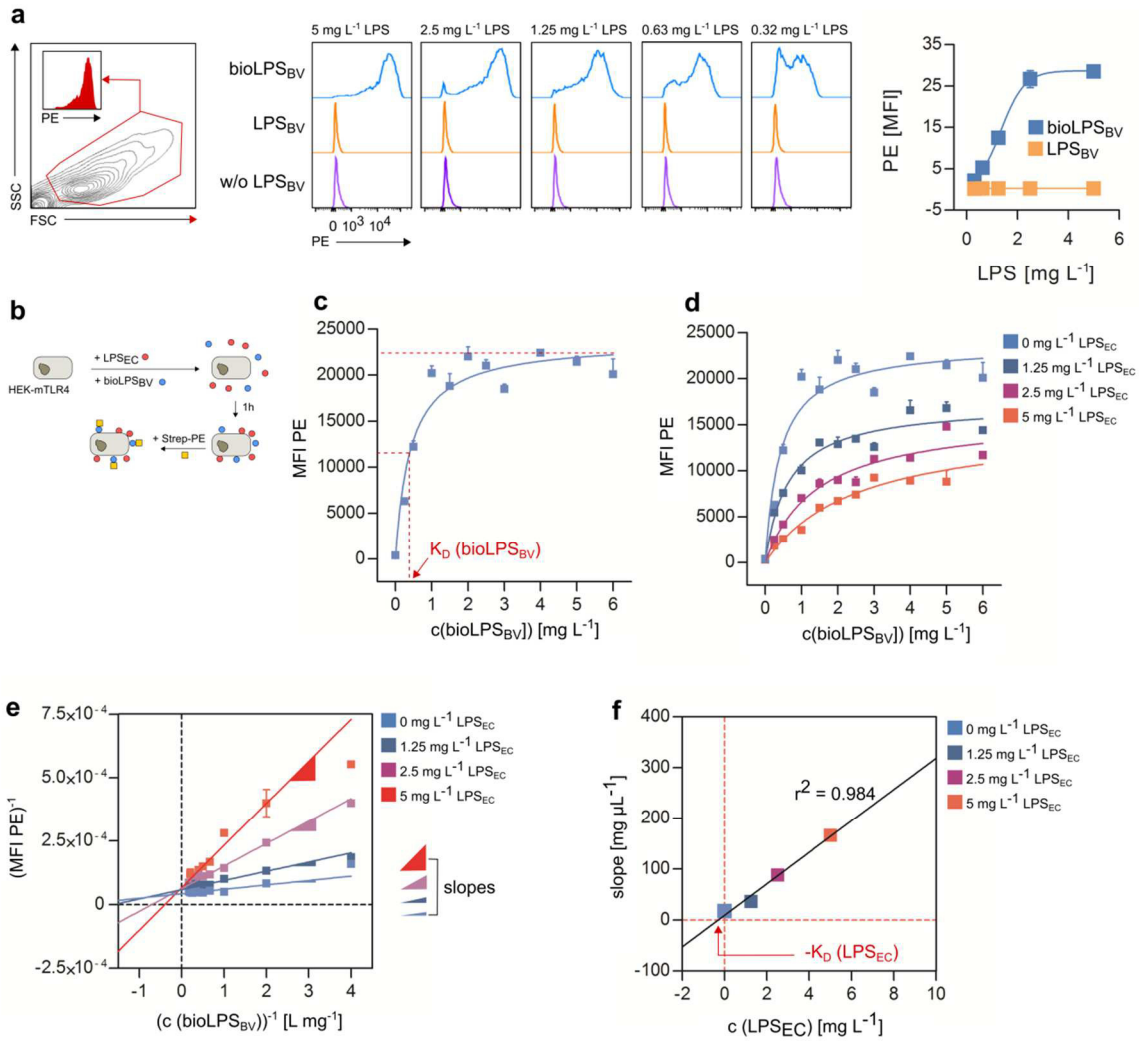

Figure 5: LPS_{BV} and LPS_{EC} provide similar binding affinity to the MD-2/TLR4 receptor complex.

a. HEK cells expressing murine CD14, MD-2 and TLR4 (HEK-mTLR4) were co-incubated with LPS_{BV}, biotinylated LPS_{BV} ($bioLPS_{BV}$) or PBS (w/o LPS_{BV}) at several concentrations. PE-coupled streptavidin (Strep-PE) was added to each sample. Cells were washed and analysed for PE fluorescence using flow cytometry. **Left panel**: gating strategy to determine intact HEK-mTLR4 cells. **Middle panel**: representative histograms of PE fluorescence of HEK-mTLR4 cells that were treated as described above. **Right panel**: Detected mean PE fluorescence intensity (PE (MFI)) as a function of used $bioLPS_{BV}$ concentration.
b. Experimental setting for the determination of LPS binding affinity: HEK-mTLR4 cells were incubated simultaneously with various concentrations of non-biotinylated LPS_{EC} or $bioLPS_{BV}$ for 1 h. Cells were washed and incubated with Strep-PE. PE fluorescence was detected afterwards.
c. HEK-mTLR4 cells were incubated with $bioLPS_{BV}$ only according to the experimental setting described in (b). By using different concentrations of $bioLPS_{BV}$ and the resulting detected PE fluorescence, a non-linear regression for a perpendicular hyperbola was created. The $bioLPS_{BV}$ concentration corresponding to the half-maximal PE intensity equals to K_D of $bioLPS_{BV}$.
d. according to (b) HEK-mTLR4 cells were simultaneously incubated with $bioLPS_{BV}$ and LPS_{EC}. For each differentially coloured perpendicular hyperbola binding curve the concentration of $bioLPS_{BV}$ varied while the concentration of LPS_{EC} was constant. According to (b), resulting PE fluorescence was detected as demonstrated in (a). The detected PE signal is directly proportional to bound $bioLPS_{BV}$. Each data point represents a distinct combination of LPS_{EC} and $bioLPS_{BV}$ concentrations (n=3).
e. Data obtained from (d) were mathematically transformed into a double reciprocal form and plotted into a graph. The binding curves from (d) are therefore transformed into straight lines.
f. Slopes which were obtained from the double reciprocal plotting in (e) which were derived from the binding curves in (d) were plotted against the corresponding concentration of LPS_{EC} which was kept constant in the experiment. A linearization led to a straight line whose intersection with the x-axis represents the negative value of the dissociation constant ($-K_D$) for the binding of LPS_{EC} to the murine MD-2/TLR4 receptor complex.

LPS_{BV} exerts therapeutic effects only in excess concentrations compared to other commensal-derived LPS

We have demonstrated that LPS_{BV} provides weakly agonistic activities and binds to the murine MD-2/TLR4 receptor complex with an affinity that is comparable to the binding affinity of strong agonistic LPS_{EC}. Since the downstream signalling, and therefore the immunogenicity, is dependent on effective $(MD\text{-}2/TLR4)_2$ heterotetramerization, we hypothesized that the specific and unique overall LPS_{BV} structure blocks the conformational change of the receptor complex which is necessary for tetramer formation (Fig. 6a). Concerning the therapeutical effects of LPS_{BV} in strong reduction of intestinal inflammation, we conclude that the concentration of LPS_{BV} located in the intestinal lumen must exceed the number of agonistic LPS from other commensal bacteria in order to induce tolerant smDCs. Exceeding LPS_{BV} concentrations are thought to enhance the probability that intestinal DCs only encounter weakly agonistic LPS_{BV} since we demonstrated that simultaneous encounter with a strong agonistic LPS prevented from DC semi-maturation and induces pro-inflammatory responses mediating DC maturation (Supplementary Fig. 3). In this case, the ability of LPS_{EC} to remove already bound LPS_{BV} from the MD-2/TLR4 receptor complex more efficiently than *vice versa* (Supplementary Fig. 2) would not be relevant. As demonstrated in Supplementary Fig. 3, the endotoxicity of LPS_{BV} depends on its concentration and very high LPS_{BV} concentration might lead to complete DC maturation. However, this concentration exceeds physiological LPS levels in the intestine. We demonstrated that using 160 $\mu g\ mL^{-1}$ in the drinking water led to the observed healing effects in *Rag1*$^{-/-}$ mice, indicating that such a concentration is sufficient to exceed the amount of already present LPS in the colon while simultaneously being in a semi-maturation inducing concentration range. Once DC semi-maturation is induced, this phenotype cannot be overcome[18, 29, 30, 31] and would therefore lead to a prevention of a *de novo* T-cell activation. Therefore, after a phase-out of ongoing inflammatory processes, newly induced smDCs through LPS_{BV} administration would prevent from a continuous T-cell activation (Fig. 6b) and, therefore, promote healing of damaged colonic tissue.

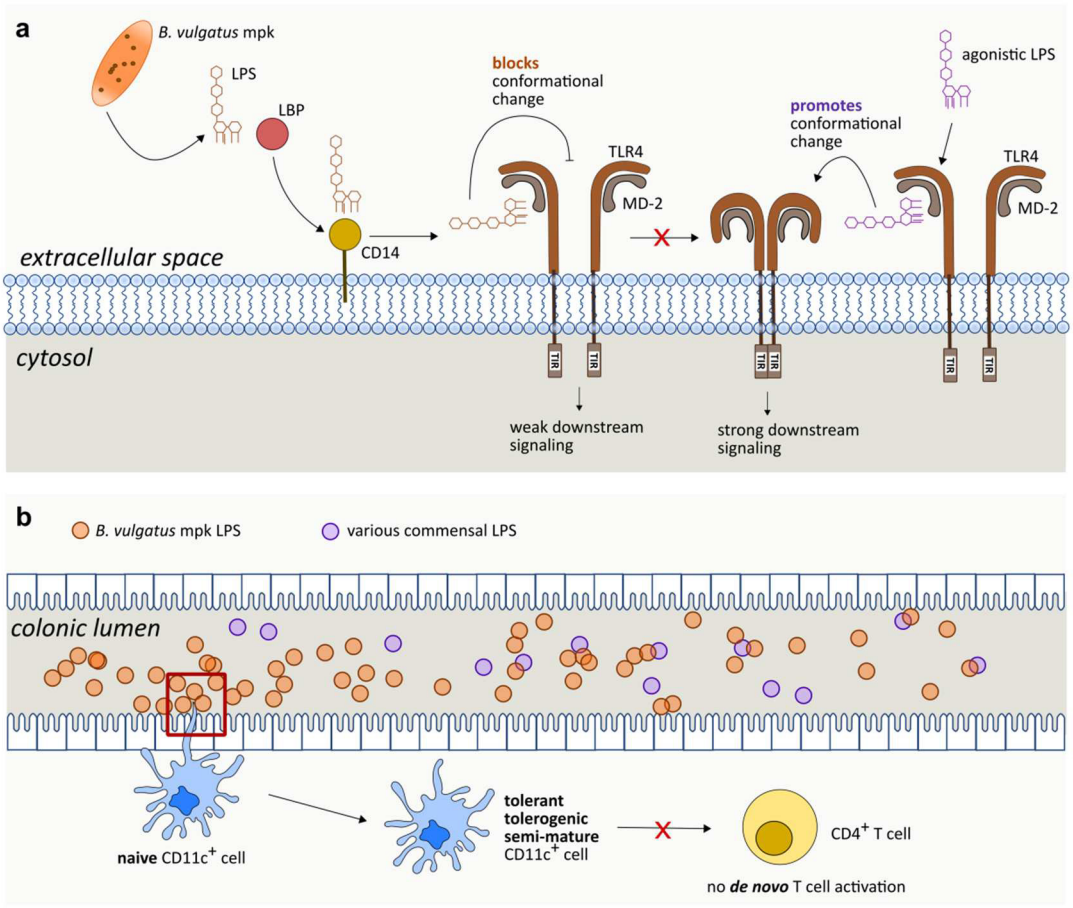

Figure 6: Proposed mechanism how weakly agonistic LPS_{BV} influences MD-2/TLR4 receptor complex activation and prevents from initiation of a $CD4^+$ T-cell mediated immune response via modulation of intestinal $CD11c^+$ cells

a. **Right side**: agonistic LPS like LPS_{EC} binds to the MD-2/TLR4 receptor complex. Its LPS structure harbouring a *bis*-phosphylated and hexaacylated lipid A leads to a conformational change in the receptor complex leading to heterotetramerization of two MD-2/TLR4-dimers resulting in efficient intracellular signalling, overshooting a pro-inflammatory signalling threshold. **Left side**: weakly agonistic LPS_{BV} binds to the MD-2/TLR4-receptor complex with a similar affinity as strong agonistic LPS_{EC}. However, its structural characteristics like harbouring a *mono*-phosphorylated, mixed tetra- and pentaacylated lipid A, as well as a unique galactofuranose-containing core OS structure probably lead to a block of the heterotetramer formation resulting in a weak intracellular signalling that does not exceed a pro-inflammatory threshold but rather mediates anti-inflammatory immune responses.

b. Therapeutical administration of LPS from symbiotic *B. vulgatus* mpk ends up in large amounts in the intestine, exceeding the amount of present LPS from other intestinal commensal bacteria. Excess LPS_{BV} primes naïve $CD11c^+$ cells into a tolerant, tolerogenic and semi-mature phenotype that fails to activate $CD4^+$ T-cells. This prevention of a *de novo* activation of $CD4^+$ T-cells leads to a phase-out of ongoing inflammatory processes while *de novo* induction of an immune response is prevented. However, our data indicate that this only happens if LPS_{BV} is the only TLR4 ligand which $CD11c^+$ cells encounter when they are still naïve and immature. LPS_{BV} needs a certain period of time to induce $CD11c^+$ cell tolerance. Simultaneous encounter with agonistic LPS does not lead to $CD11c^+$ cell tolerance and does therefore not promote abrogation of inflammatory processes.

Discussion

In this study, we report that the administration of the gut commensal bacterium, *B. vulgatus* mpk, drastically reduces established and ongoing pathological inflammatory processes in the intestine of a mouse model for experimental colitis using *Rag1*$^{-/-}$ mice. These immune response silencing properties were mediated by the bacterial LPS as the healing effects could be obtained using pure LPS_{BV} only. We therefore propose that LPS_{BV} might be a novel therapeutic agent for the treatment of chronic gut inflammatory disorders or could alternatively (bio)-inspire an *ad hoc* chemical synthesis for novel correlated compounds.

B. vulgatus mpk belongs to the Gram-negative bacterial phylum *Bacteroidetes* representing one of the two most prominent phyla in the mammalian gut[13, 14]. However, the proportion of *Bacteroidetes* in the intestinal microbiota is dependent on the inflammatory status of the gut. In ulcerative colitis patients, the proportion of *Bacteroides* spp is markedly decreased[32] supporting the idea of *Bacteroides* strains being important beneficial players in the intestinal microbiota. Additionally, we have already shown that administration of a certain mouse gut-associated intestinal commensal *Bacteroides* strain, *B. vulgatus* mpk, prevents from disease induction in different mouse models for experimental colitis[16, 17, 18], mainly by induction of tolerant semi-mature dendritic cells (smDCs) in the intestine. These smDCs are responsible for the prevention of pro-inflammatory immune responses[16, 17, 18, 29]. Here we demonstrated that *B. vulgatus* mpk is not only able to prevent from the induction of pathological inflammatory responses but it is also capable of strongly reducing established and ongoing inflammation resulting in amelioration of colitis. These colitis healing effects were not restricted to administration of live *B. vulgatus* mpk since, intriguingly, administration of isolated LPS_{BV} was able to completely mimic the observed homeostasis restoring effects in *Rag1*$^{-/-}$ mice.

Structural analysis of LPS_{BV} revealed a mixture of penta- and tetraacylated *mono*-phosphorylated lipid A, chemically related to the *B. dorei*[24] and *B. fragilis*[33] lipid As , a galactofuranose-containing core OS and an O-chain composed of rhamnose and mannose. Interestingly, the core structure revealed a novel carbohydrate composition that has not yet been detected in any other bacterial LPS. In particular, the presence of galactofuranose in the inner part of the LPS core as well as the presence of a rhamnose residue, as the first sugar linked to the Kdo, are surely an innovative hallmark for LPS. Thus it can be speculated that such an unusual architecture has a key role in the MD-2/TLR4 complexation with LPS and the following

downstream signalling. In general, LPS is a potent MD-2/TLR4 agonist leading to strong intracellular signalling in target T-cells resulting in transcription of genes associated with pro-inflammatory immune responses[12]. The immunogenicity, or the strength of this intracellular signalling, triggered by LPS is widely considered to be mostly mediated by lipid A[34, 35]. Hexaacylated and *bis*-phosphorylated *E. coli* lipid A is considered to be the most potent activator of the MD-2/TLR4-receptor complex mediated signalling since it was demonstrated that five of the six acyl chains are buried inside the MD-2 binding cavity while the sixth acyl chain points out to the MD-2 surface mediating hydrophobic interactions with the TLR4 ectodomain which is necessary for TLR4 activation.[12,42] This partly explains the lower endotoxicity of hypoacylated lipid A structures lacking this sixth acyl chain and the weakly agonistic activity of hypoacylated LPS_{BV}. Furthermore, both 1- and 4'- phosphates on the lipid A diglucosamine backbone were demonstrated to be important moieties for MD-2/TLR4 receptor complex activation[12]. Since LPS_{BV} possesses only one phosphate at position 1 of the reducing glucosamine, this may also contribute to its weakly agonistic effects as a missing 4'-phosphate was demonstrated to result in a 100-fold reduction in endotoxic activity[36]. Within this frame, the occurrence of a minor *bis*-phosphorylated lipid A species did not increase the LPS_{BV} immunogenicity as previously demonstrated for the *bis*-phosphorylated LPS lipid A from the mutant strain of *B. thetaiotaomicron* (ΔLpxFI)[37]. Additionally, recent studies revealed that not only the lipid A phosphorylation and acylation pattern determines LPS endotoxicity. Indeed, it was demonstrated that charged groups, other than glucosamine backbone associated phosphates, can increase LPS mediated endotoxicity. As examples, the positively charged aminoarabinose attached to the lipid A disaccharide backbone of the hypoacylated LPS from *Burkholderia cenocepacia* as well as the negatively charged carboxyl group present in the LPS core of a pentaacylated lipid A containing LPS of *Capnocytophaga canimorsus* were responsible for the high endotoxicity of both LPS[38, 39]. Besides Kdo-phosphate, LPS_{BV} does neither contain any further charged groups in the lipid A part nor in the core OS. Therefore, we can hypothesize that LPS_{BV} provides features and properties of a TLR4 antagonist, which is usually able to bind to MD-2 but it failed to induce receptor multimer formation and prevented from induction of any intracellular signalling[40, 41, 42]. LPS_{BV} bound to the MD-2/TLR4 receptor complex with a comparable affinity as highly agonistic LPS_{EC} but it did not lead to strong intracellular pro-inflammatory signalling. Nevertheless, LPS_{BV} did not act as a pure antagonist since it actively induced semi-maturation and tolerance

446 in dendritic cells, making it rather weakly agonistic than completely antagonistic. This is highly interesting
447 as Vatanen *et al.* demonstrated that *B. dorei* LPS, which provides the same lipid A structure as LPS_{BV}, acts as
448 a strong MD-2/TLR4 receptor complex antagonist[24]. This difference in immunogenicity of the respective
449 LPS supports the speculation of the unique LPS_{BV} core structure to contribute to its weakly agonistic activity.
450 Nevertheless, the weakly agonistic features of LPS_{BV} seem to be responsible for the observed healing effects
451 in mice suffering from intestinal inflammation. Therefore, LPS_{BV} led to weak intracellular signalling,
452 providing a basic anti-inflammatory intracellular transcription program without exceeding a pro-
453 inflammatory threshold. Furthermore, LPS_{BV} leads to the induction of tolerogenic DCs. These properties
454 clearly distinguish LPS_{BV} from strong agonistic LPS_{EC}, which induces endotoxin tolerance but also strong
455 pro-inflammatory signalling, and from antagonistic *B. dorei* LPS, which does not promote pro-inflammatory
456 reactions but does also not promote tolerance induction in TLR4-expressing cells[24]. The property of LPS_{BV}
457 of being an effective ligand for the MD-2/TLR4 receptor complex and, at the same time, of being a weak
458 agonist must of course be attributed to its chemical structure. We are not aware, whether this is a "chemical
459 paradigm" of the intestinal microbiota LPS since so far, only very few chemical structures of intestinal
460 commensals have been established. However, this is a logical follow up of the present work and further work
461 is in progress.

462 These observations led to a speculation on the potential use of such a LPS structure as a suitable tool to
463 restore homeostatic conditions not only in experimental mouse models, but also in IBD patients. Therapy of
464 IBD patients is, to date, restricted to a general suppression of the patient's immune response often associated
465 with undesirable side effects. LPS (derivative)-based treatment might avoid this problem by acting only
466 locally at the site of inflammation: the intestine.

467 Therefore, we would promote pure LPS_{BV} as an alternative for the treatment of intestinal inflammatory
468 disorders or IBD providing evidence that this compound demonstrated its beneficial effects as not being an
469 antagonist but rather a weak agonist. Alternatively, the structure of LPS_{BV} could act as a starting point for a
470 structure-activity relationship study in order to obtain a proper LPS derivative that could be used as a
471 prospective therapeutic agent. Concluding, we hope to contribute to IBD therapy-related research offering a
472 completely new approach avoiding disadvantages of current state-of-the-art IBD therapies.

Methods

T-cell mediated induction of chronic colitis in *Rag1*$^{-/-}$ mice

Germfree (GF) or conventionally colonized (CV) C57BL/6J-*Rag1*^{tm1Mom} (*Rag1*$^{-/-}$) mice were transplanted with 5 x 10^5 splenic $CD4^+CD62L^+CD45RB^{hi}C$ *wt* T-cells at 8 to 10 weeks of age. The conventional microbiota was free of Norovirus, Rotavirus and *Helicobacter hepaticus*. *Rag1*$^{-/-}$ mice were kept under SPF conditions and analyzed 8 weeks after T-cell transplantation as indicated in the results section.

In vivo positron emission tomography (PET)

High resolution PET imaging was performed using two identical small animal Inveon microPET scanner (Siemens Medical Solutions, Knoxville, USA) with a spatial resolution of 1.4 mm in reconstructed images (Field of view (FOV): transaxial 10 cm; axial: 12.7 cm)[43]. List mode data were processed by applying iterative Ordered Subset Expectation Maximization (OSEM) 2D algorithm for reconstruction. Mice were anesthetized using 1.5% isoflurane (Abbott GmbH, Wiesbaden, Germany) vaporized in O_2 (1.5 L/minute), an intravenously (i.v.) injection of 8.3 ± 1.3 MBq [^{18}F]fluorodesoxyglucose (FDG) was applied into the tail vein. After tracer injection, animals were placed on a heating pad to maintain body temperature and the animals were kept anesthetized for 60 min during tracer uptake time in an anaesthesia box. Shortly before the end of the uptake time, mice were placed in the FOV of the PET scanner on a warmed scanner bed (37 °C). Static (10 min) PET scans were performed on week 0, 4, 6 and 8 after T-cell application. Data were corrected for decay, normalized to the injected activity and analyzed using Pmod Software (PMOD Technologies Ltd., Zurich, Switzerland) by drawing regions of interest over the whole intestine.

Isolation of *B. vulgatus* mpk LPS (LPS_{BV}) and *E. coli* mpk LPS (LPS_{EC})

The Lyophilized bacterial pellet was washed several times with distilled water, ethanol and acetone followed by several ultracentrifugation steps (45,000 rpm at 4 °C), in order to remove contaminants.

Cells were extracted by hot phenol/water extraction[44]. Water and phenol phases were both dialyzed and lyophilized. After inspection by SDS-PAGE, an enzymatic treatment to remove proteins and nucleic acids was executed, followed by a dialysis step. The SDS-PAGE executed on both purified water and phenol phases highlighted the presence of LPS only in the water phase. To further purify the LPS material from a neutral polysaccharide capsular fraction, an ultracentrifugation step was executed as well.

See supplementary material for more information on experimental and analytic procedures.

Acknowledgments

Work was supported by the DFG (DFG FR 2087/6-1, DFG FR 2087/8-1, CRC685, SFB685, SFB766, SPP1656) the DFG research training group 1708, the Bundesministerium für Bildung und Forschung (BMBF) and the German Center for Infection research (DZIF). A.S. and A. M. thank the H2020-MSCA-ITN-2014-ETN TOLLerant.

Author contributions

J-S.F. and A.M. conceived the study, J-S.F., A.M., F.D.L., A.St. designed, executed the research and wrote the manuscript. All the authors contributed to execute the research, to analyze the data and to write the manuscript.

References

1. Herfarth H, Rogler G. Inflammatory bowel disease. *Endoscopy* **37**, 42-47 (2005).

2. Jostins L*, et al.* Host-microbe interactions have shaped the genetic architecture of inflammatory bowel disease. *Nature* **491**, 119-124 (2012).

3. Abegunde AT, Muhammad BH, Bhatti O, Ali T. Environmental risk factors for inflammatory bowel diseases: Evidence based literature review. *World journal of gastroenterology : WJG* **22**, 6296-6317 (2016).

4. Duboc H*, et al.* Connecting dysbiosis, bile-acid dysmetabolism and gut inflammation in inflammatory bowel diseases. *Gut* **62**, 531-539 (2013).

5. Peyrin-Biroulet L*, et al.* Systematic review of tumour necrosis factor antagonists in extraintestinal manifestations in inflammatory bowel disease. *Clin Gastroenterol Hepatol*, (2016).

6. Pigneur B, Sokol H. Fecal microbiota transplantation in inflammatory bowel disease: the quest for the holy grail. *Mucosal immunology*, (2016).

7. Gronbach K*, et al.* Endotoxicity of lipopolysaccharide as a determinant of T-cell-mediated colitis induction in mice. *Gastroenterology* **146**, 765-775 (2014).

8. Alexander C, Rietschel ET. Bacterial lipopolysaccharides and innate immunity. *J Endotoxin Res* **7**, 167-202 (2001).

9. Steimle A, Autenrieth IB, Frick JS. Structure and function: Lipid A modifications in commensals and pathogens. *Int J Med Microbiol*, (2016).

10. Silipo A*, et al.* Structural characterization of two lipopolysaccharide O-antigens produced by the endofungal bacterium Burkholderia sp. HKI-402 (B4). *Carbohydr Res* **347**, 95-98 (2012).

11. Molinaro A*, et al.* Chemistry of lipid A: at the heart of innate immunity. *Chemistry* **21**, 500-519 (2015).

12. Park BS, Song DH, Kim HM, Choi BS, Lee H, Lee JO. The structural basis of lipopolysaccharide recognition by the TLR4-MD-2 complex. *Nature* **458**, 1191-1195 (2009).

13. Kamada N, Chen GY, Inohara N, Nunez G. Control of pathogens and pathobionts by the gut microbiota. *Nat Immunol* **14**, 685-690 (2013).

14. Chassaing B, Darfeuille-Michaud A. The commensal microbiota and enteropathogens in the pathogenesis of inflammatory bowel diseases. *Gastroenterology* **140**, 1720-1728 (2011).

15. Lange A, Beier S, Steimle A, Autenrieth IB, Huson DH, Frick JS. Extensive mobilome-driven genome diversification in mouse gut-associated Bacteroides vulgatus mpk. *Genome Biol Evol*, (2016).

16. Waidmann M*, et al.* Bacteroides vulgatus protects against Escherichia coli-induced colitis in gnotobiotic interleukin-2-deficient mice. *Gastroenterology* **125**, 162-177 (2003).

17. Muller M*, et al.* Intestinal colonization of IL-2 deficient mice with non-colitogenic B. vulgatus prevents DC maturation and T-cell polarization. *PLoS One* **3**, e2376 (2008).

18. Steimle A*, et al.* Symbiotic gut commensal bacteria act as host cathepsin S activity regulators. *Journal of autoimmunity*, (2016).

19. Pellegrino D, Bonab AA, Dragotakes SC, Pitman JT, Mariani G, Carter EA. Inflammation and infection: imaging properties of 18F-FDG-labeled white blood cells versus 18F-FDG. *J Nucl Med* **46**, 1522-1530 (2005).

20. Iwasaki A, Medzhitov R. Control of adaptive immunity by the innate immune system. *Nat Immunol* **16**, 343-353 (2015).

21. Agace WW, Persson EK. How vitamin A metabolizing dendritic cells are generated in the gut mucosa. *Trends Immunol* **33**, 42-48 (2012).

22. Steimle A, Frick JS. Molecular Mechanisms of Induction of Tolerant and Tolerogenic Intestinal Dendritic Cells in Mice. *J Immunol Res* **2016**, 1958650 (2016).

23. Hall JA, Grainger JR, Spencer SP, Belkaid Y. The role of retinoic acid in tolerance and immunity. *Immunity* **35**, 13-22 (2011).

24. Vatanen T*, et al.* Variation in Microbiome LPS Immunogenicity Contributes to Autoimmunity in Humans. *Cell* **165**, 842-853 (2016).

25. Hashimoto M*, et al.* Structural study on lipid A and the O-specific polysaccharide of the lipopolysaccharide from a clinical isolate of Bacteroides vulgatus from a patient with Crohn's disease. *Eur J Biochem* **269**, 3715-3721 (2002).

26. Vinogradov E, Korenevsky A, Beveridge TJ. The structure of the carbohydrate backbone of the LPS from Shewanella putrefaciens CN32. *Carbohydr Res* **337**, 1285-1289 (2002).

27. Di Lorenzo F*, et al.* Thermophiles as potential source of novel endotoxin antagonists: the full structure and bioactivity of the lipo-oligosaccharide from Thermomonas hydrothermalis. *Chembiochem* **15**, 2146-2155 (2014).

28. Holst O, Molinaro A. Core region and lipid A components of lipopolysacchrides. *Microbial glycobiology: structures, relevance and applications*, 29-55 (2009).

29. Frick JS*, et al.* Colitogenic and non-colitogenic commensal bacteria differentially trigger DC maturation and Th cell polarization: an important role for IL-6. *European journal of immunology* **36**, 1537-1547 (2006).

30. Geisel J*, et al.* IL-6 and maturation govern TLR2 and TLR4 induced TLR agonist tolerance and cross-tolerance in dendritic cells. *J Immunol* **179**, 5811-5818 (2007).

31. Gerlach AM*, et al.* Role of CD40 ligation in dendritic cell semimaturation. *BMC Immunol* **13**, 22 (2012).

32. Kumari R, Ahuja V, Paul J. Fluctuations in butyrate-producing bacteria in ulcerative colitis patients of North India. *World journal of gastroenterology : WJG* **19**, 3404-3414 (2013).

33. Weintraub A, Zahringer U, Wollenweber HW, Seydel U, Rietschel ET. Structural characterization of the lipid A component of Bacteroides fragilis strain NCTC 9343 lipopolysaccharide. *Eur J Biochem* **183**, 425-431 (1989).

34. Brandenburg K, Mayer H, Koch MH, Weckesser J, Rietschel ET, Seydel U. Influence of the supramolecular structure of free lipid A on its biological activity. *Eur J Biochem* **218**, 555-563 (1993).

35. Seydel U, Oikawa M, Fukase K, Kusumoto S, Brandenburg K. Intrinsic conformation of lipid A is responsible for agonistic and antagonistic activity. *Eur J Biochem* **267**, 3032-3039 (2000).

36. Rietschel ET*, et al.* Bacterial endotoxin: molecular relationships of structure to activity and function. *FASEB J* **8**, 217-225 (1994).

37. Cullen TW*, et al.* Gut microbiota. Antimicrobial peptide resistance mediates resilience of prominent gut commensals during inflammation. *Science* **347**, 170-175 (2015).

38. Di Lorenzo F*, et al.* Activation of Human Toll-like Receptor 4 (TLR4).Myeloid Differentiation Factor 2 (MD-2) by Hypoacylated Lipopolysaccharide from a Clinical Isolate of Burkholderia cenocepacia. *J Biol Chem* **290**, 21305-21319 (2015).

39. Ittig S*, et al.* The lipopolysaccharide from Capnocytophaga canimorsus reveals an unexpected role of the core-oligosaccharide in MD-2 binding. *PLoS pathogens* **8**, e1002667 (2012).

40. Ianaro A, Tersigni M, D'Acquisto F. New insight in LPS antagonist. *Mini Rev Med Chem* **9**, 306-317 (2009).

41. Meng J, Drolet JR, Monks BG, Golenbock DT. MD-2 residues tyrosine 42, arginine 69, aspartic acid 122, and leucine 125 provide species specificity for lipid IVA. *J Biol Chem* **285**, 27935-27943 (2010).

42. Meng J, Lien E, Golenbock DT. MD-2-mediated ionic interactions between lipid A and TLR4 are essential for receptor activation. *J Biol Chem* **285**, 8695-8702 (2010).

43. Mannheim JG*, et al.* Quantification accuracy and partial volume effect in dependence of the attenuation correction of a state-of-the-art small animal PET scanner. *Phys Med Biol* **57**, 3981-3993 (2012).

44. Westphal O, Jann K. Bacterial lipopolysaccharides: extraction with phenol-water and further applications of procedure. *Carbohydr Chem* **5**, 83-91 (1965).

Bacteroides vulgatus mpk lipopolysaccharide acts as inflammation-silencing agent for the treatment of intestinal inflammatory disorders

Supplementary information

Supplementary Methods

Mice

C57BL/6J mice were purchased from Charles River Laboratories, C57BL/6J-*Rag1*^{tm1Mom} (*Rag1*$^{-/-}$) mice from own breeding. All animals were kept and bred under SPF conditions. For isolation of bone marrow, only female mice aged 6-12 weeks were used. Animal experiments were reviewed and approved by the responsible institutional review committee and the local authorities.

Radiopharmaceuticals

[^{18}F]fluoride was produced by using ^{18}O (p,n) ^{18}F nuclear reaction on the PETtrace cyclotron (General Electric Medical Systems, GEMS, Uppsala, Sweden). [^{18}F]FDG synthesis was performed as described elsewhere[1]. After the synthesis, specific activity was calculated and revealed > 50 GBq/mmol with a radiochemical purity of > 99%.

Bacteria

The bacteria used for stimulation of the murine dendritic cells were *Escherichia coli* mpk and *Bacteroides vulgatus* mpk[2]. The *E. coli* mpk strain was grown in Luria-Bertani (LB) medium under aerobic conditions at 37 °C. *B. vulgatus* mpk was grown in Brain-Heart-Infusion (BHI) medium and anaerobic conditions at 37 °C.

Extraction, purification and chemical analyses of lipopolysaccharide from *B. vulgatus* mpk (LPS_{BV})

Bacterial dried cells (5 g) were extracted through the hot phenol/water procedure[3]. The row LPS (300 mg) was checked by SDS-PAGE after gel silver staining[4] revealing a smooth-type LPS only in the water phase. In order to remove cell contaminants, an intensive enzymatic treatment by RNase (Roth, Germany), DNase (Roth, Germany) and Proteinase K (Roth, Germany) at 37 °C and 56 °C was executed, followed by exhaustive dialysis. In order to further purify the LPS material, an ultracentrifugation step (4 °C, 30,000 rpm, 24 h) and a gel-filtration chromatography were also performed. LPS monosaccharide content was established by analysis of the acetylated *O*-methyl glycoside derivatives obtained by treatment with HCl/MeOH (1.25 M, 85 °C, 24 h) followed by an acetylation step with acetic anhydride in pyridine (85 °C, 30 min). The absolute configuration of each sugar unit was defined through the evaluation of the *O*-octylglycoside derivatives as previously described[5]. The sugar linkage pattern was determined by the Ciucanu method[6, 7]: briefly, an aliquot of sample was suspended in DMSO to which NaOH in powder was added and then methylated with CH_3I, hydrolyzed with trifluoroacetic acid (4 M, 100 °C, 4 h), carbonyl reduced with $NaBD_4$ and acetylated with pyridine and acetic anhydride. The total fatty acid content was established on intact LPS by treating with HCl (4 M, 100 °C, 4 h) followed by NaOH (5 M, 100 °C, 30 min). The pH was adjusted to reach slight acidity. After extraction in chloroform, fatty acids were then methylated with diazomethane[8]. All chemical analyses were performed by means of gas-liquid chromatography (GLC-MS) Agilent Technologies 6850A equipped with a mass selective detector 5973N and a Zebron ZB-5 capillary column (Phenomenex, 30 m x 0.25 mm i.d., flow rate 1 mL min^{-1}, He used as carrier gas) and using the following temperature program: 140 °C/240 °C at 3 °C min^{-1}.

Isolation of the LPS_{BV} saccharide domain

An aliquot of pure LPS was treated with anhydrous hydrazine (2 mL), stirred at 37 °C for 90 min, cooled, poured into ice-cold acetone (20 mL) and allowed to precipitate. The precipitate was centrifuged (4000 x g, 30 min), washed with ice-cold acetone, dried, dissolved in water and lyophilized[9]. The *O*-deacylated product was then *N*-deacylated with 4 M KOH. The removal of salts was executed by gel-filtration chromatography on a Sephadex G-10 column (Pharmacia, 50 x 1.5 cm)[10]. The fully deacylated product was further purified on a Toyopearl TSK HW-50 (Tosoh Bioscience).

NMR spectroscopy

1D and 2D ^{1}H NMR spectra were recorded on a Bruker 600 DRX equipped with a cryo probe. The solvent employed was D_2O and the temperature was 298 K and pD was 7. Spectra calibration was performed with internal acetone (δH 2.225 ppm, δC 31.45 ppm). ^{31}P NMR experiments were carried out with a Bruker DRX-400 spectrometer, aqueous 85% phosphoric acid was used as external reference (δ = 0.00 ppm). The double-quantum filtered phase sensitive correlation spectroscopy (DQF-COSY) experiment was carried out by using data sets of 4096 x 256 points. Total correlation spectroscopy (TOCSY) experiments were executed with spinlock times of 100 ms, using data sets (t1 × t2) of 4096 x 256 points. Rotating frame Overhauser enhancement spectroscopy (ROESY) and Nuclear Overhauser enhancement spectroscopy (NOESY) experiments were recorded by using data sets (t1 × t2) of 4096 x 256 points and by using mixing times between 100 and 400 ms, In all homonuclear experiments the data matrix was zero-filled in both dimensions to give a matrix of 4 K x 2 K points and was resolution enhanced in both dimensions by a cosine-bell function before Fourier Transformation. The determination of coupling constants was obtained by 2D phase sensitive DQF-COSY.[11,12] Heteronuclear single quantum coherence (^{1}H, ^{13}C HSQC) and heteronuclear multiple bound correlation (^{1}H, ^{13}C HMBC) experiments were recorded in 1H-detection mode by single-quantum coherence with protein decoupling in the ^{13}C domain using data sets of 2048 × 256 points. ^{1}H, ^{13}C HSQC was executed using sensitivity improvement and in the phase-sensitive mode using Echo/Antiecho gradient selection, with multiplicity editing during selection step.[13] The ^{1}H, ^{13}C HMBC experiment was optimized on long-range coupling constants with low-pass *J* filter to suppress one-bound connectivity, using gradient pulses for selection. A delay of 60 ms was employed for the evolution of long-range correlations. It was used a long-range coupling constant value of 6 Hz. The data matrix in both heteronuclear experiments was extended to 2048 × 1024 points using forward linear prediction[14].

ESI MS and MS/MS analysis

MS spectra of the carbohydrate part of LPS_{BV} were acquired on an amazon SL ion trap (IT) mass spectrometer with electrospray ionization (ESI) (Bruker Daltonics, USA). The sample (75 µg) was dissolved

in 50 µL of acetonitrile/water/formic acid solution (100:100:1, v/v/v) and analyzed in negative ion mode. Ion corresponding to core OS (*m/z* 667.3) was analyzed by MS/MS. Source parameters were as follows: sample flow, 3 µL min^{-1}; ion source temperature, 200 °C; nitrogen flow, 5 L min^{-1} at a pressure of 8 psi. Spectra were scanned in the 200-2000 *m/z* range. He was used as the collision gas in the IT. The system was calibrated using ESI-L Tuning Mix (Agilent Technologies, USA)[15].

Isolation of the lipid A fraction from LPS_{BV}

Isolation of lipid A was achieved by mild acid hydrolysis by using acetate buffer (1 mL, pH = 4.4) promoted by SDS (1 mg mL^{-1}) on ca. 20 mg of isolated LPS at 100 °C. The solution was extracted 3 times with $CHCl_3$/MeOH/H_20 (100:30:30, v/v/v) and centrifuged (4 °C, 7,000 x g, 15 min). The organic phase containing the lipid A was further purified by several washes with distilled water and then freeze-dried.

MALDI MS analysis on isolated A from LPS_{BV}

Lipid A isolated after mild acid hydrolysis of LPS_{BV} was analyzed with MALDI-TOF ultrafleXtreme sptecrometer (Bruker Daltonics, USA). 100 µg of lipid A was dissolved in 100 µL of mQ water after 10 min incubation at 40 °C in the ultrasonic bath. 10 mg of 9H-pyrido(3,4)-indole was mixed with 1 mL of CHCl3/MeOH (1:1, v/v) and 0.5 µL of the matrix was spotted onto the matrix. The sample was analyzed in reflectron, negative ion mode, scan range: 700-3500 *m/z*. Instrument was calibrated within 1000-3150 Da mass range, using peptide mixture (Peptide Calibration Standard, Bruker Daltonics, USA).

Biotinylation of LPS_{BV}

10 mg of LPS_{BV} were biotinylated with EZ-Link Micro Sulfo-NHS-LC-Biotinylation Kit (Thermo Scientific) according to the manufacturer's protocol using phosphate buffered saline (PBS) as a solvent. In order to remove PBS, an exhaustive dialysis against distilled water was performed. The biotinylated LPS_{BV}

(bioLPS$_{BV}$) was then collected and lyophilized. For *in vitro* experiments lyophilized bioLPS$_{BV}$ was dissolved in distilled water in concentrations not higher than 1 mg mL^{-1}.

Cultivation of bone marrow derived dendritic cells (BMDCs)

Bone marrow cells were isolated from *wt* C57BL/6 mice (purchased from Charles River) and cultivated as described previously[16]. At day 7 after isolation, resulting CD11c positive dendritic cells (BMDCs) were used for further experiments.

Stimulation of bone marrow derived dendritic cells

2 x 10^6 BMDCs were stimulated with either PBS, *B. vulgatus* mpk or *E. coli* mpk at a MOI of 1 or respective isolated LPS at concentrations as indicated in the results section. Cells were stimulated for a maximum of 24 h. If a second challenge was used, cells were stimulated with bacteria followed by exchanging used for fresh medium followed by challenging the cells with a second stimulus for a maximum of 16 h. PBS was used as mock stimulation control.

Stimulation of human embryonic kidney (HEK) cells

2 x 10^5 HEK cells, either expressing murine CD14, MD-2 and TLR4 (HEK-mTLR4) or not, were seeded in 1 mL medium were subsequently stimulated with 1 to 1000 ng mL^{-1} isolated LPS or bacteria (MOI 1) for time points indicated in the results section.

Detection of bound biotinylated LPS$_{BV}$

After end of incubation time with biotinylated LPS$_{BV}$, HEK-mTLR4 cells were scraped off, washed once in PBS + 1%FCS and incubated with PE-coupled streptavidin (Strep-PE) for 30 min, followed by another washing step. Cell-attached strep-PE was detected by flow cytometry. All experiments to be compared were

carried out in one experimental setting to guarantee for comparability of the detected MFI (median fluorescence intensity) values of the PE fluorescence.

Cytokine analysis by ELISA

For analysis of secreted cytokines (IL-6, IL-1β, IL-12p40, TNF), ELISA-based detection kits were purchased from BD Biosciences, Germany, and used according to the manufacturer's instructions.

Flow cytometrical analysis

Multi-color FCM analyses were performed on a FACS Calibur or FACS LSRII (BD Biosciences, Germany). All fluorochrome-coupled antibodies were purchased from BD Biosciences, Germaany. Data were analyzed using FlowJo software (Tree Star Inc., USA).

Purification of RNA and Quantitative Real-Time PCR

Purification of RNA from mouse colonic scrapings was performed using Qiagen's RNeasy Mini Kit according to the manufacturer's instructions. Additional DNA digestion was conducted by using 4 U rDNase I and 40 U rRNasin for a RNA solution of 0.1 µg μL^{-1}. After 30 min of incubation at RT, DNase was inactivated using Ambion DNase inactivation reagent which was later removed by centrifugation for 1 min at 10'000 x g. SybrGreen based quantitative RT-PCR was performed on a Roche LightCycler480 using QiagenSybrGreen RT-PCR Kit. Primer annealing occurred at 60 °C. 10 to 100 ng DNA-digested RNA was used for qRT-PCR. Relative mRNA expression in BMDCs stimulated with bacteria to unstimulated BMDCs was determined with β-actin as housekeeping gene using the ΔΔCp-method that included the specific amplification efficiency of every used primer pair and each PCR run.

Primer sequences

Primers used for qRT-PCR were: *Aldh1a2,* Forward Primer: 5'- AAGACACGAGCCCATTGGAG-3'; Reverse Primer: 5'- GGAAAGCCAGCCTCCTTGAT-3'; *β-actin*, Forward Primer: 5'- CCCTGTGCTGCTCACCGA-3', Reverse Primer: 5'- ACAGTGTGGGTGACCCCGTC-3'

Isolation of lamina propria (LP) dendritic cells (DC) and T cells and adoptive transfer of T cells

Isolation of mouse LP cells was performed as published previously[17]. For adoptive transfer, splenic $CD4^+$ T cells from C57BL/6 mice were purified using a MACS-based negative selection kit (Miltenyi) according to the manufacturer's instructions. The isolated cells were stained for CD3ε, CD4 and CD62 for reanalysis, purity was generally >90% with >80% being $CD4^+CD62L^+CD45RB^{hi}$. 5 x 10^5 $CD4^+$ T cells were injected into the peritoneum (i.p.) of *Rag1*$^{-/-}$ mice as described previously [18].

Histology

Colonic tissues were fixed in neutral buffered 4% formalin. Formalin-fixed tissues were embedded in paraffin and cut into 2 µm sections. They were stained with hematoxylin (Merck) and eosin (Merck) for histological scoring. Scoring was conducted in a blinded fashion on a validated scale of 0 – 3, with 0 representing no inflammation and 3 representing severe inflammation characterized by infiltration with inflammatory cells, crypt hyperplasia, loss of goblet cells and distortion of architecture [19].

Statistics

Statistical analyses were performed using the unpaired student's t test to compare two groups with each other. For comparing *in vitro* results, samples were considered to be biologically independent if the samples were generated from BMDCs from different mice. Differences were considered to be statistically significant if $p < 0.05$. Error bars, if shown, represent ± standard deviation (SD).

Supplementary figures:

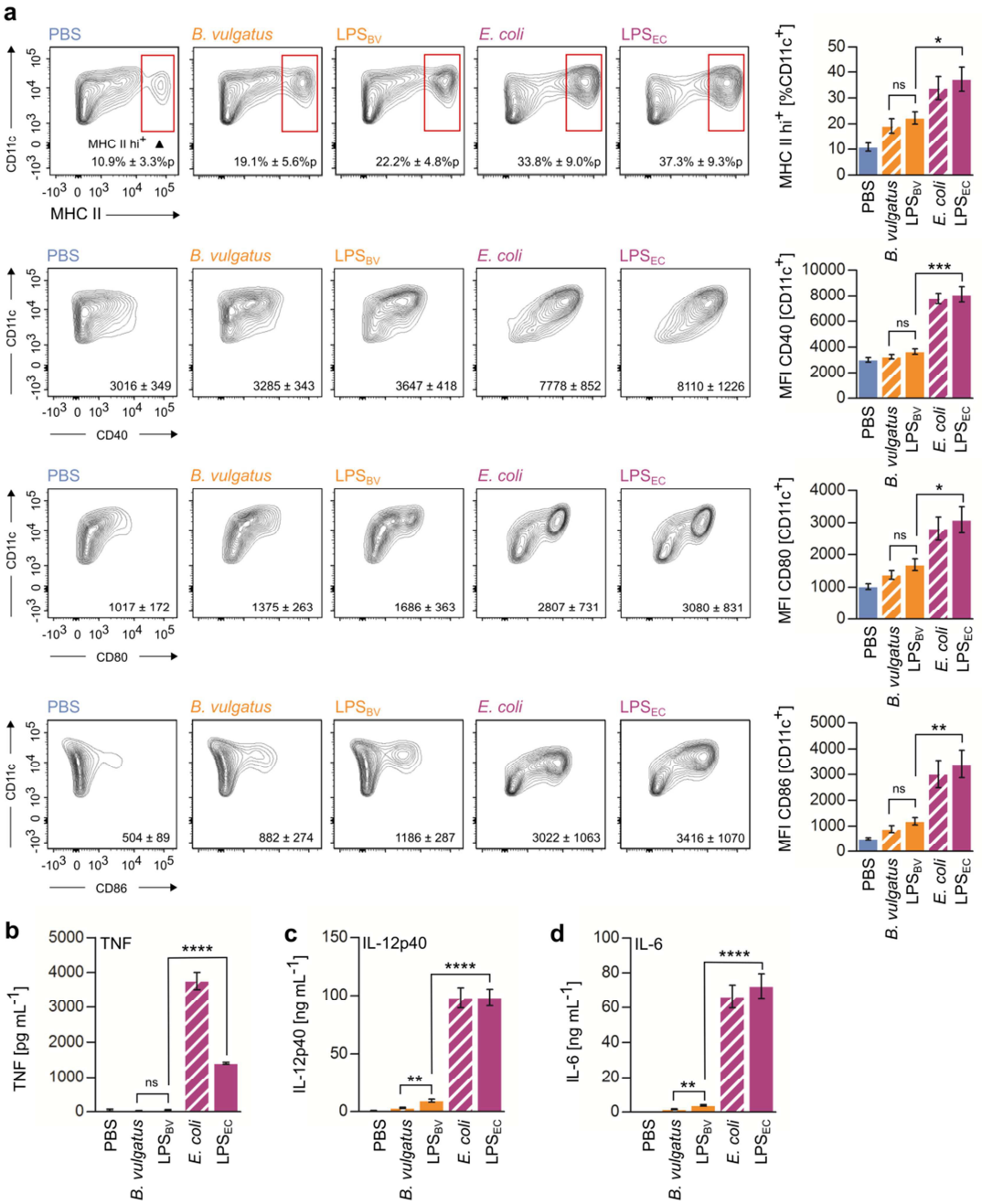

Supplementary Figure 1: Isolated LPS of *B. vulgatus* mpk and live *B. vulgatus* mpk provide similar weakly agonistic immunogenic properties on bone marrow derived dendritic cells.

Bone marrow derived dendritic cells (BMDCs) from *wt* mice were generated as described and stimulated with either PBS (mock control), *B. vulgatus* mpk (MOI 1), *E. coli* mpk (MOI 1), *B. vulgatus* mpk LPS (LPS_{BV}) (50 ng per 10^6 BMDCs) or *E. coli* mpk LPS (LPS_{EC}) (50 ng per 10^6 BMDCs) for 16 h. (a) flow cytometric analyses of BMDC surface expression of MHC-II, CD40, CD80 and CD86 among the population of $CD11c^+$ cells. (b) secretion of TNF, IL-12p40 and IL-6 into cell supernatant, determined by ELISA,

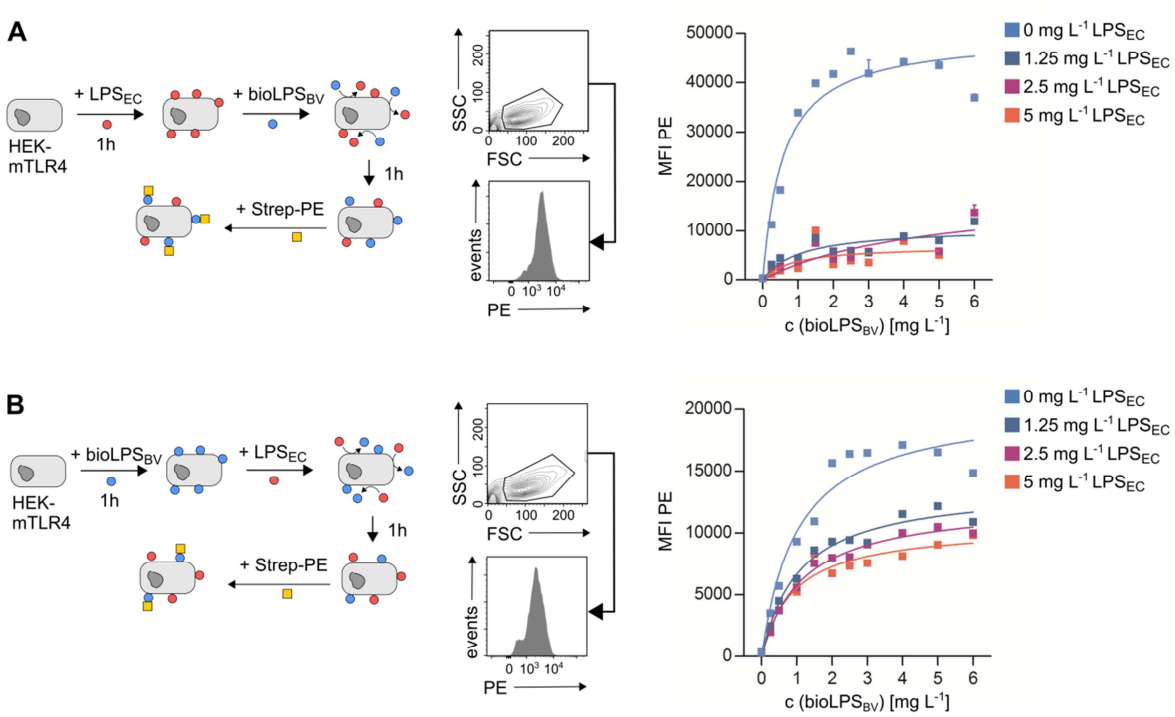

Supplementary Figure 2: Weakly agonistic LPS$_{BV}$ provides only low capacity to remove agonistic LPS$_{EC}$ from the murine MD-2/TLR4 receptor complex.

a. Left panel: experimental setting. 1 x 10^5 HEK cells expressing murine CD14, MD-2 and TLR4 (HEK-mTLR4) were incubated with a certain constant concentration of LPS$_{EC}$ ranging from 0 to 5 mg L^{-1} for 1 h. For each certain LPS$_{EC}$ concentration varying concentrations of biotinylated *B. vulgatus* mpk LPS (bioLPS$_{BV}$) were added ranging from 0 to 6 mg mL^{-1} and incubated again for 1 h. PE-coupled streptavidin (Strep-PE) was added for 30 min and the resulting PE fluorescence associated with HEK-mTLR4 cells was detected by flow cytometry. **Central panel**: gating strategy to determine PE fluorescence of intact HEK-mTLR4 cells. **Right panel**: Binding curves of 4 distinct concentrations of LPS$_{EC}$ plotted against varying concentrations of subsequently added bioLPS$_{BV}$.

b. **Left panel**: experimental setting. 1 x 10^5 HEK-mTLR4 cells were incubated with a certain concentration of bioLPS$_{BV}$ ranging from 0 to 6 mg L^{-1} for 1 h. For each certain bioLPS$_{BV}$ concentration varying concentrations of LPS$_{EC}$ was added ranging from 0 to 5 mg L^{-1} and incubated again for 1 h. Strep-PE was added for 30 min and fluorescence was detected by flow cytometry. **Central panel**: gating strategy to determine PE fluorescence of intact HEK-mTLR4 cells. **Right panel**: Binding curves of 4 distinct concentrations of LPS$_{EC}$ plotted against varying concentrations of previously added bioLPS$_{BV}$.

.

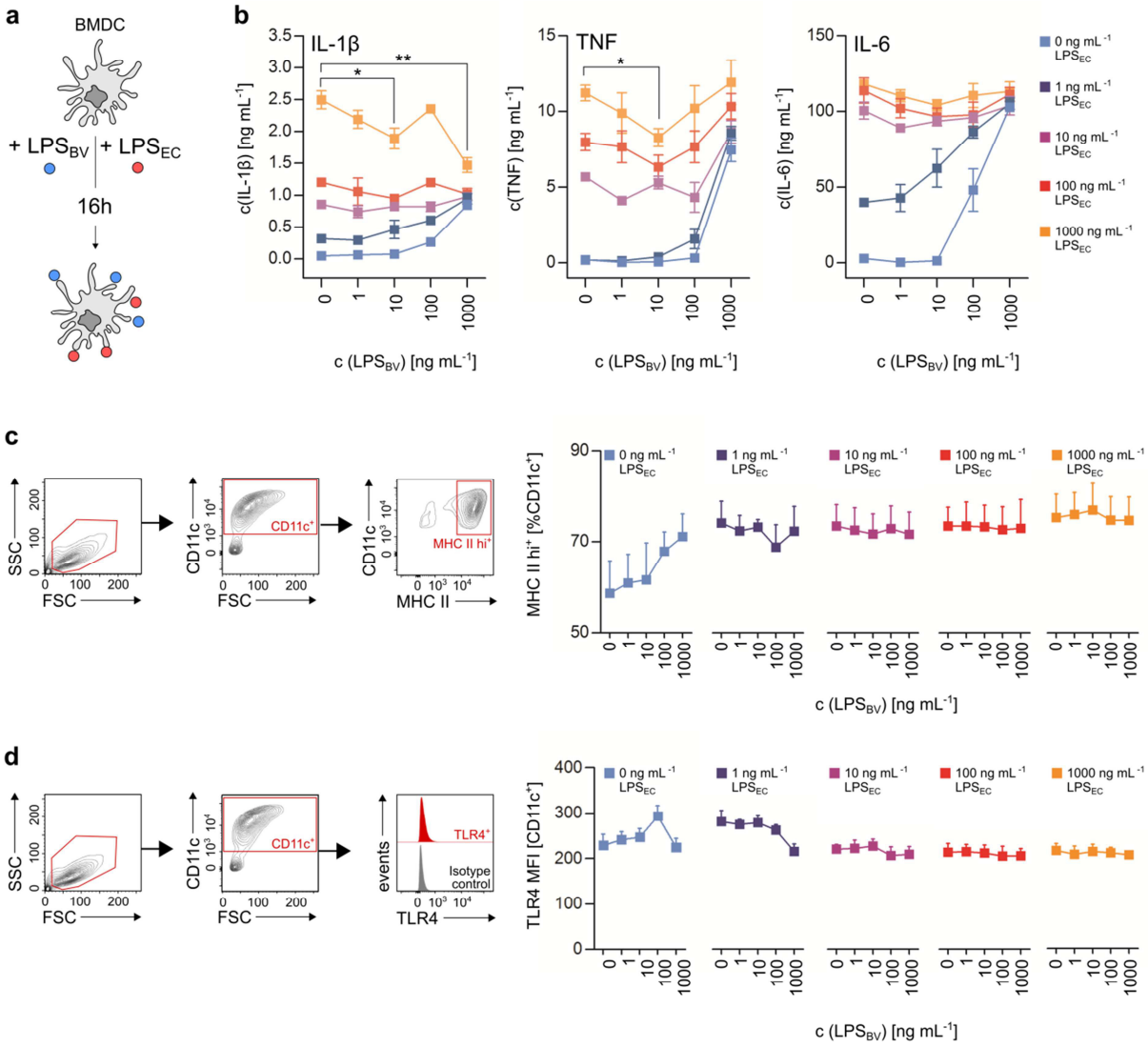

Supplementary Figure 3: Simultaneous stimulation of bone marrow derived dendritic cells with weakly agonistic semi-maturation inducing LPS_{BV} and agonistic LPS_{EC} does not anticipate dendritic cell maturation.

a. Experimental setting: bone marrow derived dendritic cells (BMDCs) were generated as described. BMDCs were simultaneously stimulated with different concentrations of LPS_{BV} and LPS_{EC} for 16 h.

b. Secretion of IL-1β, TNF and IL-6 into cell supernatant from BMDCs that were stimulated as shown in (a). Used concentrations of LPS_{BV} are depicted on the x-axes, the connected coloured lines represent a distinct concentration of LPS_{EC} each. Every data point therefore represents a certain combination of LPS_{EC} and LPS_{BV} concentrations (n=3).

c. MHC-II surface expression. BMDCs were stimulated according to (a). **Left panel**: Gating strategy to determine the proportion of MHC II high positive (MHC-II^{hi+}) cells among the population of $CD11c^+$ BMDCs. **Right panel**: Proportion of MHC-II^{hi+} $CD11c^+$ cells dependent on the used concentrations of LPS_{BV} (depicted on the x-axes) and LPS_{EC} (depicted as differentially coloured connected lines) (n=3).

d. TLR4 expression of BMDCs which were stimulated as demonstrated in (a). **Left panel**: gating strategy to determine the mean fluorescence intensity (MFI) of TLR4 expression on $CD11c^+$ BMDCs. **Right panel**: MFI of TLR4 expression of $CD11c^+$ cells dependent on the used concentrations of LPS_{BV} (depicted on the x-axes) and LPS_{EC} (depicted as differentially coloured connected lines) (n=3).

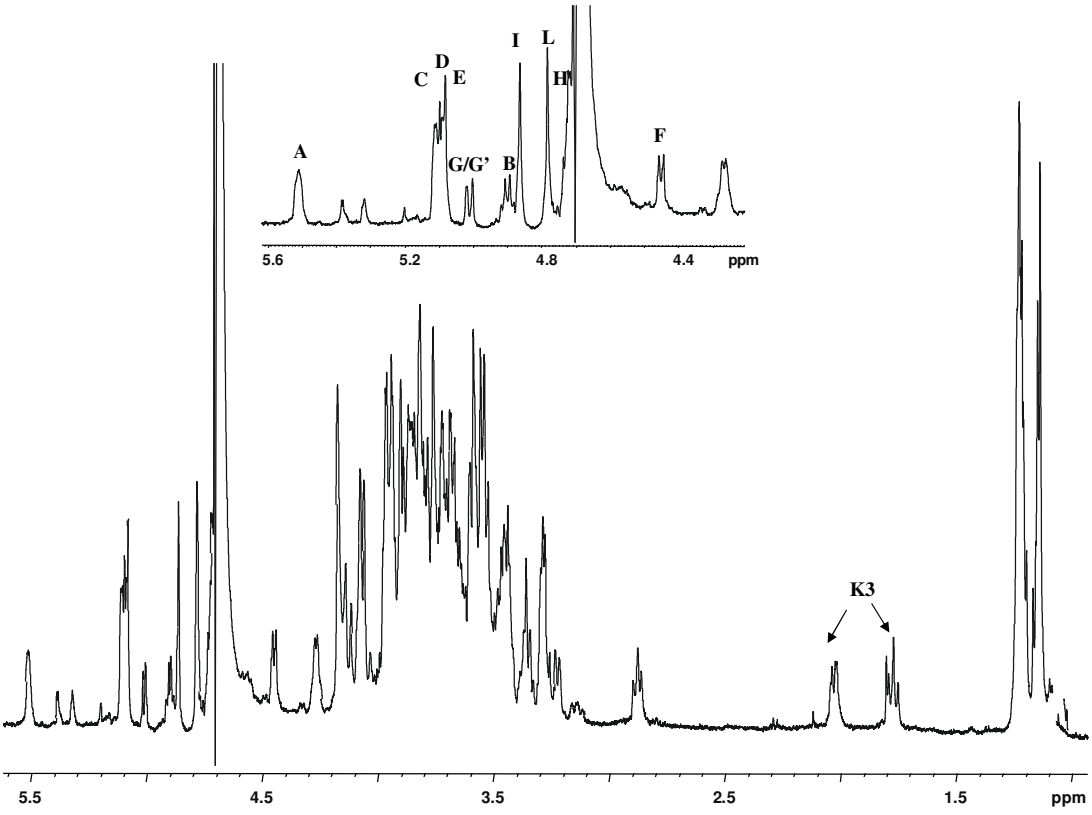

Supplementary Figure 4: ^{1}H NMR of fully deacylated LPS$_{BV}$.
^{1}H NMR spectrum of the saccharide domain of the LPS from *B. vulgatus* mpk obtained after full deacylation of the pure LPS. A zoom of the anomeric region is reported in the inset. Anomeric signals in the inset are as attributed in Supplementary Table 1.

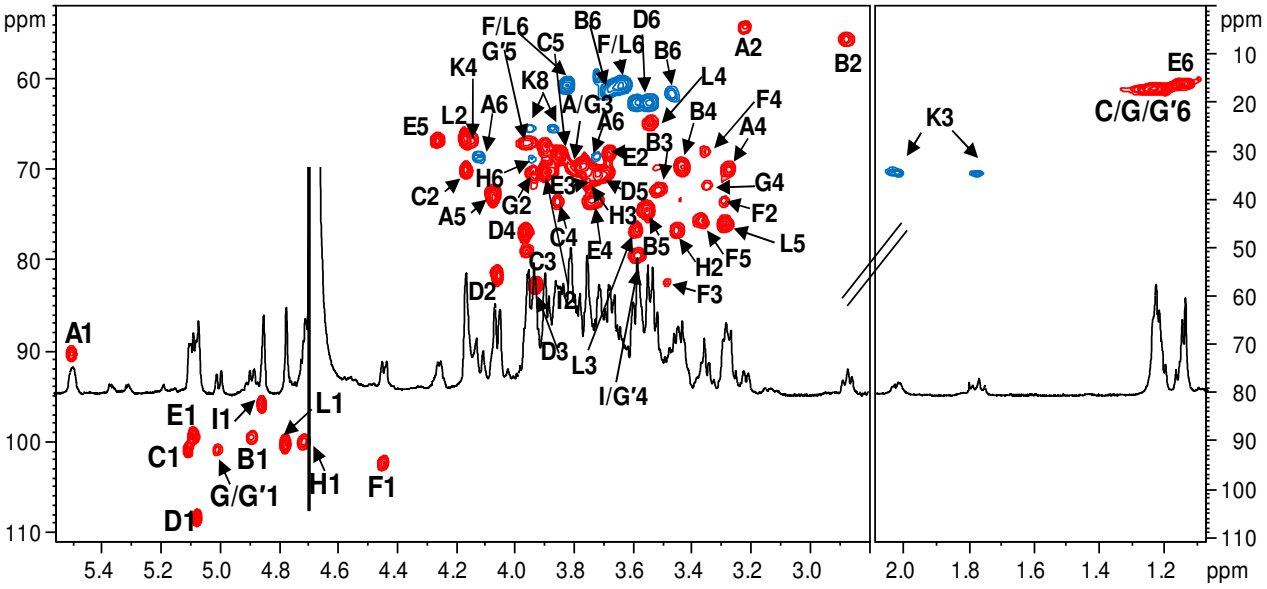

Supplementary Figure 5: ^{1}H and ^{1}H, ^{13}C HSQC NMR spectrum of fully deacylated LPS$_{BV}$.
^{1}H and ^{1}H, ^{13}C HSQC spectra of the deacylated LPS from *B. vulgatus* mpk. Key heteronuclear signals from the sugar backbone are indicated. Numbering of sugar residues is as reported in Fig. 3 and Supplementary Table 1.

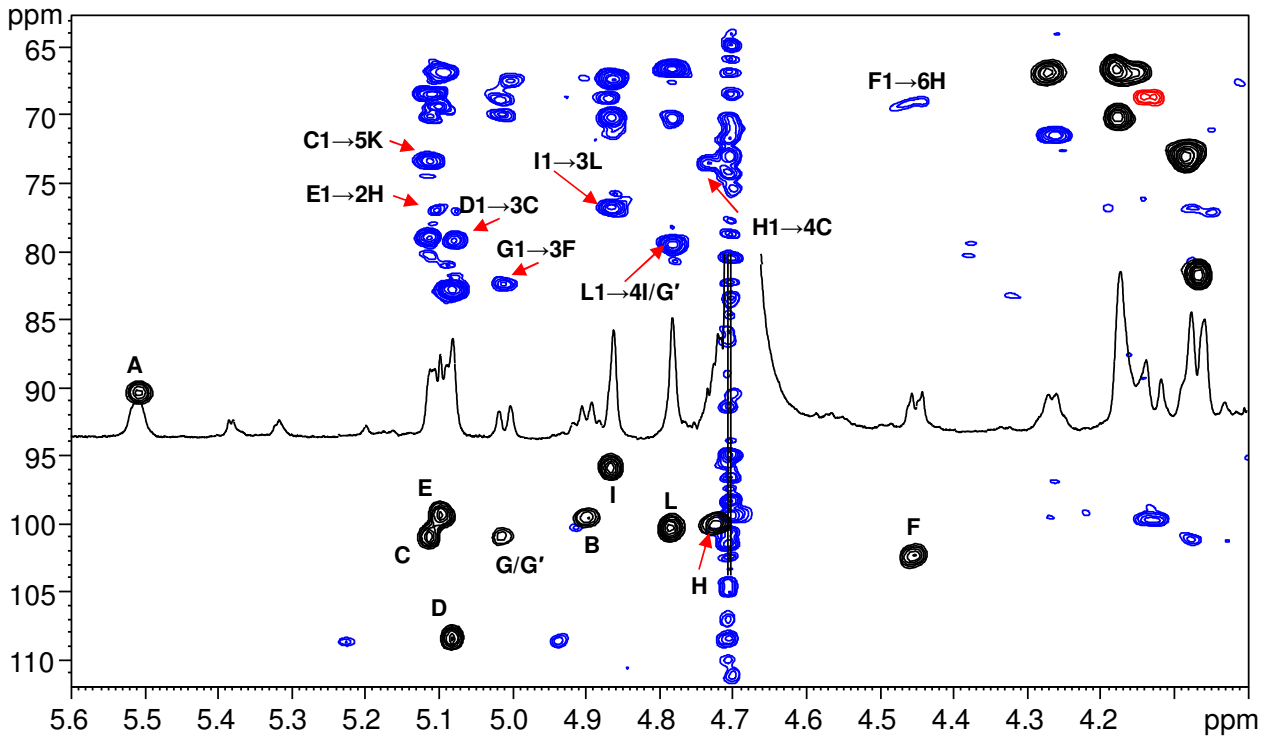

Supplementary Figure 6: Long-range correlations analysis of fully deacylated LPS_{BV}.
Zoom of the overlapped ^{1}H, ^{1}H, ^{13}C HMBC (blue) and ^{1}H, ^{13}C HSQC (black and red) NMR spectra; the key *inter*-residual long-range correlations involving sugar moieties (**A**-**L**) are indicated; letters are as in Supplementary Table 1. Anomeric one-bond heteronuclear correlations were also reported in the spectrum.

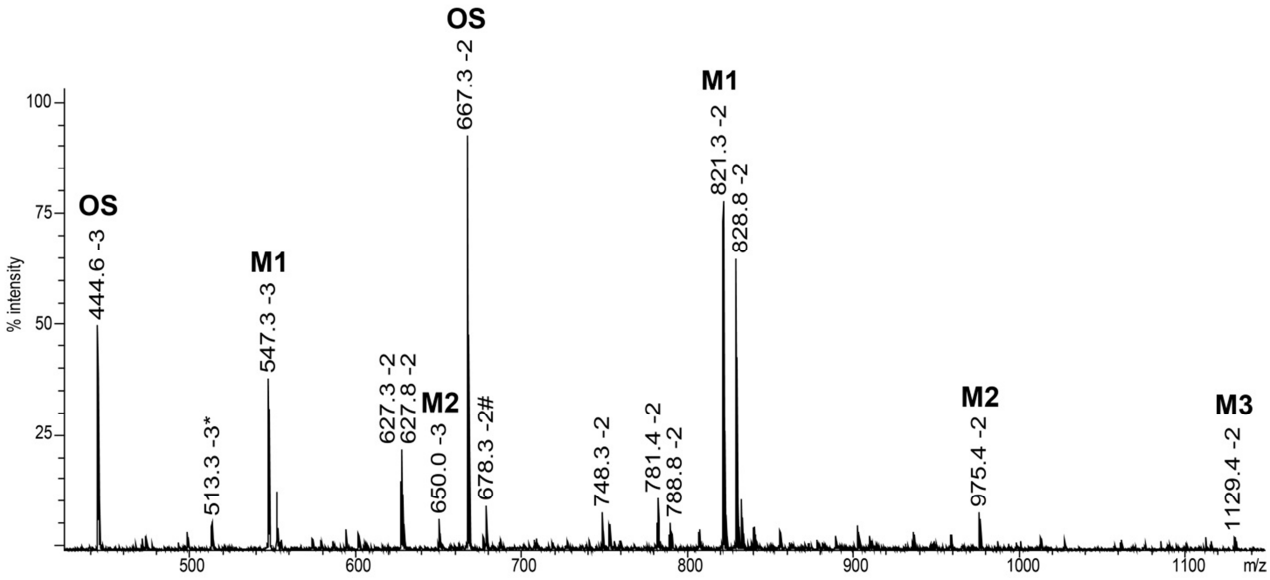

Supplementary Figure 7: ESI-MS spectrum of fully deacylated LPS_{BV}.
Zoom of mass spectrum with ions corresponding to core OS and core OS substituted with one, two and three O-chain repeating units (*m/z* 444.6 and 667.3 (**OS**), 547.3 and 821.3 (**M1**), 650.0 and 975.4 (**M2**), as well as 1129.4 (**M3)** respectively). Spectrum was acquired in negative ion mode. # indicates $[M-3H+Na]^{2-}$ ion. Ion indicated by asterisk was not interpreted.

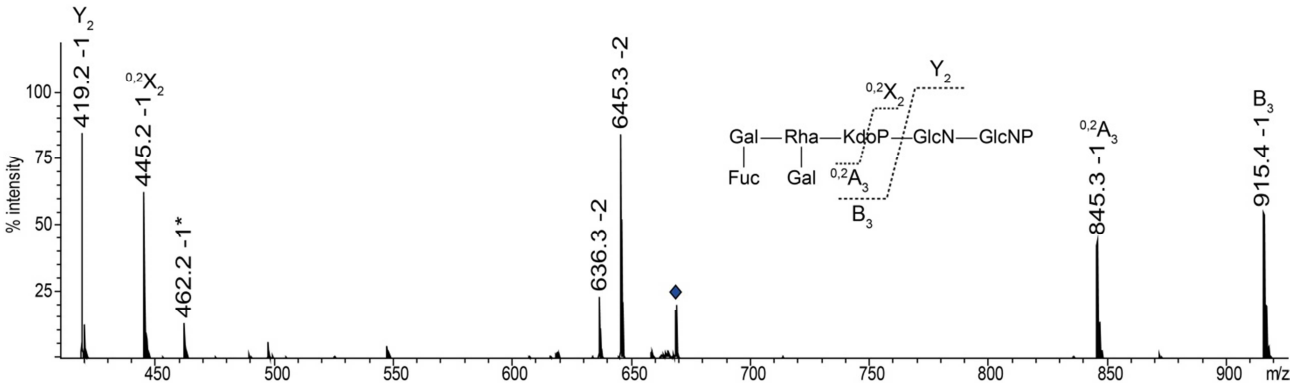

285

286 **Supplementary Figure 8: ESI-MS^2 spectrum of core OS from LPS$_{BV}$.**

287 Core OS was selected for MS^2 fragmentation. The glycosidic bond cleavage resulted in daughter ion B_3, corresponding to
288 oligosaccharide fragment containing Kdo, two hexoses, two deoxy-hexoses and phosphate, as well as complementary Y_2 ion
289 attributed to *mono*-phosphorylated dihexosamine. Other ions indicate fragmentation inside the sugar ring (A_3 and X_2) with
290 loss of formyl (*m/z* 645.3, 636.3 and X_2). The inset structure represents general structure of core OS. The precursor ion (*m/z*
291 667.3) is indicated by diamond. Ion indicated by asterisk was not interpreted.

292

293

294

295

296

297

298

299

300

301

302

303

304

305

306

Supplementary Table 1.

^{1}H, ^{13}C (*italic*) and ^{31}P (**bold**) chemical shift values of the saccharide region of the LPS_{BV}.

Chemical shifts (δ)								
Unit	**1**	**2**	**3**	**4**	**5**	**6**	**7**	**8**
A	5.50	3.22	3.81	3.27	4.07	4.12/3.80		
6-α-Glc*p*N	*90.4* **2.99**	*54.3*	*69.9*	*70.1*	*73.0*	*68.0*		
B	4.90	2.86	3.52	3.43	3.55	3.69/3.47		
6-β-Glc*p*N	*99.6*	*55.6*	*72.3*	*69.8*	*74.5*	*61.3*		
C	5.11	4.16	3.96	3.85	3.85	1.23		
3,4-α-Rha*p* (α-Rha^{I})	*101.0*	*70.2*	*78.9*	*73.6*	*68.6*	*16.9*		
D	5.07	4.06	3.96	3.92	3.72	3.56		
t-β-Gal*f*	*108.6*	*81.8*	*77.0*	*82.8*	*70.3*	*62.7*		
E	5.09	3.67	3.76	3.71	4.27	1.14		
t-α-Fuc*p*	*99.4*	*68.3*	*71.4*	*73.2*	*66.9*	*16.2*		
F	4.47	3.29	3.48	3.36	3.36	3.82/3.62		
3-β-Glc*p*	*102.5*	*73.5*	*82.4*	*69.9*	*75.6*	*60.8*		
G	5.01	3.93	3.81	3.34	3.96	1.22		
t-α-Rha*p* (α-Rha^{II})	*100.8*	*70.4*	*69.7*	*71.9*	*67.4*	*17.0*		
G′	5.00	3.93	ND	3.58	3.88	1.22		
4-α-Rha*p* (α-Rha′^{II})	*100.8*	*70.4*	*ND*	*79.4*	*67.5*	*17.0*		
H	4.72	3.45	3.75	3.80	3.71	3.93		
2,6-β-Gal*p*	*100.2*	*76.8*	*71.4*	*69.7*	*70.6*	*69.0*		
I	4.86	3.90	3.94	3.58	3.89	1.22		
4-α-Rha*p* (α-Rha^{OC})	*99.7*	*70.3*	70.3	79.4	*67.5*	*17.0*		
L	4.78	4.17	3.58	3.54	3.29	3.82/3.64		
3-β-Man*p*	*100.3*	*66.6*	*76.6*	*65.0*	*76.1*	*60.8*		
K	-	-	1.77/2.02	4.15	4.07	3.68	3.96	3.95/3.86
5-α-Kdo*p*			*34.5*	*67.2* **1.64**	*73.3*	*70.5*	*70.2*	*65.6*

Supplementary Table 2.

Interpretation of ESI-IT mass spectra of the saccharide domain of the LPS from *B. vulgatus* mpk.

Oligosaccharide composition	**Mass of the observed ion**	**Calculated mass of the ion**	**monoisotopic mass of oligosaccharides (Da)**	
	(*m/z*)	(*m/z*)	observed	calculated
Kdo·$HexN_2$·Hex_2·$DeoxyHex_2$·P	627.3	627.19	1256.6	1256.39
Kdo·HexN·Hex_3·$DeoxyHex_2$·P	627.8	627.69	1257.6	1257.38
Kdo·$HexN_2$·Hex_2·$DeoxyHex_2$·P_2	444.6 (-3) 667.3 (-2)	444.45 (-3) 667.18 (-2)	1336.6 1336.8	1336.36
Kdo·$HexN_2$·Hex_2·$DeoxyHex_2$·P_2	678.3#	-	1336.6	1336.36
Kdo·$HexN_2$·Hex_3·$DeoxyHex_2$·P_2	748.3	748.20	1498.6	1498.41
Kdo·$HexN_2$·Hex_3·$DeoxyHex_3$·P_1	781.4	781.25	1564.8	1564.50
Kdo·$HexN_3$·Hex_3·$DeoxyHex_2$·P_1	788.8	788.76	1579.6	1579.52
Kdo·$HexN_2$·Hex_3·$DeoxyHex_3$·P_2	821.3	821.23	1644.6	1644.47
Kdo·$HexN_3$·Hex_3·$DeoxyHex_2$·P_2	828.8	828.74	1659.6	1659.48
Kdo·$HexN_2$·Hex_4·$DeoxyHex_4$·P_2	650.0 (-3) 975.4 (-2)	649.86 (-3) 975.29 (-2)	1953.0 1952.8	1952.58
Kdo·$HexN_2$·Hex_5·$DeoxyHex_5$·P_2	1129.4	1129.34	2260.8	2260.69

# indicates $[M-3H+Na]^{2-}$ ion.

Supplementary Notes

Supplementary Note 1

B. vulgatus mpk LPS provides similar immunogenic properties on dendritic cells as live *B. vulgatus* mpk

It is known that apathogenic commensal bacteria can have either symbiotic or pathobiotic properties concerning the activation of the immune system. As published and mentioned previously, we identified *B. vulgatus* mpk as such a symbiotic commensal. As a representative apathogenic pathobiotic commensal, we identified and characterized *E. coli* mpk[2, 20, 21], which efficiently triggered the induction of colitis in *Il2*$^{-/-}$ mice[2]. We focused our attention on the immunological properties of the bacteria on dendritic cells *in vitro* and we tested whether such bacterial properties could be completely mimicked by their respective isolated LPS, thus explaining the observations made in *in vivo* experiments (Fig. 2). In view of this, we also isolated the LPS from *E. coli* mpk (LPS_{EC}) which contains a *bis*-phosphorylated and hexaacylated lipid A. We generated and stimulated bone marrow derived dendritic cells (BMDCs) with either live *B. vulgatus* mpk, *E. coli* mpk (both at MOI 1) or isolated LPS_{BV} or LPS_{EC}, both at concentrations of 50 ng^{-1} per 10^6 BMDCs for a total of 16 h. As shown in Fig. 4, stimulation of BMDCs with LPS resulted in the same BMDC phenotype as stimulation with the respective bacteria from which the LPS was isolated. Both, *B. vulgatus* mpk and pure LPS_{BV} stimulation led to a low expression of MHC-II, CD40, CD80 and CD86 (Supplementary Fig. 1a) as well as to very low secretion rates of pro-inflammatory cytokines, such as TNF, IL-12p40 and IL-6 (Supplementary Fig. 1b). The secretion rates of these cytokines were low but higher when compared to PBS treated controls. In contrast, stimulation of BMDCs with either *E. coli* mpk or LPS_{EC} led to a drastic increase of MHC-II and T cell co-stimulatory molecules (Supplementary Fig. 1a) as well as to strong secretion of pro-inflammatory cytokines (Supplementary Fig. 1b). Thus, it was confirmed that pure LPS was able to mimic the immunogenic properties of both commensal bacteria with LPS_{BV} providing low and LPS_{EC} providing strong immuno-stimulating properties. Therefore, it can be stated that LPS_{BV} is not a MD-2/TLR4 receptor complex antagonist as it provided weakly agonistic activity as demonstrated by low, but still detectable amounts of secreted cytokines and by slight enhancement of T cell stimulatory surface proteins as MHC-II, CD40, CD80 and CD86.

Supplementary Note 2

Weakly agonistic LPS_{BV} provides low replacement capacity at the MD-2/TLR4 receptor complex towards strong agonistic LPS_{EC}

Based on these latter results, we then tested the capability of each of these two distinct LPS to remove already bound LPS from the receptor complex. Thus, we incubated HEK-mTLR4 cells with different concentrations of either biotinylated LPS_{BV} ($bioLPS_{BV}$) or LPS_{EC} for 1 h and subsequently added the opposite LPS for 1 h and in several concentrations. Subsequent additional incubation with Strep-PE allowed for flow cytometry based visualisation of HEK-mTLR4 cell bound $bioLPS_{BV}$ (Supplementary Fig. 2). Pre-incubation with LPS_{EC} followed by subsequent incubation with $bioLPS_{BV}$ resulted in low detected PE fluorescence, more or less independent from the employed LPS_{EC} and $bioLPS_{BV}$ concentrations (Supplementary Fig. 2a). This indicated that once the murine MD-2/TLR4 receptor complex is bound by LPS_{EC}, $bioLPS_{BV}$ is not able to remove LPS_{EC} from the receptor binding site. Pre-incubation with LPS_{EC} even at low concentrations of 1.25 mg L^{-1}, resulted in a decrease of the PE-signal to about 20% of the PE-signal that arose when cells were not pre-incubated with LPS_{EC} (Supplementary Fig. 2a). Conversely, pre-incubation of HEK-mTLR4 cells with $bioLPS_{BV}$ followed by subsequent incubation with LPS_{EC} resulted in a strong reduction of the PE-signal, which is exclusively derived from bound $bioLPS_{BV}$, of about 50%, even when low concentrations of LPS_{EC} were added (Supplementary Fig. 2b). Since we assumed that the detected PE fluorescence was directly proportional to the amount of bound $bioLPS_{BV}$, it can be stated that $bioLPS_{BV}$ was able to remove about 20% of already bound LPS_{EC} (Supplementary Fig. 2a), while LPS_{EC} was able to remove about 50% of already bound $bioLPS_{BV}$ (Supplementary Fig. 2b).

Supplementary Note 3

DC semi-maturation cannot be induced in presence of agonistic LPS

We have already demonstrated that LPS_{BV} is able to induce tolerant semi-mature DCs *in vitro* (Fig. 4 and 5). However, these experiments were performed in absence of other LPS structures for the first 16 h of the semi-maturation process. Physiological conditions in the colonic lumen provide the presence

of lots of different LPS structures at the same time. Therefore, we stimulated BMDCs with both LPS molecules, weakly agonistic LPS_{BV} and strong agonistic LPS_{EC}, at the same time and at different concentrations for 16 h (Supplementary Fig. 3a). We checked for secretion of pro-inflammatory cytokines and the surface expression of MHC-II and TLR4. We detected a concentration dependent effect of LPS_{BV} stimulation on BMDCs in the absence of LPS_{EC} (light blue lines in Supplementary Fig. 3b,c). LPS_{BV} concentrations of up to 100 ng mL^{-1} (which equals to 50 ng per 10^6 BMDCs) led to a semi-mature BMDC phenotype, as previously demonstrated in Figs. 4 and 5. Using 1000 ng mL^{-1}, or 500 ng pure LPS_{BV} per 10^6 cells led to strong activation of BMDCs as indicated by high IL-1β, TNF, IL-6 (Supplementary Fig. 3b) and MHC-II surface expression (Supplementary Fig. 3c). However, 500 ng pure LPS exceeds physiological LPS-to-DC ratios in the mammalian intestine thus representing an artificial observation. Nevertheless, it underlined and confirmed the observation that LPS_{BV} is not antagonistic but rather weakly agonistic and the overall concentration determines its final endotoxicity. Addition of agonistic LPS_{EC} led to strong increases in secretion rates of pro-inflammatory cytokines (Supplementary Fig. 3a) as well as in the expression of MHC-II (Supplementary Fig. 3c) for all used LPS_{EC} concentrations. Simultaneous presence of LPS_{BV} could not anticipate LPS_{EC}-induced maturation effects on DCs as it was demonstrated in case of subsequent stimulation of DCs that were primed with LPS_{BV} and challenged with LPS_{EC} (Fig. 5). Surprisingly, TLR4 expression on the cell surface remained relatively constant among all differently stimulated BMDCs (Supplementary Fig. 3d), indicating that no significant TLR4 endocytosis is detectable upon binding of these two LPS structures to the TLR4 receptor complex in opposition to what was previously reported for other intestinal commensal-derived LPS [22].

Supplementary Note 4

Structural characterization of LPS_{BV}

In order to define the full structure of the LPS from *B. vulgatus* mpk, a multi-disciplinary approach was employed. In detail, a set of chemical analyses, on both intact and isolated LPS domains, was executed, furnishing the chemical composition of each LPS moiety. Data resulting from chemical

analyses represented the guidelines to unveil the information provided by the other techniques, NMR spectroscopy and ESI mass spectrometry (MS) which enabled the complete structural characterization of the LPS_{BV}. MALDI MS analysis also furnished fundamental information regarding the LPS_{BV} lipid A, providing important clues such as the nature of the molecular lipid A species, their heterogeneity, the type, the location and the distribution of the fatty acid chains.

Supplementary Note 5

Extraction, purification and chemical analyses of LPS_{BV}

LPS material was extracted from lyophilized bacterial cells by the hot phenol/water procedure [3]. The extracted LPS underwent an enzymatic digestion by DNase, RNase and protease in order to remove cell contaminants. A further step of purification by ultracentrifugation was also performed. The nature and purity of the LPS was determined by SDS-PAGE analysis after silver nitrate gel staining [4], disclosing the smooth-nature of the extracted LPS, as proven by the ladder-like pattern in the upper part of the gel indicating the occurrence of high molecular weight species.

Chemical analyses [5, 6, 7] executed on pure LPS revealed the presence of terminal, 4-substituted and 3,4-disubstituted rhamnopyranose (Rha*p*), terminal fucopyranose (Fuc*p*), terminal galactofuranose (Gal*f*), 3-substituted mannopyranose (Man*p*), 3-substituted glucopyranose (Glc*p*), 2,6-disubstituted galactopyranose (Gal*p*), 6-substituted aminoglucopyranose (Glc*p*N) and 5-substituted Kdo. Fatty acid analysis [8] showed the occurrence of tetradecanoic acid (C14:0), pentadecanoic acid (C15:0), hydroxypentadecanoid acid (C15:(3-OH)), hydroxyhexadecanoid acid (C16:(3-OH)) and hydroxyheptadecanoic acid (C17:(3-OH)), in full agreement with previously reported data by Hashimoto *et al*. on the structure of lipid A from *B. vulgatus* IMCJ 1204 [23].

Supplementary Note 6

NMR spectroscopy analysis

An aliquot of the pure LPS isolated from *B. vulgatus* mpk underwent a full deacylation [9, 10] furnishing the complete LPS saccharide portion. The deacylated LPS fraction was then purified by gel permeation chromatography. Monosaccharide analysis of the isolated product confirmed the presence of the sugar residues detected in the intact LPS. The deacylated product was then analyzed by 1D and 2D NMR spectroscopy. A combination of homo- and heteronuclear 2D NMR experiments (DQF-COSY, TOCSY, NOESY, ROESY, ^{1}H, ^{13}C HSQC, ^{1}H, ^{13}C HMBC, ^{31}P and ^{1}H, ^{31}P HSQC) was performed in order to elucidate the complete saccharide sequence of LPS_{BV}. In detail, each spin system was assigned on the basis of the spin connectivity observed in both the double-quantum-filtered correlation spectroscopy (DQF-COSY) and the total correlation spectroscopy (TOCSY) spectra; each carbon atom was identified through the analysis of the heteronuclear single-quantum coherence (HSQC) spectrum. The anomeric configuration of all sugar units was defined by *intra*-residual NOE contacts, detectable in the nuclear Overhauser effect spectroscopy (NOESY) spectrum and the $^{3}J_{H\text{-}1,H\text{-}2}$ coupling constants from the DQF-COSY spectrum. The assignment of the relative configuration of each sugar residue was obtained through the observation of the vicinal $^{3}J_{H,H}$ coupling constant values. The combined study of rotating-frame NOE spectroscopy (ROESY), NOESY, and HMBC (heteronuclear multiple-bond correlation spectroscopy) spectra allowed the characterization of the entire primary structure of the LPS saccharide part. Finally, ^{31}P and ^{31}P,^{1}H HSQC experiments were pivotal to establish the location of the phosphate groups decorating the LPS_{BV}.

In the ^{1}H NMR spectrum (Supplementary Fig. 4) eleven anomeric signals from eleven spin systems were clearly identified (**A**–**L**; Supplementary Table 1); Furthermore, the signals at 1.77 and 2.02 ppm were attributed to the H-3 methylene protons of the Kdo unit (**K**; Supplementary Table 1). All the monosaccharide residues, except for **D**, were present as pyranose rings, according to both ^{13}C chemical shift values and the presence of long-range correlations between C-1/H-1 and H-5/C-5 observable in the ^{1}H,^{13}C HMBC spectrum (for the Kdo residue between C-2 and H-6)[24, 25]. Conversely, residue **D** was present as furanose ring as shown by the occurrence of low-field shifted ring carbon signals resonating around 82.0 ppm, anomeric carbon over 108 ppm and further confirmed by the *intra*-residual long-range H/C 1-4 correlations in the ^{1}H,^{13}C HMBC spectrum.

Spin systems **A** (H-1 5.50 ppm) and **B** (H-1 4.90 ppm) were identified as the α-Glc*p*N and β-Glc*p*N of the lipid A moiety based on their H-2 proton signals, which correlated with two nitrogen-bearing carbon atoms at 54.3 and 55.6 ppm, respectively (Supplementary Fig. 5, Supplementary Table 1). This hypothesis was also corroborated by the presence of an *inter*-residue contact between H-1 of **B** and H-$6_{a,b}$ of **A** observed in the NOESY spectrum. Furthermore, the occurrence of a correlation, in the $^{31}P,^{1}H$ HSQC spectrum (not shown), between the signal at 2.99 ppm and the anomeric proton signal of residue **A** (5.50 ppm, Supplementary Table 1), allowed the allocation of a phosphate group at such a position. Spin systems **C**, **G**, **G′** and **I** were identified as α-rhamnopyranose residues as proven by the correlations, in the TOCSY spectrum, with the methyl group signals resonating at δ_H 1.23 and 1.24 ppm (δ_C 16.9 and 17.0 ppm; Supplementary Table 1) respectively. As mentioned above, the α-anomeric configuration was determined on the basis of the $^{3}J_{H\text{-}1,H\text{-}2}$ coupling constant values and the *intra*-residual NOE contact of H-1 with H-2; whereas the *manno* configuration was established by evaluation of $^{3}J_{H,H}$ coupling constant values.

Spin systems **D**, **E** and **H** were attributed to *galacto*-configured sugar units. In detail, residue **D** (H-1 5.07 ppm, Supplementary Table 1), as stated above, revealed to be a β-galactofuranose (anomeric carbon signal at 108.6 ppm, Supplementary Table 1 and Supplementary Fig. 5) based on its chemical shifts and *intra* residual scalar and dipolar correlations. By contrast, spin system **H** (H-1 4.72 ppm, Supplementary Table 1) was assigned to a β-galactopyranose, as proven by the chemical shift values of ring protons and the $^{3}J_{H,H}$ ring coupling constants; furthermore, the large $^{3}J_{H\text{-}1,H\text{-}2}$ values and the NOE correlations of H-1 with H-3 and H-5, were indicative of the β-anomeric configuration.

The *galacto*-configured sugar residue **E** (H-1 5.09 ppm, Supplementary Table 1) was identified as an α-fucopyranose as shown by the correlations, in the TOCSY spectrum, with the methyl proton signal at 1.14 ppm (δ_C 16.2 ppm; Supplementary Table 1) and the $^{3}J_{H\text{-}1,H\text{-}2}$ coupling constant values that confirmed the α-anomeric configuration.

Spin system **F** (H-1 4.47 ppm, Supplementary Table 1) was assigned to a β-glucopyranose as indicated by the large $^{3}J_{H,H}$ ring coupling constants and the chemical shift values of ring protons, in agreement with *gluco*-configuration of pyranose rings (Supplementary Table 1). Moreover, the large $^{3}J_{H\text{-}1,H\text{-}2}$ values, together with the NOE contacts of H-1 with H-3 and H-5, were diagnostic of the β-

anomeric configuration. Finally, spin system **L** (H-1 4.78 ppm; Supplementary Table 1) was attributed to a β-mannopyranose residue, as proved by the small $^{3}J_{\text{H-1,H-2}}$ and $^{3}J_{\text{H-2,H-3}}$ values, diagnostic of a H-2 equatorial orientation, whereas the *intra*-residual correlations between H-1 and H-5 in the NOESY and ROESY spectra allowed the β configuration assignment. The assignment of the Kdo unit (**K**) was achieved starting from the diastereotopic methylene signal, and its anomeric α-configuration was assigned on the basis of the chemical shift values of H-3 (1.77/2.02 ppm, Supplementary Table 1), and of the $^{3}J_{\text{H-7,H8a}}$ and $^{3}J_{\text{H-7,H-8b}}$ coupling constants [26, 27]. Moreover, the Kdo residue was phosphorylated at position O-4, due to the occurrence of a correlation with a signal at 1.64 ppm in the ^{31}P,^{1}H HSQC spectrum (not shown).

The down-field shifted carbon signals were indicative of glycosylation at position O-6 of **A** and **B**, O-5 of **K**, O-3 and O-4 of **C**, O-2 and O-6 of **H**, O-3 of **F** and **L** and O-4 of **I** and **G′**, whereas **D**, **E** and **G** were terminal sugar residues, in full accordance with the methylation data. The analysis of the *inter*-residual NOE contacts (observable in both the NOESY and ROESY spectra) and the long-range correlations in the HMBC spectrum allowed to define the complete sugar sequence of the LPS from *B. vulgatus* mpk. Starting from the lipid A disaccharide backbone, made up of residue **A** and **B**, this latter sugar unit was found to be substituted at position O-6 by Kdo residue (**K**); this was further confirmed by the weak downfield shift of signal of C-6 of residue **B** (61.3 ppm, Supplementary table 1), which is consistent with the α-(2→6) ketosidic linkage of Kdo with the β-GlcN of the lipid A. The Kdo unit was, in turn, substituted at position O-5 by the rhamnose residue **C**, as suggested by the long-range correlation between the anomeric proton signal of residue **C** and the carbon atom at 73.3 ppm (C-5, Supplementary Table 1) of residue **K** (Figure 3c and Supplementary Fig. 6). Rhamnose **C** revealed to be substituted at both positions O-3 and O-4 by the *galacto*-configured sugar units **D** and **H** respectively, as showed by the occurrence of the strong NOE contacts between H-1 of **D** and H-3 of **C** and between H-1 of **H** and H-4 of **C**. These glycosydic linkages were also confirmed by the observation of the respective long-range correlations in the HMBC spectrum (Figure 3c and Supplementary Fig. 6). Residue **H**, in turn, was substituted by the α-Fuc **E** at position O-2 and by the β-Glc **F** at position O-6, as proven by the long-range correlations between the H-1 of **E** and the C-2 signal of **H**, and H-1 of **F** and C-6 of **H** (Figure 3c and Supplementary Fig. 6). This latter residue **F**

turned out to be substituted at position O-3 by rhamnose **G**, as suggested by the long-range contact between the anomeric proton signal of **G** and the carbon atom signal at 82.4 ppm (C-3, Supplementary Table 1) of β-glucose **F** (Figure 3c and Supplementary Fig. 6). Interestingly, 2D NMR analysis allowed the identification of a second slight different glycoform of rhamnose **G**, referred to here as **G′**, differing for the presence of a glycosylated position, namely position O-4 (Supplementary Table 1).

Sugar units **I** and **L** were attributed to the components of the disaccharide repeating unit of the O-chain moiety as demonstrated by the long-range correlation of the anomeric proton signal of β-Man **L** with the carbon atom signal C-4 of α-Rha **I** (Figure 3c and Supplementary Fig. 6); further on, an HMBC correlation between anomeric proton signal of **I** and C-3 of β-Man **L** was also clearly visible. These data were in full agreement with the LPS O-chain repeating unit previously elucidated by Hashimoto *et al.* [18]. Finally, we were able also to establish the biological repeating unit, in fact, residue **G′**, assigned to a 4-substituted α-Rha, was identified as the sugar likely connecting the O-chain moiety to the core region, as proven by the long-range correlation between H-1 of **L** and C-4 of **G′** (Figure 3c and Supplementary Fig. 6). This hypothesis was also confirmed by MS and MS^2 data (see below).

All the above information taken together allowed to establish the complete structure of the fully deacylated LPS_{BV} as follow:

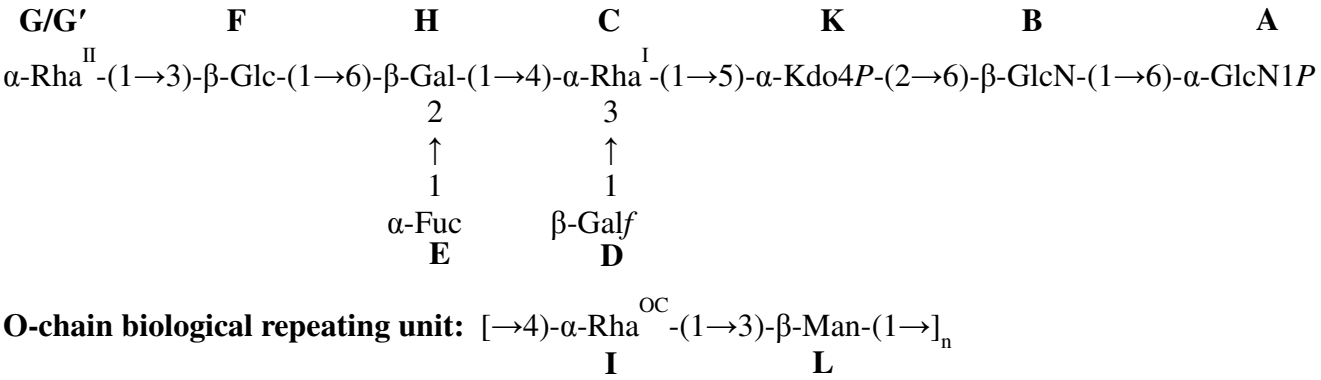

Supplementary Note 7

Mass spectrometry analysis

The fully deacylated LPS_{BV} was also analyzed by ESI MS. The corresponding spectrum is reported in Supplementary Fig. 7. The detailed investigation of the double and triple charged ions in the spectrum in the mass range *m*/*z* 400-1130 allowed the determination of the fine structure of the LPS saccharide domain. In detail, the spectrum showed three main signal clusters (**M1**–**M3**) of double charged ions (*m*/*z* 821.3, 975.4 and 1129.4, Supplementary Fig. 7 and Supplementary Table 2) originated from the monoisotopic molecules with a mass of 1644.47, 1952.58 and 2260.69 (calculated molecular masses 1644.6, 1952.8 and 2260.8 Da) respectively, differing by 308 u, which corresponded to the mass of an O-chain repeating unit (RU) built up of a hexose and a deoxyhexose, thus in full agreement with the NMR data. Briefly, **M1** (the most abundant species) and **M2** contained one and two O-chain RU respectively, whereas **M3** possessed three O-chain RU. Interestingly, the main peak *m*/*z* 667.3 was attributed to the double charged ion originated from the monoisotopic mass of 1336.36 (calculated molecular mass 1336.6 Da) which is consistent with an oligosaccharide composed of two hexosamines, one Kdo, two hexoses, two deoxyhexoses and two phosphates. The structural sequence of the core OS was also corroborated by the ESI-MS^2 investigation executed on precursor ion 1336.36 which is reported in Supplementary Fig. 8. The spectrum showed the occurrence of a daughter ion at *m*/*z* 419.2 ($\mathbf{Y_2}$) originated from the monoisotopic mass 420.11 (calculated molecular mass 420.2 Da) assignable to the *mono*-phosphorylated diglucosamine backbone of the lipid A. Moreover, the daughter ion at *m*/*z* 915.4 ($\mathbf{B_4}$) relative to a mass of 916.24 (calculated mass 916.4 Da) was attributed to the oligosaccharide fragment made up of one Kdo, one phosphate, two hexoses and two deoxy-hexoses. Finally, the ESI-MS spectrum revealed also the occurrence of the two double charged ions at *m*/*z* 627.3 and 748.3 relative to the monoisotopic masses 1256.39 and 1498.41 (calculated molecular masses 1256.6 and 1498.6 Da) respectively, which matched with the above described core OS minus a phosphate group (1256.39) or carrying a further hexose unit (1498.41). Therefore, all above mentioned MS and MS^2 data were in full accordance with the NMR structural elucidation of the saccharide moiety of the LPS_{BV}.

In order to define also the structure of the glycolipid portion of the LPS_{BV}, an aliquot of pure LPS underwent a mild acid hydrolysis in order selectively cleave the acid-labile linkage between the Kdo and the β-GlcN unit and to isolate the lipid A fraction. After purification, this latter was then analyzed by MALDI MS. The MALDI MS spectrum (Figure 3a), acquired in negative polarity, matched perfectly with the MS analysis executed by Hashimoto *et al.* [23] In detail, a high heterogeneity of lipid A species was immediately apparent as demonstrated by the occurrence of four clusters of signals differing in the number of the fatty acid chains (Figure 3a). Moreover, each of these group of ions was characterized by the presence of mass differences that can be explained with the presence of lipid A species differing in the fatty acid chain length. In detail, the most intense cluster of ions in the mass range *m/z* 1617-1717 Da (Figure 3a) was consistent with *mono*-phosphorylated pentaacylated lipid A species whose fatty acid distribution and composition, as instance for ion peak at *m/z* 1688.28, was determined as two C17:(3-OH) as *N*-linked acyl chains, two C16:(3-OH) as primary *O*-linked fatty acids and C15:0 as a secondary *O*-acyl substitution. The less intense cluster of ions visible in the mass range *m/z* 1385-1479 Da (Figure 3a) was attributed to *mono*-phosphotylated tetraacylated lipid A species with the main ion peak at *m/z* 1436.02 assigned to a lipid A possessing the above mentioned fatty acid distribution and composition but lacking one primary *O*-linked C16:(3-OH). The minor cluster of ion at about *m/z* 1257 Da (Figure 3a) was identified as *mono*-phosphotylated lipid A species bearing three fatty acid chains. Interestingly, a further minor cluster in the mass range *m/z* 1768-1797 (Figure 3a) Da was assignable to pentaacylated lipid A species carrying a further phosphate group whose location remains to be defined.

Supplementary references

1. Hamacher, K., Coenen, H. H. & Stocklin, G. Efficient stereospecific synthesis of no-carrier-added 2-[^{18}F]-fluoro-2-deoxy-D-glucose using aminopolyether supported nucleophilic substitution. *J. Nucl. Med.* **27**, 235–238 (1986).

2. Waidmann, M.*, et al. Bacteroides vulgatus* protects against *Escherichia coli*-induced colitis in gnotobiotic interleukin-2-deficient mice. *Gastroenterology* **125**, 162–177 (2003).

3. Westphal, O. & Jann, K. Bacterial lipopolysaccharides: extraction with phenol-water and further applications of procedure. *Carbohydr. Chem.* **5**, 83–91 (1965).

4. Kittelberger, R. & Hilbink, F. Sensitive silver-staining detection of bacterial lipopolysaccharides in polyacrylamide gels. *J. Biochem. Biophys. Methods* **26**, 81–86 (1993).

5. Leontein, K. Assignment of absolute configuration of sugars by glc of their acetylated glycosides formed from chiral alcohols. *Methods Carbohydr. Chem.* **62**, 359–362 (1978).

6. De Castro, C., Parrilli, M., Holst, O. & Molinaro, A. Microbe-associated molecular patterns in innate immunity: Extraction and chemical analysis of gram-negative bacterial lipopolysaccharides. *Methods Enzymol.* **480**, 89–115 (2010).

7. Ciucanu, I., Kerek,F. A simple and rapid method for the permethylation of carbohydrates. *Carbohydr. Res*, 209–217 (1984).

8. Rietschel, E. T. Absolute configuration of 3-hydroxy fatty acids present in lipopolysaccharides from various bacterial groups. *Eur. J. Biochem.* **64**, 423–428 (1976).

9. Holst, O. Deacylation of lipopolysaccharides and isolation of oligosaccharide phosphates. *Methods Mol. Biol.* **145**, 345–353 (2000).

10. Holst, O., Muller-Loennies, S., Lindner, B. & Brade, H. Chemical structure of the lipid A of *Escherichia coli* J-5. *Eur. J. Biochem.* **214**, 695–701 (1993).

11. Piantini, U., Sorensen, O. W. & Ernst, R. R. Multiple quantum filters for elucidating NMR coupling networks. *J. Am. Chem. Soc*. **104**, 6800–6801 (1982).

12. Rance, M., Sorensen, O. W., Bodenhausen, G., Wagner, G., Ernst, R. R. & Wuthrich, K. Improved spectral resolution in COSY (1)H NMR spectra of proteins via double quantum filtering. *Biochem. Biophys. Res. Commun.* **425**, 527–533 (1983).

13. States, D. J., Haberkorn, R. A. & Ruben, D. J. A two-dimensional nuclear Overhauser experiment with pure absorption phase in four quadrants. *J. Magnetic Res.* **8**, 286–292 (1982).

14. Stern, A. S., Li, K. B. & Hoch, J. C. Modern spectrum analysis in multidimensional NMR spectroscopy: comparison of linear-prediction extrapolation and maximum-entropy reconstruction. *J. Am. Chem. Soc*. **124**, 1982–1993 (2002).

15. Jachymek, W. et al. Structural Studies of the O-Specific Chain and a Core Hexasaccharide of *Hafnia Alvei* Strain 1192 Lipopolysaccharide. *Carbohydr. Res.* **269** (1), 125–38 (1995).

16. Lutz, M. B.*, et al.* An advanced culture method for generating large quantities of highly pure dendritic cells from mouse bone marrow. *J. Immunol. methods* **223**, 77–92 (1999).

17. Jeon, S. G.*, et al.* Probiotic *Bifidobacterium* breve induces IL-10-producing Tr1 cells in the colon. *PLoS pathogens* **8**, e1002714 (2012).

18. Rakoff-Nahoum, S., Paglino, J., Eslami-Varzaneh, F., Edberg, S. & Medzhitov, R. Recognition of commensal microflora by toll-like receptors is required for intestinal homeostasis. *Cell* **118**, 229–241 (2004).

19. Chow, J., Mazmanian, S. K. A pathobiont of the microbiota balances host colonization and intestinal inflammation. *Cell host & microbe* **7**, 265–276 (2010).

20. Muller, M.*, et al.* Intestinal colonization of IL-2 deficient mice with non-colitogenic B. vulgatus prevents DC maturation and T-cell polarization. *PLoS One* **3**, e2376 (2008).

21. Frick, J. S.*, et al.* Colitogenic and non-colitogenic commensal bacteria differentially trigger DC maturation and Th cell polarization: an important role for IL-6. *Eur. J. Immunol.* **36**, 1537–1547 (2006).

22. Tan, Y., Zanoni, I., Cullen, T. W., Goodman, A. L., Kagan, J. C. Mechanisms of Toll-like Receptor 4 Endocytosis Reveal a Common Immune-Evasion Strategy Used by Pathogenic and Commensal Bacteria. *Immunity* **43**, 909–922 (2015).

23. Hashimoto M*, et al.* Structural study on lipid A and the O-specific polysaccharide of the lipopolysaccharide from a clinical isolate of *Bacteroides vulgatus* from a patient with Crohn's disease. *Eur. J. Biochem.* **269**, 3715–3721 (2002).

24. Silipo, A., Leone, S., Molinaro, A., Lanzetta, R. & Parrilli, M. The structure of the phosphorylated carbohydrate backbone of the lipopolysaccharide of the phytopathogen bacterium *Pseudomonas tolaasii*. *Carbohydr. Res.* **339**, 2241–2248 (2004).

25. Silipo, A. et al. Structure Elucidation of the Highly Heterogeneous Lipid A from the Lipopolysaccharide of the Gram-Negative Extremophile Bacterium *Halomonas Magadiensis* Strain 21 M1. *Eur. J. Org. Chem.*, 2263–2271 (2004).

26. Birnbaum, G. I. Conformations of ammonium 3-deoxy-D-manno-2-octulosonate (KDO) and methyl α-and β-ketopyranosides of KDO: X-ray structure and ^{1}H NMR analyses. *J. Carbohydr. Chem.* **6**, 17–39 (1987).

27. Silipo, A. et al. Full structural characterisation of the lipooligosaccharide of a *Burkholderia pyrrocinia* clinical isolate. *Eur. J. Org. Chem.*, 4874-4883 (2006).